UNIVERSIDAD NACIONAL AUTÓNOMA DE MÉXICO

Maestría y Doctorado en Ciencias Bioquímicas

Caracterización de la fosforilación oxidativa mitocondrial de D*ebaryomyces hansenii* en diferentes fases de crecimiento

TESIS

QUE PARA OPTAR POR EL GRADO DE:

Doctor en Ciencias

PRESENTA:

LIBB. ALFREDO CABRERA OREFICE

TUTOR PRINCIPAL:

DR. SALVADOR URIBE CARVAJAL
Instituto de Fisiología Celular, UNAM

MIEMBROS DEL COMITÉ TUTOR:

DR. ANTONIO PEÑA DÍAZ
Instituto de Fisiología Celular, UNAM

DR. JUAN PABLO PARDO VÁZQUEZ
Facultad de Medicina, UNAM

MÉXICO, D. F., Septiembre, 2015

AGRADECIMIENTOS

Al **Programa de Maestría y Doctorado en Ciencias Bioquímicas** de la Universidad Nacional Autónoma de México (UNAM), por la formación y apoyos que me brindaron durante mis estudios de posgrado.

Al **Consejo Nacional de Ciencia y Tecnología (CONACYT)** por otorgarme la beca para la realización de mis estudios de posgrado (Becario 240104, No. de apoyo 335161, CVU 289024).

Al **Programa de Apoyo a los Estudios del Posgrado (PAEP)** por los apoyos otorgados para la asistencia a congresos nacionales e internacionales.

Al **CONACYT** (239487) y **DGAPA-PAPIIT** (IN204015) por los apoyos otorgados para la realización de este proyecto.

A mi tutor principal, el **Dr. Salvador Uribe Carvajal** por toda la asesoría académica, experimental y personal durante mis estudios de posgrado y trabajo de tesis.

A los integrantes del Comité Tutor:

- **Dr. Antonio Peña Díaz**
- **Dr. Juan Pablo Pardo Vázquez**

A los integrantes del Jurado de Examen:

- **Dr. Edmundo Chavez Cossío**
- **Dra. Xóchitl Pérez Martínez**
- **Dr. Oscar Flores Herrera**
- **Dra. Cecilia Zazueta Mendizábal**
- **Dr. Diego González Halphen**

A las asistentes de procesos del Programa de Maestría y Doctorado en Ciencias Bioquímicas:

- **Leticia García Gutiérrez**
- **Adelina González Pérez**
- **Sara Méndez Ibáñez**

A la **Dra. Natalia Chiquete Félix**, Técnico Académico del lab. 305-Ote, IFC, UNAM.

A **Teresa Castillo**, secretaria de la Sociedad Mexicana de Bioquímica, oficina IFC, UNAM.

A **Gabriela Valdéz**, secretaria del Departamento de Genética Molecular, IFC, UNAM.

ÍNDICE

LISTA DE ABREVIATURAS

A_{540}	Absorbencia a 540 nm
ADN	Ácido desoxirribonucleico
ADNmt	ADN mitocondrial
ADP	Difosfato de adenosina
ANT	Acarreador de adenín nucleótidos
AOX	Oxidasa alterna
ARN	Ácido ribonucleico
ATP	Trifosfato de adenosina
BLAST	Herramienta Básica de Búsquedas de Alineamientos Locales
BN-PAGE	Electroforesis nativa azul en geles de poliacrilamida
BSA	Albúmina sérica bovina
CCCP	*p*-clorocarbonilcianuro fenilhidrazona
CR	Control respiratorio
CsA	Ciclosporina A
Cyp-D	Ciclofilina D
D.E.	Desviación estándar
$_{Dh}$MUC	Canal inespecífico mitocondrial de *D. hansenii*
kDa	KiloDaltones
LDH	Lactato deshidrogenasa
MME	Membrana mitocondrial externa
MMI	Membrana mitocondrial interna
mPTP	Poro de la transición de la permeabilidad de mamíferos
MUC	Canal inespecífico mitocondrial
NAD^+	Dinucleótido de nicotinamida adenina oxidado
NADH	Dinucleótido de nicotinamida adenina reducido
NDE	NADH deshidrogenasa alterna externa
NDH2	NADH deshidrogenasa alterna tipo II
NDI	NADH deshidrogenasa alterna interna
O_2	Oxígeno molecular (diatómico)
Pi	Fosfato inorgánico
PiC	Acarreador de fosfato
PTP	Poro de la transición de la permeabilidad
Q	Ubiquinona
$Q^{\bullet-}$	Semiquinona
QH_2	Ubiquinol
ROS	Especies reactivas del oxígeno
rpm	Revoluciones por minuto
RRC	Respiración resistente al cianuro
SHAM	Ácido salicilhidroxámico
TPM	Transición de la permeabilidad mitocondrial
Tris	2-Amino-2-hidroximetil-propano-1,3-diol
VDAC	Canal aniónico dependiente de voltaje
YMUC	Canal inespecífico mitocondrial de levadura
Δp	Fuerza protón-motriz
$\Delta\Psi$	Potencial eléctrico transmembranal

RESUMEN

La levadura *Debaryomyces hansenii* posee una cadena respiratoria ramificada conformada por los complejos I, II, III y IV, una oxidasa alterna (AOX) insensible al cianuro, una NADH deshidrogenasa externa (NDH2e) y una glicerol-fosfato deshidrogenasa ($_{Mit}$GPDH). Las mitocondrias de esta levadura llevan a cabo una transición de la permeabilidad debido a que forman un canal inespecífico mitocondrial ($_{Dh}$MUC). La presencia de este canal constituye un mecanismo de desacoplamiento fisiológico de la fosforilación oxidativa. Además, la presencia de las oxidorreductasas alternas puede constituir un segundo mecanismo de este tipo. Estos mecanismos modulan la producción del ATP, evitan la sobreproducción de especies reactivas del oxígeno (ROS) y reciclan las pozas redox en condiciones de baja demanda energética (p. ej. en la fase estacionaria de crecimiento).

En estudios previos se propone que la AOX se expresa sólo en la fase estacionaria de crecimiento. Lo anterior ocurre únicamente cuando *D. hansenii* es cultivada en presencia de glucosa como fuente de carbono. En cambio, al cultivarla en presencia de lactato (fuente no fermentable), la actividad de esta enzima aparece desde la fase exponencial y se mantiene sin cambio durante la fase estacionaria. Por esta razón, en este trabajo se decidió estudiar si en *D. hansenii* la fosforilación oxidativa varía en diversas fases de crecimiento.

Para ésto se determinó el consumo de O_2 y el acoplamiento respiratorio de las mitocondrias aisladas de las levaduras cosechadas en diferentes tiempos de cultivo, en presencia de diferentes donadores de electrones. Solamente con piruvato-malato se encontró una disminución gradual en la respiración y el acoplamiento a medida que aumentó el tiempo de cultivo. Este efecto no se debió a una menor cantidad y/o actividad del complejo I ni de los otros componentes respiratorios. Por tal motivo, se sugirió que la disminución de la actividad respiratoria observada pudo deberse a una baja producción de NADH matricial.

Para explorar lo anterior, se determinaron las actividades enzimáticas de la piruvato deshidrogenasa y la malato deshidrogenasa (enzimas dependientes de NAD^+) en muestras mitocondriales de las fases exponencial y estacionaria. No se encontraron diferencias en las actividades entre las dos fases. Cabe señalar que los ensayos se realizaron en presencia de NAD^+ y otras coenzimas. Con base en esto, se sugirió que la baja actividad respiratoria observada en la fase estacionaria pudo deberse, en principio, a una menor cantidad de NAD^+ en la matriz mitocondrial.

Bajo esta premisa, se cuantificaron nuevamente la respiración, el acoplamiento respiratorio y el potencial transmembranal ($\Delta\Psi$) en presencia de piruvato-malato y agregando NAD^+ a los ensayos. Las muestras de fase exponencial no presentaron cambios con respecto a las mediciones iniciales (en ausencia del NAD^+). Sin embargo, las muestras de fase estacionaria recuperaron de manera parcial la actividad respiratoria y el acoplamiento, y de manera completa el $\Delta\Psi$ en presencia del NAD^+. La recuperación completa de los primeros dos parámetros se observó únicamente en esferoplastos permeabilizados de la fase estacionaria, en los cuales las mitocondrias se encuentran *in situ*. En este trabajo se propone que la falta del NAD^+ matricial pudo deberse a una fuga de éste a través del $_{Dh}$MUC.

En los ensayos anteriores, el NAD^+ ingresó a la matriz en condiciones donde el $_{Dh}$MUC se encuentra cerrado. Esto sugirió la posibilidad de un mecanismo de transporte específico para esta coenzima. En *Saccharomyces cerevisiae*, el NAD^+ se transporta a la matriz mitocondrial a través de dos isoformas de un acarreador específico: Ndt1p y Ndt2p. En *D. hansenii* se encontró un posible ortólogo de este acarreador. Para determinar su posible participación se determinó el consumo de O_2 en presencia de batofenantrolina, púrpura de bromocresol y piridoxal-5'-fosfato, los cuales son inhibidores del transporte del NAD^+. En presencia de éstos, la adición del NAD^+ no tuvo efecto sobre la respiración, lo que sugiere que no fue transportado a la matriz.

La pérdida sugerida del NAD^+ matricial en la fase estacionaria de crecimiento constituye un posible mecanismo de desacoplamiento fisiológico adicional a la apertura del $_{Dh}$MUC. Debido a la baja demanda energética en esta fase, este mecanismo puede disminuir, por un lado, la producción de ATP al abatir el $\Delta\Psi$ y al evitar la entrada de electrones a partir del complejo I y, por otro, la formación de ROS al transportar los electrones y consumir el O_2 de forma desacoplada.

ABSTRACT

The branched respiratory chain from *Debaryomyces hansenii* contains complexes I, II, III and IV, a cyanide-insensitive alternative oxidase (AOX), an external NADH dehydrogenase (NDH2e) and a glycerol-phosphate dehydrogenase ($_{Mit}$GPDH). In addition, this yeast species contains two possible physiological oxidative phosphorylation (OxPhos) uncoupling mechanisms: *a)* a branched respiratory chain, which contains non-proton pumping alternative oxidoreductases and *b)* a permeability transition, which is triggered by opening the mitochondrial unspecific channel ($_{Dh}$MUC). These mechanisms may modulate the ATP synthesis, prevent reactive oxygen species (ROS) overproduction and recycle redox pools during low energy demand situations (e.g. stationary growth phase).

In exponential phase grown cells, OxPhos are highly coupled and both uncoupling mechanisms inactive. However, upon aging in culture (stationary phase), the efficiency of proton pumping decreases and mitochondria become partially uncoupled, probably in an effort to deplete oxygen in the cell without synthesizing ATP. In the stationary growth phase, the complex I-dependent rate of oxygen consumption and coupling are selectively decreased. Complex I relative content and activity are not changed in this condition. In fact, all other branched respiratory chain components activities remain the same as in the exponential phase. For this reason, it is suggested that the respiratory activity change is due to a lower matrix NADH production. In order to explore this, activities of pyruvate and malate dehydrogenases (NAD^+-dependent enzymes) were measured in both growth phases. No differences were observed in these enzymes. Therefore, these results suggest a lack of matrix NAD^+ in isolated mitochondria from the stationary phase.

Here, we propose that NAD^+ possibly escapes the matrix through an open $_{Dh}$MUC. When NAD^+ is added back, coupled complex I-dependent respiratory activity in stationary phase-isolated mitochondria is recovered. This uptake occurs when $_{Dh}$MUC is closed and seems to be catalyzed by a NAD^+-specific carrier, which is inhibited by bathophenanthroline, bromcresol purple and pyridoxal-5'-phosphate as described for *S. cerevisiae*. Loss of matrix NAD^+ through an open MUC is suggested as an additional OxPhos physiological uncoupling mechanism.

1. INTRODUCCIÓN

1.1. Debaryomyces hansenii como modelo de estudio

Debaryomyces hansenii es una levadura halotolerante no patógena que suele residir en hábitats con alta salinidad, tales como el agua marina, de donde se aisló por primera vez (Norkrans y Kylin, 1969), y otros como son los quesos, la cerveza, el vino, los lácteos y diversos productos cárnicos (Breuer y Harms, 2006).

Aunque facultativa, esta levadura tiene un metabolismo aeróbico mayor que la fermentación (Sánchez y cols., 2006). Posee una gran versatilidad para metabolizar diversas fuentes de carbono (glucosa, sacarosa, galactosa, glicerol, lactato, manitol, etanol, trehalosa, celobiosa, ribitol, succinato, gluconato, entre otras) (Breuer y Harms, 2006). Además, crece a bajas temperaturas (Norkrans, 1966), en distintos intervalos de pH (Norkrans, 1966; Hobot y Jennings, 1981) y en alta salinidad (a concentraciones de NaCl y/o KCl por encima de 2 M) (Norkrans, 1966; Prista y cols., 2005).

Debido a estas cualidades, esta levadura se utiliza desde hace algunos años como modelo de gran interés para la investigación básica y aplicada, principalmente en el área biotecnológica. Además, se aprovecha en la industria para la síntesis de compuestos naturales y artificiales (carbohidratos y lípidos, principalmente), expresión y purificación de proteínas y enzimas de interés comercial, elaboración de probióticos, maduración de quesos, etc. (Fadda y cols., 2004; Breuer y Harms, 2006).

1.2. Principales estudios en Debaryomyces hansenii

La mayoría de los estudios básicos realizados en este microorganismo tratan sobre los mecanismos por los cuales se adapta a las altas concentraciones de cationes monovalentes (Na^+ y K^+) (Norkrans, 1966; Prista y cols., 1997). Al parecer, la preferencia por este tipo de hábitats no se debe únicamente a la capacidad de resistir al estrés osmótico, sino a que en estas condiciones optimiza su crecimiento (Prista y cols., 1997; Almagro y cols., 2000; González-Hernández y cols., 2002). Por ello se ha propuesto clasificar a este organismo como halófilo (González-Hernández y Peña, 2002) y no sólo como halotolerante.

Por definición, los microorganismos halófilos son aquellos que se reproducen y realizan sus funciones metabólicas con mayor eficacia en medios hipersalinos. En cambio, los halotolerantes, únicamente modulan sus funciones para resistir al estrés en dichas

condiciones (González-Hernández y Peña, 2002). *D. hansenii* se encuentra en medio de las dos clasificaciones debido a que no requiere que el medio contenga alta salinidad para poder crecer. En general, dos mecanismos principales son llevados a cabo por los organismos que resisten la hipersalinidad: el "sodio-excluyente" y el "sodio-incluyente". El primero se lleva a cabo por los halotolerantes, que expulsan la mayor cantidad de sodio posible del citoplasma y balancean la presión osmótica con solutos compatibles (sacarosa, trehalosa, glicerol, etc.). La segunda es utilizada por los halófilos, que almacenan altas concentraciones de sodio en el interior para balancear la presión osmótica, y se sugiere que poseen diversas adaptaciones internas que les permiten resistir los efectos nocivos de la sal y además beneficiarse (González-Hernández y Peña, 2002; Sánchez y cols., 2006).

En las membranas plasmática y vacuolar de *D. hansenii* existen diversos transportadores de cationes monovalentes involucrados en su movimiento (Hobot y Jennings, 1981; Prista y cols., 1997). La concentración promedio de cationes monovalentes en el agua marina es de 600 mM y 10 mM, para el Na^+ y K^+, respectivamente. En presencia de concentraciones desiguales de Na^+ y K^+, esta levadura es capaz de internalizar en mayor cantidad al catión que se encuentre más concentrado en el exterior y expulsar del citosol la mayor parte del otro que se encuentre en menor concentración. Pero en presencia de concentraciones iguales de estos cationes, *D. hansenii* acumula al K^+ preferentemente y con mayor rapidez que al Na^+ (Thomé-Ortiz y cols., 1998). Cuando se cultiva en 0.6 M de NaCl, ambos cationes se encuentran en concentraciones similares en el interior (~150 mM Na^+ y ~100 mM K^+). Por el contrario, si se incuba en ausencia de sales o en presencia de KCl, se observa un aumento en la concentración de K^+ intracelular y el Na^+ es expulsado casi por completo (González-Hernández y cols., 2004).

Diversos autores describen que en *D. hansenii* incubada en medios con alto contenido de NaCl y KCl, se induce la expresión de algunas enzimas (Alba-Lois y cols., 2004) y aumenta la actividad de las enzimas glucolíticas y la respiración (Sánchez y cols., 2006). En las mitocondrias aisladas de esta levadura se sabe que las concentraciones altas de Na^+ y K^+ mejoran el rendimiento de la fosforilación oxidativa (Cabrera-Orefice y cols., 2010). Con este último antecedente, descrito en nuestro grupo, se inicia la caracterización de la fosforilación oxidativa mitocondrial de *D. hansenii*, como parte de un proyecto global que tiene como meta describir las diferencias y similitudes en los mecanismos de desacoplamiento fisiológico de la fosforilación oxidativa en distintas especies de levaduras (Uribe-Carvajal y cols., 2011).

1.3. La mitocondria y la fosforilación oxidativa.

Las mitocondrias son organelos formados por dos membranas, una externa y otra interna; esta última forma una serie de invaginaciones denominadas crestas. Entre ambas membranas se encuentra el espacio intermembranal. El interior de la mitocondria constituye la matriz mitocondrial, donde se llevan a cabo diversos procesos como el ciclo de Krebs, la β-oxidación de ácidos grasos, el ciclo de la urea, oxidación de ciertos aminoácidos, entre otros (Nelson y Cox, 2000).

Estos organelos poseen material genético propio (ADN) y cuentan con toda la maquinaria necesaria para su expresión. No obstante, las proteínas mitocondriales se codifican por dos genomas: el nuclear y el mitocondrial (ADNmt). El genoma mitocondrial codifica diversos ARN de transferencia (ARNt) y ribosomales (ARNr) y algunas subunidades proteicas. Sin embargo, cerca del 98% de las proteínas mitocondriales son codificadas fuera de ella y una vez sintetizadas, son dirigidas y transportadas a este organelo (Pfanner y Meijer, 1997; Chacinska y cols., 2009); tal es el caso de transportadores de solutos, proteínas de importación, subunidades de la cadena respiratoria, enzimas de la replicación, etc. Por tal motivo, es necesaria la expresión coordinada de los dos sistemas genómicos para que el organelo funcione de manera óptima y en respuesta a las necesidades celulares.

La membrana mitocondrial externa (MME), además de mantener la integridad del organelo, es una estructura primordial en la comunicación intergenómica, la regulación metabólica y el transporte del organelo a través del citoplasma (unida a elementos del citoesqueleto) (Hirano y Vu, 2000; Boldogh y Pon, 2006). Por otro lado, la membrana mitocondrial interna (MMI) es una estructura con una arquitectura altamente dinámica, y modifica su organización en función del estado metabólico celular (Frey y cols., 2000; Mannella y cols. 2002). La MMI cambia su conformación para incrementar o disminuir el número, tamaño y forma de las crestas (Manella, 2006). Se cree que esto favorece la interacción y asociación de las proteínas involucradas en la fosforilación oxidativa, además de promover la formación de gradientes localizados (Gilkerson y cols., 2003; Manella, 2006).

La principal característica de las mitocondrias es su especialización en la transducción de energía y la síntesis del adenosín trifosfato (ATP), el compuesto energético de mayor importancia para las células. La producción del ATP en este organelo se lleva a cabo a través de la fosforilación oxidativa (Nelson y Cox, 2000).

Los compuestos altamente reducidos (p. ej. glucosa, ácidos grasos, etc.) son inicialmente metabolizados en el citoplasma y los productos obtenidos son llevados al interior de la mitocondria donde se continúa el catabolismo utilizando diversas rutas que incluyen el ciclo de los ácidos tricarboxílicos (o ciclo de Krebs), la β-oxidación de ácidos grasos y la oxidación de los aminoácidos. El resultado final de estas rutas es la producción de dos donadores de electrones: NADH y $FADH_2$. Los electrones que residen en estas moléculas son transferidos a través de una serie de complejos de proteínas integrales de membrana, llamados en conjunto "cadena respiratoria", hasta el O_2, el cual se reduce a agua. Este proceso ocurre en la MMI (Nicholls y Ferguson, 2002).

La cadena respiratoria tiene como finalidad la generación de un gradiente electroquímico de protones (H^+) (Mitchell, 1961). Esto ocurre gracias al acarreo de electrones a través de una serie de reacciones de óxido-reducción. Esta transferencia promueve un bombeo vectorial de H^+ a través de los complejos respiratorios desde la matriz al espacio intermembranal. Este fenómeno provoca que el espacio intermembranal quede positivo (lado P) con respecto a la matriz, que queda negativa (lado N).

Peter Mitchell estableció el término conocido como fuerza protón-motriz (Δp) al manipular algebraicamente la ecuación de Nernst (Mitchell, 1966). Este término se puede interpretar como la energía que puede transformarse en trabajo útil; en este caso la formación de un enlace fosfodiéster para sintetizar al ATP (Nicholls y Ferguson, 2002). La fuerza protón-motriz, incluye los componentes químico (ΔpH) y eléctrico ($\Delta\Psi$) de los H^+ separados por la MMI. Una vez generado el gradiente, éste es utilizado por la enzima F_1F_o-ATP sintasa (conocida también como complejo V), la cual es capaz de acoplar el paso de H^+ desde el espacio intermembranal a la matriz mitocondrial con la síntesis de ATP a partir de adenosín difosfato (ADP) y fosfato inorgánico (Pi) (Hatefi y cols., 1962).

La cadena respiratoria de la mayoría de las mitocondrias está formada por cuatro complejos "clásicos" denominados I, II, III y IV (Nicholls y Ferguson, 2002). Sin embargo, las mitocondrias de plantas, hongos, protozoarios y otros unicelulares, pueden contener enzimas respiratorias alternas (deshidrogenasas y oxidasas) involucradas en el transporte de electrones (Joseph-Horne y cols., 2001). La presencia de éstas da lugar a nuevos puntos de entrada y a la ramificación del flujo de electrones. Gracias a ésto, los electrones transportados pueden seguir dos vías hasta el O_2: la citocrómica, si son transportados por los complejos III y IV; y la alterna, cuando se transfieren hacia una oxidasa alterna (AOX, por sus

siglas en inglés *alternative oxidase*). En las mitocondrias de los mamíferos no se han encontrado esta clase de enzimas, aunque sí contienen distintas proteínas de otras vías metabólicas que participan en el transporte de electrones (Nelson y Cox, 2000).

1.3.1. Complejos respiratorios "clásicos"

El complejo I (NADH deshidrogenasa) o NADH:ubiquinona oxidorreductasa (E.C. 1.6.5.1) es la enzima respiratoria más grande (aprox. de 1 MDa en mamíferos y 500 kDa en procariontes) y contiene el mayor número de subunidades de todos los complejos respiratorios. Los modelos cristalográficos y las imágenes de microscopía electrónica revelan que este complejo posee dos dominios principales: uno hidrofóbico, embebido en la MMI y otro soluble, orientado hacia la matriz (Brandt, 2006; Efremov y Sazanov, 2011). Estructuralmente, el complejo I de los mamíferos está compuesto por alrededor de cuarenta y seis subunidades (catorce conservadas y alrededor de treinta y dos adicionales dependiendo la especie) (Nelson y Cox, 2000). Siete subunidades son codificadas por el ADNmt y cinco de ellas contienen a los grupos prostéticos FMN y hierro-azufre (centros Fe-S) (Brandt y cols., 2003; Hinchliffe y Sazanov, 2005). El complejo I puede ser inhibido por rotenona, amital y piericidina (Nelson y Cox, 2000). Esta enzima pertenece a la familia de las NADH deshidrogenasas tipo I (Kerscher y cols., 2008).

El complejo I capta los electrones acarreados por el NADH y los transfiere a un intermediario liposoluble llamado ubiquinona (Q) reduciéndolo a ubiquinol (QH_2). Tanto la Q como el QH_2 son intermediarios que se encuentran en la MMI y pueden difundir a través de ella. El complejo I toma al NADH y lo oxida a NAD^+ reduciendo a su vez al grupo prostético FMN a $FMNH_2$ en un único paso que implica la transferencia de dos electrones. Posteriormente estos electrones continúan su paso a través de siete centros Fe-S que sólo pueden aceptar un electrón a la vez. El último centro Fe-S, transfiere el primer electrón proveniente del NADH a la Q generando una de sus formas reducidas: la semiquinona ($Q^{\bullet -}$) (Galkin y Brandt, 2005). Esta semiquinona vuelve a reducirse por el centro Fe-S con el segundo electrón generando QH_2. El paso de electrones en esta enzima se encuentra acoplado a una serie de cambios conformacionales en las subunidades del dominio hidrofóbico, que durante la transferencia, permiten la translocación de cuatro protones desde la matriz hasta el espacio intermembranal (Walker, 1992).

El Complejo II (succinato deshidrogenasa) o succinato:ubiquinona oxidorreductasa (E.C. 1.3.5.1) es una enzima que forma parte del ciclo de Krebs y no bombea protones (Hederstedt y Ohnishi, 1992). Este complejo recibe electrones al oxidar succinato a fumarato y los transfiere a través de un grupo prostético FAD, tres centros Fe-S y un grupo hemo *b* hasta la Q para formar QH_2 (Ohnishi y cols., 1998; Lemire y Oyedotun, 2002). El primer aceptor de electrones es la flavina; posteriormente son transferidos de uno por uno a través de los centros Fe-S, antes de entrar a las subunidades membranales, en donde se lleva a cabo la reducción de la ubiquinona. En este mecanismo, un electrón se transporta del centro [3Fe-4S] de la subunidad Sdhb a la Q, y se produce la $Q^{\bullet-}$. La enzima debe retener este compuesto inestable hasta que otro electrón sea transferido para generar QH_2 (Guo y Lemire, 2003). En los mamíferos, el complejo II está formado por cuatro subunidades codificadas por genes nucleares (Nelson y Cox, 2000). Esta enzima se inhibe de manera competitiva por malato, oxaloacetato y malonato (Hagerhall, 1997).

El complejo III (complejo bc_1) o ubiquinol:citocromo *c* oxidorreductasa (E.C. 1.10.2.2) obtiene dos electrones de la QH_2 y los transfiere a un acarreador móvil de electrones hidrosoluble que se encuentra en el espacio intermembranal: el citocromo *c* (cit *c*). Este complejo transloca cuatro protones a través de la membrana por cada dos electrones transportados desde el ubiquinol (Hatefi y cols., 1962). En el bovino, el complejo III contiene once subunidades (una codificada por el ADNmt) y cuatro grupos prostéticos: dos hemos tipo *b* (b_L y b_H), un hemo tipo *c* y un centro hierro-azufre (2Fe-2S) (Covian y Trumpower, 2005). Este último, ubicado en una subunidad conocida como “proteína de Rieske”. El transporte de electrones en esta enzima, se lleva a cabo a través de un mecanismo conocido como ciclo Q, en el cual se transfiere un electrón al *cyt c* y otro se mantiene en una semiquinona hasta que otro ubiquinol entra y completa el ciclo (Braun y Schmitz, 1995; Darrouzet y cols., 2001). El complejo III tiene una forma dimérica obligatoria, ya que la forma monomérica no es funcional, a diferencia de los complejos I y II. Esto se debe a que las proteínas de Rieske sólo ejercen su función en monómeros contrarios (Covian y Trumpower, 2005). Esta enzima se inhibe por antimicina A, mixotiazol y estigmatelina (Nelson y Cox, 2000).

El complejo IV (citocromo *c* oxidasa) o citocromo *c*:oxígeno oxidorreductasa (E.C. 1.9.3.1) capta los electrones provenientes del *cyt c* y los transfiere al oxígeno molecular ($½O_2$). Al igual que el complejo III, esta enzima también es dimérica, aunque cada monómero de COX es funcional. En los mamíferos, cada monómero se forma por trece subunidades, de

las cuales tres (COXI, COXII y COXIII) son codificadas por el ADNmt. Este complejo, contiene dos grupos hemo (*a* y a_3) y dos centros cobre (Cu_A y Cu_B) a través de los cuales se transfieren los electrones (Tsukihara y cols., 1995). El centro Cu_A se ubica en la subunidad II y contiene dos iones cobre que forman un complejo con los grupos tiol de dos residuos de cisteína que forman un centro binuclear (Tsukihara y cols., 1995). La subunidad I contiene los dos grupos hemo y el Cu_B. En esta última, el citocromo a_3 y el Cu_B forman otro centro binuclear, el cual acepta los electrones que provienen del hemo *a* y permite la reducción de $½O_2$ a H_2O (Iwata y cols., 1995). Esta reducción del oxígeno molecular, implica centros redox que transportan un único electrón a la vez y se lleva a cabo sin la liberación de los intermediarios parcialmente reducidos, tales como el H_2O_2 o el radical hidroxilo ($OH^{\bullet -}$).

La energía de las reacciones redox se aprovecha también en este complejo para impulsar la translocación de protones. Por cada cuatro electrones que atraviesan el complejo IV, se bombean dos protones netos al espacio intermembranal, ya que otros dos protones se utilizan para formar el H_2O. La estequiometría del bombeo de H^+ de esta enzima puede variar según el valor del $\Delta\Psi$ o las concentraciones intracelulares de nucleótidos de adenina (Frank y Kadenbach, 1996). A esto se le conoce como “deslizamiento” (del inglés *slipping*) y es un tipo de desacoplamiento intrínseco de la fosforilación oxidativa que no altera la transferencia de electrones hasta el O_2 y sólo cambia el número de H^+ bombeados por par de electrones transferidos (Azzone y cols., 1985).

La actividad de la COX se inhibe por análogos del oxígeno, tales como cianuro (CN^-), azida, monóxido de carbono (CO), óxido nítrico (NO), dióxido de nitrógeno (NO_2), entre otros (Yoshikawa y Caughey, 1990).

1.3.2. F_1F_o-ATP sintasa

Debido al uso de la nomenclatura de los complejos respiratorios es frecuente encontrar a la F_1F_o-ATP sintasa (E.C. 3.6.3.14) referida como complejo V. Esta enzima se caracteriza por tener dos dominios principales: el F_1, soluble en el lado matricial y el F_o, embebido en la MMI. Además, se distingue otro dominio de importancia conocido como brazo periférico, el cual funciona como estator y participa en la dimerización de la enzima (Couoh-Cardel y cols., 2010). El dominio F_o es el responsable de captar los protones del espacio intermembranal. Los H^+ promueven la rotación de un anillo de subunidades (denominadas c) y posteriormente son liberados en el lado matricial. Cada especie tiene una

estequiometría constante y definida de las subunidades que conforman el anillo c (Frank, 2011). Sin embargo, hasta donde se sabe, ésta puede variar de 8 (Watt y cols., 2010) a 15 (Pogoryelov y cols., 2005) subunidades dependiendo del tipo de organismo. La rotación del anillo promueve una serie de cambios conformacionales acoplados a las subunidades gamma (γ) y épsilon (ε), del dominio F_1, que permiten la transición entre tres estados catalíticos responsables de la síntesis del ATP a nivel de las subunidades alfa (α) y beta (β) (Lutter y cols., 1993; Boyer, 2002). Las subunidades que catalizan la formación del enlace fosfodiéster entre el ADP y el Pi son propiamente las β; éstas atraviesan por tres importantes cambios conformacionales durante el ciclo catalítico.

La relación entre los protones utilizados por el complejo V para sintetizar el ATP es de 3-4 H^+/ATP (Stock y cols., 2000; Ferguson, 2010). En condiciones energéticas ideales, la transferencia del par de electrones proveniente del NADH hasta el O_2 permite que la cadena respiratoria bombee 10 H^+ al espacio intermembranal, los cuales al utilizarse por el complejo V, permiten la síntesis de 2.5 moléculas de ATP. En el otro caso, cuando el par de electrones ingresa a la cadena respiratoria a través de la succinato deshidrogenasa, solo se pueden sintetizar 1.5 moléculas de ATP empleando los protones bombeados por los complejos III y IV (6 H^+ totales). No obstante, dichas estequiometrías (también llamadas relaciones ATP/O o P/O) varían según el número de subunidades c contenidas en el anillo (Ferguson, 2010).

Mediante electroforesis nativa y microscopía electrónica es posible observar formas diméricas y oligoméricas de esta enzima (Couoh-Cardel y cols. 2010). De hecho, se sugiere que las estructuras oligoméricas tienen como unidad a la ATP sintasa dimérica. Además, se propone que esta forma dimérica del complejo V es la funcional (Couoh-Cardel y cols. 2010). La dimerización de esta enzima induce una marcada curvatura en la membrana interna, la cual se relaciona directamente con la morfología de esta última y con la formación de las crestas mitocondriales (Paumard y cols. 2002). Recientemente, se propone que la F_1F_O-ATP sintasa es uno de los constituyentes del poro de la transición de la permeabilidad (PTP) en mamíferos, levadura y *Drosophila melanogaster* (Bernardi y cols., 2015). Esto se describirá mas adelante con detalle.

La F_1F_o-ATP sintasa se inhibe por moléculas como la oligomicina, venturicidina y aurovertina. Estas moléculas frenan el mecanismo rotatorio o bloquean directamente a la subunidad F_1 (Nelson y Cox, 2000).

1.3.3. Componentes respiratorios alternos

La mayoría de los datos que se tienen sobre la cadena respiratoria son producto de estudios realizados en las mitocondrias de mamíferos (p. ej. hígado y corazón de rata y corazón de bovino). En estos organelos, el flujo de electrones, a partir de la poza de quinonas, se realiza de manera lineal hasta el O_2 a través de la vía citocrómica (III-cit *c*-IV). Sin embargo, las mitocondrias de plantas, hongos, protozoarios y otros unicelulares, pueden contener enzimas "alternas" que catalizan las mismas reacciones que los complejos I y IV. Este tipo de cadenas conformadas por los complejos clásicos y las oxidorreductasas alternas recibe el nombre de "cadenas respiratorias ramificadas" (Kerscher y cols., 2008). Por tal motivo, los electrones pueden ingresar y transferirse por diversas rutas hasta el O_2.

El grupo de enzimas alternas que catalizan la oxidación del NADH reciben el nombre de NADH deshidrogenasas tipo II (NDH2) (Kerscher y cols., 2008); son una familia de enzimas periféricas ubicadas en la MMI y orientadas hacia el lado matricial (internas o NDI) o hacia el lado del espacio intermembranal (externas o NDE). Las NDE utilizan como sustrato el NADH citosólico de manera directa; las NDI pueden utilizar el NADH producido en la matriz mitocondrial al igual que el complejo I.

Este tipo de proteínas son monoméricas, codificadas por genes nucleares, tienen FAD unido como grupo prostético, no bombean protones y su catálisis no es afectada por inhibidores del complejo I; en su lugar son inhibidas específicamente por flavonas (Juárez y cols., 2004). Estructuralmente, se reconocen cuatro dominios conservados en este tipo de deshidrogenasas: dos dominios de unión a dinucleótidos (que forman el sitio donde se transfieren los electrones del NADH al FAD) y dos hidrofóbicos (Kerscher y cols., 2008).

Las mitocondrias de la planta *Arabidopsis thaliana* contienen siete NADH deshidrogenadas alternas, tanto NDI como NDE, cuya expresión depende de las condiciones del medio (luz, temperatura, humedad, etc.) (González-Meler y cols., 1999). Por otro lado, las mitocondrias de la levadura *Saccharomyces cerevisiae*, que no poseen complejo I, contienen tres NADH deshidrogenasas alternas (dos NDE y una NDI) que le confieren la posibilidad de utilizar los electrones del NADH (de Vries y Grivell, 1988; Kerscher y cols., 2008). Otros hongos como *Neurospora crassa, Yarrowia lipolytica y Ustilago maydis* tienen tanto el complejo I como NDH2s (Veiga y cols., 2003a; Juarez y cols., 2004). También existen deshidrogenasas alternas que utilizan indistintamente el NADH o NADPH como sustrato donador de electrones (Joseph-Horne y cols., 2001).

Otros componentes de las cadenas respiratorias ramificadas son las oxidasas alternas (AOXs), cuya función redox es equivalente a la del complejo IV, pero no bombean protones y no están acopladas a la síntesis de ATP (Moore y Siedow, 1991). Las AOXs se encuentran codificadas en el genoma nuclear y se orientan hacia el lado matricial de la MMI. La característica principal de las AOXs es su insensibilidad a inhibidores de la vía citocrómica; por ejemplo cianuro (CN^-), azida, monóxido de carbono (CO), mixotiazol y antimicina A (Lambers, 1980; Albury y cols., 2002). Por esta razón, las AOXs confieren a diversos organismos una respiración resistente a cianuro (RRC) (Veiga y cols., 2003a).

Las AOXs están presentes en plantas superiores, algas, eubacterias, nematodos e inclusive algunos protozoarios de vida libre, parásitos y metazoarios (Shiba y cols., 2013). Asimismo, esta enzima está codificada en la mayoría de los hongos y levaduras; con algunas excepciones como *S. cerevisiae*, *Schizosaccharomyces pombe* y *Kluyveromyces lactis*. Este tipo de oxidorreductasa tampoco se encuentra codificada en mamíferos ni en arqueas (Rogov y cols., 2014). Las AOXs pueden expresarse de manera constitutiva o inducible (dependen de la fase de crecimiento o situaciones de estrés) (Medentsev y cols., 1999; Veiga y cols., 2003b). Tal es el caso de *Candida albicans* que expresa dos isoformas de AOXs: AOX1a y AOX1b. La primera se expresa constitutivamente en niveles bajos, mientras que la otra se expresa en presencia de inhibidores de la vía citocrómica, especies reactivas del oxígeno (ROS por sus siglas en ingles *reactive oxygen species*) o cuando se satura el flujo de electrones a través de la vía citocrómica (Siedow y Umbach, 2000). Por otro lado, en plantas con órganos termogénicos, la AOX libera la energía de la transferencia de electrones hacia el O_2 en forma de calor (Rogov y cols., 2014). En otro tipo de plantas, la actividad de la AOX regula a la fotosíntesis y protege a los fotosistemas en contra del estrés oxidante (Rogov y cols., 2014). En los parásitos protistas, la AOX es una enzima clave para su supervivencia y adaptación dentro del hospedero. Por ejemplo, en ciertas etapas del desarrollo de *Trypanosoma brucei*, la AOX permite la respiración al ser la única oxidasa terminal (Walker y cols., 2005). Como se puede apreciar, las funciones de esta enzima varían según el tipo de organismo que la expresa. No obstante, la AOX no solo ofrece una ruta alterna a la vía citocrómica sino que también permite reciclar las pozas redox y que continue el flujo metabólico en otras vías (Vanlerberghe y cols., 2011).

Actualmente, la AOX es considerada como un potencial agente para el tratamiento de algunas disfunciones mitocondriales. Al expresar heterólogamente la AOX de *Ciona*

intestinalis o de plantas en células humanas, disminuyen la producción de ROS, la acumulación de lactato y la sensibilidad a pro-oxidantes en líneas celulares deficientes en COX (Hakkaart y cols., 2006; Matsukawa y cols., 2009; Dassa y cols., 2009). En ratones, la expresión heteróloga de esta enzima permite el acarreo de electrones hasta el O_2 en presencia del CN^- y disminuye la generación de ROS (El-Khoury y cols., 2013).

Hasta el momento no se cuenta con la estructura cristalográfica de la AOX de hongos o levaduras, pero se sugiere que es monomérica y orientada hacia el lado matricial (Uribe-Carvajal y cols., 2011). Sin embargo, recientemente se resolvió la estructura de la AOX de *T. brucei* (Shiba y cols., 2013). En este caso la enzima es un homodímero cuyo sitio activo se encuentra oculto dentro de un "haz de cuatro hélices". En este último, se encuentra el centro redox que consta de dos átomos de hierro, denominado di-hierro di-carboxilato (Albury y cols., 2002; Shiba y cols., 2013). Además, existen dos cavidades hidrofóbicas por monómero, las cuales parecen constituir el sitio en donde se une el ubiquinol (Shiba y cols., 2013). En plantas, la AOX también es homodimérica gracias a una cisteína conservada en el extremo N-terminal que forma un enlace disulfuro entre los monómeros (Siedow y Umbach, 2000). Esta cisteína no está presente en las AOXs de hongos y levaduras, razón por la cual no son capaces de formar homodímeros (Rogov y cols., 2014).

Las AOXs son inhibidas específicamente por ácidos hidroxámicos y *n*-alquil-galatos (Veiga y cols, 2003b). En contraparte, los nucleótidos de adenina (AMP, ADP) y guanina (GMP), incrementan su actividad por un mecanismo hasta ahora desconocido (Medentsev y cols. 2004); Además, en plantas, los α-cetoácidos (principalmente el piruvato) incrementan su actividad, probablemente a través de la reducción del enlace disulfuro (Day y cols. 1995).

Adicionalmente, es posible encontrar otras enzimas que donan electrones a la Q diferentes a los complejos I, II y las NDH2. Este tipo de proteínas se encuentran también en las mitocondrias de los mamíferos. Durante la β-oxidación de los ácidos grasos, los electrones extraídos de los acil-CoAs por diversas acil-CoA deshidrogenasas (contienen FAD como grupo prostético), pueden llegar a la poza de quinonas a través de una proteína transferidora de electrones (ETF) y una ETF:ubiquinona oxidorreductasa (Nicholls y Ferguson, 2006). En otro caso, el glicerol-fosfato, liberado en la hidrólisis de triacilgliceroles, así como en la reducción de la dihidroxiacetona-fosfato en la glucólisis, se oxida por una isoforma mitocondrial de glicerol-fosfato deshidrogenasa ($_{Mit}$GPDH) localizada en la cara externa de la MMI (Nelson y Cox, 2000). Esta enzima también dona electrones a la Q.

1.3.4. Supercomplejos respiratorios

El modelo original de la cadena respiratoria (o modelo de “estado fluido”) considera a las proteínas que la constituyen como entidades independientes y libres de difundir a lo largo de la MMI (Hackenbrock y cols. 1986). En este modelo, el transporte de electrones entre los complejos ocurre a través de moléculas acarreadoras que también difunden en la membrana (p. ej. la ubiquinona). Sin embargo, en las bacterias y en las mitocondrias de mamíferos, plantas y hongos, se describen asociaciones supramoleculares de los complejos I, III y IV, conocidas como “supercomplejos respiratorios” (Schägger y Pfeiffer, 2000). Este modelo, el cual se conoce como del “estado sólido”, propone que los complejos respiratorios forman heteroligómeros y que es posible la canalización de sustratos entre ellos. En este caso, la transferencia de electrones se puede dar a través de los sitios redox de cada complejo y de moléculas acarreadoras atrapadas entre éstos. Además de la canalización de sustratos, se proponen otras funciones para estas estructuras, por ejemplo: acelerar la catálisis de transferencia de electrones (Bianchi y cols., 2004), impedir la liberación de radicales libres (Acín-Pérez y Enríquez, 2014) y estabilizar la estructura de los complejos individuales dentro del supercomplejo (Lapuente-Brun y cols., 2013).

Es posible observar las bandas que corresponden a los supercomplejos respiratorios por medio de la electroforesis nativa azul (BN-PAGE). Para ello, las proteínas mitocondriales membranales son previamente solubilizadas con detergentes suaves y neutros como la digitonina (Schägger, 2001). Actualmente, se cuenta con imágenes y estructuras en baja resolución de distintos supercomplejos respiratorios de plantas y levaduras obtenidas por microscopía electrónica (Dudkina y cols., 2005; Schafer y cols, 2007).

Recientemente, se propone que los supercomplejos se organizan en estructuras de mayor tamaño que constituyen una red supramolecular conocida como “respirasoma”. En las mitocondrias de los mamíferos se observa que los respirasomas están formados por los supercomplejos $I_1III_2IV_4$ y III_2IV_4 en una proporción de 2:1, respectivamente (Krause y cols., 2004). Asimismo, se sugiere que estas estructuras forman ensambles lineales repetidos de alto peso molecular denominados “cuerdas respiratorias” (Wittig y cols., 2006). Sin embargo, otros autores consideran al respirasoma como una unidad funcional completa en la que la asociación de los complejos respiratorios I, III y IV (e inclusive el II) mantiene unidos al citocromo *c* y a la Q (Acin-Pérez y Enríquez, 2014). De hecho, este respirasoma se logró

aislar de un gel nativo y es capaz de transferir electrones desde el NADH hasta el O_2, sin la necesidad de agregar Q y citocromo *c* al medio de reacción (Acín-Pérez y cols., 2008).

Adicionalmente, existe un tercer modelo de la organización de la cadena respiratoria: el modelo de plasticidad (Acin-Pérez y Enríquez, 2014). En este caso se propone la coexistencia de complejos respiratorios y acarreadores de electrones que pueden o no encontrarse asociados en supercomplejos. Este modelo se ajusta de mejor forma con las cadenas respiratorias ramificadas en donde se sabe que el complejo II y las enzimas alternas no forman supercomplejos; sin embargo, los electrones que reciben pueden transferirse a través de la vía citocrómica. De hecho, se sugiere que los supercomplejos respiratorios están sujetos a un proceso dinámico de asociación-disociación que depende del estado energético celular y de la expresión de proteínas que sirven como chaperonas durante el ensamblaje de los mismos (Lapuente-Brun y cols., 2013).

En *S. cerevisiae* se observan únicamente los supercomplejos III_2IV_{1-2} debido a la ausencia del complejo I en esta levadura. Tampoco se observan asociaciones de las NADH deshidrogenasas alternas (NDH2s) con estos supercomplejos. Esto se debe posiblemente a que se trata de proteínas periféricas (Schägger y Pfeiffer, 2000). No obstante, en *Y. lipolytica* se observa la asociación de la NDH2 externa (NDH2e) con los complejos de la vía citocrómica (III y IV) (Guerrero-Castillo y cols., 2009). El supercomplejo NDH2e-III-IV es posiblemente el único caso descrito hasta el momento que involucra una enzima alterna. Por otro lado, no se tienen reportes que demuestren la asociación de la AOX con este tipo de estructuras (Eubel y cols. 2003).

1.4. La cadena respiratoria mitocondrial de Debaryomyces hansenii

D. hansenii posee una cadena respiratoria (Figura 1) formada básicamente por los complejos I, II, III y IV y una AOX insensible al cianuro e inhibida por ácido salicilhidroxámico (SHAM) (Veiga y cols., 2003a) y *n*-alquil-galatos (Sánchez y cols., 2006; Cabrera-Orefice y cols., 2010). Esta última se activa con AMP y es insensible al piruvato (Cabrera-Orefice y cols., 2014). Además, esta levadura expresa una NADH deshidrogenasa tipo II externa (NDH2e) sensible a flavona y una isoforma mitocondrial de glicerol-fosfato deshidrogenasa ($_{Mit}$GPDH) (Cabrera-Orefice y cols., 2014), capaces de utilizar NADH y glicerol-fosfato exógenos, respectivamente, como donadores de electrones (Figura 1). La presencia de las tres enzimas alternas permite que el flujo de electrones se encuentre ramificado (Figura 1).

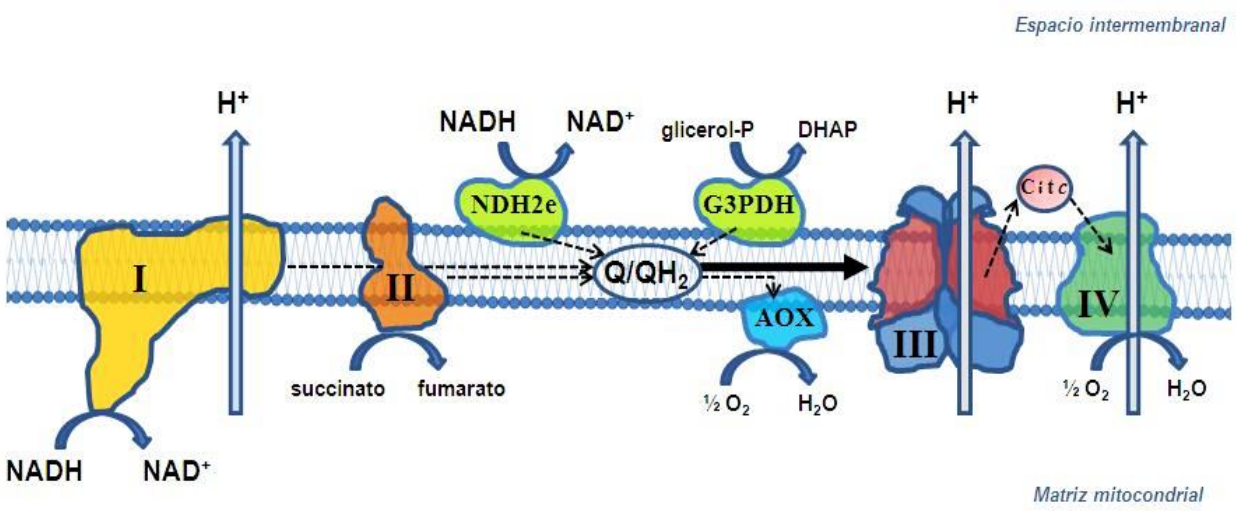

Figura 1. Componentes de la cadena respiratoria de *Debaryomyces hansenii*. La transferencia de electrones en los complejos I, III y IV se utiliza para el bombeo de protones a través de la MMI desde la matriz al espacio intermembranal. A nivel de la poza de quinonas (Q/QH_2), el flujo de electrones se puede desviar hacia la vía *citocrómica* a través de los complejos III y IV o a la vía *alterna* a través de la oxidasa alterna (AOX). NADH deshidrogenasa (I); succinato deshidrogenasa (II); citocromo bc_1 (III); citocromo *c* oxidasa (IV); citocromo *c* (Cit *c*); NADH deshidrogenasa alterna externa (NDH2e); glicerol-3-fosfato deshidrogenasa (G3PDH).

D. hansenii codifica una sola isoforma de cada una de las enzimas alternas (Veiga y cols., 2003; Cabrera-Orefice y cols., 2014). La NDH2e de esta levadura es homóloga con las tres NDH2 de *S. cerevisiae* y la NDH2e de *Y. lipolytica*. Esta secuencia está anotada como proteína hipotética *DEHA2D07568p* y corresponde a un precursor de 568 residuos (PM ~63 kDa). El alineamiento de secuencias arroja una identidad entre las cuatro proteínas por arriba del 45% y una similitud por arriba del 60%. Un alineamiento adicional de los motivos conservados de las NDH2 muestra una gran conservación entre la secuencia de *Y. lipolytica* y la de *D. hansenii* (Cabrera-Orefice y cols., 2014). La $_{Mit}$GPDH de *D. hansenii* es homóloga a las isoformas de *S. cerevisiae* (Gut2p) y *Y. Lipolytica* (YALI0B13970p). La secuencia aparece como proteína hipotética *DEHA2E08624p* y corresponde a un precursor de 652 residuos (PM ~72.5 kDa). El alineamiento calcula una identidad por arriba del 49% y una similitud por arriba del 64% entre las proteínas (Cabrera-Orefice y cols., 2014). La AOX es homóloga con las isoformas constitutiva (1) e inducible (2) de *Y. lipolytica* y *C. albicans.* La secuencia aparece como proteína hipotética *DEHA2C03828p* y corresponde a un precursor de 338 residuos (PM ~39.4 kDa) con 97.1% de probabilidad de importarse a la mitocondria (Cabrera-Orefice y cols., 2014).

Por otro lado, en *D. hansenii*, los complejos respiratorios I, III y IV se organizan en forma de supercomplejos respiratorios (Cabrera-Orefice y cols., 2014), dada la presencia de bandas de alto peso molecular con actividad de NADH deshidrogenasa (Figura 2B) y citocromo *c* oxidasa (Figura 2C) que se observan en geles nativos azules (BN-PAGE). Además, la F_1F_o-ATP sintasa se observa en la forma dimérica (V_2) y monomérica (V) (Figura 2D). En este estudio no se observaron bandas con actividad de complejo II, NDH2e o $_{Mit}$GPDH en las regiones de los supercomplejos (datos no mostrados) por lo que parecen encontrarse libres en la MMI. Con base en estos resultados, se propone que los componentes de la cadena respiratoria de esta levadura pueden estar organizados según el modelo de plasticidad (Acín-Pérez y Enríquez, 2014).

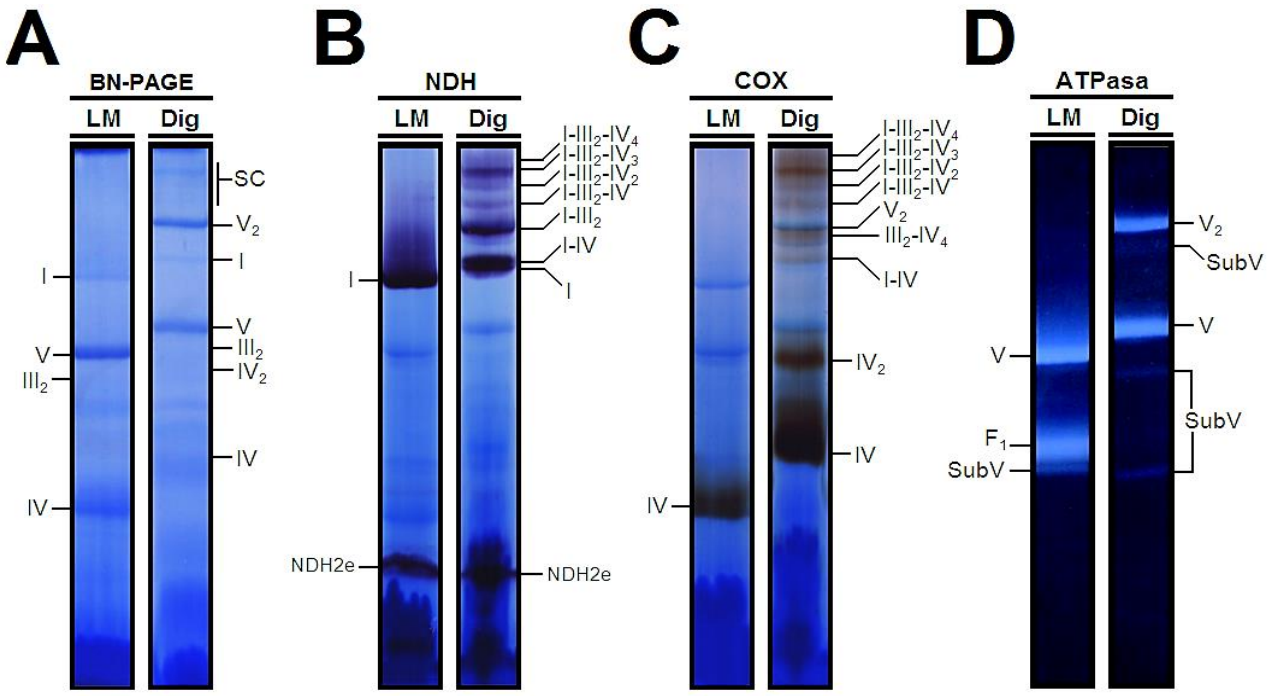

Figura 2. Supercomplejos respiratorios encontrados en *D. hansenii*. (A) Las muestras mitocondriales solubilizadas con lauril-maltósido (LM) (para separar los complejos en su forma individual) y digitonina (Dig) (para preservar las asociaciones supramoleculares entre los complejos) se cargaron y corrieron en un gel nativo azul (BN-PAGE) de gradiente (4-12%). **(B)** Tinción de actividad de NADH deshidrogenasa (NDH). **(C)** Tinción de actividad de citocromo *c* oxidasa (COX). **(D)** Tinción de actividad de ATPasa (en vista negativa). I, III_2, IV y V corresponden a los complejos respiratorios "clásicos". NDH2e: NADH deshidrogenasa alterna externa; F_1: Fracción soluble de la ATP sintasa; SubV: subcomplejos de ATP sintasa. Las estequiometrías de los supercomplejos (SC) se indican con subíndices y se estimaron con base en los pesos moleculares de los complejos monoméricos de *Y. lipolytica* (no mostrado). Imagen modificada de Cabrera-Orefice y cols., 2014.

1.5. Mecanismos de desacoplamiento fisiológico en levaduras

En ausencia de síntesis de ATP (estado no fosforilante), el potencial transmembranal mitocondrial ($\Delta\Psi$) se mantiene alto y la actividad de la cadena respiratoria disminuye. En esta condición, los electrones pasan lentamente a través de las diferentes oxidorreductasas aumentando la probabilidad de que los radicales libres producidos a nivel de los complejos respiratorios I, II y III reaccionen con el O_2 y se generen especies reactivas de oxígeno (ROS) (Koshkin y cols., 2003; Rottenberg y cols., 2009). La sobreproducción de ROS puede desencadenar procesos involucrados en la muerte celular, en el envejecimiento celular y en el desarrollo de varios estados patológicos. No obstante, las ROS tienen implicaciones fisiológicas ya que participan en la señalización celular y en la regulación metabólica y transcripcional (Nicholls y Ferguson, 2006).

En las mitocondrias existen mecanismos de eliminación de ROS, como la superóxido dismutasa, la glutatión peroxidasa, etc. Sin embargo, con el fin de prevenir la sobreproducción de ROS, se ha propuesto que las mitocondrias pueden mantener un alto flujo de electrones al activar diferentes sistemas de desacoplamiento fisiológicos de la fosforilación oxidativa finamente regulados (Guerrero-Castillo y cols., 2011). En general, son de dos tipos: *disipadores del gradiente de H^+* y *oxidorreductasas que no bombean protones*. El primer tipo corresponde a los canales inespecíficos mitocondriales (MUCs, por sus siglas en inglés *mitochondrial unspecific channels*) y las proteínas desacoplantes (UCPs, por sus siglas en inglés *uncoupling proteins*). En el segundo encontramos a las NADH deshidrogenasas tipo II (NDH2), oxidasas insensibles a cianuro (AOXs) y otras proteínas transferidoras de electrones que no bombean H^+ (p. ej. glicerol-fosfato deshidrogenasa mitocondrial).

Estos mecanismos se conocen en muchos organismos y en particular en diferentes especies de levaduras. *S. cerevisiae* y *D. hansenii* expresan MUCs sensibles a la concentración de iones y moléculas como Mg^{2+}, Ca^{2+}, fosfato inorgánico, ATP, entre otras (Uribe-Carvajal y cols., 2011). Por otro lado, *Y. lipolytica* posee un acarreador mitocondrial de oxaloacetato con actividad protonofórica; como las UCPs (Luévano-Martínez y cols., 2010). Además, las tres especies expresan enzimas alternas junto a los otros complejos que bombean H^+ o bien, pueden sustituir la función redox de alguna bomba que no esté presente. Tal es el caso de *S. cerevisiae* que carece del complejo I pero la función de NADH deshidrogenasa es catalizada por la NDI (Guerrero-Castillo y cols., 2011).

1.5.1. Canales inespecíficos mitocondriales (MUCs)

En diversos organismos, ocurre una transición de la permeabilidad (TPM) cuando un canal inespecífico de alta conductancia denominado canal inespecífico mitocondrial (MUC) o poro de transición de la permeabilidad (PTP) se abre y permite el libre paso de solutos a través de la MMI. Éste permite el paso de moléculas de entre 1.1 y 1.5 kDa (Jung y cols., 1997). Una característica particular de estos poros es su fluctuación entre un estado abierto y otro cerrado. La apertura del canal permite que los iones fluyan libremente entre el espacio intermembranal y la matriz, abatiendo los gradientes químicos ($\Delta\mu$) y eléctricos ($\Delta\Psi$). En consecuencia, se acelera el consumo de oxígeno y las mitocondrias se hinchan (Bernardi y cols., 1994; Zoratti y Szabo, 1995; Manon y Guérin, 1998). Originalmente, este canal se describió en las mitocondrias de los mamíferos (referido como mPTP por sus siglas en inglés *mitochondrial permeability transition pore*) (Beutner y cols., 1998). Más tarde, se encontró en las mitocondrias de *S. cerevisiae*, en donde se le conoce como canal inespecífico mitocondrial de levadura (YMUC por sus siglas en inglés *yeast mitochondrial unspecific channel*) (Manon y Guérin, 1998).

Hasta ahora no se conoce el papel fisiológico de estos canales, aunque su función los involucra en la modulación del acoplamiento de la fosforilación oxidativa, la disipación de energía en forma de calor, la detoxificación de las ROS, la regulación del volumen mitocondrial y en la muerte celular (Bernardi y Petronilli, 1996; Crompton y cols., 1999; DeJean y cols., 2000; Rostovtseva y cols., 2004). Diversos estudios sobre la sensibilidad del mPTP a iones inorgánicos como el Ca^{2+}, sugieren su participación en la homeostasis de este catión (Uribe-Carvajal y cols., 2011). Dicha regulación se involucra en la transducción de diversas señales, la importación de proteínas mitocondriales o la termogénesis producida por la disipación del gradiente de H^+ (Crompton y cols., 1987).

Hipotéticamente, estos canales se forman por la interacción de diversas proteínas en sitios específicos entre la MMI y la MME (Figura 3). Los componentes del canal en las mitocondrias de mamífero suelen tener otras funciones celulares; tal es el caso del canal aniónico dependiente de voltaje (VDAC), el acarreador de adenín nucleótidos (ANT), la ciclofilina D (Cyp-D) y el acarreador de fosfatos (PiC) (Manon y cols., 1998). La propuesta de que estas proteínas son parte del mPTP se debe a que la TPM es específicamente promovida o inhibida por diversas moléculas que interactúan con ellas (Figura 3A) (Halestrap, 1991; Baines y cols., 2005). El VDAC es un canal localizado en la MME que

permite el paso de iones, sustratos y moléculas pequeñas del citosol al espacio intermembranal. Se sugiere como una de las partes del canal debido a la sensibilidad de la TPM al voltaje en estudios *in vitro.* En estudios de cromatografía de afinidad (usando Cyp-D anclada), se retiene al VDAC, unido a su vez, con el ANT (Crompton y cols., 1998). El ANT se ubica en la MMI y tiene como función primordial internalizar ADP a la matriz y sacar el ATP sintetizado en la fosforilación oxidativa. Además, la TPM se inhibe con carboxiatractilósido; un inhibidor específico del translocador (Halestrap, 1991). La Cyp-D es una proteína matricial involucrada en el plegamiento de las proteínas que son importadas a este compartimento. Su participación en el mPTP se sugiere por la inhibición de la TPM por ciclosporina A (CsA). La CsA se une específicamente a la Cyp-D (Kroemer y cols., 1995). La sensibilidad de la TPM a la variación de la concentración de fosfato inorgánico sugiere que el PiC es otro componente del canal. Actualmente se cuenta con mayor evidencia que apoya la interacción de estas proteínas en mitocondrias de mamíferos (Leung y cols., 2008; Uribe-Carvajal y cols., 2011). Por otra parte, dependiendo del tipo de mitocondria y el organismo o tejido de donde se obtengan, se pueden asociar otras proteínas al mPTP, p. ej., la hexocinasa o la creatín cinasa (Manon y cols., 1998) (Figura 3A).

En estudios recientes se sugiere que los dímeros del complejo V forman canales y participan en la formación del mPTP (Bernardi, 2013). Una de las evidencias que sustentan lo anterior es la asociación de la Cyp-D con la subunidad OSCP del tallo periférico (Giorgio y cols., 2013). En este caso, al disminuir la cantidad de OSCP se observa una menor TPM inducida por Ca^{2+}, el cual es un potente activador del mPTP. Los autores consideran que al no ocurrir la interacción de la Cyp-D con OSCP, disminuye la probabilidad de que el mPTP se abra (Figura 3B panel a) y aumenta considerablemente la $[Ca^{2+}]$ requerida para que ocurra la TPM (Figura 3B panel c). En contraste, cuando ocurre la unión de la Cyp-D, la cual es favorecida por el Pi (Giorgio y cols., 2009) (Figura 3B panel b), incrementa la accesibilidad del Ca^{2+} a los sitios de unión a metales y permite la apertura del mPTP (Figura 3B panel d). La participación del complejo V en la TPM también se observa en *S. cerevisiae* (Carraro y cols., 2014) y *D. melanogaster* (von Stockum y cols., 2015).

De primera mano, se puede pensar que los modelos de la estructura del mPTP difieren; sin embargo, se sabe que tanto el ANT como el PiC se encuentran asociados con el complejo V formando el “sintasoma” (Chen y cols., 2004). Por tal motivo, no hay razón para eliminar aún la posibilidad de que todas las anteriores formen parte del mPTP.

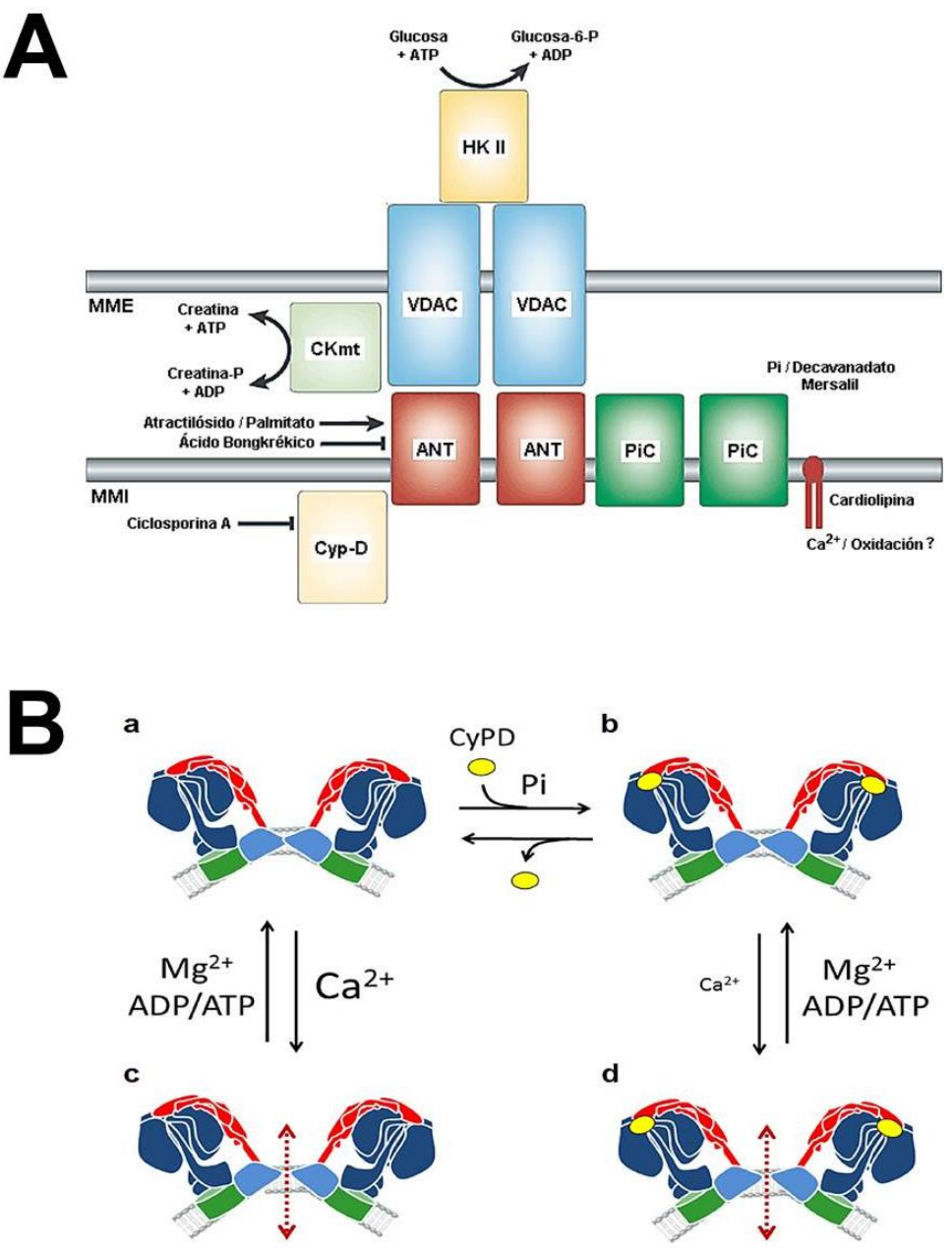

Figura 3. Estructuras hipotéticas del PTP de mamíferos. (A) La estructura mas aceptada del mPTP se compone principalmente del canal aniónico dependiente de voltaje (VDAC), el acarreador de adenín nucleotidos (ANT), el acarreador de fosfatos (PiC) y la ciclofilina-D (Cyp-D). En algunos casos se asocian la hexocinasa II (HK II) y la creatín cinasa mitocondrial (CKmt) con la estructura principal. En este panel, se muestran algunos de los iones y moléculas que promueven la apertura o el cierre del mPTP. Membrana mitocondrial interna (MMI) y externa (MME) **(B)** Estructura propuesta por el grupo de Bernardi en donde la F_1F_O-ATP sintasa en su forma dimérica constituye directamente el mPTP. El canal se cierra en ausencia de Ca^{2+} y Cyp-D (a). En esta condición, una elevada [Ca^{2+}] puede inducir la TPM (c). La presencia de Pi favorece la unión de la Cyp-D a la subunidad OSCP del tallo periférico (mostrada en rojo) (b) e induce la TPM a menor [Ca^{2+}] (d). Imagenes modificadas de Zamzami y Kroemer, 2001 (A) y Bernardi, 2013 (B).

En las mitocondrias de *S. cerevisiae*, también existe un canal inespecífico de alta conductancia: el YMUC, equivalente al mPTP (Jung y cols., 1997). La sensibilidad del YMUC es diferente a la descrita para el mPTP y no se cuenta con un modelo concertado de su estructura. Algunos estudios sugieren que la composición del YMUC es muy similar a la del mPTP con la diferencia de que en levaduras no se encuentra la Cyp-D (Manon y cols., 1998). En trabajos de nuestro grupo se describen la participación del VDAC (Gutiérrez-Aguilar y cols., 2007) y del PiC (Gutiérrez-Aguilar y cols., 2009) en la TPM de esta levadura, lo que sugiere que tanto el mPTP como el YMUC poseen una estructura altamente conservada (Uribe-Carvajal y cols., 2011).

La regulación de los canales inespecíficos varía de acuerdo con las características tanto del YMUC como del mPTP (Tabla A). Al comparar ambos poros se observa que son principalmente aniónicos y permiten el paso de moléculas de tamaño similar (Jung y cols., 1997; Manon y cols., 1998). Ambas estructuras atraviesan las MMI y MME, por lo que deben encontrarse en los sitios de contacto intermembranales (Uribe-Carvajal y cols., 2011). La apertura del mPTP se induce cuando aumenta la concentración de fosfato inorgánico y es inhibida por ATP, mientras que el YMUC se cierra en presencia de Pi y se abre con ATP (Manon y Guérin, 1997; Pérez-Vázquez y cols., 2003). Esto sugiere que la carga energética controla la apertura del canal (Wallace y cols., 1994). Al abrirse éste, se disipa el $\Delta\Psi$ y permite la aceleración del flujo de electrones y la disminución de ROS. Al igual que el Pi, otros aniones como son el arsenato, el sulfato (Cortés y cols., 2000), el propionato y el decavanadato (Manon y cols., 1998) son capaces de cerrar el YMUC. Ante esto, se plantea la existencia de sitios específicos de interacción en los componentes del poro (Gutierrez-Aguilar y cols., 2007; Uribe-Carvajal y cols., 2011).

En contraste con lo observado en el mPTP, el Ca^{2+} no es capaz de abrir el YMUC ni promover la TPM por sí solo (Jung y cols., 1997). Sin embargo, las mitocondrias de *S. cerevisiae* pueden ser capaces de llevar a cabo una TPM inducida por Ca^{2+}, cuando se agregan ionóforos como el ETH129 o la alameticina (Yamada y cols., 2009). En cambio, el Mg^{2+} es capaz de inhibir la transición de la permeabilidad en ambos poros (Bernardi y cols., 1994; Pérez-Vázquez y cols., 2003). Por otro lado, el carboxiatractilósido y el ácido bongkrékico cierran tanto el mPTP como el YMUC (Halestrap, 1991), al unirse específicamente al ANT (Halestrap y Brennerb, 2003). En estudios recientes, se ha observado que el mersalil es capaz de inducir el hinchamiento mitocondrial, posiblemente por

unirse al PiC e inducirle un cambio conformacional que permite su apertura (Gutiérrez-Aguilar y cols., 2009). Como se mencionó, la CsA inhibe el PTP a nivel de la Cyp-D (Baines y cols., 2005) pero no tiene actividad en el YMUC, probablemente porque en la levadura no se codifica esta proteína. Además, la hexil y octilguanidina cierran el YMUC a nivel del VDAC1 (Pérez-Vázquez y cols., 2003; Gutierrez-Aguilar y cols., 2007).

En las mitocondrias de *D. hansenii* ocurre una TPM modulada por la apertura y cierre de un MUC. En este caso el canal ($_{Dh}$MUC) es sensible a cambios en la concentración de diversos iones como el fosfato, el Ca^{2+}, el Mg^{2+} y particularmente, por los cationes monovalentes Na^{+} y K^{+} (Cabrera-Orefice y cols., 2010). Esta sensibilidad es atípica, ya que no se presenta en ninguna de las mitocondrias caracterizadas. Por esta razón, se propone que las mitocondrias de *D. hansenii* poseen capacidades de adaptación que les permiten por un lado, resistir la alta concentración de cationes monovalentes que ingresan al citosol y por otro, modular y optimizar su funcionamiento sólo en presencia de éstos (Sánchez y cols., 2008; Cabrera-Orefice y cols., 2010).

Tabla A. Principales efectores de los canales inespecíficos mitocondriales de mamífero (mPTP), *S. cerevisiae* (YMUC) y *D. hansenii* ($_{Dh}$MUC)

Efector	mPTP	YMUC	$_{Dh}$MUC
Fosfato	+	–	–
Ca^{2+}	+	–	–
Mg^{2+}	–	–	–
Na^{+}/K^{+}	×	×	–
ATP	–	+	+
Ciclosporina A	–	×	×
Ácido Bongkrékico	–	–	?
Alquil-guanidinas	–	–	?
Carboxiatractilósido	+	–	?
Decavanadato	+	–	–
Mersalil	+	+	+

*Simbología: abre el poro **(+)**; cierra el poro **(–)**; no tiene efecto **(x);** no se sabe el efecto **(?)**

1.5.2. Enzimas redox que no bombean protones

En las cadenas respiratorias ramificadas, además de la reacción llevada a cabo por el complejo I, la Q puede ser reducida por diferentes oxidorreductasas que no funcionan como bombas de protones. Ejemplos de éstas son el complejo II, las NDH2s (internas y externas), la dihidroorotato deshidrogenasa mitocondrial, la flavoproteína transferidora de electrones (ETF:ubiquinona oxidorreductasa) y la $_{Mit}$GPDH. Además, el ubiquinol puede ser oxidado por dos diferentes rutas: la vía citocrómica (III-cit *c*-IV) o por la vía alterna, que consta únicamente de la AOX. Producto de lo anterior, existen múltiples rutas de transporte de electrones desde los equivalentes reductores (p. ej. NADH, succinato, glicerol-fosfato) hasta el O_2.

En general, se proponen diversas funciones para los componentes alternos: a) disipar la energía en forma de calor; b) continuar con el transporte de electrones en condiciones de saturación del flujo (cuando hay elevado $\Delta\Psi$); c) consumir equivalentes reductores sin generar ATP (desacoplamiento fisiológico) y d) permitir el reciclaje de la poza de piridín nucleótidos y otros intermediarios para continuar con el ciclo de Krebs y otras vías asociadas a ésta (Lambers, 1982). Además, se sugiere que tienen un papel importante sobre la prevención de la formación de ROS (Popov y cols. 1997) y en la regulación del estado redox del citosol.

La estequiometría del bombeo de protones acoplado a la transferencia de electrones depende del número de bombas que intervienen en cada ruta (Figura 4). Por tal motivo, el número de protones bombeados por par de electrones puede variar de 10 $H^+/2e^-$ (cuando se utilizan los complejos I, III y IV) (Figura 4A) a cero (Figura 4E). Esto último en el caso de que el QH_2 se genere por las NDH2i o el complejo II y se oxide por la AOX. Por ende, en estas reacciones redox no hay cambios en el gradiente electroquímico de protones. En el caso de las mitocondrias aisladas puede disminuir hasta -1 $H^+/2e^-$ (Guerrero-Castillo y cols., 2011). Esto último se da en el caso de que los electrones sean transferidos del NADH al oxígeno por medio de la NDH2e y la AOX (Figura 4F). Esto se debe a que la flavina de la NDH2e recibe un anión hidruro del NADH, el cual es transferido a la ubiquinona para generar la especie QH^- (ubiquinol desprotonado). Esta especie capta un protón del espacio intermembranal para formar QH_2. Al ser oxidado el ubiquinol por la AOX, los protones son liberados hacia la matriz o utilizados en la formación de agua a partir de oxígeno. Como

resultado neto, un protón desaparece del espacio intermembranal, y disminuye así el gradiente electroquímico de protones.

Cuando los complejos III y IV son las únicas bombas de protones involucradas (Figura 4B y C) se espera que el número de protones bombeados sea el mismo (6 $H^+/2e^-$). No obstante, en mitocondrias aisladas un protón del espacio intermembranal es utilizado para la reducción de la Q a QH_2 y, posteriormente, el complejo III lo regresa al mismo espacio. En este caso no se puede considerar como bombeado y el cociente disminuye a 5 $H^+/2e^-$ (Guerrero-Castillo y cols. 2011).

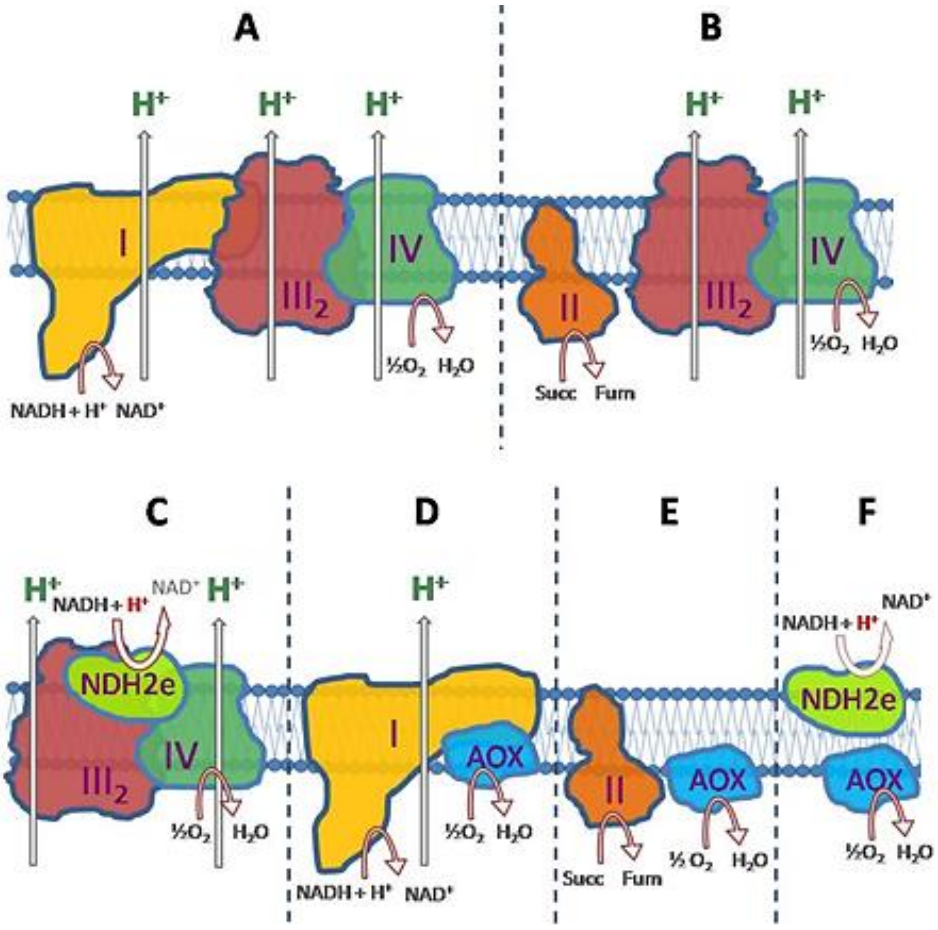

Figura 4. Diferencias en el número de bombas de protones que participan en el transporte de electrones de las cadenas respiratorias ramificadas. (A) Al tener las tres bombas activas se transportan 10 $H^+/2e^-$ al espacio intermembranal. (**B)** Dos bombas activas, 6 $H^+/2e^-$. (**C)** Dos bombas activas, 5 $H^+/2e^-$. (**D)** Una bomba activa, 4 $H^+/2e^-$; (**E)** cero bombas, 0 $H^+/2e^-$; (**F)** cero bombas, -1 $H^+/2e^-$. I, II, III_2 y IV: complejos respiratorios "clásicos"; NDH2e: NADH deshidrogenasa alterna externa; AOX: oxidasa alterna. Imagen modificada de Guerrero-Castillo y cols., 2011.

2. PLANTEAMIENTO DEL PROBLEMA

Debaryomyces hansenii contiene dos posibles mecanismos de desacoplamiento fisiológicos de la fosforilación oxidativa: a) el canal inespecífico mitocondrial ($_{Dh}$MUC) y b) la cadena respiratoria ramificada. Ambos se describen únicamente en mitocondrias aisladas de células cosechadas en la fase exponencial de crecimiento (Cabrera-Orefice y cols., 2010; 2014). En ésta, los requerimientos energéticos celulares son elevados, por lo que el flujo de electrones debe ocurrir preferencialmente a través de la vía citocrómica. Lo anterior debe ocurrir para garantizar la mayor eficiencia de la fosforilación oxidativa posible (en términos de ATP producido por par de electrones transferidos al O_2) (Guerrero-Castillo y cols., 2012). En dicho escenario deben evitarse la transferencia de electrones por las oxidorreductasas alternas y/o que el $_{Dh}$MUC se abra y se pierda el $\Delta\Psi$. Sin embargo, cuando las necesidades energéticas disminuyen (p. ej. en la fase estacionaria de crecimiento), la activación de estos sistema de desacoplamiento resultan más útiles.

En primer lugar, la posibilidad de enviar electrones al oxígeno por la vía alterna (no acoplada con el bombeo de protones ni la síntesis del ATP) establece un consumo de oxígeno constante que evita la acumulación de acarreadores reducidos (NADH, $FADH_2$, QH_2, etc.) y de la semiquinona que puede generar anión superóxido (Guerrero-Castillo y cols., 2011). En *D. hansenii*, el antecedente más importante que sugiere que hay diferencias a nivel de la cadena respiratoria ramificada entre diferentes fases de crecimiento es que la respiración resistente a cianuro se manifiesta únicamente en la fase estacionaria (en medio fermentable, YPD-Na^+) (Veiga y cols., 2003b).

En segundo lugar, la apertura del $_{Dh}$MUC abate el $\Delta\Psi$ y ocasiona que el consumo de oxígeno se mantenga alto gracias a que las bombas trabajan más rápido y desacopladas de la síntesis del ATP. Paradójicamente, no se cuenta con estudios reportados que describan el funcionamiento del MUC en situaciones de baja demanda energética.

Por estas razones, resulta interesante estudiar la fosforilación oxidativa de esta levadura en la fase estacionaria de crecimiento y describir la participación de los dos sistemas de desacoplamiento en esta condición.

3. HIPÓTESIS

Los sistemas de desacoplamiento fisiológico de la fosforilación oxidativa de *D. hansenii* deben activarse en la fase estacionaria de crecimiento.

4. OBJETIVOS

4.1. Objetivo General

Caracterizar la fosforilación oxidativa y los sistemas de desacoplamiento fisiológicos mitocondriales de *D. hansenii* en distintas fases de crecimiento.

4.2. Objetivos Particulares

- Determinar el consumo de oxígeno y el acoplamiento respiratorio en mitocondrias aisladas de *D. hansenii* en diferentes fases y tiempos de crecimiento.
- Comparar la actividad respiratoria de mitocondrias aisladas de células cultivadas en fuente de carbono fermentable y no fermentable.
- Determinar la respiración resistente a cianuro en mitocondrias aisladas de células cultivadas en diferentes fases de crecimiento y fuentes de carbono.
- Caracterizar la transición de la permeabilidad en mitocondrias aisladas de células cultivadas hasta la fase estacionaria de crecimiento.

5. MATERIALES Y MÉTODOS

5.1. Materiales químicos

Todos los materiales químicos que se utilizan son de la más alta pureza asequible comercialmente. Los materiales para realizar los ensayos experimentales, como D-sorbitol, D-glucosa, D-galactosa, Trizma® base (Tris), antiespumante A, ácido málico, ácido pirúvico, ácido succínico, ácido maléico, DL-α-glicerofosfato, ditionita de sodio, ADP, NADH, NAD^+, rotenona, batofenantrolina, piridoxal-5'-fosfato, púrpura de bromocresol, β-mercaptoetanol, EGTA, nistatina, *n*-dodecil β-D-maltósido (LM), cloruro de nitrotetrazolio azul (NTB), CCCP, safranina-O son de Sigma Chem Co. (St. Louis, MO, EUA). La diaminobencidina (tetracloruro hidrato) es de Fluka. La Probulmin™ (albúmina sérica bovina, BSA) es de Millipore (Billerica, MA, EUA). La bacto-peptona y el extracto de levadura, son de BD Bioxon (Franklin Lakes, NJ, EUA). El NaCl, KCl, $MgCl_2$, NaCN, ácido fosfórico, ferricianuro de potasio y el ácido DL-láctico son de J.T. Baker (Center Valley, PA, EUA). La zimoliasa 20 T es de Seigaku Corp. (Tokio, Japón). El azul de Coomassie G es de SERVA (Heidelberg, Alemania). La acrilamida, el azul de Coomassie® brillante G-250 y todos los reactivos utilizados para electroforesis son de BIO-RAD (Richmond, CA, EUA).

5.2. Materiales biológicos

Se utilizó la cepa Y7426 de *Debaryomyces hansenii* (US Department of Agriculture, Peoria, IL). Ésta se mantuvo en cajas de cultivo con medio sólido YPGal–NaCl (extracto de levadura 1%, bacto-peptona 2%, galactosa 2%, NaCl 1 M y bacto-agar 2%) a 4 °C.

5.3. Cultivo de las levaduras

Se emplearon como medios de crecimiento el YPLac–NaCl (extracto de levadura 1%, bacto-peptona 2%, lactato 2% y NaCl 0.6 M, pH 5.5) y el YPD-NaCl (extracto de levadura 1%, bacto-peptona 2%, dextrosa 2% y NaCl 0.6 M). Para obtener una biomasa suficiente de levadura, se inocularon tres precultivos de 100 mL del medio líquido (YPD-NaCl o YPD-NaCl) y se colocaron en agitación continua a 250 rpm durante 24 hrs en un cuarto de temperatura constante (~30°C). Posteriormente, los precultivos se vaciaron en matraces con 750 mL del mismo medio y se continuó la incubación bajo las mismas condiciones hasta llegar a las 15, 20, 24, 48, 72 y 96 hrs (en YPLac-NaCl) o 12, 18, 22, 48, 72 y 96 hrs (en YPD-NaCl).

5.4. Aislamiento de las mitocondrias

Las células se cosechan por centrifugación y se lavan con agua bidestilada. A continuación, se resuspenden en el medio de aislamiento (D-sorbitol 1 M, Tris-maleato 10 mM y BSA 0.2%, pH 6.8) y se mantienen en hielo durante diez minutos. Para la obtención de las mitocondrias, se homogenizan las células con perlas de vidrio (0.5 mm de diámetro). La levadura resuspendida se vacía en una cámara del "bead-beater" (Biospec products, EUA) enfriada con hielo durante media hora y se somete a cuatro ciclos de ruptura de 20 seg con intervalos de 2 min de reposo entre cada ciclo. Después de la homogeneización, las mitocondrias se aislan por centrifugación diferencial a 4°C (Cabrera-Orefice y cols., 2010), en una centrífuga Sorvall RC-5B y rotores FIBERlite® *F21-8x50y* y *F14-6x250y*. El primer homogenado se centrifuga a 5000 rpm durante 5 min; se recupera el sobrenadante y se centrifuga a 12,000 rpm durante 15 min. El paquete obtenido se resuspende en medio de aislamiento fresco con un pincel fino y a continuación se centrifuga nuevamente según lo descrito arriba. El paquete mitocondrial final se resuspende en 500 µL del medio de aislamiento a 4°C y se mantiene en hielo durante la cuantificación de proteína y los experimentos.

5.5. Obtención de esferoplastos permeabilizados

Los esferoplastos de *D. hansenii* se generaron a partir de un protocolo desarrollado para *S. cerevisiae* (Avéret y cols., 1998) con algunas modificaciones. Las células se cultivan hasta la fase exponencial (24 hrs) o estacionaria (96 hrs) en YPLac-NaCl. Posteriormente, se cosechan por centrifugación (5000 rpm, 5 min), se lavan con agua bidestilada y se vuelven a centrifugar. El paquete de células se resuspende en amortiguador SH (β-mercaptoetanol 0.5 M, Tris 0.1 M, pH 9.3) y se incuba durante 10 minutos a 30°C. Las células se centrifugan y se lavan dos veces con medio de lavado (KCl 0.5 M, Tris 10 mM, pH 7). A continuación, las células se resuspenden en medio de digestión (Sorbitol 1.35 M, EGTA 1 mM, fosfatos 0.2 M, pH 7.4) y se agrega zimoliasa 20 T (5 mg/g peso seco) para romper la pared. La progresión de la digestión se monitorea espectrofotométricamente a 600 nm y se detiene cuando la turbidez de la muestra diluida en agua bidestilada (1:10) disminuye al valor que tiene una dilución 1:100 del control (sin enzima). Los esferoplastos resultantes se centrifugan (2500 rpm, 5 min) y se lavan tres veces con el amortiguador de protoplastos (sorbitol 1.2 M, Tris-maleato 10 mM, pH 6.8) y el paquete final se resuspende en amortiguador de esferoplastos

(sorbitol 1 M, KCl 75 mM, $MgCl_2$ 5 mM, EGTA 0.5 mM, Tris-fosfato 20 mM, Tris-maleato 10 mM, BSA 0.2%, pH 6.8). Para permeabilizar se adiciona nistatina (20 μg/mL) a una suspensión de esferoplastos (1 mgProt/mL) y se burbujea aire a la solución durante 10 minutos para consumir los sustratos respiratorios endógenos.

5.6. Cuantificación de proteína

La concentración de proteína se determina por el método de Biuret (Gornal *et al.*, 1949) en un espectrofotómetro Beckman DU-50 a 540 nm. A 2 mL del reactivo de Biuret (que contiene $CuSO_4$) se le añaden 125 μL de desoxicolato de sodio al 5%, 350 μl de agua destilada y 25 μl de la suspensión de mitocondrias o esferoplastos. La interacción del ión Cu^{2+} con los enlaces peptídicos genera una coloración violeta cuya absorbencia es proporcional a la concentración de proteína de la muestra. Se emplea BSA para realizar la curva estándar.

5.7. Consumo de oxígeno y acoplamiento respiratorio

La velocidad del consumo de oxígeno en mitocondrias aisladas se determina en estado de reposo (edo. IV, en presencia de un sustrato oxidable y sin ADP) y en estado fosforilante (edo. III, en presencia de un sustrato oxidable y ADP) con un electrodo tipo Clark conectado a un oxímetro Strathkelvin Instruments® modelo 782 (North Lanarkshire, Escocia) acoplado a una computadora para el registro de los datos. La cámara de reacción (vol. final 1 mL) se mantiene a 30°C. Como medio de respiración se utiliza una solución de sorbitol desionizado 1 M, Tris-maleato 10 mM (pH 6.8), Tris-fosfato 10 mM, KCl 75 mM y $MgCl_2$ 1 mM. Como sustratos respiratorios se utilizan piruvato 10 mM - malato 10 mM, succinato 10 mM, glicerol-fosfato 10 mM o NADH 1 mM, según el ensayo. La concentración de fosfato, Mg^{2+} y K^+ se modulan para abrir o cerrar el MUC (Cabrera-Orefice y cols., 2010). Para inducir el estado fosforilante (III) se agrega a la mezcla de reacción 500 μM de ADP. Los valores del control respiratorio (CR) se obtienen al dividir el valor del consumo de O_2 en estado III sobre el del estado IV. Se utiliza una concentración final de proteína mitocondrial o de esferoplastos de 0.5 ó 1 mg/mL, respectivamente. Para inhibir específicamente a los componentes de la cadena respiratoria se agregan distintos inhibidores como son rotenona, flavona, antimicina A, cianuro y propil-galato (Cabrera-Orefice y cols., 2014). Las concentraciones de los sustratos e inhibidores se muestran debajo de cada figura.

5.8. Electroforesis nativa azul (BN-PAGE) y actividades en gel.

La separación de los complejos respiratorios se realiza mediante electroforesis nativa azul (BN-PAGE) (Schägger y von Jagow, 1991; Wittig y cols., 2006). Para esto, la preparación mitocondrial se resuspende en un amortiguador de ácido aminocaproico 750 mM e imidazol 25 mM (pH 7.0) y se solubiliza con lauril-maltósido (LM) en una relación de 2 mg/mg Prot. Después, se ultracentrifugan las muestras a 33,000 rpm durante 20 min a 4°C. A los sobrenadantes se les agrega azul de Coomassie 5% (10 μL/mgProt) y se cargan en geles de gradiente de poliacrilamida (4-12 %) y se corre la electroforesis a un amperaje constante de 30 mA/gel aprox. tres horas a 4°C. La poliacrilamida del gel concentrador se encuentra al 4%. En el caso de los geles BN, primero se utiliza el amortiguador del cátodo 1 (Tricina 50 mM, imidazol 7.5 mM, azul de Coomassie G Serva 0.02 %) hasta un tercio del gel; para los dos tercios siguientes es necesario cambiar al amortiguador del cátodo 2 (Tricina 50 mM, imidazol 7.5 mM, azul de Coomassie G Serva 0.002 %). En cada carril se cargan 0.5 mgProt para geles grandes (17x12 cm). Al finalizar la corrida electroforética, los geles se deben incubar en el amortiguador de la actividad que se desea revelar o bien teñirse con azul de Coomassie® brillante G-250 para incrementar la definición de las bandas de proteína.

Para determinar la actividad de NADH deshidrogenasa (NDH) se incuba al gel BN en una solución que contiene Tris 10 mM (pH 7.0), 0.5 mg de cloruro de nitrotetrazolio azul (NTB)/mL y NADH 1 mM (Vol. final 50 mL). Normalmente, la tinción de NDH se revela entre 15 y 30 min como un precipitado de color morado. En esta reacción, el NADH puede oxidarse por la flavina del complejo I, NDH2 y otras deshidrogenasas dependientes de NAD^+; esta última reduce directamente al NTB.

Por otro lado, para determinar la actividad de citocromo *c* oxidasa (COX) el gel BN se incuba en un amortiguador de fosfatos de sodio 50 mM (pH 7.4), 10 mg de citocromo *c* y 20 mg de diaminobencidina. La actividad de COX se revela entre 30 min y 2 hrs como un precipitado de color café oscuro. Esta tinción es específica para el complejo IV, aunque si se realiza en ausencia del citocromo *c* puede revelarse con menor sensibilidad la actividad de otras proteínas que contienen citocromos (p. ej. complejo III) (Wittig y cols., 2007).

5.9. Contenido de citocromos

Se determinan mediante la obtención de espectros diferenciales. Primero, se obtienen los espectros oxidados con mitocondrias solubilizadas con LM agregando ferricianuro de

potasio 0.25 mg/mL a la celda de reacción. Estos espectros se asignan como líneas basales. Después, se agrega ditionita de sodio en las mismas celdas para obtener los espectros reducidos. El barrido se realiza de 500 a 675 nm en un espectrofotómetro AMINCO DW2000. Se utiliza una concentración de 5 mg/mL. Se pueden utilizar mitocondrias aisladas directamente para estos ensayos; sin embargo la solubilización con LM incrementa la señal de los citocromos y además disminuye el ruido durante las lecturas. El contenido de citocromos por mgProt se calcula con los siguientes valores de los coeficientes de extinción molar: $\Delta\varepsilon_{605-630}$ = 16.5 mM^{-1} cm^{-1} (citocromos a+a_3); $\Delta\varepsilon_{563-577}$ = 28 mM^{-1} cm^{-1} (citocromo b) y $\Delta\varepsilon_{553-539}$ = 19.1 mM^{-1} cm^{-1} (citocromos c+c_1) (Yonetani y cols., 1960; Berden y Slatter, 1970).

5.10. Actividad enzimática de las deshidrogenasas dependientes de NAD^+

Para determinar la actividad de la piruvato deshidrogenasa (PDH) y malato deshidrogenasa (MDH), enzimas del ciclo de Krebs, se utiliza el protocolo descrito por Cooney y cols. (1981) La generación de NADH se sigue espectrofotométricamente a 340 nm a temperatura ambiente. Para iniciar la reacción se adiciona piruvato 10 mM o malato 10 mM, respectivamente. En cada caso, se determinan las actividades en condiciones de sustrato saturantes y en presencia de NAD^+ 1 mM para las dos enzimas. La concentración de proteína mitocondrial que se usa es de 0.5 mg/mL. Mezcla de reacción: Sorbitol 1 M, Tris-maleato 10 mM (pH 6.8), Triton X-100 0.05%. El Triton X-100 se agrega para permeabilizar las mitocondrias. Sólo para medir la PDH se agrega a la mezcla de reacción Coenzima A 0.63 mM, pirofosfato de tiamina 1 mM y ditiotreitol 1 mM. Para prevenir la reoxidación del NADH matricial se agrega rotenona 50 μM para inhibir al complejo I. Las líneas basales se obtienen en ausencia de sustratos y el valor de sus pendientes se resta en cada caso. El coeficiente de extinción molar del NADH que se utiliza es de 6.22 x 10^3 $(M\ cm)^{-1}$.

5.11. Potencial transmembranal ($\Delta\Psi$)

El potencial transmembranal se determina con el colorante catiónico naranja de safranina (safranine-O). Esta molécula interactúa con la membrana mitocondrial cuando se genera el $\Delta\Psi$ (negativo al interior), cambiando de color. Los cambios se determinan a 511-533 nm en un espectrofotómetro Aminco DW 2000 en modo dual a temperatura ambiente. En este caso, la absorbencia aumenta cuando hay un incremento en el $\Delta\Psi$ (Akerman y Wikström, 1976). Para estos ensayos se emplean las mismas condiciones y medio de

respiración que en las oximetrías; sólo se agrega naranja de safranina 10 µM a la celda de reacción. Se utiliza una concentración final de proteína mitocondrial de 0.5 mg/mL. Para abatir el $\Delta\Psi$, se agrega a la celda de reacción el protonóforo *p*-clorocarbonilcianuro fenilhidrazona (CCCP) 5 µM.

5.12. Búsqueda, alineamiento y análisis de secuencias de proteínas

El genoma de *D. hansenii* se encuentra completamente secuenciado (Dujon y cols., 2004; Sherman y cols., 2009) y disponible en la base de datos del Centro Nacional de Información Biotecnológica (NCBI por sus siglas en inglés *National Center for Biotechnology Information*). Para buscar y comparar secuencias proteicas de diferentes especies se utiliza la interfaz web de la Herramienta Básica de Búsquedas de Alineamientos Locales (BLAST por sus siglas en inglés *Basic Local Alignment Search Tool*). Las secuencias de aminoácidos candidatas de *D. hansenii*, se alinean por pares y de manera simultánea con las de otras levaduras como *S. cerevisiae* y *Y. lipolytica*. Además, con esta herramienta se obtienen los porcentajes de identidad y similitud y otros parámetros de la comparación entre las secuencias de aminoácidos analizadas.

6. RESULTADOS

Hasta este momento, la fosforilación oxidativa de *D. hansenii* se estudió únicamente en mitocondrias aisladas de células cultivadas hasta la fase exponencial tardía (24 hrs). En dichas muestras se encontraron dos posibles mecanismos de desacoplamiento fisiológicos: *a)* la presencia de enzimas alternas que no bombean protones y *b)* el $_{Dh}$MUC. En condiciones experimentales óptimas, es decir, en presencia de sustratos respiratorios, fosfato, K^+ y Mg^{2+}, las mitocondrias aisladas presentan acoplamiento respiratorio, sintetizan ATP y generan un $\Delta\Psi$ elevado (Cabrera-Orefice y cols., 2010). Sin embargo, en esta fase de crecimiento, donde los requerimientos energéticos celulares son elevados, los sistemas de desacoplamiento deben encontrarse inactivos para evitar pérdidas de energía. Por tal motivo, se sugiere que estos mecanismos ofrecen una mayor utilidad en condiciones de baja demanda energética; por ejemplo, en la fase estacionaria de crecimiento (Guerrero-Castillo y cols., 2011). Con esto en mente, se caracterizó la fosforilación oxidativa y los dos posibles mecanismos de desacoplamiento fisiológicos en la fase estacionaria de crecimiento de esta levadura.

6.1. En D. hansenii, la respiración resistente a cianuro depende de la fase de crecimiento y de la fuente de carbono del medio.

La respiración resistente a cianuro (RRC) se presenta en especies que expresan a la oxidasa alterna (AOX) (Veiga y cols., 2000). Previamente, Veiga y cols. (2003c), encontraron este fenómeno únicamente en células completas de *D. hansenii* en la fase estacionaria de crecimiento. Además, reportaron la existencia del gen de la AOX en esta levadura. Sin embargo, en estudios recientes de nuestro grupo, se demuestra la presencia de RRC en mitocondrias aisladas de *D. hansenii* obtenidas de cultivos cosechados en la fase exponencial (Cabrera-Orefice y cols., 2010). Ésto nos llamó mucho la atención porque contrasta con lo reportado por Veiga y cols. (2003c), quienes no observaron RRC en dicha fase. Cabe señalar que dicho estudio se realizó en células cultivadas en YPD-NaCl (medio fermentable); mientras que nosotros utilizamos el YPLac-NaCl (medio no fermentable). Este último se utiliza para obtener una mayor cantidad de biomasa mitocondrial (Cabrera-Orefice y cols., 2010). Con base en lo anterior, se estudió la RRC en mitocondrias aisladas de células de *D. hansenii* cultivadas en ambos medios y en diferentes fases de crecimiento.

Se determinó la actividad de la AOX y su activación por AMP (Cabrera-Orefice y cols., 2014) en diferentes tiempos de cultivo con ensayos de consumo de oxígeno. Se aislaron las mitocondrias de células cultivadas en YPLac-NaCl y cosechadas a las 15, 20, 24, 48, 72 y 96 hrs; y cultivadas en YPD-NaCl y cosechadas a las 12, 18, 22, 48, 72 y 96 hrs. Los primeros tres tiempos de cultivo corresponden a la fase exponencial de crecimiento y los tres últimos a la fase estacionaria de crecimiento en cada medio. La diferencia de horas de cultivo en la fase exponencial se debe a que en YPD-NaCl el tiempo de duplicación es menor. Las medias logarítmicas en YPLac-NaCl y YPD-NaCl son 20 y 18 hrs, respectivamente. La actividad respiratoria se determinó antes y después de agregar NaCN 500 μM (para inducir la RRC) y en presencia de succinato 10 mM como sustrato respiratorio. En todos los casos, se agregaron las concentraciones de iones inorgánicos ideales para inhibir la TPM (Tris-fosfato 10 mM, $MgCl_2$ 1 mM y KCl 75 mM) (Cabrera-Orefice y cols., 2010).

En el caso de las muestras obtenidas de YPLac-NaCl, la RRC fue de ~20-25% del total de la actividad respiratoria en todos los tiempos de cultivo (Figura 5A, círculos negros). Además, estos ensayos se realizaron en ausencia y presencia de AMP 1 mM para observar la activación de la AOX en cada fase (Figura 5A, círculos vacíos). En cada caso, la RRC aumentó en ~13-15% y no encontramos diferencias significativas entre los tiempos de cultivo.

En contraste, en las muestras obtenidas de YPD-NaCl, no se observó RRC a 12 hrs de cultivo, ésta apareció en menor valor a las 18 hrs (~13%) y alcanzó su valor máximo a partir de las 22 hrs (~25%) (Figura 5B, círculos vacíos). Este último no aumentó en las muestras de la fase estacionaria (48, 72 y 96 hrs). La adición de AMP 1 mM no mostró efecto a las 12 hrs, lo que confirmó que la AOX no está presente aún (Figura 5B, círculos vacíos). A las 18 hrs, el AMP promovió una pequeña activación de ~5% (Figura 5B, círculos vacíos). La máxima activación se observó en las muestras de 22, 48, 72 y 96 hrs, en donde tuvo un valor de ~15% (Figura 5B, círculos vacíos).

Este resultado es interesante debido a que se observó un efecto de la fuente de carbono sobre la expresión de la AOX. Estos datos sugirieron que la expresión de esta proteína no necesariamente depende de la fase de crecimiento, como lo postulan Veiga y cols., (2003c). Cuando se utilizó dextrosa como fuente de carbono, la RRC máxima se obtuvo en la fase exponencial tardía (22 hrs), mientras que en presencia de lactato, ésta se encontró presente en ambas fases de crecimiento.

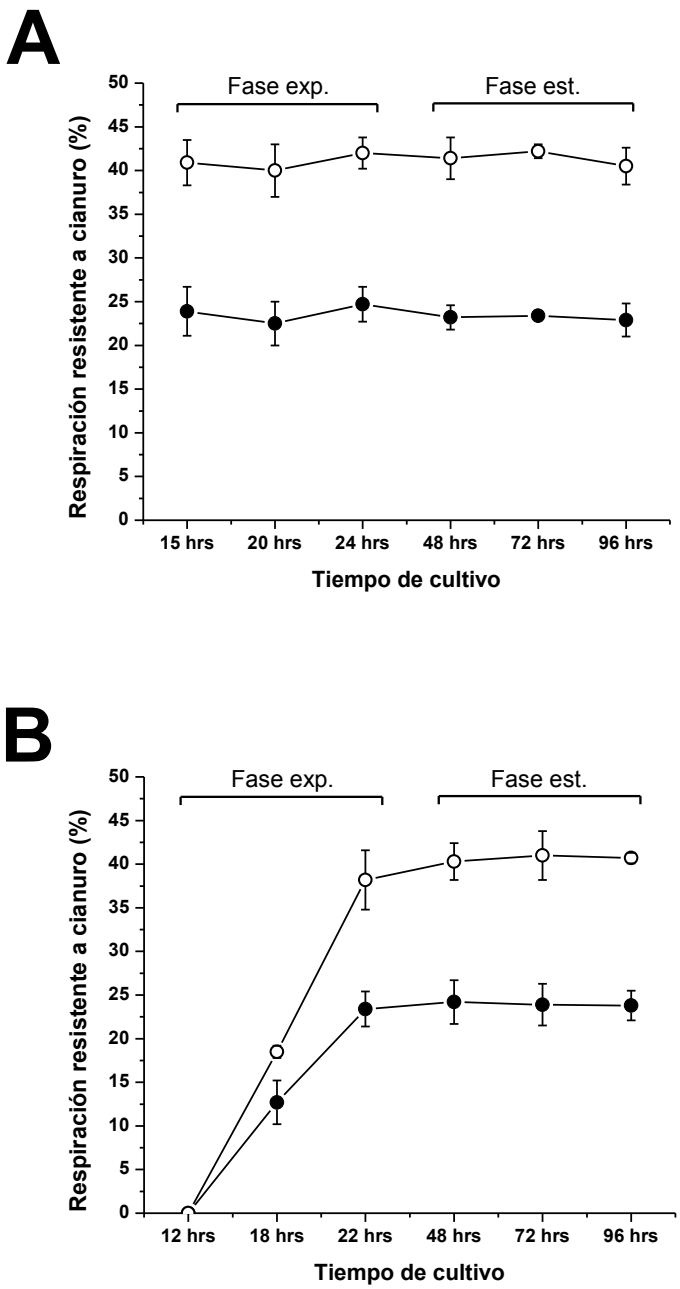

Figura 5. Respiración resistente a cianuro (RRC) en mitocondrias aisladas de *D. hansenii* en diferentes fases de crecimiento y tiempos de cultivo. El consumo de oxígeno se determinó en estado IV (no fosforilante) con succinato 10 mM como sustrato respiratorio. Se agregó NaCN 500 μM para promover la RRC. Los porcentajes de la RRC de muestras de fase exponencial (exp.) y fase estacionaria (est.) obtenidas de células cultivadas en **(A)** YPLac-NaCl o **(B)** YPD-NaCl a diferentes tiempos de cultivo se muestran en círculos rellenos (●). Los porcentajes de la RRC en presencia de AMP 1 mM se muestran en círculos vacíos (○). Mezcla de reacción: Sorbitol 1 M, Tris-maleato 10 mM (pH 6.8), KCl 75 mM, Tris-fosfato 10 mM, $MgCl_2$ 1 mM (vol. final 1 mL; temperatura 30 °C). Datos de tres experimentos independientes (promedio ± D.E.).

6.2. En D. hansenii, la actividad respiratoria dependiente del complejo I disminuye en la fase estacionaria de crecimiento.

Los datos anteriores dieron la pauta para estudiar si otros componentes de la cadena respiratoria ramificada de *D. hansenii* cambian su expresión o actividad en la fase estacionaria. Se aislaron mitocondrias de células cultivadas a diferentes tiempos en YPLac-NaCl (15, 20, 24, 48, 72 y 96 hrs) o YPD-NaCl (12, 18, 22, 48, 72 y 96 hrs). Se determinó el consumo de oxígeno en estado III y IV de las diferentes preparaciones mitocondriales (Tabla B y C) con cuatro sustratos diferentes: piruvato-malato 10 mM, succinato 10 mM, NADH 1 mM y glicerol-fosfato 10 mM. Se agregó rotenona 50 μM al utilizar los tres últimos sustratos para inhibir al complejo I. En todos los casos, se agregaron las concentraciones de iones inorgánicos ideales para inhibir la TPM (fosfato 10 mM, $MgCl_2$ 1 mM y KCl 75 mM) (Cabrera-Orefice y cols., 2010).

En presencia de la mayoría de los sustratos respiratorios (succinato, NADH y glicerol-fosfato), las velocidades de consumo de oxígeno en la fase exponencial no mostraron cambios significativos, mientras que en la fase estacionaria aumentaron ligeramente (Tablas B y C). Además, con estos tres sustratos, los controles respiratorios (CRs) no cambiaron significativamente entres los tiempos de cultivo (Tablas B y C). Por otro lado, en presencia de piruvato-malato, las muestras de la fase exponencial presentaron el máximo acoplamiento respiratorio; CR 2.33 ± 0.03 y 2.2 ± 0.13, en YPLac-NaCl y YPD-NaCl, respectivamente (Figura 6). Con el mismo sustrato, se observó una disminución considerable en el consumo de oxígeno (Tablas B y C) y el acoplamiento respiratorio (Figura 6) de las preparaciones obtenidas de ambos medios en la fase estacionaria (48, 72 y 96 hrs). Los CRs disminuyeron a 1.27 ± 0.05 y 1.25 ± 0.11, en YPLac-NaCl y YPD-NaCl, respectivamente (Figura 6). Las velocidades de consumo de oxígeno en estado III y IV disminuyeron a valores que corresponden aproximadamente al 15-20% de las que se registraron en la fase exponencial (Tablas B y C). Durante la transición de la fase exponencial a la estacionaria, el consumo de oxígeno y el acoplamiento respiratorio disminuyeron únicamente en presencia de sustratos que alimentan al complejo I. Por el contrario, no se observaron cambios en estos parámetros cuando los sustratos donan electrones al complejo II, a la NDH2e o a la $_{Mit}$GPDH. Esto sugiere un posible cambio a nivel del complejo I, lo cual se describe en la siguiente sección. Asimismo, no se observaron cambios promovidos por la fuente de carbono. Por esta razón para los siguientes experimentos se utilizó sólo el YPLac-NaCl como medio de cultivo.

Tabla B. Velocidades de consumo de oxígeno de mitocondrias aisladas de células de *D. hansenii* cultivadas en YPLac-NaCl por diferentes tiempos.

Sustrato	Tiempo de cultivo (hrs)	Velocidad de consumo de O_2 (natgO·(min·mgProt)$^{-1}$)		Control respiratorio (III/IV)
		Estado IV*	Estado III**	
Piruvato + malato	15	115 ± 14	248 ± 10	2.16 ± 0.09
	20	116 ± 11	262 ± 14	2.25 ± 0.08
	24	120 ± 10	279 ± 12	2.33 ± 0.07
	48	74 ± 8	152 ± 7	2.04 ± 0.05
	72	42 ± 5	59 ± 10	1.41 ± 0.06
	96	22 ± 7	28 ± 8	1.27 ± 0.05
Succinato	15	165 ± 14	280 ± 10	1.69 ± 0.10
	20	176 ± 11	282 ± 5	1.60 ± 0.08
	24	173 ± 15	285 ± 17	1.64 ± 0.10
	48	187 ± 6	284 ± 15	1.52 ± 0.10
	72	219 ± 12	379 ± 10	1.73 ± 0.11
	96	222 ± 8	382 ± 4	1.72 ± 0.05
NADH	15	225 ± 14	279 ± 15	1.24 ± 0.15
	20	235 ± 16	285 ± 13	1.21 ± 0.14
	24	228 ± 5	289 ± 13	1.26 ± 0.04
	48	237 ± 12	293 ± 10	1.24 ± 0.08
	72	283 ± 4	365 ± 9	1.29 ± 0.06
	96	326 ± 7	395 ± 4	1.21 ± 0.03
Glicerol-fosfato	15	211 ± 12	267 ± 11	1.27 ± 0.10
	20	215 ± 8	276 ± 15	1.28 ± 0.09
	24	218 ± 6	279 ± 13	1.28 ± 0.09
	48	232 ± 8	290 ± 12	1.25 ± 0.01
	72	266 ± 14	342 ± 10	1.29 ± 0.12
	96	300 ± 16	351 ± 15	1.17 ± 0.13

Las velocidades de consumo de oxígeno se midieron en estado de reposo (IV)* y estado fosforilante (III)**. El estado III se indujo al agregar ADP 500 μM. Muestras de fase exponencial: 15, 20 y 24 hrs; muestras de fase estacionaria: 48, 72 and 96 hrs. Las concentraciones de los sustratos respiratorios fueron: piruvato + malato 10 mM; succinato 10 mM; NADH 1 mM y glicerol-fosfato 10 mM. Mezcla de reacción igual a la de la Figura 5. Datos de tres experimentos independientes (promedio ± D.E.).

Tabla C. Velocidades de consumo de oxígeno de mitocondrias aisladas de células de *D. hansenii* cultivadas en YPD-NaCl por diferentes tiempos.

Sustrato	Tiempo de cultivo (hrs)	Velocidad de consumo de O_2 (natgO·(min·mgProt)$^{-1}$)		Control respiratorio (III/IV)
		Estado IV*	Estado III**	
Piruvato + malato	12	127 ± 12	250 ± 14	1.97 ± 0.12
	18	123 ± 13	270 ± 15	2.19 ± 0.11
	22	125 ± 15	275 ± 17	2.20 ± 0.13
	48	78 ± 15	149 ± 17	1.91 ± 0.12
	72	45 ± 14	65 ± 16	1.44 ± 0.10
	96	28 ± 17	35 ± 18	1.25 ± 0.11
Succinato	12	166 ± 10	275 ± 18	1.65 ± 0.13
	18	174 ± 14	286 ± 21	1.64 ± 0.14
	22	178 ± 10	295 ± 17	1.65 ± 0.10
	48	180 ± 15	289 ± 9	1.61 ± 0.08
	72	202 ± 18	314 ± 18	1.55 ± 0.12
	96	210 ± 17	345 ± 20	1.64 ± 0.10
NADH	12	222 ± 15	277 ± 14	1.24 ± 0.11
	18	238 ± 15	258 ± 23	1.08 ± 0.13
	22	238 ± 16	282 ± 20	1.18 ± 0.12
	48	244 ± 14	283 ± 14	1.16 ± 0.09
	72	289 ± 18	328 ± 10	1.13 ± 0.11
	96	312 ± 17	351 ± 15	1.13 ± 0.12
Glicerol-fosfato	12	215 ± 12	272 ± 21	1.27 ± 0.14
	18	220 ± 18	269 ± 18	1.22 ± 0.12
	22	222 ± 10	270 ± 11	1.21 ± 0.09
	48	243 ± 13	295 ± 18	1.21 ± 0.10
	72	256 ± 10	330 ± 13	1.29 ± 0.12
	96	290 ± 17	332 ± 18	1.14 ± 0.13

Las velocidades de consumo de oxígeno se midieron en estado de reposo (IV)* y estado fosforilante (III)**. El estado III se indujo al agregar ADP 500 μM. Muestras de fase exponencial: 12, 18 y 22 hrs; muestras de fase estacionaria: 48, 72 and 96 hrs. Las concentraciones de los sustratos respiratorios fueron: piruvato + malato 10 mM; succinato 10 mM; NADH 1 mM y glicerol-fosfato 10 mM. Mezcla de reacción igual a la de la Figura 5. Datos de tres experimentos independientes (promedio ± D.E.).

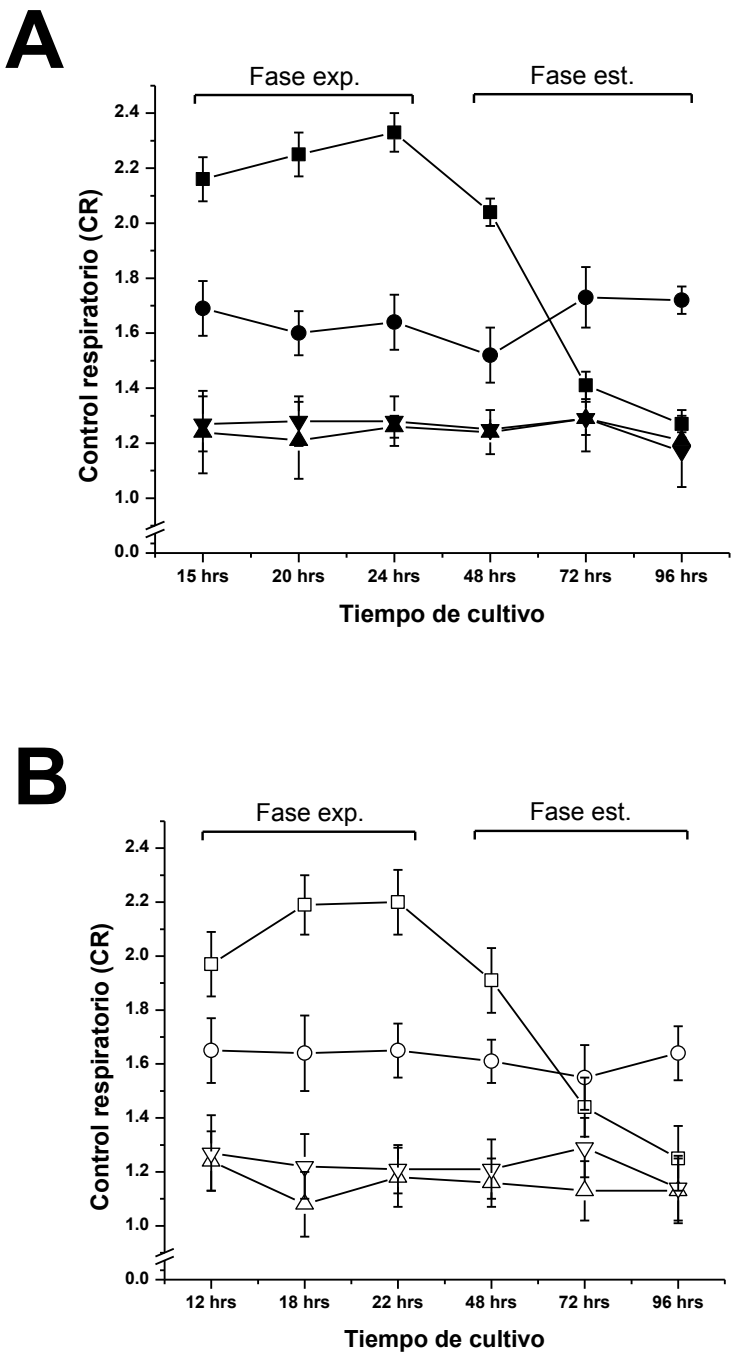

Figura 6. Controles respiratorios (CRs) de mitocondrias aisladas de *D. hansenii* en diferentes fases de crecimiento y tiempos de cultivo. El acoplamiento respiratorio se determinó con diferentes sustratos respiratorios: piruvato-malato 10 mM (cuadrados); succinato 10 mM (círculos); NADH 1 mM (triángulos) y glicerol-fosfato 10 mM (triángulos invertidos) en muestras mitocondriales obtenidas de células cultivadas en **(A)** YPLac-NaCl (símbolos rellenos) y en **(B)** YPD-NaCl (símbolos vacíos). Los tres primeros tiempos de cultivo corresponden a la fase exponencial (exp.) y los últimos tres a la fase estacionaria (est.). Mezcla de reacción igual a la de la Figura 5. Datos de tres experimentos independientes (promedio ± D.E.).

6.3. *La cantidad y actividad del complejo I no cambian durante la fase estacionaria de crecimiento.*

En *D. hansenii*, el consumo de oxígeno promovido por sustratos que alimentan al complejo I disminuyó exclusivamente durante la fase estacionaria de crecimiento. La evidencia experimental sugirió, en principio, cambios en la cantidad o actividad del complejo I en dicha fase. Para explorar lo anterior, se determinó la cantidad relativa y la actividad de NADH deshidrogenasa (NDH) mediante la separación electroforética de los complejos respiratorios de las muestras obtenidas de los diferentes tiempos de cultivo por BN-PAGE. Al término de la electroforesis, se observó que la cantidad relativa de proteína correspondiente al complejo I no cambió en la fase estacionaria (48, 72 y 96 hrs) con respecto a la fase exponencial (15, 20 y 24 hrs) (Figura 7A). El complejo V se usó como control de carga. No se detectaron diferencias visibles en las cantidades de otros complejos (p. ej. IV y V) (Figura 7A). A continuación, se realizó la tinción de NDH para determinar si la actividad del complejo I disminuye en la fase estacionaria, pero no se encontraron diferencias significativas (Figura 7B). Con esta evidencia se descartó la hipótesis de que el complejo I estuviera alterado. Además, en estos geles nativos, se reveló la actividad de la NDH2e durante la misma tinción (Figura 7B). Dicha actividad fue semejante en todos los casos, lo que sugirió que esta enzima se expresa constitutivamente y no se altera entre las fases. Por otra parte, se realizó la tinción de COX y tampoco se hallaron diferencias entre las fases (Figura 7C).

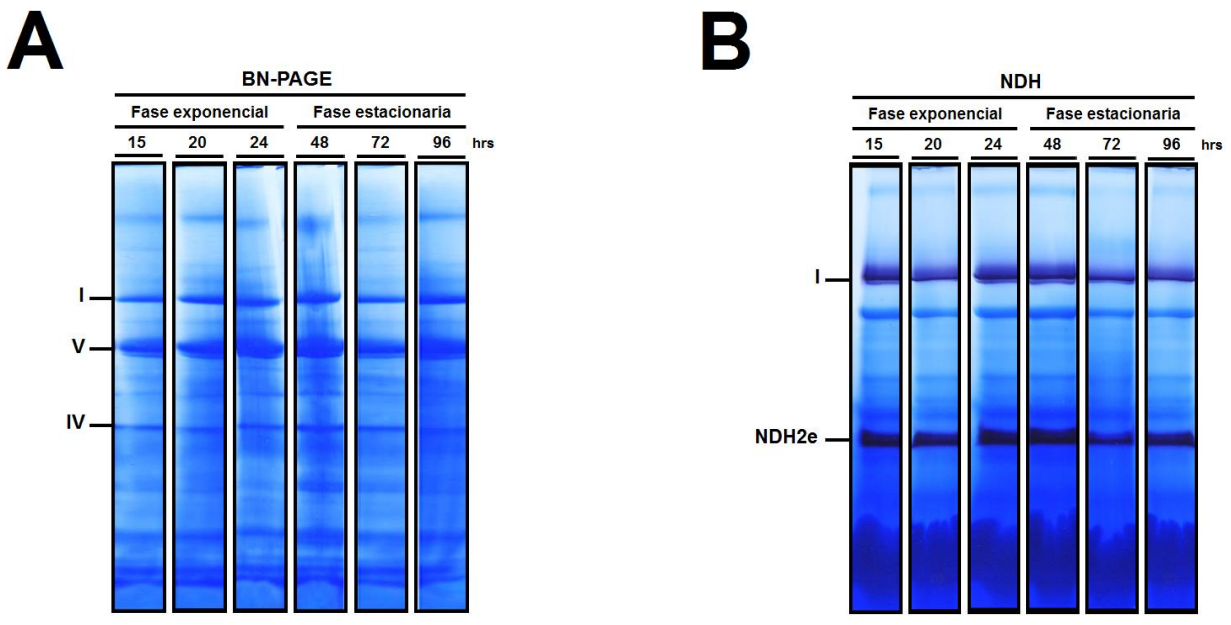

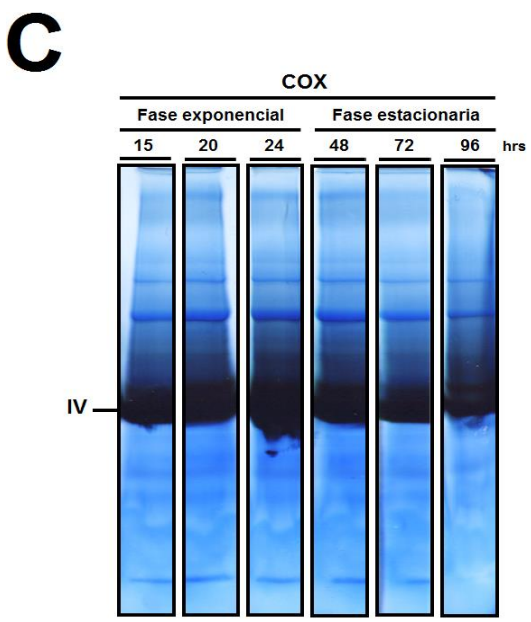

Figura 7. Separación electroforética y actividades en geles nativos de los complejos respiratorios de *D. hansenii* en diferentes fases de crecimiento y tiempos de cultivo. Las mitocondrias aisladas se solubilizaron con lauril-maltósido (LM) 2 mg/mgProt y se cargaron en geles de gradiente de poliacrilamida (4-12 %). Las fases de crecimiento y los tiempos de cultivo se muestran sobre cada carril. **(A)** Los solubilizados se cargaron en un gel BN y al término de la electroforesis se tiño con azul de Coomassie® brillante G-250. El complejo V se usó como control de carga. **(B)** Actividad en gel de NADH deshidrogenasa (NDH). **(C)** Actividad en gel de citocromo c oxidasa (COX). I, IV y V corresponden a la NADH deshidrogenasa, citocromo *c* oxidasa y ATP sintasa, respectivamente. NDH2e: NADH deshidrogenasa alterna externa. Geles representativos de tres experimentos independientes.

6.4. La vía citocrómica no se modifica durante el crecimiento.

El transporte de electrones promovido por la adición de sustratos como el NADH, glicerol-fosfato o succinato no se afectó durante el crecimiento de las levaduras (Tablas B y C). Además, la cantidad relativa y actividad del complejo IV fue igual en todos los tiempos de cultivo (Figura 7C). Esto sugirió que la vía citocrómica se mantiene igual durante las fases de crecimiento. En *D. hansenii*, resulta difícil detectar la banda que corresponde al complejo III por BN-PAGE (Cabrera-Orefice y cols., 2014). Sin embargo, es posible estimar su concentración a través de la cuantificación de los citocromos con espectros diferenciales. Para el complejo III, se midieron los citocromos *b* y $c+c_1$; para estimar la cantidad de complejo IV se cuantificaron los citocromos $a+a_3$. Para estas cuantificaciones, se utilizaron únicamente dos tiempos de cultivo representativos de cada fase de crecimiento: 24 hrs y 96 hrs; fase exponencial y estacionaria, respectivamente. Se encontró una menor cantidad de

citocromos *b* y $c+c_1$ en la fase estacionaria (~40% menos) mientras que el contenido de citocromos $a+a_3$ se mantuvo constante en ambas fases. La concentración de citocromos $a+a_3$ a las 24 hrs fue de 0.217 ± 0.07 nmol/mgProt y a 96 hrs de 0.202 ± 0.13 nmol/mgProt. A las 24 hrs, el contenido de citocromos *b* y $c+c_1$ fue de 0.318 ± 0.06 nmol/mgProt y 0.375 ± 0.03 nmol/mgProt, respectivamente. En cambio, a las 96 hrs el contenido de citocromos *b* y $c+c_1$ fue de 0.2 ± 0.07 nmol/mgProt y 0.227 ± 0.05 nmol/mgProt, respectivamente. No obstante, la actividad respiratoria a través de la vía citocrómica no resultó afectada entre las fases.

6.5. En la fase estacionaria de crecimiento, la adición de NAD^+ recupera parcialmente la actividad respiratoria y el acoplamiento mitocondrial.

Los datos mostrados hasta el momento sugirieron que la pérdida de actividad respiratoria y acoplamiento con los sustratos del complejo I (piruvato-malato) no se debieron a una menor concentración y/o actividad del complejo I, ni por cambios en la vía citocrómica. Con esto se propuso que, en la fase estacionaria, las deshidrogenasas dependientes de NAD^+ del ciclo de Krebs pudieron disminuir su actividad generando menor cantidad de poder reductor (NADH). Por tal motivo, se determinaron las actividades de la piruvato deshidrogenasa (PDH) y de la malato deshidrogenasa (MDH) a las 24 (fase exponencial) y 96 hrs (fase estacionaria) de cultivo. A las 24 hrs, las actividades de PDH y MDH fueron de 15.7 ± 1.38 nmoles de producto/min·mgProt y 2976 ± 88 nmoles de producto/min·mgProt, respectivamente. A las 96 hrs estas actividades no mostraron cambios significativos y fueron para la PDH de 14.56 ± 1.53 nmoles de producto/min•mgProt y para la MDH 3010 ± 125 nmoles de producto/min·mgProt. Los valores de la actividad de MDH son similares a los reportados por Sánchez y cols., (2008).

Al no encontrar diferencias en estas enzimas, se pensó que la menor actividad y acoplamiento pudieron deberse a una falta de sustratos matriciales para estas enzimas; particularmente de la coenzima NAD^+. En un estudio previo, se describe que las mitocondrias aisladas del alga *Polytomella sp.*, son incapaces de consumir oxígeno a menos que se les adicione NAD^+ exógeno durante las mediciones (Jiménez-Suárez y cols., 2012). Por esta razón, se decidió agregar NAD^+ (1 mM) a la mezcla de reacción y se determinó de nueva cuenta el consumo de oxígeno en ambas fases.

La adición del NAD^+ no tuvo efecto sobre el consumo de oxígeno y el CR en las mitocondrias de fase exponencial (Tabla D), pero provocó que las mitocondrias aisladas de fase estacionaria tuvieran mayor actividad respiratoria y acoplamiento (Tabla D) con piruvato-malato. Aun así, estos parámetros no alcanzaron los valores observados en la fase exponencial. En las muestras de fase estacionaria (96 hrs), el CR aumentó de 1.27 ± 0.05 a 1.72 ± 0.05 con la adición del NAD^+. La recuperación parcial del acoplamiento se observó desde las 48 hrs y se mantuvo en el mismo valor en tiempos de cultivo superiores (Figura 8). Se corroboró que el efecto de esta coenzima solo fuera a nivel de las deshidrogenasas que alimentan al complejo I, al cuantificar el consumo de oxígeno y acoplamiento con succinato. En este caso, no se encontraron diferencias significativas en ningún tiempo de cultivo (Figura 8). Esto nos sugirió que, en la fase estacionaria de crecimiento, se perdió el NAD^+ matricial y se frenó la generación de NADH por las deshidrogenasas del ciclo de Krebs. Estos resultados sugirieron que, cuando *D. hansenii* alcanza la fase estacionaria y experimenta el desacoplamiento relacionado con el complejo I, la adición de NAD^+ puede revertirlo y reestablecer el consumo de O_2.

Tabla D. Efecto del NAD^+ sobre la actividad respiratoria y el acoplamiento de mitocondrias aisladas de células de *D. hansenii* cultivadas durante 24 y 96 hrs.

Sustratos	Fase exponencial (24 h)			Fase estacionaria (96 h)		
	Velocidad de consumo de O_2 ($natgO \cdot (min \cdot mgProt)^{-1}$)		CR (III/IV)	Velocidad de consumo de O_2 ($natgO \cdot (min \cdot mgProt)^{-1}$)		CR (III/IV)
	Edo. IV*	Edo. III**		Edo. IV*	Edo. III**	
Piruvato + malato						
– NAD^+	120 ± 10	279 ± 12	2.33 ± 0.07	22 ± 7	28 ± 8	1.27 ± 0.05
+ NAD^+	130 ± 12	307 ± 15	2.36 ± 0.13	72 ± 10	126 ± 17	1.75 ± 0.15
Succinato						
– NAD^+	173 ± 15	285 ± 17	1.64 ± 0.10	222 ± 8	382 ± 4	1.72 ± 0.05
+ NAD^+	170 ± 3	270 ± 18	1.59 ± 0.10	215 ± 14	348 ± 16	1.62 ± 0.13

Las velocidades de consumo de oxígeno se midieron en estado de reposo (IV)* y estado fosforilante (III)**. El estado III se indujo al agregar ADP 500 μM. Se utilizó piruvato + malato 10 mM ó succinato 10 mM como sustratos respiratorios. El NAD^+ se agregó a una concentración final de 1 mM. Mezcla de reacción igual a la de la Figura 5. Datos de tres experimentos independientes (promedio ± D.E.).

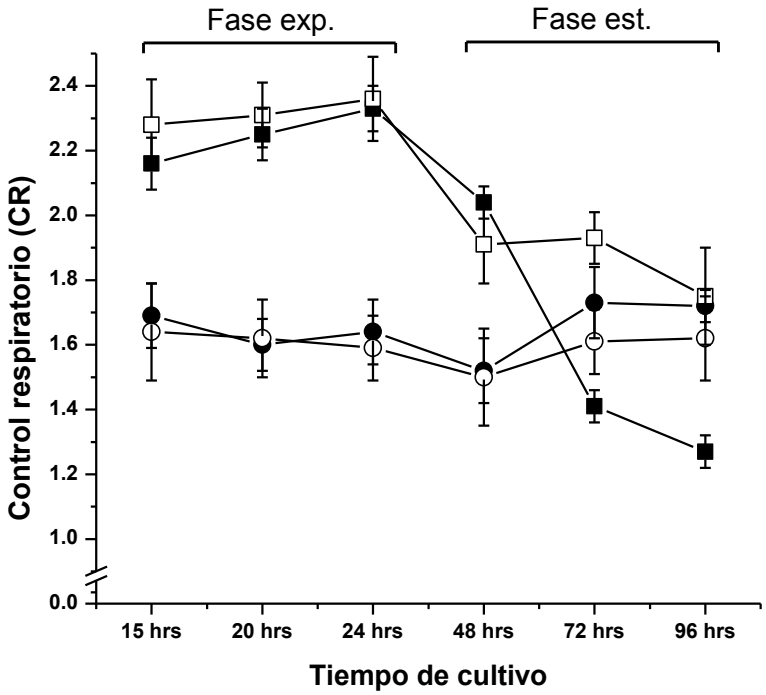

Figura 8. Efecto del NAD^+ sobre el acoplamiento respiratorio de mitocondrias aisladas de *D. hansenii* en diferentes fases de crecimiento y tiempos de cultivo. Para cada condición se determinó el control respiratorio (CR) con dos diferentes sustratos respiratorios: a) piruvato-malato 10 mM (cuadrados) y b) succinato 10 mM (círculos). En ambos casos, los CRs en presencia de NAD^+ 1 mM se muestran en símbolos vacíos. Mezcla de reacción igual a la de la Figura 5. Datos de tres experimentos independientes (promedio ± D.E.).

6.6. En la fase estacionaria de crecimiento, las mitocondrias de D. hansenii pierden el NAD^+ matricial posiblemente a través del $_{Dh}$MUC.

Los resultados descritos en la sección anterior, nos hicieron pensar que el NAD^+ matricial se fugó al citosol a través del segundo mecanismo de desacoplamiento fisiológico que tiene *D. hansenii*: el $_{Dh}$MUC (en su estado abierto). Para explorar esta posibilidad, se determinó cualitativamente el potencial transmembranal ($\Delta\Psi$) en muestras de ambas fases (24 y 96 hrs) en las mismas condiciones que los ensayos de oximetría; en presencia y en ausencia de NAD^+ 1 mM y con piruvato-malato 10 mM o succinato 10 mM como sustratos respiratorios. Se utilizaron dos concentraciones de fosfato para evaluar los estados abierto (0.4 mM) y cerrado (10 mM) del canal inespecífico.

En el caso de los sustratos de complejo I, el valor del $\Delta\Psi$ a las 24 hrs, fue alto y estable en presencia de alto fosfato (10 mM; $_{Dh}$MUC cerrado) (Figura 9A, trazo a). En presencia de NAD^+, la velocidad de generación del $\Delta\Psi$ fue más rápida que en la condición anterior, pero con un valor máximo similar (Figura 9A, trazo c). En bajo fosfato (0.4 mM; $_{Dh}$MUC abierto), no se estableció el $\Delta\Psi$ y el NAD^+ no tuvo efecto (Figura 9A, trazos b y d). A las 96 hrs, en alto fosfato y en ausencia de NAD^+, el valor máximo del $\Delta\Psi$ fue menor que el observado a 24 hrs (Figura 9C, trazo a). En cambio, cuando se les agregó el NAD^+, el valor de $\Delta\Psi$ alcanzó el valor del mostrado a las 24 hrs (Figura 9C, trazo c). Nuevamente, en bajo fosfato, no se observó efecto del NAD^+ ni se estableció el $\Delta\Psi$ (Figura 9C, trazos b y d).

Cuando se utilizó succinato como donador de electrones, no se encontraron diferencias entre los tratamientos, ni entre las fases (Figura 9B, D). Para ambos tiempos de cultivo, en alto fosfato, se estableció un alto valor de $\Delta\Psi$ (Figura 9 B, D, trazos a); mientras que, en bajo fosfato, lo anterior no ocurrió (Figura 9 B, D, trazos c). La adición de NAD^+ tampoco mostró efecto en ambas condiciones de fosfato y fases de crecimiento (Figura 9 B, D, trazos b y d). Con estos resultados se demostró que la adición del NAD^+ fue importante sólo cuando se utilizaron sustratos generadores de NADH matricial (a través de las deshidrogenasas del ciclo de Krebs).

Por otro lado, el hecho de que el NAD^+ tuvo efecto en la condición del $_{Dh}$MUC cerrado, sugirió que esta molécula puede ser transportada por otra vía. Para explorar esto, se usó al piruvato-malato 10 mM, se agregó el NAD^+ durante la medición del $\Delta\Psi$ (a los 60 s del trazo) en presencia de alto fosfato y se observó un incremento súbito en su valor (Figura 10A, trazo a). El experimento se realizó únicamente en las muestras de fase estacionaria (96 hrs); que es en donde el NAD^+ tuvo efecto sobre el $\Delta\Psi$. Este resultado sugirió que el NAD^+ ingresa rápidamente a la matriz mitocondrial. En contraste, en bajo fosfato, la adición provocó un muy pequeño aumento en la señal pero no fue significativo (Figura 10A, trazo b). Para descartar que el incremento en la señal fuera un efecto directo sobre el canal inespecífico, las mitocondrias se incubaron 30 s durante el trazo en bajo fosfato y en la ausencia (Figura 10B, trazo a) o presencia (Figura 10B, trazo b) del NAD^+ y en ningún caso se observó $\Delta\Psi$. A continuación, se agregó fosfato 10 mM para establecer el $\Delta\Psi$ y en el caso la muestra incubada con NAD^+ su valor fue mayor (Figura 10B, trazo b) que la control. Esto descartó la posibilidad de que este compuesto tuviera efecto directo sobre el $_{Dh}$MUC.

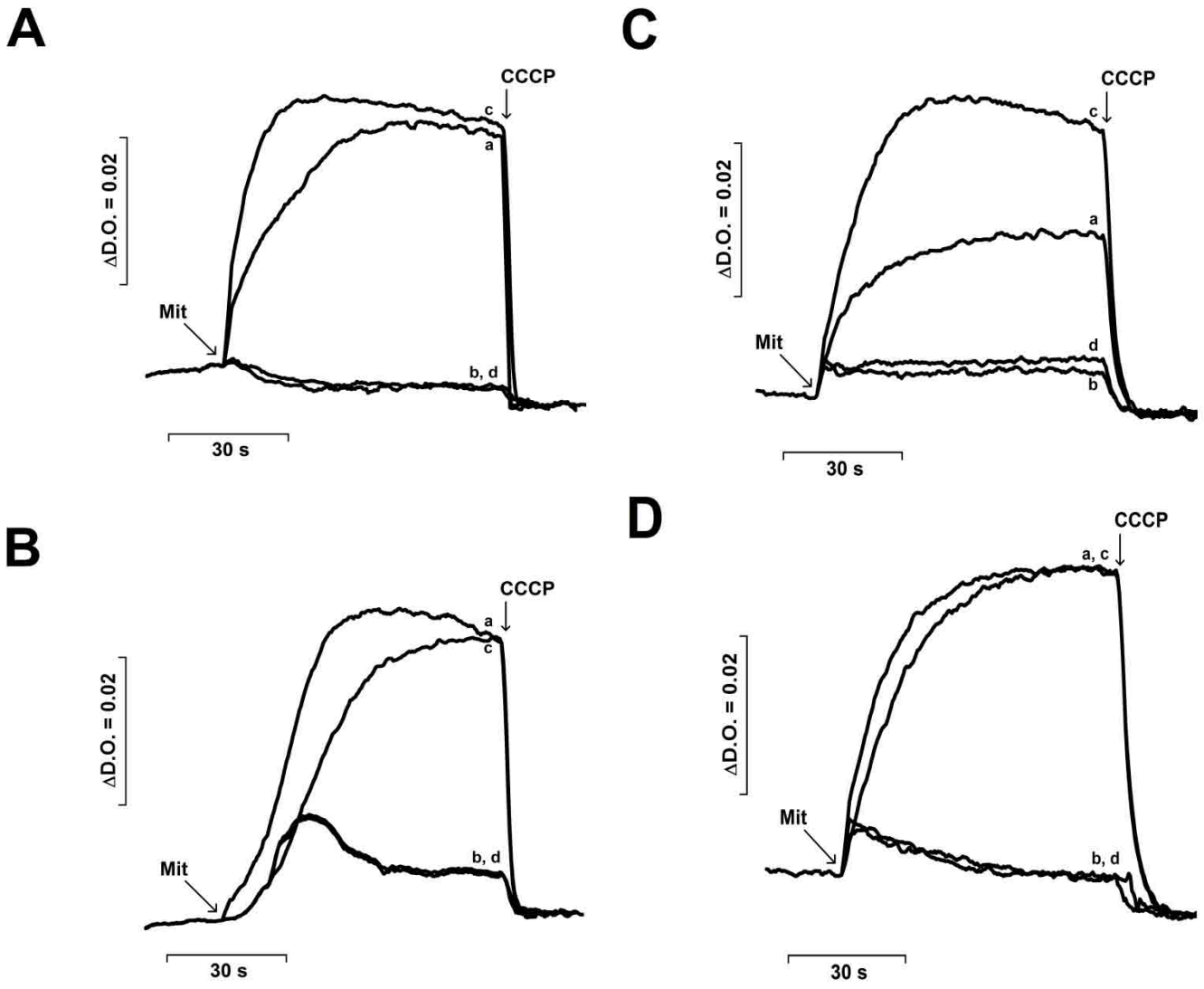

Figura 9. Efecto del NAD^+ sobre el potencial transmembranal ($\Delta\Psi$) de mitocondrias aisladas de *D. hansenii* cosechadas en la fase exponencial y estacionaria. Mezcla de reacción: Sorbitol 1 M, Tris-maleato 10 mM (pH 6.8) y naranja de safranina 10 μM (vol. final 2 mL; temperatura ambiente). Las concentraciones de Tris-fosfato fueron: 0.4 mM (trazos b, d) y 10 mM (trazos a, c). Se determinó el $\Delta\Psi$ en presencia de piruvato-malato 10 mM **(A)** y succinato 10 mM **(B)** en mitocondrias de fase exponencial (24 hrs)**.** Además, se determinó el $\Delta\Psi$ en presencia de piruvato-malato 10 mM **(C)** y succinato 10 mM **(D)** en mitocondrias de fase estacionaria (96 hrs). Se adicionó NAD^+ 1 mM a la celda de reacción en los trazos c y d. Se agregaron mitocondrias 0.5 mg/mL (Mit) y CCCP 5 μM en donde se indica. Trazos representativos de tres experimentos independientes.

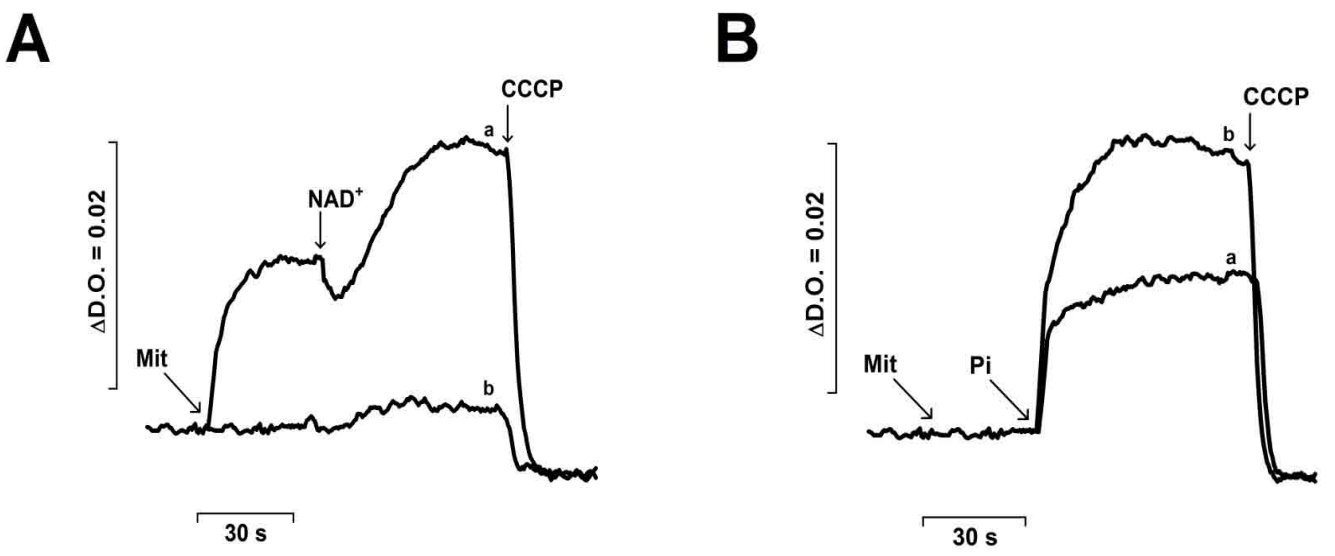

Figura 10. Efecto del NAD^+ sobre el $\Delta\Psi$ de mitocondrias aisladas de *D. hansenii* cosechada en la fase estacionaria (96 hrs). Se utilizó piruvato-malato 10 mM como sustrato respiratorio. La mezcla de reacción es igual a la de la figura 9. **(A)** Concentraciones de fosfato: alto fosfato (10 mM) (trazo a) y bajo fosfato (0.4 mM) (trazo b). **(B)** Concentraciones de NAD^+: 0 mM (trazo a) y 1 mM (trazo b); no se agregó fosfato antes de la adición marcada. En donde se indica, se agregaron mitocondrias 0.5 mg/mL (Mit), NAD^+ 1 mM, fosfato 10 mM y CCCP 5 µM. Trazos representativos de tres experimentos independientes.

6.7. La pérdida del NAD^+ no ocurre durante el aislamiento mitocondrial y se observa en esferoplastos permeabilizados de D. hansenii.

Existen dos posibilidades que pueden explicar la falta de NAD^+ en las mitocondrias obtenidas de células cultivadas hasta la fase estacionaria sin considerar su degradación: *a)* pérdida durante el aislamiento mitocondrial por dilución o fragilidad de las mitocondrias y *b)* pérdida fisiológica a través del $_{Dh}$MUC. Para ésto, se determinó la actividad respiratoria en esferoplastos permeabilizados con nistatina. Los esferoplastos se obtienen al romper la pared celular de las levaduras con zimoliasa. La nistatina es una molécula que se une al ergosterol de la membrana celular y forma poros por donde pueden permear sustratos e intermediarios metabólicos (Averet y cols., 1998). En esta condición las mitocondrias se encuentran en el ambiente citosólico y permite extrapolar su comportamiento a la realidad (Avéret y cols., 1998).

Para determinar el efecto del NAD^+ sobre el consumo de O_2 y el acoplamiento respiratorio se utilizaron esferoplastos permeabilizados obtenidos de la fase exponencial (24 hrs) y estacionaria (96 hrs), en presencia de piruvato-malato y succinato (Tabla E). La

respiración de los esferoplastos fue mucho más lenta que la registrada en las mitocondrias aisladas, mientras que el valor del CR fue ligeramente menor; por ejemplo los esferoplastos permeabilizados de 24 hrs tuvieron un CR = 1.83, mientras que las mitocondrias aisladas un CR = 2.33 (Tablas D y E). En el caso de la fase exponencial, no se encontraron diferencias en estos parámetros en presencia o ausencia del NAD^+ y con ambos sustratos (Tabla E). Sin embargo, los esferoplastos de fase estacionaria mostraron una menor actividad respiratoria y acoplamiento en presencia de piruvato-malato (Tabla E). Sin embargo, ambos parámetros aumentaron con la adición del NAD^+ 1 mM (Tabla E). Cabe señalar que en este caso, los valores de actividad y control respiratorios regresaron a valores similares mostrados por los esferoplastos de fase exponencial. Esto contrasta con lo que se observó en las mitocondrias aisladas en donde la adición de la coenzima no recupera la respiración ni el CR al máximo mostrado en fase exponencial (Tabla D). Al utilizar succinato en las muestras de fase estacionaria, la adición de NAD^+ no tuvo efecto alguno sobre los dos parámetros (Tabla E).

Tabla E. Efecto del NAD^+ sobre la actividad respiratoria y el acoplamiento de esferoplastos permeabilizados de *D. hansenii* obtenidos a 24 y 96 hrs.

Sustratos	Fase exponencial (24 h)			Fase estacionaria (96 h)		
	Velocidad de consumo de O_2 (natgO·(min·mgProt)$^{-1}$)		CR (III/IV)	Velocidad de consumo de O_2 (natgO·(min·mgProt)$^{-1}$)		CR (III/IV)
	Edo. IV*	Edo. III**		Edo. IV*	Edo. III**	
Piruvato + malato						
– NAD^+	11.5 ± 0.2	21.1 ± 2.0	1.83 ± 0.18	4.9 ± 1.3	5.3 ± 1.3	1.08 ± 0.02
+ NAD^+	11.8 ± 1.2	22.5 ± 3.2	1.91 ± 0.12	11.1 ± 1.2	20.7 ± 3.3	1.86 ± 0.10
Succinato						
– NAD^+	12.6 ± 0.7	18.7 ± 0.4	1.49 ± 0.08	12.2 ± 2.8	18.5 ± 2.8	1.54 ± 0.15
+ NAD^+	11.9 ± 1.4	17.9 ± 0.4	1.51 ± 0.21	13.3 ± 2.4	18.8 ± 2.4	1.42 ± 0.08

Los esferoplastos se permeabilizaron con nistatina 20 μg/mL en la presencia de aeración constante (aire burbujeado con una manguera). Las velocidades de consumo de oxígeno se midieron en estado de reposo (IV)* y estado fosforilante (III)**. El estado III se indujo al agregar ADP 5 mM. Se utilizó piruvato + malato 20 mM ó succinato 20 mM como sustratos respiratorios. El NAD^+ se agregó a una concentración final de 5 mM. Mezcla de reacción: Sorbitol 1 M, Tris-maleato 10 mM (pH 6.8), KCl 75 mM, Tris-fosfato 20 mM, $MgCl_2$ 5 mM, EGTA 0.5 mM (vol. final 1 mL; temperatura 30 °C). Datos de tres experimentos independientes (promedio ± D.E.).

Con base en estos resultados, se sugirió que la falta de NAD^+ matricial no ocurrió durante el aislamiento mitocondrial, sino que ésta ocurre en las células durante su crecimiento. Además, se propuso que la diferencia encontrada en los esferoplastos permeabilizados, con respecto a los resultados en las mitocondrias aisladas, se debió a que en los primeros se mantuvo intacta la integridad mitocondrial. Otro dato que apoya esta propuesta es que en las mitocondrias de fase exponencial, que se obtuvieron por el mismo método de aislamiento, presentaron la máxima actividad respiratoria y acoplamiento. Si la fuga de NAD^+ ocurrió por dilución, entonces las mitocondrias de fase exponencial debieron perderlo de igual manera. Sin embargo, esto no fue así, por lo que se descartó esta posibilidad y fortaleció la hipótesis de que el NAD^+ se pierde por el $_{Dh}$MUC.

6.8. En D. hansenii, el NAD^+ se transporta hacia la matriz por un posible acarreador mitocondrial específico.

Los resultados anteriores mostraron que al agregar el NAD^+ a las mitocondrias aisladas, éste pudo ingresar a la matriz mitocondrial aún con el $_{Dh}$MUC cerrado (en presencia de Pi 10 mM) (Figura 10). Esto sugiere la existencia de otro mecanismo diferente para su transporte hacia la matriz mitocondrial. Al revisar la literatura, se encontró que *S. cerevisiae* expresa dos isoformas (Ndt1p y Ndt2p) de un acarreador mitocondrial específico de NAD^+ (Todisco y cols., 2006). Este transportador debe incorporar el NAD^+ a la mitocondria, ya que las enzimas involucradas en su síntesis se encuentran en el citoplasma (Todisco y cols., 2006). Con base en lo anterior, se realizó una búsqueda en la base de datos del NCBI con las secuencias de estas isoformas para encontrar posibles secuencias candidatas de un acarreador de este tipo en *D. hansenii*. En este caso, se encontró un posible ortólogo anotado como *DEHA2B09284p* (390 residuos). La secuencia aparece anotada como un acarreador hipotético de piruvato similar al ANT. No obstante, esta secuencia tiene 49% de identidad y 63% de similitud con Ndt1p y 45% de identidad y 60% de similitud con Ndt2p. Los "*E*-values" para cada alineamiento fueron 8×10^{-102} y 2×10^{-88}, respectivamente. Estos valores fueron muy pequeños e indicaron un excelente alineamiento y cobertura de la secuencia (83-86%). Por tales razones, se sugirió que la secuencia *DEHA2B09284p* corresponde a un acarreador de NAD^+ que pertenece a la superfamilia de acarreadores mitocondriales.

Para continuar la caracterización del mecanismo de transporte del NAD^+, se probaron una serie de compuestos que inhiben el acarreo de esta molécula en *S. cerevisiae*. Ambas

isoformas se inhiben por distintos compuestos, entre ellos, la batofenantrolina (BAT), el púrpura de bromocresol (PBrC) y el piridoxal-5'-fosfato (Px5P) (Todisco y cols., 2006). Se determinó el consumo de O_2 de mitocondrias aisladas de la fase estacionaria (96 hrs) en presencia de piruvato-malato 10 mM, con o sin NAD^+ 1 mM y con los tres inhibidores (Figura 11). El consumo de O_2 control fue menor en ausencia del NAD^+ y aumentó al añadírsele (Figura 11). En cambio, al agregarse cada uno de los inhibidores se perdió el incremento de actividad respiratoria en presencia del NAD^+ (Figura 11). El consumo de oxígeno en ausencia de NAD^+ no se afectó en presencia de estos inhibidores (Figura 11, barras negras). El efecto de estos inhibidores se exploró en mitocondrias de fase exponencial, pero no se encontraron cambios (datos no mostrados); ésto se debió posiblemente a que el NAD^+ no tuvo efecto a las 24 hrs (Tabla B). Estos resultados sugieren que las mitocondrias de *D. hansenii* son capaces de incorporar al NAD^+ a través de un acarreador con características similares a los de *S. cerevisiae*. Aun así, la pérdida de la coenzima (en la fase estacionaria), no ocurrió a través de este transportador, ya que en la otra fase se observó una considerable actividad respiratoria en presencia de piruvato-malato (Tabla B).

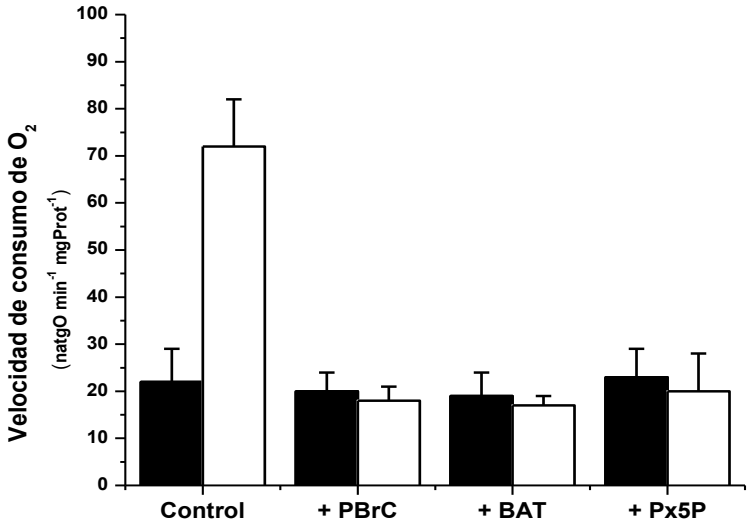

Figura 11. Efecto de los inhibidores del transporte de NAD^+ sobre el consumo de oxígeno de mitocondrias aisladas de *D. hansenii* cosechadas en la fase estacionaria (96 hrs). Las velocidades de consumo de oxígeno se midieron en estado de reposo (IV) con (barras blancas) o sin (barras negras) NAD^+ 1 mM. Se utilizó piruvato + malato 10 mM como donador de electrones. Inhibidores: púrpura de bromocresol (PBrC) 0. 3 mM; batofenantrolina (BAT) 5 mM y piridoxal-5'-fosfato (Px5P) 5 mM. Mezcla de reacción igual a la de la Figura 5. Datos de tres experimentos independientes (promedio ± D.E.).

7. DISCUSIÓN

Durante las diferentes etapas de crecimiento, las levaduras experimentan cambios metabólicos notables en respuesta a las necesidades energéticas. En la fase exponencial de crecimiento las células se dividen constantemente, por lo que deben sintetizar una gran cantidad de ATP para su uso en las vías anabólicas activas. Sin embargo, al entrar en la fase estacionaria de crecimiento, la división celular se detiene y los requerimientos de ATP disminuyen considerablemente (Veiga y cols., 2003; Guerrero-Castillo y cols., 2011). En esta situación, se sugiere que la cadena respiratoria mitocondrial puede funcionar a una velocidad baja, lo que promueve la formación de ROS y pérdida del control del estado redox celular (Guerrero-Castillo y cols., 2011; 2012). De ocurrir lo anterior, resulta en una mayor desventaja para las levaduras no fermentativas o Crabtree-negativas (p. ej. *Y. lipolytica*, *D. hansenii*, *C. albicans*, etc.), en donde la fosforilación oxidativa mitocondrial es la fuente principal de ATP (Veiga y cols., 2000). En cambio, las levaduras Crabtree-positivas (fermentativas), tales como *S. cerevisiae*, probablemente enfrentan este problema exclusivamente en la presencia de fuentes de carbono no fermentables (p. ej. glicerol-etanol y lactato). Para evitar estos efectos negativos, deben existir sistemas intrínsecos que mantengan alto el consumo de O_2 sin generar fuerza protón-motriz (Δp). En conjunto, reciben el nombre de mecanismos de desacoplamiento fisiológicos (Guerrero-Castillo y cols., 2011) y deben encontrarse finamente regulados; inactivos en condiciones de alta demanda energética (p. ej. en la fase exponencial) y activos sólo en condiciones de baja demanda energética (p. ej. en la fase estacionaria) (Guerrero-Castillo y cols., 2012).

D. hansenii contiene dos posibles mecanismos de desacoplamiento fisiológicos (Cabrera-Orefice y cols., 2010, 2014). El primero involucra a las oxidorreductasas alternas; NDH2e, $_{Mit}$GPDH y AOX. La transferencia de electrones a través de estas enzimas redox hasta el O_2 es independiente de la síntesis del ATP ya que no bombean protones. Aunque este tipo de enzimas no tengan actividad protonofórica (como los desacoplantes clásicos (p. ej. CCCP o 2,4-dinitrofenol) o las UCPs), el resultado final es el aumento en la velocidad de consumo de O_2 (Kadenbach, 2003; Guerrero-Castillo y cols., 2011). El segundo es la transición de la permeabilidad (TPM) provocada por la apertura del canal inespecífico mitocondrial ($_{Dh}$MUC) (Cabrera-Orefice y cols., 2010). La TPM se define como el aumento en el transporte inespecífico de iones y metabolitos con un peso molecular de hasta 1.5 kDa a

través de la MMI [62, 63]. Como resultado de esto, se disipan todos los gradientes electroquímicos y se promueve la entrada de agua al organelo (hinchamiento mitocondrial) (Manon y cols., 1998).

En *D. hansenii*, estos dos mecanismos se describen en las mitocondrias aisladas de células cosechadas en la fase exponencial de crecimiento. Ambos se estudiaron con mayor detalle en este trabajo y en diferentes fases de crecimiento con el objetivo de entender el desacoplamiento fisiológico en esta especie.

En primer lugar, se estudió la actividad de la AOX, la cual se puede detectar en la fase exponencial de crecimiento utilizando lactato como fuente de carbono (Cabrera-Orefice y cols., 2010, 2014a) y se mantiene al mismo nivel durante la estacionaria (Figura 5A). Por el contrario, en medios que contienen glucosa, dicha actividad aparece en la fase de crecimiento exponencial tardía y se mantiene durante la estacionaria (Veiga y cols., 2003c). En nuestras manos, a tiempos menores a la media logarítmica (p. ej. 12 hrs), no se detectó la RRC (Figura 5B). Esto sugiere que la expresión de la AOX de *D. hansenii* parece estar controlada por la fuente de carbono y no sólo por la fase de crecimiento, como sugieren Veiga y cols. (2003c).

En *S. cerevisiae*, el lactato se oxida directamente por dos lactato deshidrogenasas mitocondriales (LDH) situadas en la cara exterior de la membrana mitocondrial interna o por otra isoforma matricial (Chelstowska y cols., 1999; Mourier y cols., 2008; Rigoulet y cols., 2010). Las isoformas de LDH membranales oxidan D-lactato o L-lactato a piruvato y son capaces de donar electrones directamente al citocromo *c* (Mourier y cols., 2008). En cambio, la isoforma matricial utiliza D-lactato para producir piruvato, en una reacción dependiente de NAD^+ (Chelstowska y cols., 1999). *D. hansenii* debe contener al menos una de estas proteínas por su capacidad de asimilar al lactato durante el crecimiento en YPLac-NaCl. En presencia de esta fuente de carbono, se espera una mayor producción del ATP y un intenso flujo de electrones a través de la vía citocrómica, la cual podría encontrarse saturada en algún momento. Se propone que para evitar esto, esta especie expresa a la AOX en todas las fases de crecimiento (Figura 5A), lo que le permite tener una vía de escape para los electrones en caso de que el consumo de O_2 se vuelva lento, el flujo esté saturado y aumenten los radicales libres. Esta función hipotética de la AOX se propone ampliamente en la literatura desde hace casi dos décadas (Umbach y Siedow, 2000; Veiga y cols., 2003b; Guerrero-Castillo y cols., 2011).

Sin embargo, al utilizar glucosa, ésta puede oxidarse completamente en la mitocondria o bien ser fermentada en el citosol y generar parte del ATP por esta vía (Sánchez y cols., 2006). En este último escenario, la producción del ATP mitocondrial debe ser menor que con lactato y la cadena respiratoria no se encontraría comprometida para requerir de una vía de escape para los electrones. Otra premisa es que exista una modulación río arriba de la expresión de la AOX dependiente de la fuente de carbono. En cualquiera de los casos, se necesitan más estudios para entender estos comportamientos.

La diferencia en la aparición de la respiración resistente a cianuro que se observó en YPD-NaCl (Figura 5B), se tradujo como una diferencia en la expresión de la AOX en esta levadura. Tomando en cuenta lo anterior, se exploraron las actividades y/o niveles relativos de otros componentes de la cadena respiratoria ramificada de *D. hansenii*. Las actividades y cantidades relativas de NDH2e, complejo I y complejo IV no cambiaron durante todo el crecimiento (Figura 7). En cambio, el complejo III tuvo una disminución de alrededor del 40% en muestras de la fase estacionaria (96 hrs) en comparación con las de exponencial (24 hrs). En *D. hansenii*, los complejos I, III y IV se organizan en forma de supercomplejos (Cabrera-Orefice y cols., 2014). Estas asociaciones se relacionan con la canalización de electrones (Schägger y Pfeiffer, 2000) y estabilidad de los complejos, principalmente de la NADH deshidrogenasa (I) (Acín-Pérez y Enríquez, 2014). Por lo tanto, la disminución que se observó en el complejo III, podría afectar el ensamblaje de los supercomplejos, dejando libre una fracción de complejos I y IV. De ocurrir así, se esperaría una transferencia de electrones menor a través de la vía citocrómica al utilizar donadores de electrones para el complejo I. Sin embargo, hasta el momento no podemos sugerir más debido a que las actividades respiratorias y acoplamientos en presencia de succinato, NADH o glicerol-fosfato no se afectaron por la disminución del complejo III (Tabla B). Este comportamiento se pudo deber a que el complejo II, NDH2e o $_{Mit}$GPDH no forman parte de los supercomplejos en esta especie (Cabrera-Orefice y cols., 2014). Por estas razones, resulta atractivo explorar a futuro, la dinámica y ensamblaje de los supercomplejos respiratorios.

Además, en *Y. lipolytica*, se describe una asociación formada entre la NADH deshidrogenasa alterna externa ($_{Yl}$NDH2e) y los complejos III y IV (Guerrero-Castillo y cols., 2009; 2012). Esta asociación sólo se observa en la fase exponencial e impide el flujo de electrones desde el NADH exógeno al O_2 por la vía alterna. Sin embargo, durante la fase estacionaria, se disocia el supercomplejo $_{Yl}$NDH2e-III-IV y se permite el flujo de electrones

por ambas vías. En *D. hansenii* aún no es claro si los componentes alternos se pueden asociar a los supercomplejos. A diferencia de lo que se reporta en *Y. lipolytica*, se sugiere que en *D. hansenii* no hay asociación entre la NDH2e y los complejos III y IV en la fase exponencial al no detectarse actividad de NDH en la región del gel donde migran estos complejos (Guerrero-Castillo y cols., 2009; Cabrera-Orefice y cols., 2014). Esto resulta interesante, porque tanto *Y. lipolytica* como *D. hansenii* poseen cadenas respiratorias ramificadas con idéntica composición y sin embargo, las asociaciones entre las complejos clásicos y los componente alternos son diferentes, al menos en la fase exponencial. En *D. hansenii*, independientemente del sustrato, los electrones son transferidos por ambas vías.

Por otra parte, en la fase estacionaria de crecimiento, las mitocondrias presentaron una gran disminución en el consumo de oxígeno (Tablas B y C) y el acoplamiento (Figura 6), en presencia de piruvato-malato, un sustrato de complejo I. Este fenómeno no ocurrió en presencia de otros donadores de electrones, tales como el NADH, succinato o glicerol-fosfato (Tablas B y C, Figura 6). Este comportamiento fue aparentemente causado por una pérdida del NAD^+ localizado en la matriz mitocondrial. En dicha fase, se propone que el NAD^+ se liberó a través del $_{Dh}$MUC. En esta condición de baja demanda energética, el canal pudo abrirse para disipar el $\Delta\Psi$ y los gradientes electroquímicos (Palmieri y cols., 2006). En general, la apertura del canal y la subsecuente caída del $\Delta\Psi$, incrementan el consumo de O_2 al activarse las bombas (I, III y IV) de la cadena respiratoria (Manon y cols., 1998). En consecuencia, incrementa el flujo de electrones que entran en la cadena y llegan al O_2, lo que disminuye considerablemente la duración de la semiquinona durante el acarreo. Con ésto disminuye la generación de superóxido y otras ROS, se puede mantener el control de las pozas redox (p. ej. $NADH/NAD^+$) y la fosforilación oxidativa se desacopla (Kadenbach, 2003; Guerrero-Castillo y cols., 2011). En el caso de *D. hansenii*, si durante la TPM hipotética de la fase estacionaria, se pierde además el NAD^+ matricial, se previene la entrada de electrones por la ruta que brinda mayor rendimiento para la síntesis del ATP (I-Q-III-cit c-IV; 10 $H^+/2e^-$). En un futuro se evaluará si el $_{Dh}$MUC tiene diferente sensibilidad a sus efectores en la fase estacionaria. Un punto adicional será determinar si la fuga del NAD^+ y la apertura del MUC son reversibles en condiciones fisiológicas.

Previamente, la pérdida del NAD^+ matricial a través del MUC se describió en *S. cerevisiae* y en una línea celular de endotelio microvascular humano (HMEC-1) por Bradshaw y Pfeiffer (2006) y por Dumas y cols. (2009), respectivamente. En el primer caso,

el NAD^+ matricial se libera únicamente en las mitocondrias hinchadas y se observa menor actividad respiratoria en presencia de sustratos de complejo I. La adición de NAD^+ restableció la velocidad de consumo de oxígeno en estas mitocondrias (Bradshaw y Pfeiffer, 2006). Por otro lado, en las células HMEC-1 se abre el canal (PTP) en presencia del A23187; un ionóforo de Ca^{2+} (Dumas y cols., 2009). En esta situación, el NAD(P)H matricial es liberado y también se observa hinchamiento mitocondrial. Asimismo, cuando se agrega ciclosporina A se previenen ambos eventos (Dumas y cols., 2009).

En mitocondrias aisladas de células de *D. hansenii* cosechadas en la fase estacionaria de crecimiento (96 hrs), la velocidad de consumo de O_2 y el acoplamiento fueron parcialmente restaurados con la adición de NAD^+ 1 mM a la mezcla de reacción (Tabla D, Figura 8). Además, este efecto se exploró en esferoplastos permeabilizados (Tabla E), en donde ambos parámetros se observaron disminuidos en la fase estacionaria pero recuperaron su valor por completo con la adición de la coenzima (Tabla E). Por otro lado, se añadió una concentración alta de fosfato (10 o 20 mM) para mantener cerrado el $_{Dh}$MUC y se determinó el potencial transmembranal. En esta condición (96 hrs), la adición del NAD^+ durante el trazo aumentó el $\Delta\Psi$ (Figura 10). En este caso (con el canal inespecífico cerrado), las mitocondrias incorporaron el NAD^+ por otro mecanismo. Con base en esto, se sugirió la presencia de un transportador similar al reportado en *S. cerevisiae*.

En *S. cerevisiae*, el NAD^+ se sintetiza fuera de la mitocondria y se importa por dos isoformas de un acarreador específico, designados Ndt1p y Ndt2p, respectivamente (Todisco y cols., 2006). Se sugiere que estas proteínas mueven al NAD^+ a través de transporte unidireccional o por intercambio con nucleótidos monofosfato, tales como AMP y GMP (Palmieri y cols., 2006). Estas proteínas son codificadas en el núcleo y, al pertenecer a la superfamilia de acarreadores mitocondriales, poseen la estructura altamente conservada de seis hélices transmembranales (Palmieri y cols., 2011). Por medio del BLAST, se encontró un ortólogo anotado como DEHA2B09284p en la base de datos del NCBI. Esta secuencia candidata mostró una gran similitud con Ndt1p y Ndt2p. Además, el transporte de NAD^+ en *D. hansenii* se inhibió por batofenantrolina, piridoxal-5'-fosfato y púrpura de bromocresol. Estos compuestos son inhibidores específicos de los transportadores de *S. cerevisiae* y *A. thaliana* (Todisco y cols., 2006; Palmieri y cols., 2009).

Los resultados obtenidos sugieren la pérdida fisiológica del NAD^+ matricial durante la fase estacionaria. La pérdida del NAD^+ matricial se observa también en las mitocondrias de

Polytomella sp. (Jiménez-Suárez y cols., 2012) y de *S. cerevisiae* (Bradshaw y Pfeiffer, 2006). En esta última, la fuga no se relaciona con la fase de crecimiento, sino como consecuencia de la apertura directa del MUC *in vitro*.

En *D. hansenii*, parece que las mitocondrias de la fase estacionaria retuvieron parte del NAD^+, ya que se observó un pequeño consumo de oxígeno y valor del $\Delta\Psi$ (Tablas B y C, Figuras 6 y 9) con piruvato-malato; sustratos generadores de NADH matricial. Se piensa que esta cantidad residual de NAD^+ podría ser útil para mantener el flujo de metabolitos través del ciclo de Krebs y otras vías mitocondriales dependientes de NAD^+ (p. ej. ciclo del glioxilato, oxidación de aminoácidos, etc.) de manera basal.

Hasta el momento tenemos evidencia sólida que sugiere que la fosforilación oxidativa en esta levadura es diferente en las dos fases de crecimiento. Se propone que la disminución en la actividad del complejo I se debió a la pérdida del NAD^+ por la activación del canal inespecífico. Esta fuga constituye un mecanismo adicional de desacoplamiento fisiológico que previene, en principio, la sobreproducción de ATP al desacoplar la vía con mayor eficiencia de bombeo de protones. Además, el hecho de que en todos los tiempos de cultivo se observó la misma actividad de AOX (en medio no fermentable), sugiere que la AOX no participa en gran medida como un mecanismo de desacoplamiento fisiológico en esta especie. No obstante, la función de la AOX en esta levadura debe estudiarse con mayor detalle para esclarecer su papel fisiológico. Finalmente, la activación del $_{Dh}$MUC en la fase estacionaria parece ser el principal mecanismo de desacoplamiento fisiológico en conjunto con la pérdida del NAD^+.

8. CONCLUSIONES

- Al cultivar a *D. hansenii* en lactato, la AOX se encuentra activa desde la fase exponencial temprana. En cambio, al cultivar la levadura en glucosa, dicha actividad aparece cerca de la fase estacionaria.

- En la fase estacionaria disminuye el consumo de oxígeno y el acoplamiento respiratorio con sustratos de complejo I, sin cambiar la cantidad y actividad de los complejos I y IV ni las actividades de las enzimas dependientes de NAD^+ estudiadas.

- Debido a que la suplementación de NAD^+ recupera la actividad y acoplamiento respiratorios en las muestras de fase estacionaria, es posible sugerir la falta de esta coenzima en la matriz. En este caso, el NAD^+ pudo perderse a través del $_{Dh}$MUC.

- Las mitocondrias de *D. hansenii* transportan NAD^+ hacia la matriz por un acarreador similar a los Ndt1p y Ndt2p de *S. cerevisiae*. Dicho transporte se pierde en presencia de batofenantrolina, piridoxal-5'-fosfato y púrpura de bromocresol.

9. PERSPECTIVAS

Hasta el momento se tiene una idea clara de la composición de la cadena respiratoria ramificada de *D. hansenii* y sobre las diferencias en la fosforilación oxidativa mitocondrial en diferentes fases de crecimiento. En este trabajo proponemos que en la fase estacionaria de crecimiento se abre el $_{Dh}$MUC, lo que parece relacionarse con la menor demanda energética. En este caso, iones y metabolitos matriciales (como el NAD^+) pueden liberarse y disminuir el flujo metabólico a través de las vías que alimentan el complejo I (p. ej. ciclo de Krebs). Este mecanismo, por un lado, puede evitar la generación de ROS al mantener activos los puntos alternos de la cadena ramificada para consumir O_2 y, por el otro, disminuir la síntesis del ATP, cuya demanda es menor. No obstante, este mecanismo debe explorarse de manera fisiológica y con mayor detalle. Una propuesta inicial es comprobar que efectivamente hay una menor cantidad de NAD^+ matricial en la fase estacionaria y que dicha falta no sea producto de la degradación enzimática de la coenzima. Actualmente se cuenta con sondas fluorescentes que permiten ver la localización del NAD(H) y seguir los cambios a nivel de la poza. Además es necesario estudiar el papel del MUC *in vivo* para saber si realmente un mecanismo de desacoplamiento fisiológico en esta y otras especies.

Por otro lado, el papel fisiológico de las oxidorreductasas alternas en esta y otras levaduras permanece en discusión. Se propone que estas enzimas aceleran el flujo de electrones a través de la cadena cuando la vía citocrómica está saturada y previenen la sobreproducción de ROS (Guerrero-Castillo y cols., 2011). En este trabajo se observó que la actividad de la AOX depende tanto de la fase de crecimiento como de la fuente de carbono (Figura 5). Por esta razón, en experimentos recientes se estudió el efecto de otras fuentes de carbono sobre la expresión de la AOX. Para esto, se determinó el consumo de oxígeno basal y en presencia de inhibidores de la vía citocrómica y alterna en células íntegras cultivadas en las diferentes fuentes de carbono. Con lactato o succinato se detectó la RRC en todas las fases de crecimiento. En cambio, con glucosa o galactosa, la RRC se detectó cerca de la fase estacionaria. El lactato y el succinato, no son fermentables, por lo que se espera una saturación de la vía citocrómica y la AOX sería una alternativa óptima para liberar electrones. Es por esto que proponemos que la expresión de la AOX puede estar ligada directamente con el flujo de electrones y de metabolitos en la mitocondria.

Sin embargo, en células cultivadas en glicerol, que es no fermentable, no se observó RRC independientemente de la fase de crecimiento. Este resultado contrastó con nuestra línea de pensamiento y se debe estudiar con mayor detalle. De hecho, la biomasa celular fue mayor en glicerol que en las otras fuentes no fermentables. Además, al romper las células de fase estacionaria para extraer las mitocondrias, se observó una gran cantidad de material insoluble en el sobrenadante, el cual pensamos que contiene una gran cantidad de lípidos. Este comportamiento es similar a lo descrito en otras levaduras como *Y. lipolytica*; una levadura oleaginosa al igual que *D. hansenii*. *Y. lipolytica* fabrica una gran cantidad de lípidos en presencia de glicerol y los almacena en forma de corpúsculos lipídicos. En este caso, proponemos que bajo estas condiciones *D. hansenii* no expresa a la AOX para mantener acoplada la fosforilación oxidativa y cubrir las necesidades de ATP que requiere la posible biosíntesis lipídica promovida por glicerol. Recientemente, se utilizan microorganismos para la producción de biodiesel a partir de los desperdicios de glicerol que se obtienen durante este proceso. Es por esto que nuestros resultados preliminares en *D. hansenii* sugieren que es una opción para producir lípidos en esta condición, lo cual es muy interesante desde el punto de vista biotecnológico. Por esta razón, se debe continuar con el estudio del metabolismo energético en esta levadura y entender los mecanismos que regulan la fosforilación oxidativa mitocondrial.

BIBLIOGRAFÍA

Acín-Pérez, R. y Enriquez, J.A. (2014). The function of the respiratory supercomplexes: the plasticity model. *Biochim. Biophys. Acta* 1837: 444-450.

Acín-Pérez, R., Fernández-Silva, P., Peleato, M. L., Pérez-Martos, A. y Enriquez, J. A. (2008). Respiratory active mitochondrial supercomplexes. *Mol. Cell*. 32: 529-539.

Akerman, K. E. O. y Wikström, M. K. (1976). Safranine as a probe of the mitochondrial membrane potential. *FEBS Lett.* 68: 191-197.

Alba-Lois, L., Segal, C., Rodarte, B., Valdés-López, V., DeLuna, A. y Cárdenas, R. (2004). NADP-glutamate dehydrogenase activity is increased under hyperosmotic conditions in the halotolerant yeast *Debaryomyces hansenii. Curr. Microbiol.* 48: 68-72.

Albury, M. S., Affourtit, C., Crichton, P. G. y Moore, A. L. (2002). Structure of the plant alternative oxidase. Site-directed mutagenesis provides new information on the active site and membrane topology. *J. Biol. Chem*. 277: 1190-1194.

Almagro, A., Prista, C., Castro, S., Quintas, C., Madeira-Lopes, A., Ramos, J. y Loureiro-Dias M. C. (2000). Effects of salts on *Debaryomyces hansenii* and *Saccharomyces cerevisiae* under stress conditions. *Int. J. Food Microbiol*. 56: 191–197.

Avéret, N., Fitton, V., Bunoust, O., Rigoulet, M. y Guérin, B. (1998). Yeast mitochondrial metabolism: from in vitro to in situ quantitative study. *Mol. Cell. Biochem.* 184: 67-79.

Azzone, G. F., Zoratti, M. Petronilli, V. y Pietrobon, D. (1985). The stoichiometry of H^+ pumping in cytochrome oxidase and the mechanism of uncoupling. *J. Inorg. Biochem*. 23: 349-356.

Baines, C. P., Kaiser, R. A., Purcell, N. H., Blair, N. S., Osinska, H., Hambleton, M. A., Brunskill, E. W., Sayen, M. R., Gottlieb, R. A., Dorn, G. W., Robbins, J. y Molkentin, J. D. (2005). Loss of cyclophilin D reveals a critical role for mitochondrial permeability transition in cell death. *Nature.* 434: 658-662.

Berden, J. A. y Slater E. C. (1970). The reaction of antimycin with a cytochrome *b* preparation active in reconstitution of the respiratory chain. *Biochim. Biophys. Acta* 216: 237-249.

Bernardi, P. y Petronilli, V. (1996). The permeability transition pore as a mitochondrial calcium release channel: a critical appraisal. *J. Bioenerg. Biomembr.* 28: 131-138.

Bernardi, P., Broekemeier, K. M., y Pfeiffer, D. R. (1994). Recent progress on regulation of the mitochondrial permeability transition pore; a cyclosporin-sensitive pore in the inner mitochondrial membrane. *J. Bioenerg. Biomembr*. 26: 509-517.

Bernardi, P., Rasola, A., Forte M. y Lippe, G. (2015). The Mitochondrial Permeability Transition Pore: Channel Formation by F-ATP Synthase, Integration in Signal Transduction, and Role in Pathophysiology. *Physiol. Rev.* 95: 1111-1155.

Beutner, G., Ruck, A., Riede, B., y Brdiczka, D. (1998). Complexes between porin, hexokinase, mitochondrial creatine kinase and adenylate translocator display properties of the permeability transition pore. Implication for regulation of permeability transition by the kinases. *Biochim. Biophys. Acta* 1368: 7-18.

Bianchi, C., Genova M. L., Parenti Castelli, G. y Lenaz, G. (2004). The mitochondrial respiratory chain is partially organized in a supercomplex assembly: kinetic evidence using flux control analysis. *J. Biol. Chem.* 279: 36562-36569.

Boldogh, I. R. y Pon, L. A. (2006). Interactions of mitochondria with the actin cytoskeleton. *Biochim. Biophys. Acta* 1763: 450-462.

Boyer, P. D. (2002). Catalytic site occupancy during ATP synthase catalysis. *FEBS Lett*. 512: 29-32.

Bradshaw, P.C. y Pfeiffer D.R. (2006). Loss of NAD(H) from swollen yeast mitochondria. *BMC Biochemistry* 7: 3.

Brandt, U. (2006). Energy converting NADH:quinone oxidoreductase (complex I). *Annu. Rev. Biochem*. 75: 69-92.

Brandt, U., Kerscher, S., Dröse, S., Zwicker, K. y Zickermann, V. (2003). Proton pumping by NADH:ubiquinone oxidoreductase. A redox driven conformational change mechanism? *FEBS Letters* 545: 9-17.

Braun, H. P. y Schmitz, U. K. (1995). Are the "core" proteins of the mitocondrial bc_1 complex evolutionary relics of a processing protease?. *Trends Biochem. Sci*. 20: 171-175.

Breuer, U. y Harms, H. (2006). *Debaryomyces hansenii* – an extremophilic yeast with biotechnological potential. *Yeast* 23: 415-437.

Cabrera-Orefice, A, Chiquete-Félix, N, Espinasa-Jaramillo, J, Rosas-Lemus, M, Guerrero-Castillo S, Peña A, Uribe-Carvajal, S. (2014). The branched mitochondrial respiratory chain from *Debaryomyces hansenii*: Components and supramolecular organization. *Biochim. Biophys. Acta* 1837: 73-84.

Cabrera-Orefice, A., Guerrero-Castillo, S., Luevano-Martinez, L.A., Peña A. y Uribe-Carvajal, S. (2010). Mitochondria from the salt-tolerant yeast *Debaryomyces hansenii* (halophilic organelles?), *J. Bioenerg. Biomembr.* 42: 11-19.

Carraro, M., Giorgio, V., Šileikytė, J., Sartori, G., Forte, M., Lippe, G., Zoratti, M., Szabò, I. y Bernardi, P. (2014). Channel formation by yeast F-ATP synthase and the role of dimerization in the mitochondrial permeability transition. *J. Biol. Chem*. 289: 15980-15985.

Chacinska, A., Koehler, C. M., Milenkovic, D., Lithgow, T. y Pfanner, N. (2009). Importing mitochondrial proteins: machineries and mechanisms. *Cell* 138: 628-44.

Chelstowska A., Z. Liu, Y. Jia, D. Amberg, R.A. Butow. (1999). Signalling between mitochondria and the nucleus regulates the expression of a new D-lactate dehydrogenase activity in yeast. *Yeast* 15: 1377-1391.

Chen, C., Ko, Y., Delannoy, M., Ludtke, S. J., Chiu, W. y Pedersen, P. L. (2004). Mitochondrial ATP synthasome: three-dimensional structure by electron microscopy of the ATP synthase in complex formation with carriers for Pi and ADP/ATP. *J. Biol. Chem.* 279: 31761-31768.

Cooney, G.J., Taegtmeyer, H. y Newsholme, E.A. (1981). Tricarboxylic acid cycle flux and enzyme activities in the isolated working rat heart. *Biochemical J.* 200: 701-703.

Cortés, P., Castrejón, V., Sampedro, J.G. y Uribe, S. (2000). Interactions of arsenate, sulfate and phosphate with yeast mitochondria. *Biochim. Biophys. Acta* 1456: 67-76.

Couoh-Cardel, S. J., Uribe-Carvajal S., Wilkens, S. y García-Trejo, J.J. (2010). Structure of dimeric F_1F_0-ATP synthase. *J. Biol. Chem.* 285: 36447-36455.

Covian, R. y Trumpower, B. L. (2005). Rapid electron transfer between monomers when the cytochrome bc_1 complex dimer is reduced through center N. *J. Biol. Chem*. 280: 22732-22740.

Crompton, M., Costi, A. y Hayat, L. (1987). Evidence for the presence of a reversible Ca^{2+}-dependent pore activated by oxidative stress in heart mitochondria. *Biochem J.* 245: 915-918.

Crompton, M., Virji, S. y Ward, J. M. (1998). Cyclophilin-D binds strongly to complexes of the voltage-dependent anion channel and the adenine nucleotide translocase to form the permeability transition pore. *Eur. J. Biochem*. 258: 729-735.

Crompton, M., Virji, S., Doyle, V., Johnson, N. y Ward, J. M. (1999). The mitochondrial permeability transition pore. *Biochem. Soc. Symp*. 66: 167-179.

Darrouzet, E., Moser, C. C., Dutton, P. L. y Daldal, F. (2001). Large scale domain movement in cytochrome bc_1: a new device for electron transfer in proteins. *Trends in Biochem. Sci*. 26: 445-451.

Dassa, E. P., Dufour, E., Goncalves, S., Jacobs, H. T. y Rustin, P. (2009). The alternative oxidase, a tool for compensating cytochrome *c* oxidase deficiency in human cells. *Physiol. Plant.* 137: 427-434.

Day, D.A. y Wiskich, J.T. (1995). Regulation of alternative oxidase activity in higher plants. *J. Bioenerg. Biomembr.* 27: 379-385.

de Vries, S. y Grivell, L. A. (1988). Purification and characterization of a rotenone-insensitive NADH:Q6 oxidoreductase from mitochondria of *Saccharomyces cerevisiae. Eur. J. Biochem*. 176: 377-384.

DeJean, L., Beauvoit, B., Guérin, B. y Rigoulet, M. (2000). Growth of the yeast *Saccharomyces cerevisiae* on a non-fermentable substrate: control of energetic yield by the amount of mitochondria. *Biochim. Biophys. Acta*. 1457: 45-56.

Dudkina N.V., Heinemeyer J., Sunderhaus S., Boekema E.J. y Braun H.P. (2006). Respiratory chain supercomplexes in the plant mitochondrial membrane. *Trends Plant Sci*. 11: 232-240.

Dujon, B., Sherman, D., Fischer, G., Durrens, P., Casaregola, S., Lafontaine, I., De Montigny, J., Marck, C., Neuvéglise, C., Talla, E., Goffard, N., Frangeul, L., Aigle, M., Anthouard, V., Babour, A., Barbe, V., Barnay, S., Blanchin, S., Beckerich, J. M., Beyne, E., Bleykasten, C., Boisramé, A., Boyer, J., Cattolico, L., Confanioleri, F., De Daruvar, A., Despons, L., Fabre, E., Fairhead, C., Ferry-Dumazet, H., Groppi, A., Hantraye, F., Hennequin, C., Jauniaux, N., Joyet, P., Kachouri, R., Kerrest, A., Koszul, R., Lemaire, M., Lesur, I., Ma, L., Muller, H., Nicaud, J. M., Nikolski, M., Oztas, S., Ozier-Kalogeropoulos, O., Pellenz, S., Potier, S., Richard, G. F., Straub, M. L., Suleau, A., Swennen, D., Tekaia, F., Wésolowski-Louvel, M., Westhof, E., Wirth, B., Zeniou-Meyer, M., Zivanovic, I., Bolotin-Fukuhara, M., Thierry, A., Bouchier, C., Caudron, B., Scarpelli, C., Gaillardin, C., Weissenbach, J., Wincker, P. y Souciet, J. L. (2004). Genome evolution in yeasts. *Nature*. 430: 35-44.

Dumas, L. Argaud, C. Cottet-Rousselle, G. Vial, C. Gonzalez, D. Detaille, X. Leverve, E. Fontaine (2009). Effect of transient and permanent permeability transition pore opening on NAD(P)H localization in intact cells. *J. Biol. Chem*. 284: 15117-15125.

Efremov, R. G. y Sazanov L. A. (2011). Structure of the membrane domain of respiratory complex I. *Nature* 476: 414-420.

El-Khoury, R., Dufour, E., Rak, M., Ramanantsoa, N., Grandchamp, N., Csaba, Z., Duvillie, B., Benit, P., Gallego, J., Gressens, P., Sarkis, C., Jacobs, H. T. y Rustin, P. (2013). Alternative oxidase expression in the mouse enables bypassing cytochrome *c* oxidase blockade and limits mitochondrial ROS overproduction. *PLoS Genet.* 9: e1003182.

Eubel, H., Jansch L. y Braun H. P. (2003). New insights into the respiratory chain of plant mitochondria. Supercomplexes and a unique composition of complex II. *Plant Physiol.* 133: 274-286.

Fadda, M. E., Mossa, V., Pisano, M. B., Deplano, M. y Cosentino, S. (2004). Occurrence and characterization of yeasts isolated from artisanal Fiore Sardo cheese. *Int. J. Food Microbiol.* 95: 51-59.

Ferguson, S. J. (2010). ATP synthase: From sequence to ring size to the P/O ratio. *Proc. Natl. Acad. Sci.* 107: 16755–16756.

Frank, J. (2011). Molecular Machines in Biology – Workshop of the Cell. Cap. 11. Cambridge University Press.

Frank, V. y Kadenbach B. (1996). Regulation of the H^+/e^- stoichiometry of cytochrome *c* oxidase from bovine heart by intramitochondrial ATP/ADP ratios. *FEBS Lett.* 382: 121-124.

Frey, T. G. y Mannella, C. (2000). The internal structure of mitochondria. *Trends Biochem. Sci*. 25: 319-324.

Galkin, A. y Brandt U. (2005). Superoxide radical formation by pure complex I (NADH:ubiquinone oxidoreductase) from *Yarrowia lipolytica. J. Biol. Chem*. 280: 30129-30135.

Gilkerson, R. W., Selker, J. M. y Capaldi, R. A. (2003). The crystal membrane of mitochondria is the principal site of oxidative phosphorylation. *FEBS Lett*. 546: 355-358.

González-Hernández, J. C. y Peña, A. (2002). Estrategias de adaptación de microorganismos halófilos y *Debaryomyces hansenii* (levadura halófila). *Rev. Latinoam. Microbiol*. 44 (3-4): 137-156.

González-Hernández, J. C., Cárdenas-Monroy C. A. y Peña, A. (2004). Sodium and potassium transport in the halophilic yeast *Debaryomyces hansenii*. *Yeast* 21: 403-412.

Gonzalez-Meler, M. A., Ribas-Carbo, M., Giles, L. y Siedow, J. N. (1999). The effect of growth and measurement temperature on the activity of the alternative respiratory pathway. *Plant Physiol*. 120: 765-772.

Gornal, A. G., Bardavill, C. J. y David, M. M. (1949). Determination of serum protein by means of the biuret reaction. *J. Biol. Chem*. 177: 751-760.

Guerrero-Castillo, S., Araiza-Olivera, D., Cabrera-Orefice, A., Espinasa-Jaramillo, J., Gutierrez-Aguilar, M., Luevano-Martinez, L.A., Zepeda-Bastida, A. y Uribe-Carvajal, S. (2011). Physiological uncoupling of mitochondrial oxidative phosphorylation. Studies in different yeast species. *J. Bioenerg. Biomembr*. 43: 323-331.

Guerrero-Castillo, S., Vázquez-Acevedo, M., González-Halphen, D. y Uribe-Carvajal, S. (2009). In *Yarrowia lipolytica* mitochondria, the alternative NADH dehydrogenase interacts specifically with the cytochrome complexes of the classic respiratory pathway. *Biochim. Biophys. Acta*. 1787: 75-85

Guo, J. y Lemire, B. D. (2003). The ubiquinone-binding site of the *Saccharomyces cerevisiae* succinate-ubiquinone oxidoreductase is a source of superoxide. *J. Biol. Chem*. 278: 47629-47635.

Gutiérrez-Aguilar, M., Pérez-Martínez, X., Chávez, E. y Uribe-Carvajal S. (2009). In *Saccharomyces cerevisiae*, the phosphate carrier is a component of the mitochondrial unselective channel. *Arch. Biochem. Biophys*. 494 (2): 184-191.

Gutiérrez-Aguilar, M., Pérez-Vázquez, V., Bunoust, O., Manon, S., Rigoulet, M. y Uribe, S. (2007). In yeast, Ca^{2+} and octylguanidine interact with porin (VDAC) preventing the mitochondrial permeability transition. *Biochim. Biophys. Acta*. 1767: 1245-1251.

Hackenbrock, C.R., Chazotte, B. y Gupte, S.S. (1986). The random collision model and a critical assessment of diffusion and collision in mitochondrial electron transport. *J. Bioenerg. Biomembr*. 18: 331-368.

Hagerhall, C. (1997). Succinate:quinone oxidoreductases. Variations on a conserved theme. *Biochim. Biophys. Acta*. 1320: 107-141.

Hakkaart, G. A., Dassa, E. P., Jacobs, H. T. y Rustin, P. (2006). Allotopic expression of a mitochondrial alternative oxidase confers cyanide resistance to human cell respiration. *EMBO Rep.* 7: 341-345.

Halestrap, A. P. (1991). Calcium-dependent opening of a non-specific pore in the mitochondrial inner membrane is inhibited at pH values below 7. Implications for the protective effect of low pH against chemical and hypoxic cell damage. *Biochem. J.* 278: 715-719.

Halestrap, A. P. y Brennerb, C. (2003). The adenine nucleotide translocase: a central component of the mitochondrial permeability transition pore and key player in cell death. *Curr. Med. Chem.* 10: 1507-1525.

Hatefi, Y., Haavik, A. G. y Griffiths D. E. (1962). Studies on the electron transfer system. XLI. Reduce coenzyme Q (QH_2)-cytochrome *c* reductase. *J. Biol. Chem*. 237: 1681-1685.

Hederstedt, L. y Ohnishi, T. (1992). Molecular Mechanisms in Bioenergetics (Ernster, L.). Elsevier Science Publishers, New York. págs. 163-197.

Hinchliffe, P. y Sazanov, L. A. (2005). Organization of the iron-sulfur clusters in respiratory complex I. *Science* 309: 771-774.

Hirano, M. y Vu, T. H. (2000). Defects of intergenomic communication: where do we stand? *Brain Pathology* 10: 451-461.

Hobot, J. A. y Jennings, D. H. (1981). Growth of *Debaryomyces hansenii* and *Saccharomyces cerevisiae* in relation to pH and salinity. *Exp. Mycol*. 5: 217-228.

Iwata, S., Ostermeier, C., Ludwig, B. y Michel, H. (1995). Structure at 2.8 Å resolution of cytochrome *c* oxidase from *Paracoccus denitrificans*. *Nature*. 376: 660-669.

Jiménez-Suárez, A., Vazquez-Acevedo, M., Rojas-Hernandez A., Funes S., Uribe-Carvajal S., Gonzalez-Halphen D. (2012). In *Polytomella* sp. mitochondria, biogenesis of the heterodimeric COX2 subunit of cytochrome *c* oxidase requires two different import pathways. *Biochim. Biophys. Acta* 1817: 819-827.

Joseph-Horne, T., Hollomon, D. W. y Wood, P. M. (2001). Fungal respiration: a fusion of standard and alternative components. *Biochim. Biophys. Acta*. 1504: 179-195.

Juárez, O., Guerra, G., Martínez, F., Pardo, J. P. (2004). The mitochondrial respiratory chain of *Ustilago maydis*. *Biochim. Biophys. Acta*. 1658: 244-251.

Jung, D. W., Bradshaw, P. C. y Pfeiffer, D. R. (1997). Properties of a cyclosporin-insensitive permeability transition pore in yeast mitochondria. *J. Biol. Chem*. 272: 21104-21112.

Kerscher, S., Dröse, S., Zickermann, V. y Brandt, U. (2008). The three families of respiratory NADH dehydrogenases. *Results Probl. Cell Differ*. 45: 185-222.

Koshkin, V., X. Wang, Scherer, P. E., Chan, C. B. y Wheeler, M. B. (2003). Mitochondrial functional state in clonal pancreatic beta-cells exposed to free fatty acids. *J. Biol. Chem*. 278: 19709-19715.

Krause, F., Reifschneider, N. H., Vocke, D., Seelert, H., Rexroth, S. y Dencher, N. A. (2004). Respirasome-like supercomplexes in green leaf mitochondria of spinach. *J Biol Chem* 279: 48369-48375.

Kroemer, G., Petit, P., Zamzami, N., Vayssière, J. L. y Mignotte, B. (1995). The biochemistry of programmed cell death. *FASEB J*. 9: 1277-1287.

Lambers, H. (1980). The physiological significance of the cyanide-resistant respiration in higher plants. *Plant Cells Env*. 3: 293-302.

Lambers, H. (1982). Cyanide-resistant respiration: a nonphosphorylating electron transport pathway acting as an energy flow. *Physiologia Plantarum* 55: 478-485.

Lapuente-Brun E, Moreno-Loshuertos R, Acín-Pérez R, Latorre-Pellicer A, Colás C, Balsa E, Perales-Clemente E, Quirós PM, Calvo E, Rodríguez-Hernández MA, Navas P, Cruz R, Carracedo Á, López-Otín C, Pérez-Martos A, Fernández-Silva P, Fernández-Vizarra E y Enríquez JA. (2013). Supercomplex assembly determines electron flux in the mitochondrial electron transport chain. *Science*. 340: 1567-1570.

Lemire, B. D. y Oyedotun, K. S. (2002). The *Saccharomyces cerevisiae* mitocondrial succinate:ubiquinone oxidoreductase. *Biochim. Biophys. Acta*. 1553: 102-116.

Leung, A. W., Varanyuwatana, P. y Halestrap, A. P. (2008). The mitochondrial phosphate carrier interacts with cyclophilin D and may play a key role in the permeability transition. *J. Biol. Chem*. 283: 26312-26323.

Luévano-Martinez L.A., Moyano E., de Lacoba M.G, Rial E. y Uribe-Carvajal S. (2010). Identification of the mitochondrial carrier that provides *Yarrowia lipolytica* with a fatty acid-induced and nucleotide-sensitive uncoupling protein-like activity. *Biochim. Biophys. Acta*, 1797: 81-88.

Lutter, R., Abrahams, J. P., van Raaij, M. J, Todd, R. J., Lundqvist, T., Buchanan, S. K., Leslie, A. G. y Walker, J. E. (1993). Crystallization of F_1-ATPase from bovine heart mitochondria. *J. Mol. Biol.* 229: 787-790.

Mannella, C. A. (2006). Structure and dynamics of the mitochondrial inner membrane cristae. *Biochim. Biophys. Acta* 1763: 542-548.

Mannella, C. A., Pfeiffer, D. R., Bradshaw, P. C., Moraru, I. I., Slepchenko, B., Loew, L. M., Hsieh, C. E., Buttle, K. y Marko, M. (2002). Topology of the mitochondrial inner membrane: dynamics and bioenergetic implications. *IUBMB Life*. 52: 93-100.

Manon, S. y Guérin, M. (1997). The ATP-induced K^+-transport pathway of yeast mitochondria may function as an uncoupling pathway. *Biochim. Biophys. Acta* 1318: 317-321.

Manon, S., Roucou, X., Guerin, M., Rigoulet, M. y Guerin, B. (1998). Characterization of the yeast mitochondria unselective channel: a counterpart to the mammalian permeability transition pore? *J. Bioenerg. Biomembr.* 30: 419-429.

Manon, S., y Guérin, M. (1998). Investigation of the yeast mitochondrial unselective channel in intact and permeabilized spheroplasts. *Biochem. Mol. Biol. Int.* 44: 565-575.

Matsukawa, K., Kamata, T. e Ito, K. (2009). Functional expression of plant alternative oxidase decreases antimycin A-induced reactive oxygen species production in human cells. *FEBS Lett.* 583: 148-152.

Medentsev, A. G., Arinbasarova A. Y., y Akimenko, V.K. (1999). Regulation and physiological role of cyanide-resistant oxidases in fungi and plants. *Biochemistry (Mosc)* 64: 1230-1243.

Medentsev, A. G., Y. Arinbasarova A. y Akimenko, V.K. (2004). Reactivation of the alternative oxidase of *Yarrowia lipolytica* by nucleoside monophosphates. *FEMS Yeast Res* 5: 231-236.

Mitchell, P. (1961). Coupling of phosphorylation to electron and hydrogen transfer by a chemi-osmotic type of mechanism. *Nature* 191: 144-148.

Mitchell, P. (1966). Chemiosmotic coupling in oxidative and photosynthetic phosphorylation. *Biol. Rev. Camb. Philos. Soc*. 41: 445-502.

Moore, A. L. y Siedow, J. N. (1991). The regulation and nature of the cyanide-resistant alternative oxidase of plant mitochondria. *Biochim. Biophys. Acta*. 1059: 121-140.

Mourier A., J. Vallortigara, E.D. Yoboue, M. Rigoulet, A. Devin (2008). Kinetic activation of yeast mitochondrial D-lactate dehydrogenase by carboxylic acids. *Biochim. Biophys. Acta* 1777:1283-1288.

Nelson, D. L. y Cox M. M. (2000). Lehninger Principles of Biochemistry, 3a. Ed, Cap. 19. W. H. Freeman.

Nicholls, D. G. y Ferguson, S. J. (2002). Bioenergetics, 3a. Ed, Cap. 5. Academic Press.

Norkrans, B. (1966). Studies on marine occurring yeasts: growth related to pH, NaCl concentration and temperature. *Arch. Mikrobiol*. 54: 374-392.

Norkrans, B. y Kylin, A. (1969). Regulation of potassium to sodium ratio and of the osmotic potential in relation to salt tolerance in yeasts. *J. Bacteriol*. 100: 836-845.

Ohnishi, T., Sled, V. D., Yano, T., Yagi, T., Burbaev, D.S. y Vinogradov AD. (1998). Structure-function studies of iron-sulfur clusters and semiquinones in the NADH-Q oxidoreductase segment of the respiratory chain. *Biochim. Biophys. Acta* 1365: 301-308.

Palmieri F., B. Rieder, A. Ventrella, E. Blanco, P.T. Do, A. Nunes-Nesi, A.U. Trauth, G. Fiermonte, J. Tjaden, G. Agrimi, S. Kirchberger, E. Paradies, A.R. Fernie, H.E. Neuhaus (2009). Molecular identification and functional characterization of Arabidopsis thaliana mitochondrial and chloroplastic NAD^+ carrier proteins. *J. Biol. Chem*. 284: 31249-31259.

Palmieri F., C.L. Pierri, A. De Grassi, A. Nunes-Nesi, A.R. Fernie, (2011) Evolution, structure and function of mitochondrial carriers: a review with new insights. *The Plant journal: for cell and molecular biology* 66: 161-181.

Palmieri F., G. Agrimi, E. Blanco, A. Castegna, M.A. Di Noia, V. Iacobazzi, F.M. Lasorsa, C.M. Marobbio, L. Palmieri, P. Scarcia, S. Todisco, A. Vozza, J. Walker (2006). Identification of mitochondrial carriers in *Saccharomyces cerevisiae* by transport assay of reconstituted recombinant proteins. *Biochim. Biophys. Acta* 1757: 1249-1262.

Paumard, P., Vaillier J., Coulary, B., Schaeffer, J., Soubannier. V., Mueller, D.M., Brèthes, D., di Rago, J.P. y Velours, J. (2002). The ATP synthase is involved in generating mitochondrial cristae morphology. *EMBO J*. 21: 221-230.

Pérez-Vázquez, V., Saavedra-Molina, A. y Uribe, S. (2003). In *Saccharomyces cerevisiae*, cations control the fate of the energy derived from oxidative metabolism through the opening and closing of the yeast mitochondrial unselective channel. *J. Bioenerg. Biomembr*. 35(3): 231-241.

Pfanner, N. y Meijer, M. (1997). Mitochondrial biogenesis: The Tom and Tim machine. *Current Biology* 7: R100-R103.

Pogoryelov, D., Yu, J., Meier, T., Vonck, J., Dimroth, P., Muller, D.J. (2005). The c15 ring of the *Spirulina platensis* F-ATP synthase: F_1/F_0 symmetry mismatch is not obligatory. *EMBO Rep.* 6: 1040-1044.

Popov, V. N., Simonian R. A., Skulachev, V. P., Starkov, A. A. (1997). Inhibition of the alternative oxidase stimulates H_2O_2 production in plant mitochondria. *FEBS Lett.* 415: 87-90.

Prista, C., Almagro, A., Loureiro-Dias, M. C. y Ramos, J. (1997). Physiological basis for the high tolerance of *Debaryomyces hansenii*. *Appl. Environ. Microbiol*. 63: 4005-4009.

Prista, C., Loureiro-Dias, M. C., Montiel V, García, R. y Ramos, J. (2005). Mechanisms underlying the halotolerant way of *Debaryomyces hansenii*. *FEMS Yeast Res*. 5: 693-670.

Rigoulet M., A. Mourier, A. Galinier, L. Casteilla, A. Devin (2010). Electron competition process in respiratory chain: regulatory mechanisms and physiological functions. *Biochim. Biophys. Acta* 1797: 671-677.

Rogov, A. G., Sukhanova, E. I., Uralskaya, L. A., Aliverdieva, D. A. y Zvyagilskaya, R. A. Alternative oxidase: distribution, induction, properties, structure, regulation, and functions. (2014) *Biochemistry (Mosc).* 79: 1615-1634.

Rostovtseva, T. K., Tan, W. y Colombini, M. (2005). On the role of VDAC in apoptosis: fact and fiction. *J. Bioenerg. Biomembr*. 37: 129-142.

Rottenberg, H., Covian R. y Trumpower B. L. (2009). Membrane potential greatly enhances superoxide generation by the cytochrome bc_1 complex reconstituted into phospholipid vesicles. *J. Biol. Chem*. 284: 19203-19210.

Sánchez, N. S., Arreguín, R., Calahorra, M. y Peña, A. (2008). Effects of salts on aerobic metabolism of *Debaryomyces hansenii*. *FEMS Yeast Res*. 8: 1303-1312.

Sánchez, N. S., Calahorra M., González-Hernández, J.C. y Peña, A. (2006). Glycolytic sequence and respiration of *Debaryomyces hansenii* as compared to *Saccharomyces cerevisiae*. *Yeast* 23: 361-374.

Schafer, E., Dencher N. A., Vonck, J. y Parcej, D.N. (2007). Three-dimensional structure of the respiratory chain supercomplex $I_1III_2IV_1$ from bovine heart mitochondria. *Biochemistry* 46: 12579-12585.

Schägger H. (2001). Respiratory chain supercomplexes. *IUBMB Life*. 52:119-128.

Schägger H. y Pfeiffer K. (2000). Supercomplexes in the respiratory chains of yeast and mammalian mitochondria. *EMBO J.* 19: 1777–1783.

Schägger H. y von Jagow G. (1991). Blue native electrophoresis for isolation of membrane protein complexes in enzymatically active form. *Anal. Biochem*. 199: 223–231.

Sherman, D. J., Martin, T., Nikolski, M., Cayla, C., Souciet, J. L. y Durrens, P. (2009). Génolevures: protein families and synteny among complete hemiascomycetous yeast proteomes and genomes. *Nucleic Acids Res*. 37: D550-D554.

Shiba, T., Kido, Y., Sakamoto, K., Inaoka, D. K., Tsuge, C., Tatsumi, R., Takahashi, G., Balogun, E. O., Nara, T., Aoki, T., Honma, T., Tanaka, A., Inoue, M., Matsuoka, S., Saimoto, H., Moore, A. L., Harada, S., y Kita, K. (2013). Structure of the trypanosome cyanide-insensitive alternative oxidase, *Proc. Natl. Acad. Sci. USA*, 110: 4580-4585.

Siedow, J. N. y Umbach, A. L. (2000). The mitochondrial cyanide-resistant oxidase: structural conservation amid regulatory diversity. *Biochim. Biophys. Acta*. 1459: 432-439.

Stock, D., Gibbons, C., Arechaga, I., Leslie, A. G. y Walker, J. E. (2000). The rotary mechanism of ATP synthase. *Curr. Opin. Struct. Biol*. 10: 672-679.

Thomé-Ortiz, P., Peña, A. y Ramírez, J. (1998). Monovalent cation fluxes and physiological changes of *Debaryomyces hansenii* grown at high concentrations of KCl and NaCl. *Yeast* 14: 1355-1371.

Todisco S., G. Agrimi, A. Castegna, F. Palmieri (2006). Identification of the mitochondrial NAD^+ transporter in *Saccharomyces cerevisiae*. *J. Biol. Chem*. 281: 1524-1531.

Todisco, S., Agrimi, G., Castegna A. y Palmieri F. (2006). Identification of the mitochondrial NAD^+ transporter in *Saccharomyces cerevisiae*. *J. Biol. Chem*. 281: 1524-1531.

Tsukihara, T., Aoyama, H., Yamashita, E., Tomizaki, T., Yamaguchi, H., Shinzawa-Itoh, K., Nakashima, R., Yaono, R. y Yoshikawa, S. (1995). Structures of metal sites of oxidized bovine heart cytochrome *c* oxidase at 2.8 Å. *Science* 269: 1069-1074.

Uribe-Carvajal, S., Luevano-Martinez, L.A., Guerrero-Castillo, S., Cabrera-Orefice, A., Corona-de-la-Pena, N.A. y Gutierrez-Aguilar, M. (2011). Mitochondrial Unselective Channels throughout the eukaryotic domain. *Mitochondrion* 11: 382-390.

Vanlerberghe, G. C., Vanlerberghe, A. E., y McIntosh, L. (2011). Molecular genetic evidence of the ability of alternative oxidase to support respiratory carbon metabolism, *Plant Physiol.* 113: 657-661.

Veiga, A., Arabaça, J. D. y Loureiro-Dias, M. C. (2003a). Cyanide-resistant respiration, a very frequent metabolic pathway in yeasts. *FEMS Yeast. Res*. 3: 239-245.

Veiga, A., Arrabaça, J. D. y Loureiro-Dias, M. C. (2003b). Stress situations induce cyanide-resistant respiration in spoilage yeasts. *J. Appl. Microbiol*. 95: 364-371.

Veiga, A., Arrabaça, J. D., Sansonetty, F., Ludovico P., Corte-Real, M. y Lourerio-Dias M. C. (2003c). Energy conversion coupled to cyanide-resistant respiration in the yeasts *Pichia membranifaciens* and *Debaryomyces hansenii*. *FEMS Yeast Res*. 3: 141–148.

von Stockum, S., Giorgio, V., Trevisan, E., Lippe, G., Glick, G. D., Forte, M. A., Da-Rè, C., Checchetto, V., Mazzotta, G., Costa, R., Szabò, I. y Bernardi, P. (2015). F-ATPase of Drosophila melanogaster forms 53-picosiemen (53-pS) channels responsible for mitochondrial Ca^{2+}-induced Ca^{2+} release. *J. Biol. Chem.* 2015. 290: 4537-4544.

Walker, J. E. (1992). The NADH:ubiquinone oxidoreductase (complex I) of respiratory chains. *Q. Rev. Biophys.* 25: 253-324.

Walker, R. Jr., Saha, L., Hill, G. C. y Chaudhuri, M. (2005). The effect of over-expression of the alternative oxidase in the procyclic forms of *Trypanosoma brucei*. *Mol. Biochem. Parasitol.* 139: 153-162.

Wallace, P. G., Pedler, S. M., Wallace, J.C. y Berry, M.N. (1994). A method for the determination of the cellular phosphorylation potential and glycolytic intermediates in yeast. *Anal Biochem.* 222: 404-408.

Watt, I.N., Montgomery, M.G., Runswick, M.J., Leslie, A.G. y Walker, J.E. (2010). Bioenergetic cost of making an adenosine triphosphate molecule in animal mitochondria. *Proc. Natl. Acad. Sci.* 107: 16823–16827.

Wittig I., Karas M. y Schägger H., (2007). High resolution clear native electrophoresis for in-gel functional assays and fluorescence studies of membrane protein complexes. *Mol. Cell. Proteomics* 6: 1215–1225.

Wittig, I., Carrozzo R., Santorelli, F.M y Schägger, H. (2006). Supercomplexes and subcomplexes of mitochondrial oxidative phosphorylation. *Biochim. Biophys. Acta* 1757: 1066-1072.

Yamada, A., Yamamoto, T., Yoshimura, Y., Gouda, S., Kawashima, S., Yamazaki, N., Yamashita, K., Kataoka, M., Nagata, T., Terada, H., Pfeiffer, D. R. y Shinohara, Y. (2009). Ca^{2+}-induced permeability transition can be observed even in yeast mitochondria under optimized experimental conditions. *Biochim. Biophys. Acta*. 1787:1486-91.

Yonetani, T. (1960). Studies on cytochrome oxidase. I. Absolute and difference absorption spectra. *J. Biol. Chem*. 235: 845-852.

Yoshikawa, S. y Caughey, W. S. (1990). Infrared evidence of cyanide binding to iron and copper sites in bovine heart cytochrome *c* oxidase. Implications regarding oxygen reduction. *J. Biol. Chem.* 265: 7945-7958.

Zamzami, N. y Kroemer, G. (2001). The mitochondrion in apoptosis: how Pandora's box opens. *Nature Rev. Mol. Cell Biol*. 2: 67-71.

Zoratti, M. y Szabo, I. (1995). The mitochondrial permeability transition. *Biochim. Biophys. Acta* 1241: 139-176.

ANEXO

Articulos publicados:

- Cabrera-Orefice A, Guerrero-Castillo S, Luévano-Martínez LA, Peña A, Uribe-Carvajal S. (2010) Mitochondria from the salt-tolerant yeast *Debaryomyces hansenii* (halophilic organelles?). *J Bioenerg Biomembr*. 42(1): 11-9.

- Uribe-Carvajal S, Luévano-Martínez LA, Guerrero-Castillo S, Cabrera-Orefice A, Corona-de-la-Peña NA, Gutiérrez-Aguilar M. (2011) Mitochondrial Unselective Channels throughout the eukaryotic domain. *Mitochondrion* 11(3): 382-390.

- Guerrero-Castillo S, Araiza-Olivera D, Cabrera-Orefice A, Espinasa-Jaramillo J, Gutiérrez-Aguilar M, Luévano-Martínez LA, Zepeda-Bastida A, Uribe-Carvajal S. (2011) Physiological uncoupling of mitochondrial oxidative phosphorylation. Studies in different yeast species. *J Bioenerg Biomembr.* 43(3): 323-331.

- Guerrero-Castillo S, Cabrera-Orefice A, Vázquez-Acevedo M, González-Halphen D, Uribe-Carvajal S. (2012). During the stationary growth phase, *Yarrowia lipolytica* prevents the overproduction of reactive oxygen species by activating an uncoupled mitochondrial respiratory pathway. *Biochim Biophys Acta* 1817(2): 353-362.

- Cabrera-Orefice A, Chiquete-Félix N, Espinasa-Jaramillo J, Rosas-Lemus M, Guerrero-Castillo S, Peña A, Uribe-Carvajal S. (2014). The branched mitochondrial respiratory chain from *Debaryomyces hansenii*: Components and supramolecular organization. *Biochim Biophys Acta* 1837(1): 73-84.

- Cabrera-Orefice A, Guerrero-Castillo S, Díaz-Ruíz R, Uribe-Carvajal S. (2014). Oxidative phosphorylation in *Debaryomyces hansenii*: Physiological uncoupling at different growth phases. *Biochimie* 102: 124-136.

- Emilio Espinoza Simón, Mónica Rosas Lemus, Alfredo Cabrera Orefice, Cristina Uribe Álvarez, Natalia Chiquete Félix, Salvador Uribe Carvajal. (2014). Oxígeno, para bien y para mal. *Revista de la Facultad de Medicina* Vol. 57, No. 6.

J Bioenerg Biomembr (2010) 42:11–19
DOI 10.1007/s10863-009-9264-0

Mitochondria from the salt-tolerant yeast *Debaryomyces hansenii* (halophilic organelles?)

Alfredo Cabrera-Orefice · Sergio Guerrero-Castillo · Luís A. Luévano-Martínez · Antonio Peña · Salvador Uribe-Carvajal

Received: 3 September 2009 / Accepted: 4 December 2009 / Published online: 21 January 2010

Abstract The yeast *Debaryomyces hansenii* is considered a marine organism. Sea water contains 0.6 M Na^+ and 10 mM K^+; these cations permeate into the cytoplasm of *D. hansenii* where proteins and organelles have to adapt to high salt concentrations. The effect of high concentrations of monovalent and divalent cations on isolated mitochondria from *D. hansenii* was explored. As in *S. cerevisiae*, these mitochondria underwent a phosphate-sensitive permeability transition (PT) which was inhibited by Ca^{2+} or Mg^{2+}. However, *D. hansenii* mitochondria require higher phosphate concentrations to inhibit PT. In regard to K^+ and Na^+, and at variance with mitochondria from all other sources known, these monovalent cations promoted closure of the putative mitochondrial unspecific channel. This was evidenced by the K^+/Na^+-promoted increase in: respiratory control, transmembrane potential and synthesis of ATP. PT was equally sensitive to either Na^+ or K^+. In the presence of propyl-gallate PT was still observed while in the presence of cyanide the alternative pathway was not active enough to generate a $\Delta\Psi$ due to a low AOX activity. In *D. hansenii* mitochondria K^+ and Na^+ optimize oxidative phosphorylation, providing an explanation for the higher growth efficiency in saline environments exhibited by this yeast.

Keywords Branched respiratory chain · Divalent cations · Monovalent cations · *Debaryomyces hansenii* · Isolated mitochondria · Permeability transition

A. Cabrera-Orefice · S. Guerrero-Castillo · L. A. Luévano-Martínez · S. Uribe-Carvajal
Department of Biochemistry, Instituto de Fisiología Celular, Universidad Nacional Autónoma de México, Mexico City, México

A. Peña
Department of Molecular Genetics, Instituto de Fisiología Celular, Universidad Nacional Autónoma de México, Mexico City, México

S. Uribe-Carvajal (✉)
Instituto de Fisiología Celular, Universidad Nacional Autónoma de México, Apdo. Postal 70-242, Ciudad Universitaria, Coyoacán, Mexico City, Mexico
e-mail: suribe@ifc.unam.mx

Introduction

Debaryomyces hansenii is normally found among the microorganisms populating sea waters and other habitats with low water activity where its halotolerance is an advantage (Norkrans 1966; Norkrans and Kylin 1969). This yeast has found diverse biotechnological applications in recent years, such as production of dairy products and of lytic enzymes of commercial interest (Breuer and Harms 2006). In cheese manufacturing, *D. hansenii* is a choice for starter cultures as it catalyzes proteolysis and lipolysis without fermenting sugars (Fadda et al. 2004). This yeast is also attractive for study due to its ability to grow under extreme conditions such as very low temperatures (Norkrans 1966), widely different pHs (Norkrans 1966; Hobot and Jennings 1981) and high salt concentrations (Norkrans 1966, Norkrans and Kylin 1969; Prista et al. 2005; Ramos 2006). The genome of *D. hansenii* was reported by the génolevure project (Sherman et al. 2004).

At least part of the halotolerance of *D. hansenii* may be due to its potent monovalent cation transporters, present both in the plasma membrane (Hobot and Jennings 1981; Prista et al. 1997; Thomé-Ortiz et al. 1998) and in the vacuole (Montiel and Ramos 2007). However, its proteins and enzymes have to be resistant to salts, because in the

presence of high (0.5–1.0 M) external NaCl the cytoplasmic concentrations of monovalent cations (Na^+ and K^+) reach the hundred mM range (Gónzalez-Hernández et al. 2004). Given the choice, *D. hansenii* accumulates KCl instead of NaCl (Norkrans and Kylin 1969; Thomé-Ortiz et al. 1998) but both cations seem to have the same effects on *D. hansenii*, e.g. the expression of NADP-glutamate dehydrogenase and glutamine synthetase is modified by either Na^+ or K^+; this regulation has not been observed in *Saccharomyces cerevisiae* (Alba-Lois et al. 2004). The Na^+/K^+ effect provides an explanation for the increase in biomass obtained when *D. hansenii* is grown in the presence of high salt concentrations (Prista et al. 1997) and fuels the notion that *D. hansenii* is halophilic and not just osmotolerant (Gónzalez-Hernández et al. 2004).

In the cytoplasm of *D. hansenii,* enzymes are not the only structures exposed to high salts. Organelles also have to deal with concentrations around 0.4 M NaCl/KCl (Neves et al. 1997; González-Hernández et al. 2004). Thus, it would be interesting to analyze the physiology and salt adaptability of each organelle. To do this, we decided to characterize the effect of high salt concentrations on the isolated mitochondria from *D. hansenii*. We theorized that the mitochondrial adaptation to high salt concentrations would have to include strict regulation of cation permeability; otherwise, an electrophoretic cycling of the monovalent cation across the inner mitochondrial membrane would result in the depletion of the transmembrane potential ($\Delta\Psi$) and in uncoupling (Garlid 1988). Indeed, in mitochondria isolated from the yeast *S. cerevisiae* addition of increasing concentrations of K^+ or Na^+ in the presence of low phosphate results in depletion of the $\Delta\Psi$ and a decrease in the synthesis of ATP (Castrejón et al. 1997). By contrast, at high phosphate concentrations monovalent cations do not affect the $\Delta\Psi$, and in these conditions a Mg^{2+}- and quinine-sensitive uptake of $^{86}Rb^+$ is observed (Castrejón et al. 2002).

The permeability transition (PT) occurs when a large mitochondrial unspecific channel (MUC) opens in the inner mitochondrial membrane allowing ions to flow freely into and out from the matrix depleting chemical and electrical gradients (Bernardi et al. 1994; Zoratti and Szabo 1995). The most studied MUCs are those from mammalians and from *S. cerevisiae* (Manon et al. 1998). The mammalian MUC is open by Ca^{2+} in the presence of high phosphate and is closed by ATP and the cyclophylin-D inhibitor cyclosporine-A (Halestrap and Davidson 1990). In *S. cerevisiae* mitochondria, both phosphate (Guérin et al. 1994) and Ca^{2+} (Pérez-Vázquez et al. 2003) prevent the PT. Thus, it was of interest to determine whether Ca^{2+} opens or closes the *D. hansenii* MUC. The structure, properties and regulating factors of the MUCs vary between different species (Pavlovskaya et al. 2007; Brustovetsky et al. 2002; Kusano et al. 2009). However, an organelle normally exposed to high monovalent cation concentrations should be able to block its own conductance to the salts found in high concentrations.

The mitochondria from at least two salinity-adapted yeast species, *Endomyces magnusii* and *Yarrowia lipolytica*, do not seem to undergo PT unless a high concentration of Ca^{2+} plus the Ca^{2+} ionophore ETH129 are added (Deryabina et al. 2004; Kovaleva et al. 2009).

We characterized the PT in isolated mitochondria from *D. hansenii.* We detected a MUC which exhibits a sensitivity to Ca^{2+} and Mg^{2+} which was similar to the *S. cerevisiae* channel. Also, the *D. hansenii* MUC was closed by phosphate, although at higher concentrations than the *S. cerevisiae* channel. In addition, we observed that this channel was different to the MUCs from *S. cerevisiae,* plants or mammalians, in that it was regulated by monovalent cations, i.e. increasing concentrations of Na^+ or K^+ closed the *D. hansenii* mitochondrial channel. It is becoming increasingly evident that the physiological role and the control mechanisms of mitochondrial unspecific channels may be different depending of the species under study.

Materials and methods

Chemicals

All chemicals were reagent grade. Sorbitol, Trizma® base, maleic acid, pyruvic acid, malic acid, NADH, NADP, antifoam emulsion, ADP, safranine-O, hexokinase and bovine serum albumin (BSA) type V were from Sigma Chem Co. (St Louis, MO). Lyophilyzed glucose-6-phosphate dehydrogenase was from Boerhinger-Manheim.

Yeast strains The yeast *Debaryomyces hansenii* strain Y7426 (US Dept. of Agriculture) was used throughout this work. The strain was maintained in Na-YPGal (1% yeast extract, 2% bacto-peptone, 2% galactose, 1 M NaCl and 2% bacto-agar) plate cultures.

Yeast growth media for mitochondrial isolation

Cells were grown as follows: three 100 mL pre-cultures were prepared immersing a loophole of yeast into 100 mL of Na-YPLac (1% yeast extract, 2% bacto-peptone, 2% lactate, pH 5.5 adjusted with NaOH plus NaCl to reach a final 0.6 M Na^+ concentration). Antifoam emulsion 50 µL/L was added to the medium. Flasks were incubated for 36 hours under continuous agitation in an orbital shaker at 250 rpm in a constant-temperature room (30°C). Then,

each 100 mL flask was used to inoculate 750 mL of fresh medium. Incubation was continued for 24 h under the same conditions. At a final optical density of 1.6–2.0, the culture was in the mid to late logarithmic growth phase; the cells were harvested at this stage, before they became resistant to disruption.

Isolation of coupled mitochondria from *Debaryomyces hansenii*

D. hansenii cells were collected and washed by centrifugation and suspended in distilled water. After a second centrifugation, the cells were suspended in ice-cold isolating medium containing 1 M sorbitol, 10 mM maleate, 0.2% bovine serum albumin, pH 6.8 (Tris). The cells were poured into a Bead-Beater 300 mL flask containing 70% v/v 0.5-mm-diameter glass beads. The container was introduced in an ice-jacketed chamber and cells were subjected to four 20 s pulses at 2 min intervals. After homogenization, mitochondria were isolated by differential centrifugation following a protocol described for *S. cerevisiae* mitochondria (Peña et al. 1977). The final mitochondrial pellet was resuspended in 500 μL ice-cold isolation medium.

Some details on the isolation of mitochondria seem pertinent as the procedure is slightly different to the usual procedures (Uribe et al. 1985). Sorbitol was deionized before use (Averet et al. 1998). Osmolarity was 1 OsM; lower osmolarities resulted in uncoupled mitochondria. The same osmolarity was used during all experiments. We did not use zymolyase and/or lyticase to disrupt the membrane due to the rapid inactivation of mitochondria that ensues during the isolation procedure. Instead, we used a Bead-Beater with a large amount (70% v/v) of glass beads. The speed of the Bead-Beater was maintained at half maximum by means of a rheostat, to avoid disruption and uncoupling of mitochondria.

Protein quantification

The concentration of mitochondrial protein was determined by the biuret method (Gornal et al. 1949). Optical absorbance was determined at 540 nm in a Beckman DU-50 spectrophotometer. Protein was determined using BSA as a standard.

Oxygen consumption

The rate of oxygen consumption was measured in the resting state (State IV) and in the phosphorylating state (State III), using an YSI-5300 Oxygraph equipped with a Clark-Type electrode (Yellow Springs Instruments Inc. OH) interfaced to a chart recorder. The reaction vessel was a water-jacketed chamber maintained at 30 °C. Mitochondria, 0.5 mg protein·(mL)$^{-1}$. The reaction mixture was 1 M sorbitol, 10 mM maleate, pH 6.8 (Tris); 10 mM pyruvate-malate was added as a substrate. Final volume was 1.5 mL. The concentrations of phosphate (Pi) and K^+ used are indicated in the legends of each illustration. Stock solutions were 2 M KCl or NaCl and 1 or 0.1 M phosphate buffer pH 6.8 (Tris).

Transmembrane potential ($\Delta\Psi$)

The transmembranal potential was determined using safranine-O, following the absorbance changes at 511–533 nm in a DW2000 Aminco spectrophotometer in dual-wavelength mode (Akerman and Wikström 1976). We used a final concentration of 0.5 mg protein/mL of mitochondria. Yeast mitochondria were assayed in the respiration medium plus 10 μM safranine-O. The concentrations of K^+ and Pi are indicated under each figure. Where indicated, the uncoupler *p*-chloromethoxycarbonylcyanide phenylhydrazone (CCCP) was added to a final concentration of 5 μM.

ATP synthesis

An enzyme–coupled assay system containing 162.5 μg/mL hexokinase, 2 U/mL glucose-6-phosphate dehydrogenase, 20 mM glucose, 1.4 mM $NADP^+$, 200 μM $MgCl_2$ and 10 mM pyruvate-malate, was used to measure the rate of ATP synthesis. The reaction was started by adding 200 μM ADP. The reduction of $NADP^+$ was followed in a DW2C Aminco/Olis spectrophotometer in dual mode at 340–390 nm (Cortés et al. 2000). The NADPH extinction coefficient used was 6.22×10^3 $(M\cdot cm)^{-1}$. The lyophilized enzymes were suspended prior to each experiment as follows: hexokinase was suspended in water to 13 mg/mL and glucose-6-phosphate dehydrogenase was suspended in a 5 mM citrate buffer pH 7 to a final concentration of 200 U/mL. Oligomycin (10 μg/mg prot) was used to determine the basal ATP synthesis; which was subtracted from the experimental data. The concentrations of Pi are indicated in the legend to the figure.

Results and discussion

In *D. hansenii* mitochondria oxygen consumption is coupled by phosphate and by monovalent cations

In all cases, the isolated mitochondria from *D. hansenii* exhibited the same sensitivity to KCl or NaCl. Thus, we are presenting mainly the results obtained with KCl. We chose to show the K^+ effect because in the presence of both cations *D. hansenii* prefers to concentrate K^+; faster and with more affinity than Na^+ (Thomé-Ortiz et al. 1998; González-Hernández et al. 2004). The isolated mitochon-

dria from *D. hansenii* exhibited a slow rate of oxygen consumption both in state IV and in state III, suggesting that the respiratory chain needed the presence of a monovalent cation in order to work at full speed (Table 1). The role of K^+ as an activator of the respiratory chain of mitochondria from yeast (Uribe et al. 1991) and mammalians (Peña et al. 1964; Gómez-Puyou et al. 1969; Gómez-Puyou and Tuena de Gómez Puyou 1977) has been described. The respiratory control (RC) is a measure of the 'integrity' of mitochondria preparation and coupling efficiency between the respiratory chain and the F_1F_0-ATP synthase (Nicholls and Ferguson 2001). In *D. hansenii* it was observed that at 0.4 mM Pi mitochondria were uncoupled as evidenced by a RC of 1.0 (Table 1). Then, addition of different concentrations of K^+ led to higher rates of oxygen consumption and to an increased RC (Table 1) as follows: At 0 to 20 mM K^+, RC was 1.0. However, at 50 mM K^+ RC was 1.33 and increased to 1.73 at the maximum K^+ concentration tested (75 mM) (Table 1). When the phosphate concentration was raised to 4.0 mM, the rates of oxygen consumption were higher (Table 1) and a RC of 1.27 was observed in the absence of K^+ (Table 1). Then, as different K^+ concentrations were added, the RC increased such that at 75 mM K^+, RC=2.29 (Table 1). In the presence of 10 mM Pi, the rates of oxygen consumption were similar to those obtained at 4 mM Pi (Table 1) and the RC was 2.14 in the absence of K^+, and increased only slightly at the K^+ concentrations tested (Table 1), i.e. 10 mM Pi closed the channel without K^+. Even though Pi has the same coupling effect in *D. hansenii* mitochondria as in those from *S. cerevisiae* (Manon and Guérin 1997), the *D. hansenii* organelles need ten times more Pi to close the unspecific channel. In isolated mitochondria from *S. cerevisiae* (Gutiérrez-Aguilar et al. 2010) or mammalians (Leung and Halestrap 2008) the Pi site has been located in the inner membrane and it has been tentatively identified as the phosphate carrier.

In *D. hansenii* mitochondria, opening of a Pi/K^+-sensitive unspecific channel results in depletion of the transmembrane potential ($\Delta\Psi$)

The oxygen consumption data suggested that there is a MUC in *D. hansenii*. Another yeast species, *S. cerevisiae* contains a MUC which is closed by 1–2 mM phosphate (Manon and Guérin 1997). Thus, in order to further explore the sensitivity of the putative MUC from *D. hansenii* mitochondria to Pi, the electric transmembrane potential ($\Delta\Psi$) was measured in the presence of 0.4, 4.0 and 10 mM Pi (Fig. 1). At 0.4 mM Pi, the $\Delta\Psi$ was low and unstable (Fig. 1a, trace a). Then in the presence of 4.0 mM Pi the $\Delta\Psi$ became higher and gained stability (Fig. 1b, trace a) and it reached a high, stable $\Delta\Psi$ at 10 mM Pi (Fig. 1c, trace a) or higher (Result not shown). These results suggested that *D. hansenii* contain a permeability transition pore similar to that observed in *S. cerevisiae* mitochondria, although the organelle from *D. hansenii* requires a higher Pi concentration to close. The oxygen consumption effects reported in Table 1 also suggested that Pi and monovalent cations exhibit synergistic effects. Thus, to further explore the monovalent cation effect, the $\Delta\Psi$ was measured at each of the Pi concentrations tested and in the presence of increasing K^+. At 0.4 mM Pi where the $\Delta\Psi$ was unstable, increasing concentrations of K^+ resulted in higher, more stable $\Delta\Psi$, indicating that at the low Pi concentrations the monovalent cation aided to seal the unspecific channel (Fig. 1a, traces b to e). At 4 mM Pi, the $\Delta\Psi$ was low in the absence of K^+ and increased with K^+ concentrations. This result probably indicates that Pi was able to partially close the channel, although K^+ was still needed to achieve full closure (Fig. 1b). At 10 mM Pi, the highest concentration tested, MUC was completely closed and the monovalent cation did not have further effects (Fig. 1c).

Table 1 Effect of phosphate (Pi) and K^+ on the rate of oxygen consumption and respiratory control of isolated mitochondria from *Debaryomyces hansenii*

	0.4 mM Pi			4.0 mM Pi			10.0 mM Pi		
[K^+] (mM)	IV	III	RC	IV	III	RC	IV	III	RC
0	75±6	75.0±6	**1.0**	130±9	165±8	**1.27**	129±6	277±9	**2.14**
10	79±3	79.0±3	**1.0**	127 ± 10	191 ± 13	**1.51**	127±6	273 ± 14	**2.16**
20	79±3	79.0±3	**1.0**	128±8	220 ± 16	**1.72**	129±6	281 ± 12	**2.18**
50	127±3	168±5	**1.33**	122 ± 6	249±4	**2.05**	124±5	285±3	**2.31**
75	127±3	219 ± 1	**1.73**	114±9	261 ± 9	**2.29**	131 ± 7	293±5	**2.24**

The rates of oxygen consumption in resting state (IV) and phosphorylating state (III) are expressed in natgO_2(min·mg prot)$^{-1}$. The respiratory control (RC) is the III/IV quotient. Reaction mixture: 1 M sorbitol, 10 mM maleate, pH 6.8 (Tris). The subtrate was always 10 mM pyruvate-malate. Three different phosphate (Pi) concentrations and five different KCl concentrations were used as indicated. State III was initiated by adding 500 μM ADP. Mitochondria 0.5 mg prot·(mL)$^{-1}$. Temp 30 °C, final vol 1.5 mL. Data from 3 different experiments.

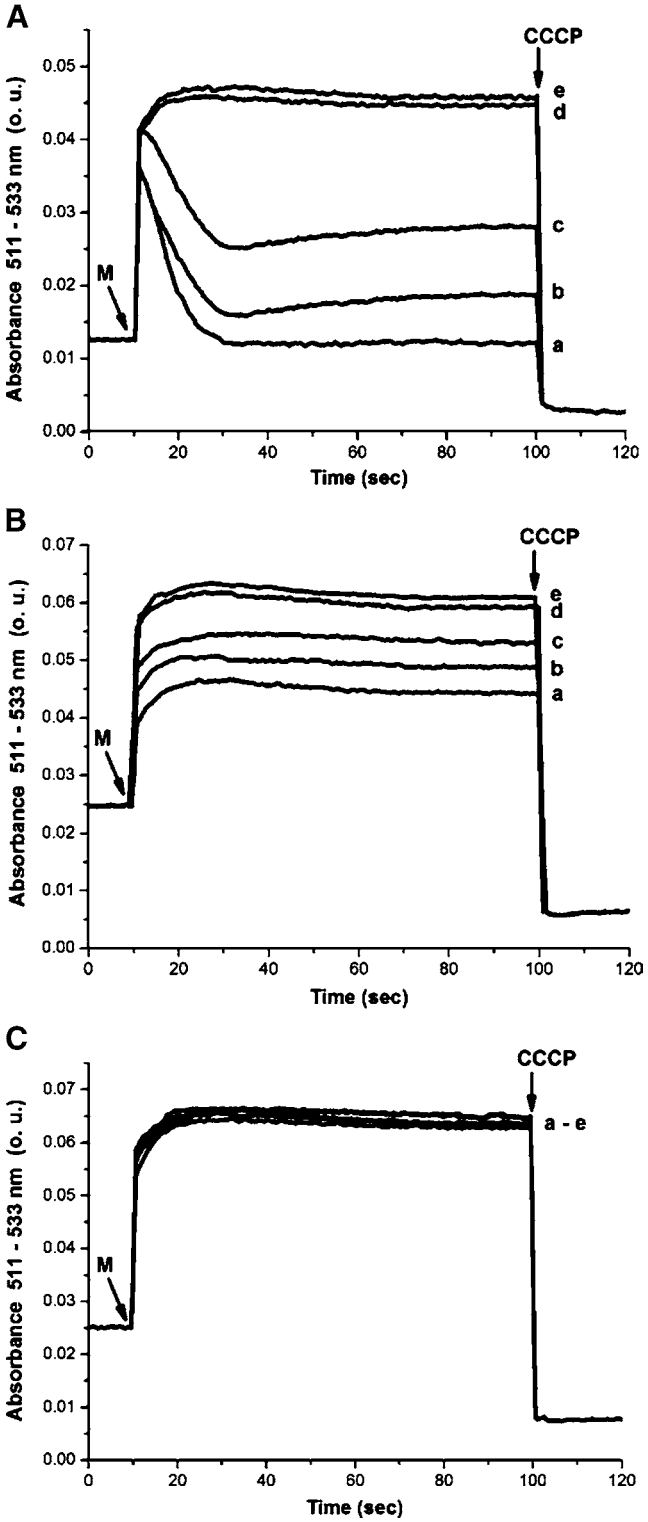

Fig. 1 Effect of K^+ and phosphate on the transmembrane potential ($\Delta\Psi$) of isolated mitochondria from *D. hansenii.* Reaction mixture as in Table 1 except 10 μM safranine-O was added. Final vol. 2 mL; room temperature. Pi concentrations were **A** 0.4 mM; **B** 4.0 mM and **C** 10.0 mM. K^+ concentrations were: **a**, 0; **b**, 10 mM; **c**, 20 mM; **d**, 50 mM; **e**, 75 mM. Where indicated, mitochondria (M) 0.5 mg prot $(ml)^{-1}$ and CCCP 5 μM were added. Representative traces from three independent experiments

The $\Delta\Psi$ sensitivity to monovalent cations does not discriminate between Na^+ or K^+

The possibility that K^+ or Na^+ exhibited different effects was explored by measuring the $\Delta\Psi$ in the presence of three different cation concentrations and in the presence of 0.4 mM Pi. In the absence of cations (Fig. 2 trace a), no increase in $\Delta\Psi$ was observed. In the presence of 18.75 mM Na^+ (Fig. 2 trace b) or K^+ (Fig. 2 trace c), a partial $\Delta\Psi$ was observed. Then, at 37.5 mM monovalent cation, the $\Delta\Psi$ increased to a higher extent regardless of whether the cation was Na^+ (Fig. 2 trace d), K^+ (Fig. 2 trace e), or a mixture of 18.75 mM Na^+ plus 18.75 mM K^+ (Fig. 2 trace f). At 75 mM monovalent cation, a still higher $\Delta\Psi$ was obtained, which again was the same regardless of whether the cation was Na^+ (Fig. 2 trace g), K^+ (Fig. 2 trace h) or a mixture of 37.5 mM Na^+ plus 37.5 K^+ (Fig. 2 trace i). Thus, the opening of the MUC seemed to be equally sensitive to Na^+ or to K^+.

The mitochondrial permeability transition results in decreased synthesis of ATP

In *D. hansenii* mitochondria, PT was triggered by lowering Pi or K^+ and resulted in lower CR and decreased $\Delta\Psi$, leading us to propose that oxidative phosphorylation might be optimized in the presence of increasing concentrations of Pi and K^+. When we tested the synthesis of ATP at three different Pi concentrations and in the presence of different concentrations of K^+, we observed that the rate of synthesis

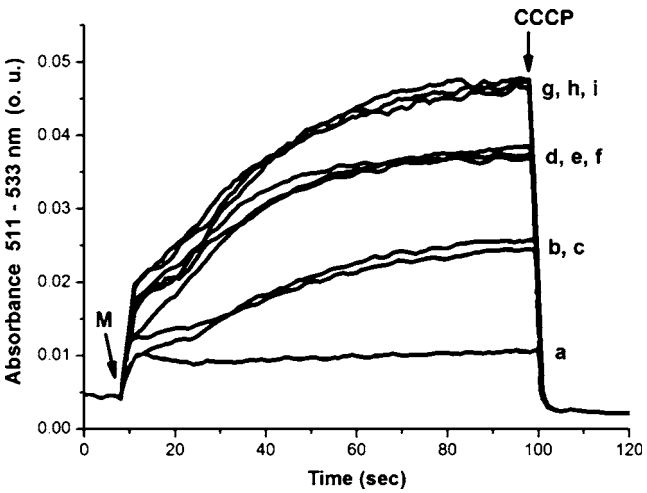

Fig. 2 Effect of Na^+ and K^+ mixtures on the transmembrane potential ($\Delta\Psi$) of isolated mitochondria from *D. hansenii.* Reaction mixture as in Fig. 1. Final volume 2 mL; room temperature. 0.4 mM Pi. Na^+ and/or K^+ concentrations were: **a**, 0; **b**, 18.75 mM Na^+; **c**, 18.75 mM K^+; **d,** 37.5 mM Na^+;18.75 mM Na^+ plus 18.75 mM K^+; **e**, **f**, 37.5 mM K^+; **g**, 37.5 mM Na^+ plus 37.5 mM K^+; **h**, 75 mM Na^+; **i**, 75 mM K^+. Where indicated, mitochondria (M) 0.5 mg prot $(ml)^{-1}$ and CCCP 5 μM were added. Representative traces from three independent experiments

of ATP increased proportionally to Pi and/or K^+, i.e. at 0.4 mM Pi a slow rate of ATP synthesis was observed which increased as the K^+ concentration was raised (Fig. 3). At 4 mM Pi higher rates of ATP synthesis were obtained and a slight optimization of this rate by K^+ was still observed (Fig 3). At the highest concentration of Pi tested, a high rate of synthesis of ATP was observed which was not further increased by the presence of different concentrations of K^+. Thus, the effect on the synthesis of ATP provide further support to the notion that there is an unspecific channel in *D. hansenii* mitochondria which is closed by high concentrations of Pi and by intermediate concentrations of monovalent cations.

The *D. hansenii* MUC is regulated by Ca^{2+} and by Mg^{2+}

Divalent cations modulate the opening of the MUC from different species. However, the effects are opposite as in mammalians Ca^{2+} opens the MUC (Halestrap and Davidson 1990) while in *S. cerevisiae* Ca^{2+} closes the MUC (Pérez-Vázquez et al. 2003) probably acting at the level of the porine (Gutiérrez-Aguilar et al. 2007). By contrast, Mg^{2+} seems to close all known MUCs (Bernardi 1999; Kowaltowski et al. 1998; Pérez-Vázquez et al. 2003). Thus, we decided to characterize the effects of Ca^{2+} and Mg^{2+} on the $\Delta\Psi$ in the presence of 0.4 mM Pi. In the absence of cations (Fig. 4a trace a; Fig. 4b trace a), a low $\Delta\Psi$ was observed. In the presence of increasing Ca^{2+} concentrations, $\Delta\Psi$ increased (Fig. 4a traces a-f); reaching a maximum at 1 mM Ca^{+2}. $[Ca^{+2}]$ above 1 mM did not promote further changes in $\Delta\Psi$ (data not shown). In regard

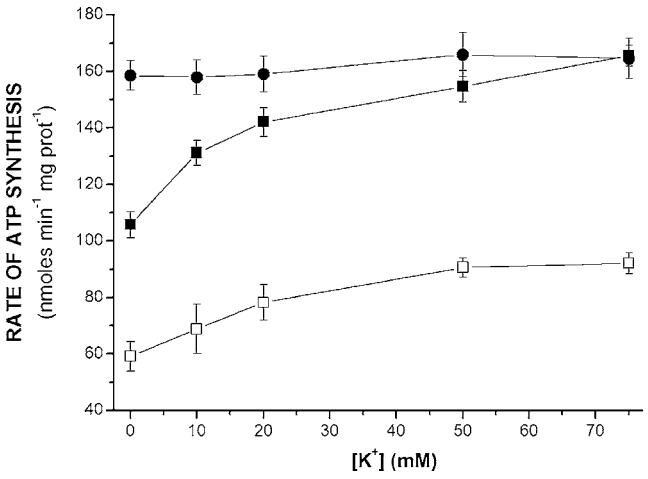

Fig. 3 Effect of K^+ and phosphate on the rate of ATP synthesis mediated by isolated mitochondria from *D. hansenii*. Experimental conditions as in Table 1, 200 μM ADP. In addition, an enzyme coupled ATP assay system was included: 200 μM $MgCl_2$, 20 mM glucose, 1.4 mM $NADP^+$, hexokinase 162.5 μg/mL and glucose-6-phosphate dehydrogenase 2 U/mL. Pi concentrations were: 0.4 mM (□), 4.0 mM (■) and 10.0 mM (●). The reaction was initiated with 200 μM ADP. Each point is the mean of four independent experiments ± SD

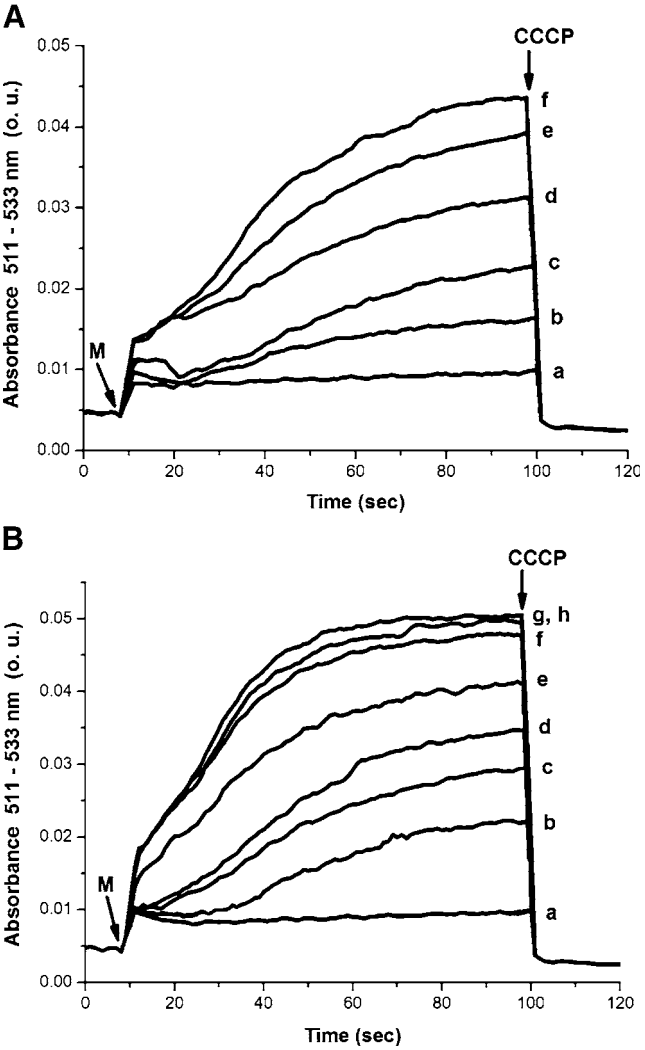

Fig. 4 Effect of divalent cations on the transmembrane potential ($\Delta\Psi$) of isolated mitochondria from *D. hansenii*. Reaction mixture as in Fig. 2, Pi concentration was 0.4 mM. A: Different Ca^{2+} concentrations were: a, 0; b, 100 μM Ca^{2+}; c, 200 μM Ca^{2+}; d, 500 μM Ca^{2+}; e, 750 μM Ca^{2+}; f, 1 mM Ca^{2+}. B: Different Mg^{2+} concentrations were: a, 0; b, 100 μM Mg^{2+}; c, 200 μM Mg^{2+}; d, 500 μM Mg^{2+}; e, 1 mM Mg^{2+}; f, 2 mM Mg^{2+}; g, 5 mM Mg^{2+}; h, 10 mM Mg^{2+}. Where indicated, mitochondria (M) 0.5 mg prot $(ml)^{-1}$ and CCCP 5 μM. Representative traces from three independent experiments

to Mg^{2+}, 100 μM and 200 μM resulted in a partial increase in $\Delta\Psi$ (Fig. 4b, traces a,b). At Mg^{2+} 500 μM and 1 mM, $\Delta\Psi$ was increased to a value near the maximum obtainable (Fig. 4b, traces d,e). At and above 2 mM Mg^{2+} the maximum $\Delta\Psi$ was obtained (Fig. 4b, traces f,g,h). These results suggest that both divalent cations closed the MUC from *D. hansenii*, but this closure was promoted at lower $[Ca^{2+}]$ than $[Mg^{2+}]$.

Selective inhibition of each oxidase and its effect on PT

In *D. hansenii* mitochondria there are two terminal oxidases. In addition to cytochrome oxidase (COX), there

is an alternative oxidase (AOX) (Veiga et al. 2003). The presence of AOX allowed us to explore whether PT might depend on whether electrons were accepted by COX or AOX. Oxygen consumption experiments were conducted in the presence of cyanide (to block COX) or propyl-gallate (to block AOX) (Table 2). The rate of oxygen consumption was measured in state IV and in state III. In the presence of cyanide the rate of oxygen consumption was about one third of the non-inhibited rate (shown in Table 1), although increasing concentrations of K^+ did promote an increase in the rate of oxygen consumption both in state IV and state III, such that the CR remained low (Table 2). This effect suggests that under our conditions AOX expression was low and thus the lack of proton pumping activity by the blocked complexes III and IV failed to establish a high protonmotive force. By contrast, when AOX was blocked, the effect of K^+ on the rate of oxygen consumption did lead to an increase in RC (Table 1) to a similar extent as the increase obtained in the absence of propyl-gallate (see Table 1), indicating that in the absence of the (low) AOX activity PT still occurred.

The possible physiological meaning of the unusual sensitivity to monovalent cations observed in the *D. hansenii* MUC

The monovalent cation-mediated prevention of opening of the *D. hansenii* MUC has not been detected in mitochondria from any other species studied so far. It had always been considered that the permeability to these ions had to be closely controlled in order to avoid a recycling of the cation following a uniport mechanism for uptake and a H^+ antiport mechanism for export that would result in depletion of the electrical gradient and the consequent mitochondrial uncoupling and loss of ATP synthesis (Garlid 1988; Castrejón et al. 1997). This monovalent cation-mediated coupling makes sense when it is considered that *in situ*, *D. hansenii* mitochondria are exposed to high K^+ or Na^+ concentrations. It should be noted that the monovalent cation-promoted increase in the efficiency of the oxidative phosphorylation by *D. hansenii* mitochondria may explain, at least partially the increase in the growth rate of the *D. hansenii* cells when these are exposed to high concentrations of monovalent cations (González-Hernández et al. 2004; Sánchez et al. 2008).

Table 2 Effect of cyanide and propyl-gallate on the rate of oxygen consumption and respiratory control of isolated mitochondria from *Debaryomyces hansenii*

	Cyanide			Propyl Gallate		
$[K^+]$ (mM)	IV	III	RC	IV	III	RC
0	18±0.7	19±0.8	1.02	145±9	162± 11	1.12
10	24.7±0.4	26.8± 1.2	1.08	151± 5	193± 10	1.27
20	25.5±0.3	26.8±0.3	1.05	136±3	203±4	1.50
50	28.6± 1.7	29.7± 2	1.04	144±5	221 ± 7	1.53
75	34±6	36±8	1.06	138±8	240± 13	1.73

Experimental conditions and data as in Table 1 except 100 μM Cyanide or 25 μM propyl gallate were indicated. Data from 4–5 independent experiments.

As more mitochondria are isolated from different species, it is becoming obvious that these organelles are evolving together with the cell to adapt to the environment. As a result, there are variations in the protein composition of the organelle, e.g. the proteins in the respiratory chain vary widely specially in species with branched respiratory chains. It is noteworthy that the components of the respiratory chain do not seem to vary at random, e.g., from 21 yeast species analyzed, 12 contain both an alternative oxidase and complex I (Veiga et al. 2003), while there is only one species, *Pichia anomala*, that contains an alternative oxidase but no complex I (Nosek and Fukuhara 1994).

The effectors regulating the activity of the mitochondrial unspecific channels from different species may vary widely. In many cases, a given molecule has opposite effects in MUCs from different species (Manon and Guérin 1998). This could be an indication of the different functions the MUC might have depending on the species. The mammalian MUC, widely known as the permeability transition pore (PTP) and the *S. cerevisiae* MUC (YMUC) are the best characterized systems. Both channels have a molecule cutoff size of 1.5 kDa (Zoratti and Szabó 1995; Jung et al. 1997) and some cations such as Mg^{2+} and alkylamines close both MUCs (Chávez et al. 2000; Castrejón et al. 2002; Pérez-Vázquez et al. 2003). Here we demonstrated that the *D. hansenii* MUC is also closed by Mg^{2+}. Differences in sensitivity for MUCs from different species to cyclosporin A (CsA) have been reported (Tanveer et al. 1996; Jung et al. 1997). CsA is a potent PT inhibitor in mammalian (Halestrap and Davidson 1990), potato (Fortes et al. 2001) and wheat mitochondria (Pavlovskaya et al. 2007) but has no effect on yeast (Jung et al. 1997) or brine shrimp mitochondria (Menze et al. 2005). In the mammalian PTP, Pi is needed for Ca^{2+}-mediated opening, but it is also required by CsA to inhibit opening (Halestrap and Davidson 1990). In mitochondria from the yeast species *S. cerevisiae* (Velours et al. 1977; Roucou et al. 1997) and *D. hansenii* (this work), Pi always inhibits PT. Ca^{2+} opens the MUC in mammals (Crompton et al. 1988; Bernardi et al. 1994), potato (Fortes et al. 2001) and *N. crassa* (Brustovetsky et al. 2002) but it is inhibitory in *S. cerevisiae* (Jung et al. 1997) and in *D. hansenii* (this work). A Ca^{2+}-porin interaction site has been located both in *S. cerevisiae* (Gutiérrez-Aguilar et al. 2007) and mammals (Israelson et al. 2007). The inability of Ca^{2+} to

open the *S. cerevisiae* MUC might be explained if it is considered that there is no specific carrier for Ca^{2+} in these mitochondria and thus the Ca^{2+} uptake is slow (Uribe et al. 1992). Furthermore, addition of a Ca^{2+} ionophore to *S. cerevisiae* mitochondria enables Ca^{2+} to induce PT (Jung et al. 1997). It would be interesting to analyze the Ca^{2+} transport activity of the isolated mitochondria from *D. hansenii*. Adding to the wide variability in the pattern of PT in mitochondria from different species, recently it was reported that the yeast species *Yarrowia lipolytica* (Deryabina et al. 2004) and *Endomyces magnusii* (Kovaleva et al. 2009) fail to undergo PT unless a high concentration of Ca^{2+} plus the Ca^{2+} ionophore ETH129 are added. Remarkably, *D. hansenii* and *Y. lipolytica* are closely related (Dujon et al. 2004), but the first undergoes PT while the second does so only under very specific conditions (Kovaleva et al. 2009). A comparison between the proteins that have been proposed to constitute the channel might yield abundant information on the mechanisms that lead to PT and on the control mechanisms.

Acknowledgements The authors thank Martha Calahorra, Sergio Couoh, Ramón Méndez, Rocío Romualdo and Norma S. Sánchez for technical assistance. Partially funded by grants from: CONACYT-79989 and UNAM/DGAPA-PAPIIT-IN217109-3. ACO is recipient of a CONACYT undergraduate fellowship 102803.

References

Akerman KEO, Wikström MK (1976) FEBS Lett 68:191–197
Alba-Lois L, Segal C, Rodarte B, Valdés-López V, De Luna A, Cárdenas R (2004) Curr Microbiol 48:68–72
Averet N, Fitton V, Bunoust O, Rigoulet M, Guerin B (1998) Mol Cell Biochem 184:67–79
Bernardi P (1999) Physiol Rev 79:1127–1155
Bernardi P, Broekemeier KM, Pfeiffer DR (1994) J Bioenerg Biomembr 26:509–517
Breuer U, Harms H (2006) Yeast 23:415–437
Brustovetsky N, Tropschug M, Heimpel S, Heidkämper D, Klingenberg M (2002) Biochemistry 41:11804–11811
Castrejón V, Parra MC, Moreno R, Peña A, Uribe S (1997) Arch Biochem Biophys 346:37–44
Castrejón V, Peña A, Uribe S (2002) J Bioenerg Biomemb 34:299–306
Chávez E, Peña A, Zazueta C, Ramírez J, García N, Carrillo R (2000) J Bioenerg Biomembr 32:193–198
Cortés P, Castrejón V, Sampedro JG, Uribe S (2000) Biochim Biophys Acta 1456:67–76
Crompton M, Ellinger H, Costi A (1988) Biochem J 255:357–360
Deryabina YI, Isakova EP, Shurubor EI, Zvyagilskaya RA (2004) Biochemistry (Mosc) 69:1025–1033
Dujon B, Sherman D, Fischer G, Durrens P, Casaregola S, Lafontaine I, De Montigny J, Marck C, Neuvéglise C, Talla E, Goffard N, Frangeul L, Aigle M, Anthouard V, Babour A, Barbe V, Barnay S, Blanchin S, Beckerich JM, Beyne E, Bleykasten C, Boisramé A, Boyer J, Cattolico L, Confanioleri F, De Daruvar A, Despons L, Fabre E, Fairhead C, Ferry-Dumazet H, Groppi A, Hantraye F, Hennequin C, Jauniaux N, Joyet P, Kachouri R, Kerrest A, Koszul R, Lemaire M, Lesur I, Ma L, Muller H, Nicaud JM, Nikolski M, Oztas S, Ozier-Kalogeropoulos O, Pellenz S, Potier S, Richard GF, Straub ML, Suleau A, Swennen D, Tekaia F, Wésolowski-Louvel M, Westhof E, Wirth B, Zeniou-Meyer M, Zivanovic I, Bolotin-Fukuhara M, Thierry A, Bouchier C, Caudron B, Scarpelli C, Gaillardin C, Weissenbach J, Wincker P, Souciet JL (2004) Nature 430:35–44
Fadda ME, Mossa V, Pisano MB, Deplano M, Cosentino S (2004) Int J Food Microbiol 95:51–59
Fortes F, Castilho RF, Catisti R, Carnieri EG, Vercesi AE (2001) J Bioenerg Biomembr 33:43–51
Garlid KD (1988) In: Lemasters JJ, Hackenbrock CR, Thurman RG, Westerhoff HV (eds) Integration of Mitochondrial Function. Mitochondrial volume control. Plenum Publishing Corp, New York, pp 259–278
Gómez-Puyou A, Sandoval F, Peña A, Chávez E, Tuena M (1969) J Biol Chem 244:5339–5345
Gómez-Puyou A, Tuena de Gómez Puyou M (1977) J Bioenerg Biomemb 9:91–102
González-Hernández JC, Cárdenas-Monroy CA, Peña A (2004) Yeast 21:403–412
Gornal AG, Bardavill CJ, David MM (1949) J Biol Chem 177:751–760
Guérin B, Bunoust O, Rouqueys V, Rigoulet M (1994) J Biol Chem 269:25406–25410
Gutiérrez-Aguilar M, Pérez-Vázquez V, Bunoust O, Manon S, Rigoulet M, Uribe S (2007) Biochim Biophys Acta 1767:1245–1251
Gutiérrez-Aguilar M, Pérez-Martínez X, Chávez E, Uribe S (2010) Arch Biochem Biophys (in press)
Halestrap AP, Davidson AM (1990) Biochem J 268:153–160
Hobot JA, Jennings DH (1981) Exp Mycol 5:217–228
Israelson A, Abu-Hamad S, Zaid H, Nahon E, Shoshan-Barmatz V (2007) Cell Calcium 41:235–244
Jung DW, Bradshaw P, Pfeiffer DR (1997) J Biol Chem 272:21104–21112
Kovaleva MV, Sukhanova EI, Trendeleva TA, Zyl'kova MV, Ural'skaya LA, Popova KM, Saris NE, Zvyagilskaya RA (2009) J Bioenerg Biomembr 41:239–249
Kowaltowski AJ, Naia-Da-Silva ZS, Castilho RF, Vercesi AE (1998) Arch Biophys Biochem 359:77–81
Kusano T, Tateda C, Berberich T, Takahashi Y (2009) Plant Cell Rep 28(9):1301–1308
Leung AW, Halestrap AP (2008) Biochim Biophys Acta 1777:946–952
Manon S, Guerin M (1997) Biochem Biophys Acta 1318:317–321
Manon S, Guerin M (1998) Biochem Mol Biol Int 44:565–575
Manon S, Roucou X, Guerin M, Rigoulet M, Guerin B (1998) J Bioenerg Biomembr 30:419–429
Menze MA, Hutchinson K, Laborde SM, Hand SC (2005) Am J Physiol Regul Integr Comp Physiol 289:R68–R76
Montiel V, Ramos J (2007) FEMS Yeast Res 7:102–109
Neves ML, Oliveira RP, Lucas CM (1997) Microbiol 143:1133–1139
Nicholls DG, Ferguson SJ (2001). In Bioenergetics 3. Chapter IV, The chemiosmotic proton circuit. Academic Press, pp. 57–87
Norkrans B (1966) Mikrobiol 54:374–392
Norkrans B, Kylin A (1969) J Bacteriol 100:836–845
Nosek J, Fukuhara H (1994) J Bacteriol 176:5622–5630
Pavlovskaya NS, Savinova OV, Grabel'nykh OI, Pobezhimova TP, Koroleva NA, Voinikov VK (2007) Dokl Biol Sci 417:446–448
Peña A, Campillo Serrano C, de Gómez T, Puyou M (1964) Arch Biochem Biophys 106:461–466
Peña MZ, Piña E, Escamilla E, Piña A (1977) FEBS Lett 80:209–213
Pérez-Vázquez V, Saavedra-Molina A, Uribe S (2003) J Bioenerg Biomembr 35:231–241
Prista C, Almagro A, Loureiro-Dias MC, Ramos J (1997) Appl Environ Microbiol 63:4005–4009
Prista C, Loureiro-Dias MC, Montiel V, Garcia R, Ramos J (2005) FEMS Yeast Res 5:693–701

Ramos J (2006) In: Gunde-Cimerman N, Oren A, Plemenitas A (eds) Introducing *Debaryomyces hansenii*, a salt loving yeast. Adaptation to life at high salt concentrations in archaea, bacteria and eukarya. Springer, Berlin, pp 443–451
Roucou X, Manon S, Guerin M (1997) Biochem Mol Biol Int 43:53–61
Sánchez NS, Arreguín R, Calahorra M, Peña A (2008) FEMS Yeast Res 8:1303–1312
Sherman D, Durrens P, Beyne E, Nikolski MJ-L (2004) Nucleic Acids Res 32:D315–D318
Tanveer A, Virji S, Andreeva L, Totty NF, Hsuan JJ, Ward JM, Crompton M (1996) Eur J Biochem 238:166–172
Thomé-Ortiz P, Peña A, Ramírez J (1998) Yeast 14:1355–1371
Uribe S, Ramírez J, Peña A (1985) J Bacteriol 161:1195–1200
Uribe S, Sánchez N, Peña A (1991) Biochem Int 24:615–624
Uribe S, Rangel P, Pardo JP (1992) Cell Calcium 13:211–217
Veiga A, Arabaca JD, Loureiro-Dias MC (2003) FEMS Yeast Res 3:239–245
Velours J, Rigoulet M, Guerin B (1977) FEBS Lett 81:18–22
Zoratti M, Szabo I (1995) Biochim Biophys Acta 1241:139–176

Mitochondrion 11 (2011) 382–390

Contents lists available at ScienceDirect

Mitochondrion

journal homepage: www.elsevier.com/locate/mito

Review

Mitochondrial Unselective Channels throughout the eukaryotic domain

Salvador Uribe-Carvajal [a], Luís A. Luévano-Martínez [a], Sergio Guerrero-Castillo [a], Alfredo Cabrera-Orefice [a], Norma A. Corona-de-la-Peña [b], Manuel Gutiérrez-Aguilar [a,*]

[a] Depto. de Genética Molecular, Inst. de Fisiología Celular, Universidad Nacional Autónoma de México, México City, Mexico
[b] U. de Inv. en Trombosis, Hemostasia y Aterogénesis, Hospital Gabriel Mancera, IMSS, México City, Mexico

ARTICLE INFO

Article history:
Received 30 November 2010
Received in revised form 16 February 2011
Accepted 25 February 2011
Available online 6 March 2011

Keywords:
Mitochondria
Permeability transition pore
Mitochondrial Unselective Channel
Bioenergetics
Cell death
Yeast

ABSTRACT

Mitochondria from diverse species can undergo a massive permeability increase known as the permeability transition, a process first thought to be an artifact. It is currently accepted that in the inner mitochondrial membrane there is a Mitochondrial Unselective Channel (MUC), also known as the permeability transition pore. Regardless of the species, MUC opening leads to uncoupling of oxidative phosphorylation. In each species, MUC regulation appears to be different, probably as a result of the adaptation of each organism to its specific environment. To date, the components and the putative physiological role of MUCs are still a matter of debate. Current hypothesis suggests that proteins normally participating in diverse metabolic functions constitute MUCs. Among these proteins, the Adenine Nucleotide Translocase and the phosphate carrier have been proposed as putative MUC components in mammalian and yeast mitochondria. In this review, the characteristics of MUCs from different species and strains are discussed. The data from the literature reinforce the current notion that these channels are preserved through evolution albeit with different control factors. We emphasize the knowledge available of Mitochondrial Unselective Channels from different yeast species.

Contents

Abbreviations: PT, mitochondrial permeability transition; MUC, Mitochondrial Unselective Channel; ROS, reactive oxygen species; MCC, Multiple Conductance Channel; CsA, cyclosporin A; CypD, cyclophilin D; PTP, permeability transition pore; ANT, Adenine Nucleotide Translocase; VDAC, voltage-dependent anion channel; PiC, phosphate carrier; TEA, triethanolamine; CCCP, carbonyl cyanide 3-chlorophenylhydrazone; BSA, bovine serum albumin; dVO_4, decavanadate.

* Corresponding author at: Dept. of Molecular Genetics, Instituto de Fisiología Celular, Universidad Nacional Autónoma de México, Apdo. postal 70-242, 04510 Mexico City, Mexico. Tel.: +52 55 5622 5632.
E-mail address: manu@unam.mx (M. Gutiérrez-Aguilar).

1567-7249/$ – see front matter
doi:10.1016/j.mito.2011.02.004

1. What are Mitochondrial Unselective Channels?

In eukaryotes, oxidative phosphorylation is a highly efficient energy producing process located in the inner mitochondrial membrane. The importance of this pathway is underlined by the fact that its dysfunction is seldom compatible with cell survival (Bernardi et al., 2006). Since the first protocols for the isolation of mitochondria were established, diverse compounds were used to inhibit the swelling and uncoupling of these organelles. Later on, it was suggested that such uncoupling was due to the opening of an unspecific pore, (Haworth and Hunter, 1979; Hunter and Haworth, 1979a,b) eventually termed the permeability transition pore (PTP). Opening of the PTP accelerates the onset of the mitochondrial permeability transition (PT). PT is defined as the increase in the unselective transport of ions and metabolites across the mitochondrial inner membrane with a molecular mass cutoff of 1.5 kDa (Halestrap, 2009; Jung et al., 1997). Since conditions used to isolate mitochondria inhibited PT, it was concluded that these channels were not active during standard experimental conditions (Guerin et al., 1994). Through the years, the number of groups studying these channels has increased steadily and now, most consider the PT as the starting point of a series of events leading to the death of the cell.

In addition to the mammalian PTPs, many pores have been identified in mitochondria from several eukaryotic species (Table 1). From studies in these organisms, it has become obvious that these channels are tightly and diversely regulated, that their opening is reversible and that probably their physiological role is another besides participating in cell death. Thus, to acknowledge all these properties the term Mitochondrial Unselective Channel (MUC) was coined by Bernard Guerin and his group while studying permeability transition in yeast mitochondria (Manon et al., 1998).

In the species studied so far, the modulation of each MUC is different and appears to have evolved in response to the living conditions of each organism, i.e. MUC modulation may be different for mitochondria from a halophilic yeast such as *Debaryomyces hansenii* (Cabrera-Orefice et al., 2010) when compared to the baker's yeast *Saccharomyces cerevisiae* (Guerin et al., 1994; Manon et al., 1998). This indeed suggests that any MUC characteristic may change according to the environment where each species develop.

Understanding the structure, physiological role and regulation of the MUCs from each of these organisms may help to understand the evolution of these channels; the availability of data on the function and structure of many MUCs will help to truly understand whether the role of MUCs diversified through evolution and if their structure is similar in all species.

Those MUCs that have been already characterized have many features in common although they also possess species-specific characteristics (Azzolin et al., 2010a). Thus in this review we attempt to systematically analyze those general characteristics.

2. Mitochondrial Unselective Channels throughout the eukaryotic domain

The mitochondrial permeability transition has been detected in plant, yeast, invertebrate, fish and mammalian mitochondria (Table 1) (Arpagaus et al., 2002; Bernardi et al., 1998; Curtis and Wolpert, 2002; Manon et al., 1998). PT may be triggered by pathological, physiological or experimental conditions (Haworth and Hunter, 1979; Menze et al., 2005; Prieto et al., 1992). Upon MUC opening, mitochondria depolarize (Crompton, 1999; Manon et al., 1998). The collapse in the mitochondrial transmembrane potential ($\Delta\Psi$) induces an immediate arrest in ATP synthesis (Bernardi, 1999; Rossi and Lehninger, 1964).

Upon MUC opening, a futile cycle ensues, where the respiratory complexes pump protons from the matrix to the intermembrane space and these protons return to the matrix through the open MUC (Beauvoit and Rigoulet, 2001). The$\Delta\Psi$is not reestablished until MUC is closed (Castrejón et al., 1997). As a result of the unselective transport of ions and other molecules across the mitochondrial membrane, osmotically active chemical species accumulate within the mitochondrial matrix, causing swelling of the organelle (Halestrap, 1994).

When the opening of MUCs is restricted to a small mitochondrial population, mitochondrial autophagy is the most likely outcome (Lemasters, 2007; Pereira et al., 2008). When large mitochondrial populations undergo PT, cellular homeostasis is compromised: at this point, cytochrome *c* (Cyt *c*) is released from mitochondria, inhibiting the respiratory chain (Grimm and Brdiczka, 2007). Then, if the cellular ATP levels are not heavily depleted, apoptosis is likely to occur (Nicotera et al., 2000; Skulachev, 2006). Otherwise, when cellular ATP levels fall to less than half of the normal values, the most likely event to occur is necrotic cell death (Crompton, 1999).

3. Yeast Mitochondrial Unselective Channels

3.1. The S. cerevisiae Mitochondrial Unselective Channel

3.1.1. Historical outline

Nearly 40 years ago, the mitochondrial permeability transition in yeast was inadvertently reported (de Chateaubodeau et al., 1974, 1976). Then, in the 1990s, the experiments performed by various groups led to propose the existence of a large conductance unselective channel in this yeast. This mitochondrial pore has been termed the Yeast Mitochondrial Unselective Channel (YMUC) (Manon et al., 1998) and later on, the Yeast Permeability Transition Pore (yPTP) (Jung et al., 1997). As there are other yeast species possessing MUCs with different properties we propose to call it $_{Sc}$MUC. The $_{Sc}$MUC opens by nucleotide triphosphate (NTP) addition and is closed by ADP or phosphate (Guerin et al., 1994; Jung et al., 1997; Prieto et al., 1992). The physiological role and composition of the $_{Sc}$MUC are still a matter

Table 1
Occurrence of Mitochondrial Unselective Channels in non-mammalian eukaryotes.

Kingdom	Species	Common name	Reference
Animalia	*Danio rerio*	Zebra fish	Azzolin et al. (2010a)
	Oncorhynchus mykiss	Rainbow trout	Krumschnabel et al. (2005)
	Lepidophthalmus louisianensis	Ghost shrimp	Hand and Menze (2008) and Holman and Hand (2009)
	Lampetra fluviatilis	Baltic lamprey	Savina et al. (2006)
Plantae	*Zinnia elegans*	Zinnia	Yu et al. (2002)
	Solanum tuberosum	Potato (tuber)	Arpagaus et al. (2002)
	Arabidopsis thaliana	*Arabidopsis*	Scott and Logan, 2008 and Tiwari et al. (2002)
	Nicotiana tabacum	Tobacco	Lin et al. (2006)
	Pissum sativum	Pea	Vianello et al. (1995)
	Triticum spp.	Wheat	Curtis and Wolpert, (2002)
	Avena sativa	Oat	Virolainen et al. (2002)
Fungi	*Saccharomyces cerevisiae*	Baker's yeast	Jung et al. (1997)
	Debaryomyces hansenii	*D. hansenii*	Cabrera-Orefice et al. (2010)

of debate (Manon et al., 1998; Prieto et al., 1996). Nevertheless, opening of this channel has been proposed to represent a regulatory mechanism for energy production (Prieto et al., 1992). While some of its structural aspects still remain obscure, mitochondrial proteins with other metabolic roles had been suggested to play either a regulatory or structural role in the $_{Sc}$MUC. Among others, the Voltage Dependent Anion Channel (VDAC) (Gutiérrez-Aguilar et al., 2007), the phosphate carrier (PiC) (Gutiérrez-Aguilar et al., 2010) and the Adenine Nucleotide Translocase (ANT) (Jung et al., 1997; Roucou et al., 1995, 1997) have been proposed to form or at least to regulate this channel.

3.1.2. Strain dependent characteristics

Early studies on *S. cerevisiae* mitochondria from the Yeast Foam strain evidenced the pH and Mg^{2+}-sensitive unselective transport of anions such as Cl^- and succinate by measuring the swelling of isolated mitochondria(de Chateaubodeau et al., 1974, 1976). This transport was triggered by respiration and inhibited by antimycin. Transport of the uncharged molecule mannitol was also observed (Velours et al., 1977). In further studies by the same group, isolated mitochondria were shown to transport K^+, Na^+, gluconate, glutamate and Cl^- but not phosphate or ammonium when incubated in the presence of ATP or when ethanol was used as respiratory substrate (Guerin et al., 1994). In the same work, inhibitors of the K^+/H^+ exchange such as propranolol, Zn^{2+} and *N, N*-dicyclohexyl-carbodiimide but not quinine were reported to close the channel. The degree of permeabilization was dependent on the pH; i.e., mitochondrial swelling was inhibited at pH 6.5, while maximal swelling was achieved at pH 8.5. Hence, Guerin's group proposed that the ATP, pH and respiratory substrate-mediated mitochondrial swelling could result from the opening of a unique channel (Guerin et al., 1994).

By the same time, Rial's group discovered a proton-uncoupling pathway in mitochondria from the W303 laboratory strain (Prieto et al., 1992). Transport was activated by the purine nucleotides ATP, GTP, dATP, dGTP, and GDP, while ADP, AMP, GMP, and pyrimidine nucleotides were ineffective. Finally, ADP was characterized as a competitive inhibitor of the ATP-mediated transport while phosphate inhibition was noncompetitive (Prieto et al., 1996).

The ATP-induced proton channel detected in W303 mitochondria, and the ATP-induced unselective transport pathway in the industrial strain Yeast Foam were analyzed by Guerin's group who proposed that these were different aspects of the same MUC (Roucou et al., 1997). In an extensive set of experiments, the partial inhibitory effect of atractyloside was measured in $\Delta\Psi$ and oxygen consumption experiments when PT was triggered either by ATP or GDP. The potent $_{Sc}$MUC activation by the non-hydrolyzable analog GDP-βS at concentrations up to ten times lower than those required for hydrolyzable NTP's was demonstrated. This work further confirmed Rial's group finding suggesting that laboratory strains exhibited a GDP-activated proton channel. This channel was shown to be absent in the industrial strain Yeast Foam. The basis for such a difference is still not known, although this may be an adaptation to suboptimal growth conditions (Ferea et al., 1999). During industrial fermentations yeasts are subjected to stress (Volfson et al., 2006; Yvert et al., 2003) probably leading to different gene expression patterns (Varela et al., 2005). Thus, adaptive evolution can account for the differences between laboratory and industrial strains where up to 22% of the total transcripts detected in industrial strains do not match annotated sequences for laboratory strains (Fay et al., 2004; Ferea et al., 1999; Townsend et al., 2003; Varela et al., 2005).

3.1.3. The $_{Sc}$MUC-promoted mitochondrial permeability transition

The possible relationship between $_{Sc}$MUC and the mammalian permeability transition pore, that we will call mammalian MUC or $_{m}$MUC, was explored and determined to be a cyclosporin A (CsA) and Ca^{2+}-insensitive permeability transition (Jung et al., 1997). The effect of Pi restriction on mitochondrial swelling, on changes of mitochondrial ultrastructure, and matrix solute release was described. In these studies, carboxyatractyloside did not affect the ATP-induced transition while it had a partial inhibitory effect on the ethanol-mediated swelling. Finally, the $_{Sc}$MUC pore size determination by means of the solute size exclusion method used in $_{m}$MUC (Haworth and Hunter, 1979) indicated that the $_{Sc}$MUC had a maximal cutoff size for solutes larger than 1.5 kDa. This suggests that the $_{m}$MUC and the $_{Sc}$MUC have a diameter in the vicinity of 2.0 nm (Crompton, 1999).

During the time when the $_{Sc}$MUC was detected, electrophysiological studies detected two channels in the inner mitochondrial membrane of *S. cerevisiae* (Ballarin and Sorgato, 1995, 1996; Ballarin et al., 1996). While one channel displayed a conductance of 45 pS (in symmetrical conditions), the other presented conductance values near 0.8 nS. Interestingly, ATP (Mg^{2+}-free) locked the smaller channel in a closed state, while it kept the large channel open. The possibility that the large channel is $_{Sc}$MUC still remains to be tested (Ballarin and Sorgato, 1995).

In the same years, Kinnally's group reported the existence of the so-called Multiple Conductance Channel (MCC) in yeast inner mitochondrial membranes (Lohret and Kinnally, 1995a,b; Lohret et al., 1996). This channel displayed a conductance similar to the large channel detected by Ballarin and Sorgato (1nS). Interestingly, upon addition of peptides matching the signal sequence of mitochondrially-targeted proteins, the MCC displayed conductance shifts from open to fast flickering semi-closed substates (Lohret and Kinnally, 1995b). This channel was unequivocally proved to be unrelated to VDAC or ANT by using knock out strains (Lohret and Kinnally, 1995a; Lohret et al., 1996). MCC activity was lost in a Tim23 conditional mutant strain suggesting this channel may be the Tim23 pore (Martínez-Caballero et al., 2007). To this, the role of the PIM as the core component of the $_{m}$MUC has been proposed (Zoratti et al., 2005, 2010). This may also be the case for yeast since protein import is powered by conditions where the $_{Sc}$MUC is partially inhibited by Mg^{2+} (Stuart and Koehler, 2007).

3.1.4. The Ca^{2+}-sensitive, cyclosporin A-insensitive $_{Sc}$MUC

The fact that yeast mitochondria lack a fast energy-linked Ca^{2+} transport system demonstrated that Ca^{2+} transport is not a universal attribute of mitochondria in the eukaryotic domain (Carafoli et al., 1970; Uribe et al., 1992). Ghost shrimp also lack a Ca^{2+} transport system (Holman and Hand, 2009). This could explain the absence of a Ca^{2+}-triggered PT in these organisms which additionally are remarkably resistant to oxidative stress (Cortés-Rojo et al., 2007; Holman and Hand, 2009; Jung et al., 1997). In mammalian mitochondria, Ca^{2+} transport and PT are inhibited with ruthenium red but may be further triggered by the addition of an uncoupler. Under such conditions, mammalian mitochondrial PT is inhibited (not activated) by Ca^{2+} addition with an $IC_{50} = 0.25$ mM (Bernardi et al., 1993). Since *S. cerevisiae* mitochondria seem to lack an endogenous Ca^{2+} uniporter, the most logical hypothesis would be that Ca^{2+} suppresses PT in this organism. This was demonstrated in experiments showing that Ca^{2+} ($IC_{50} = 0.3$ mM) could control the fate of the energy derived from oxidative metabolism through regulating the closure of the $_{Sc}$MUC (Table 2) (Pérez-Vázquez et al., 2003). This is a similar (but non-physiological) value for the Ca^{2+}-mediated inhibition of $_{m}$MUC (Bernardi et al., 1993). For *S. cerevisiae* mitochondria, this value may be lowered to the micromolar range when in the presence of non-inhibitory levels of Mg^{2+} and Pi (unpublished results).

Finally, a Ca^{2+} induced permeability transition in *S. cerevisiae* under optimized experimental conditions was reported (Yamada et al., 2009). This work showed that mitochondria incubated in the presence of the Ca^{2+} ionophore ETH129 plus 100 μM Ca^{2+} and low phosphate concentrations, suffered a collapse in $\Delta\Psi$. Similar effects were obtained for mitochondria from *Yarrowia lypolytica* and *Endomyces magnusii* (Kovaleva et al., 2009). This suggests that high matrix free Ca^{2+}can trigger PT in these yeast species, as long as mitochondria are incubated with low Pi levels. Also, *S. cerevisiae* mitochondria depolarize transiently upon Ca^{2+} and ETH129 addition, triggering Ca^{2+} release (Bradshaw and

Table 2
Mitochondrial Unselective Channel effectors from diverse species.

Modulator	Possible target	Effect	MUC(s)	Reference(s)
Bonkrekic acid and ADP	ANT	Inhibition	$_{m}$MUC, $_{Lf}$MUC and $_{pea}$MUC	Crompton et al. (1998) and Savina et al. (2006)
CAT and agaric acid	ANT	Activation	$_{m}$MUC	García et al. (2009)
CAT	ANT	Partial inhibition	$_{Sc}$MUC	Roucou et al. (1995, 1997)
Ruthenium red	MCU, VDAC	Inhibition	$_{m}$MUC and $_{Zf}$MUC,	Azzolin et al. (2010b) and Bernardi et al. (1993)
Cyclosporin A and Sangliferin A	CypD	Inhibition	$_{m}$MUC, $_{Zf}$MUC,$_{Om}$MUC, $_{Lf}$MUC, $_{Ze}$MUC, $_{Pt}$MUC, $_{At}$MUC, $_{Nt}$MUC and $_{pea}$MUC	Arpagaus et al. (2002), Azzolin et al. (2010a), Crompton et al. (1992), Fortes et al. (2001), Krumschnabel et al. (2005), Lin et al. (2006), Savina et al. (2006), Scott and Logan (2008), Tiwari et al. (2002), Vianello et al. (1995) and Yu et al. (2002)
Hydroxy-decylubiquinone	Unknown	Activation	$_{m}$MUC	Walter et al. (2002)
Ubiquinone 0,decylubiquinone	Unknown	Inhibition	$_{Zf}$MUC and $_{m}$MUC	Azzolin et al. (2010a) and Walter et al. (2002)
Ca^{2+}, Cu^{2+},Cd^{2+}, Pb^{2+} and Hg^{2+}	Unknown	Activation	$_{m}$MUC, $_{Sc}$MUC, $_{Zf}$MUC, $_{Om}$MUC, $_{Gs}$MUC$_{Ze}$MUC, $_{Pt}$MUC, $_{oat}$MUC, $_{wheat}$MUC and $_{Af}$MUC	Arpagaus et al. (2002), Azzolin et al. (2010a), Curtis and Wolpert (2002), Holman and Hand (2009), Hunter and Haworth (1979a), Krumschnabel et al. (2005), Menze and Hand (2009), Menze et al. (2005), Virolainen et al. (2002), Yamada et al. (2009) and Yu et al. (2002)
Me^{2+} and La^{3+}	Unknown	Inhibition	$_{m}$MUC, $_{Sc}$MUC, $_{Lf}$MUC, $_{At}$MUC and $_{Dh}$MUC	Bernardi et al. (1993), Cabrera-Orefice et al. (2010), Pérez-Vázquez et al. (2003), Savina et al. (2006), Scott and Logan (2008) and Tiwari et al. (2002)
Alkylamines	Unknown/VDAC	Inhibition	$_{m}$MUC and $_{Sc}$MUC	Gutiérrez-Aguilar et al. (2007), Pavón et al. (2009) and Pérez-Vázquez et al. (2003)
Thiol oxidizing reagents	ANT and PiC	Activation	$_{m}$MUC, $_{Sc}$MUC and $_{Zf}$MUC	Azzolin et al. (2010a), Gutiérrez-Aguilar et al. (2010) and Leung et al. (2008)
Maleimides	ANT and PiC	Inhibition	$_{m}$MUC and $_{Zf}$MUC	Azzolin et al. (2010a) and Leung et al. (2008)
dVO_4	VDAC	Inhibition	$_{Sc}$MUC	Gutiérrez-Aguilar et al. (2007, 2010), Manon and Guerin (1997), Manon et al. (1998) and Roucou et al. (1997)
As_2O_3	VDAC	Activation	$_{m}$MUC and $_{Sc}$MUC	Zheng et al. (2004)
Mitochondrial signal peptides and mastoparan	Unknown (PIM?)	Activation	$_{m}$MUC and $_{oat}$MUC	Curtis and Wolpert (2002), Kushnareva et al. (1999, 2001); Pfeiffer et al. (1995), Sokolove and Kinnally (1996)
Reactive oxygen species	Specific thiols	Activation	$_{m}$MUC, $_{Sc}$MUC and $_{Af}$MUC	García et al. (2005), Kowaltowski et al. (2000), McStay et al. (2002) and Menze et al. (2005)
Phosphate	Unknown	Inhibition	$_{m}$MUC, $_{Sc}$MUC, $_{Zf}$MUC and $_{Dh}$MUC	Azzolin et al. (2010a), Basso et al. (2008), Cabrera-Orefice et al. (2010), Chavez et al. (1997), Guerin et al. (1994), Gutiérrez-Aguilar et al. (2007, 2010), Prieto et al. (1992)
Phosphate	Unknown	Activation (with Ca^{2+})	$_{m}$MUC	Halestrap (2009)

Abbreviations used:MUC: Mitochondrial Unselective Channel. MCU: Mitochondrial Ca^{2+} uniporter, PIM: mitochondrial protein import machinery, CAT: carboxyatractyloside, m: mammalian, *Sc*: *Saccharomyces cerevisiae*, *Zf*: *Zebrafish*, *Om*: *Oncorhynchus mykiss*, *Gs*: ghost shrimp, *Ze*: *Zinnia elegans*, *Pt*: potato tuber, *Dh*: *Debaryomyces hansenii*, *At*: *Arabidopsis thaliana*, *Nt*: *Nicotiana tabacum*; *pea*: *Pissum sativum* and *Af*: *Artemia franciscana.*

Pfeiffer, 2006). This is a typical feature of the $_{m}$MUC (Ichas and Mazat, 1998). In the work by Yamada et al. (2009), the effect of Ca^{2+} plus the ionophore was shown to be insensitive to dVO_4. Thus it was suggested that this oxovanadate should be reevaluated as a *bona fide* $_{Sc}$MUC effector. However, dVO_4 inhibits $_{Sc}$MUC as a competitor for ATP-binding sites on putative $_{Sc}$MUC components (Roucou et al., 1997). This means ATP and dVO_4 should be acting at sites that are different to the Ca^{2+} site that opens the $_{Sc}$MUC. The site of action for dVO_4 has been proposed to be located at VDAC (Gutiérrez-Aguilar et al., 2007).

The $_{Sc}$MUC is not sensitive to CsA. Still, *S. cerevisiae* expresses a matricial cyclophilin involved in the CsA-sensitive protein folding (Matouschek et al., 1995). While there is no apparent relationship between this protein and the $_{Sc}$MUC, mammalian cyclophilin D does interact with yeast ANT (Woodfield et al., 1998). CsA-insensitive MUCs have also been detected in other organisms such as *Drosophila melanogaster* and *Triticum aestivum* (wheat). Nevertheless both MUCs are triggered by Ca^{2+}, which makes these MUCs share traits with the yeast and mammalian unselective channels (Virolainen et al., 2002; von Stockum et al., 2010) (Table 2).

3.1.5. $_{Sc}$MUC structure–function relationships

Most of the structural characteristics of the $_{Sc}$MUC remain to be determined. Proteins usually having another role in mitochondrial physiology have been proposed to form part or at least modulate the $_{Sc}$MUC (Gutiérrez-Aguilar et al., 2007, 2010; Roucou et al., 1997). The first evidence suggesting the dispensability of VDAC as a component of the $_{Sc}$MUC was suggested in experiments where mitochondria from a ΔVDAC strain exhibited a small increase in the NADH-supported oxygen consumption rate upon ATP addition. This was interpreted as the opening of the $_{Sc}$MUC (Roucou et al., 1997). Later reports demonstrated that the permeability of the outer membrane to external nucleotides is reduced 20-fold in the porin-less strain and that NADH is specifically transported into mitochondria through the VDAC (Averet et al., 2002; Lee et al., 1998). Thus, experiments reinforcing the notion that the VDAC is not necessary for PT in yeast were missing. These experiments were later performed in a wild type and ΔVDAC strain by monitoring the opening of the $_{Sc}$MUC through oxygen consumption, $\Delta\Psi$ and swelling experiments. The opening of the $_{Sc}$MUC was triggered by Pi depletion and the respiratory chain was fueled by ethanol thus avoiding the diffusion issue with NADH in the ΔVDAC strain (Gutiérrez-Aguilar et al., 2007). Indeed, PT was monitored in the mutant strain; nevertheless its regulation by Ca^{2+}, OG and dVO_4 was lost. When the same experiments were performed in wild type yeast mitoplasts i.e., in outer membrane depleted mitochondria, the same results were obtained (unpublished results). This suggests that although ΔVDAC mitochondria undergo PT, the porin is involved in the $_{Sc}$MUC sensitivity to Ca^{2+}, OG and dVO_4. In other words, it is possible that VDAC is a regulatory component of the $_{Sc}$MUC.

The putative role of the ANT in the $_{Sc}$MUC has been explored as it has been observed that the ATP-induced mitochondrial depolarization

was partially inhibited by the addition of CAT to isolated mitochondria from the Yeast Foam and YPH250 strains, an opposite regulation observed for the $_m$MUC (García et al., 2009; Jung et al., 1997; Roucou et al., 1997). In a mutant strain lacking the three isoforms of the ANT, ATP still induced a drop in $\Delta\Psi$, strongly suggesting that the ANT is at best a dispensable but regulatory component of the $_{Sc}$MUC (Roucou, et al., 1997). This is the current notion for the role of the ANT in the $_m$MUC (Kokoszka et al., 2004; Leung and Halestrap, 2008).

Since the $_{Sc}$MUC is inhibited by Pi (Prieto et al., 1992) and triggered by mersalyl, we studied the relationship between the phosphate carrier (PiC) and the $_{Sc}$MUC (Cortés et al., 2000; Gutiérrez-Aguilar et al., 2010). The effects of mersalil on mitochondria were reversed by dVO_4. In mitochondria from a ΔPiC strain, the mersalyl-induced opening of $_{Sc}$MUC was not detected, while an ATP-triggered, dVO_4-sensitive PT was still present. In this mutant strain, high loads of phosphate (around 5-fold) were needed to seal the channel, possibly through matrix acidification (Velours et al., 1977). In ΔPiC mitochondria, solute size exclusion experiments indicated that the $_{Sc}$MUC in the mutant strain was smaller, with a maximal cutoff size of around 1.1 kDa as compared to the 1.5 kDa WT-$_{Sc}$MUC cutoff size.

Thus the $_{Sc}$MUC is a complex structure whose regulation appears to be opposite in some cases but similar to that reported for other MUCs. It's molecular nature and possible role in cell life and death still remains to be unequivocally established. Nonetheless, the relative ease of use, the viability of mutants lacking mitochondrial proteins and the possibility of expression of mutated or recombinant proteins, make facultative yeasts such as *S. cerevisiae* an ideal model for the study of MUC's.

3.2. Mitochondrial Unselective Channels in non-conventional yeasts

Attempts to find a "typical" MUC in some non-conventional yeasts such as *Pichia pastoris* (González-Barroso et al., 2006), *Yarrowia lipolytica* and *E. magnusii* have been unsuccessful due to the apparent lack of an unspecific channel modulated by nucleotides or by phosphate, such as the $_{Sc}$MUC (Kovaleva et al., 2009; Manon et al., 1998).

In a recent report, a MUC was detected in *D. hansenii* ($_{Dh}$MUC) (Cabrera-Orefice et al., 2010). The $_{Dh}$MUC is regulated by Pi, Ca^{2+} and Mg^{2+}. This yeast is considered a halophilic organism since in its environment high levels of extracellular Na^+ may permeate into the cytosol affecting proteins and organelles. Interestingly, Na^+ and K^+ salts, close the $_{Dh}$MUC. This feature is at variance with the effect of monovalent cations on other MUCs including the $_{Sc}$MUC and the $_m$MUC, suggesting that MUC modulation may differ as a response to the changing environment where a given organism develops. Experiments comparing the $_{Sc}$MUC and the $_{Dh}$MUCs showed that both structures are sensitive to submicromolar amounts of the potent $_m$MUC facilitator mastoparan (Fig. 1). Mastoparan is a peptide known to trigger PT in mitochondria from different sources (Curtis and Wolpert, 2002; Pfeiffer et al., 1995; Sokolove and Kinnally, 1996). At submicromolar levels, the effects of mastoparan on *D. hansenii* mitochondria seem to occur at the level of the $_{Dh}$MUC opening since these are reversed with micromolar amounts of decavanadate (dVO_4) (Fig. 1A trace e). Under analog conditions, the mastoparan-triggered $_{Sc}$MUC is inhibited with dVO_4 (Fig. 1B trace e). The mechanism of action of this peptide has not been solved to date. Its cationic and helical nature may suggest that mastoparan triggers MUC opening through a similar pathway as that achieved using mitochondrial signal peptides (Kushnareva et al., 1999, 2001; Pfeiffer et al., 1995; Sokolove and Kinnally, 1996).

4. The mitochondrial permeability transition in mammals

In mammals, the Mitochondrial Unselective Channel ($_m$MUC) has been thoroughly studied (Bernardi et al., 1998; Zoratti and Szabo, 1995). Many useful reviews on the $_m$MUC are available to the reader (Baines, 2009a,b; Crompton, 1999; Halestrap and Pasdois, 2009; Lemasters et al., 2009; Rasola and Bernardi, 2007; Zoratti et al., 2005). Since its discovery, several groups have characterized relevant structure–function features in the $_m$MUC suggesting an important role in cell homeostasis and pathology (Haworth and Hunter, 1979; Hunter and Haworth, 1979a,b; Ichas and Mazat, 1998).

Commonly, Ca^{2+} plus an additional effector e.g. phosphate, oxidative stress or high pH levels are used to trigger $_m$MUC opening in a CsA-sensitive fashion (Bernardi, 1999). Other molecules known to promote $_m$MUC opening are mastoparan or mitochondrial signal peptides (Kushnareva et al., 1999, 2001; Pfeiffer et al., 1995; Sokolove and Kinnally, 1996). As described above, both effectors also trigger MUC opening in yeasts from different species (Fig. 1). The modulation of $_m$MUC by diverse effectors has helped to elucidate its possible structure–function relationships and role in cell life and death (Elrod et al., 2010; Lemasters, 2007; Malhi et al., 2006). Today, an increasing number of reagents known either to activate or inhibit $_m$MUC have been described (Table 2). In addition, both *in vitro* and *in vivo* $_m$MUC opening correlates with the damage induced by ischemia–reperfusion and storage–reperfusion injuries (Lemasters et al., 2009). In these cases, addition of $_m$MUC inhibitors has been shown to protect cells and tissues (Correa et al., 2007; Pavón et al., 2009; Zazueta et al., 2007). It is noteworthy to mention that PT is an organ- and tissue-dependent phenomenon. Differences in the PT behavior of different organs and tissues in response to diverse effectors such as Ca^{2+}, Pi and thiol reagents have been reported (Berman et al., 2000; Friberg et al., 1999).

Regulated $_m$MUC opening/closing cycles, i.e. flickering, has been previously proposed and suggested to constitute a energetic dissipation (uncoupling) pathway (Giorgio et al., 2009; Petronilli et al., 1999, 2001); flickering occurs when an initial Ca^{2+} signal from the Endoplasmic Reticulum (ER) reaches mitochondria (Rizzuto et al., 2009). Then, transient physiological opening of the $_m$MUC would decrease $\Delta\Psi$ and release accumulated Ca^{2+} (Ichas and Mazat, 1998). The decrease in$\Delta\Psi$ would promote mitochondrial matrix acidification, a strong inhibitory signal for $_m$MUC (Bernardi et al., 1992) activating the respiratory chain to pump protons to reestablish the $\Delta\Psi$ (Zoratti and Szabo, 1995). Ca^{2+} cycling would also increase the semiquinone radical turnover rate, thus diminishing the production of reactive oxygen species (ROS) (Ichas and Mazat, 1998; Korshunov et al., 1997). Thus, $_m$MUC flickering could constitute a regulated metabolic and ROS dissipation mechanism.

While the behavior of the $_m$MUC is well characterized, the structure of this entity has been difficult to establish. As for *S. cerevisiae* mitochondria, solute exclusion-mediated mitochondrial shrinkage experiments determined the $_m$MUC solute size cutoff to be close to 1.5 kDa (Hunter and Haworth, 1979b). This means that smaller solutes will tend to flow through mitochondria unselectively. Several proteins and molecules exhibiting a function different to the formation of the $_m$MUC have been reported to constitute or at least regulate the pore: the Voltage Dependent Anion Channel (VDAC), the Adenine Nucleotide Translocase (ANT), the phosphate carrier (PiC), components of the Protein Import Machinery (PIM), respiratory complex I and accessory proteins/molecules such as cyclophilin D (CypD) (Fig. 2) have been proposed to play either a regulatory or a structural role in the unselective permeability(Alcalá et al., 2008; Crompton et al., 1992, 1998; Fontaine and Bernardi, 1999; García et al., 2005; Halestrap et al., 1997; Kushnareva et al., 1999, 2001; Leung and Halestrap, 2008; Leung et al., 2008; Palma et al., 2009; Sokolove and Kinnally, 1996; Szabo and Zoratti, 1993; Szabo et al., 1993; Woodfield et al., 1998; Zheng et al., 2004; Zoratti et al., 2010). Nevertheless, upon deletion of most of these proteins, some kind of PT or PT-derived cell death still takes place (Alcalá et al., 2008; Baines, 2007, 2009b; Baines et al., 2005; Basso et al., 2005; Kokoszka et al., 2004) strengthening the notion that the unspecificity of MUCs may not be limited to the transported species, but also to its structural components.

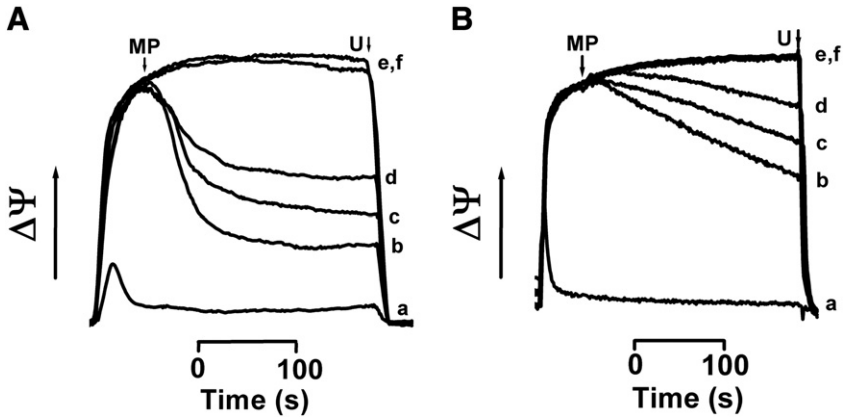

Fig. 1. Opening of the $_{Dh}$MUC (A) and $_{Sc}$MUC (B) can be achieved in the presence of submicromolar amounts of the wasp venom peptide mastoparan. Experimental conditions: (A) *Debaryomyces hansenii* mitochondria: 1 M sorbitol pH 6.8 (Tris–maleate), 10 mM pyruvate–malate. a: 0.4 mM Pi, b: 10 mM Pi plus 1 μM mastoparan, c: 10 mM Pi plus 0.75 μM mastoparan, d: 10 mM Pi plus 0.5 μM mastoparan, e: 10 mM Pi plus 1 μM mastoparan and 10 μM dVO_4 and f: 10 mM Pi. (B) *Saccharomyces cerevisiae* mitochondria: 0.6 M mannitol pH 6.8 (Tris–maleate), 5 μL/mL ethanol. a: 0.4 mM Pi, b: 4 mM Pi plus 1 μM mastoparan, c: 4 mM Pi plus 0.75 μM mastoparan, d: 4 mM Pi plus 0.5 μM mastoparan, e: 4 mM Pi plus 1 μM mastoparan and 10 μM dVO_4 and f: 4 mM Pi. The mitochondrial ΔΨ was determined spectrophotometrically using a DW2 Aminco spectrophotometer in dual mode at 511–533 nm monitoring the changes in absorbance of 10 μM safranine-O as in Gutiérrez-Aguilar et al. (2007). 6 μM of the uncoupler FCCP was added at the end of each trace.

5. Mitochondrial Unselective Channels in non-mammalian animal mitochondria

Most of the studies on mitochondrial PT have been centered in mammalian and yeast models. Nonetheless, PT has been reported in mitochondria from many sources (Table 1).In trout hepatocytes, the acute toxicity of Cu^{2+} leading to an excess in free radical formation and cell death was described (Manzl et al., 2003, 2004). In addition to ROS formation, an increase in intracellular free $Ca^{2+}$and depletion of the glutathione pool was monitored. Further experiments demonstrated a Cu^{2+} induced-CsA-sensitive PT in rainbow trout mitochondria (Table 2) (Krumschnabel et al., 2005).

In a recent report, a MUC has been detected and characterized in *Danio rerio* (Azzolin et al., 2010b). This fish has been considered a very attractive model for developmental biology studies and for understanding key aspects of mitochondrial diseases (Dooley and Zon, 2000; Navarro et al., 2008; Telfer et al., 2010). Zebra fish mitochondria may be used to test novel pore inhibitors and perhaps to unveil the molecular structure of MUCs. The $_{Zf}$MUC is responsive to known MUC effectors such as CsA, ΔΨ, pH, ruthenium red, ubiquinone analogues, ANT ligands and dithiol reagents (Table 2) (Azzolin et al., 2010a).

As suggested for mammalian and yeast models, MUC flickering may work as an energy dissipation mechanism (Petronilli et al., 1999, 2001; Prieto et al., 1992). This could be considered a physiological role of MUCs and this has been also evaluated in the Baltic lamprey *Lampetra fluviatilis* MUC ($_{Lf}$MUC) (Savina et al., 2006). During the winter season, the $_{Lf}$MUC is continuously open in a low conductance state. This has been suggested to be due to the low levels of adenine nucleotides that possibly render the ANT inactive for nucleotide translocation promoting unselective permeability to H^+, K^+ and Cl^- in a CsA, Mg^{2+}, EGTA and ADP sensitive fashion. The low conductance opening observed in $_{Lf}$MUC might be similar to that observed in the mammalian structure (Ichas and Mazat, 1998). Upon arrival of spring, lamprey mitochondria resume a highly oxidative metabolism prior to

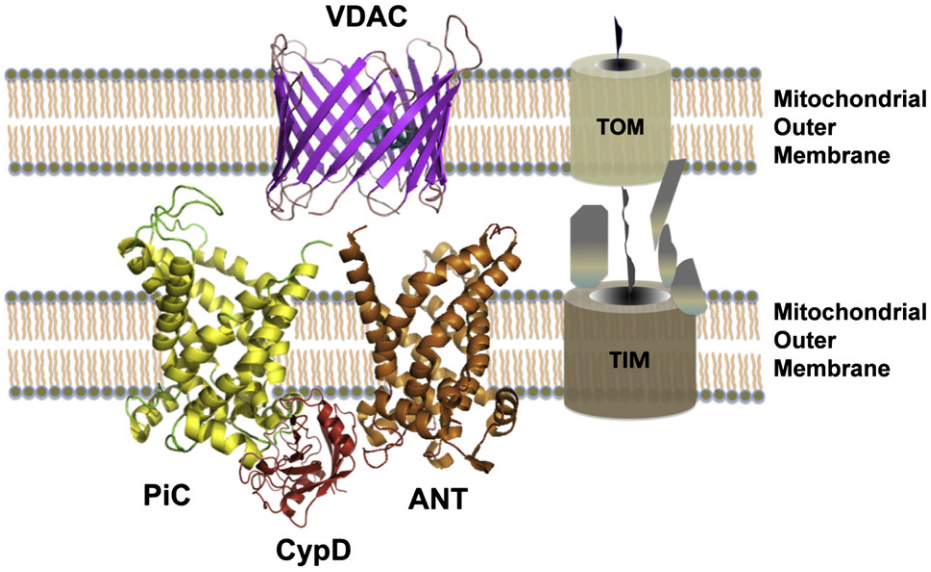

Fig. 2. Putative components of the mammalian MUC. To date, the only certain (but regulatory) component of this structure appears to be the mitochondrial cyclophylin (CypD). Nevertheless, several proteins usually having another physiological role have been proposed to at least regulate such structure. VDAC: Voltage Dependent Anion Channel, PiC: phosphate carrier, ANT: Adenine Nucleotide Translocase and TIM/TOM: pore components of the protein import machinery. Protein models were generated with PyMol software (The PyMOL Molecular Graphics System, Version 1.2r3pre, Schrödinger, LLC).

spawning and death of the organism. This kind of cell death induced by oxidative damage has been reported during reperfusion injury in mammalian mitochondria. In this scenario, the respiratory chain may be triggering $_{Lf}$MUC in its high conductance state through ROS production (Theruvath et al., 2006).

In the invertebrate *Artemia franciscana* no MUC was detected upon Ca^{2+} addition (Hand and Menze, 2008; Menze and Hand, 2009; Menze et al., 2005). Nevertheless, *A. franciscana* mitochondria show an active Ca^{2+} uptake system (Menze et al., 2005). This was also the case for *Lepidophthalmus louisianensis* (ghost shrimp) mitochondria, where a permeability transition could not be triggered by Ca^{2+} addition (Holman and Hand, 2009). In both cases, PT was achieved in the presence of Hg^{2+}. This was interpreted as a MUC-independent permeabilization mechanism. In addition, the lack of sensitivity to Ca^{2+} and CsA led to suggest that ghost shrimp mitochondria do not undergo a classical PT. It is worth to mention that there are increasing reports that detect CsA-insensitive $_{m}$MUC opening triggered even by classical effectors (Basso et al., 2008; García et al., 2009; Sokolove and Kinnally, 1996). This probably reflects the currently growing notion that CsA is not a *bona fide* $_{m}$MUC blocker since PT is only delayed in its presence. This may be possibly because MUC opening is achieved even in the absence of CypD (Baines et al., 2005). In fact, it has been proposed that the main $_{m}$MUC trigger is the oxidation of critical residues inducing conformational changes facilitated by Ca^{2+} in membrane proteins (Halestrap, 2009).

6. Mitochondrial Unselective Channels in plants

The presence of MUCs in plants ($_{p}$MUC) from diverse species has been reported. The first piece of evidence points to a similar modulation as in mammalian mitochondria: in most cases, Ca^{2+} is necessary to induce a high amplitude mitochondrial swelling although the Ca^{2+} uptake mechanism is not evident (Curtis and Wolpert, 2002). As in the $_{Sc}$MUC, the presence of Ca^{2+} ionophores such as A23187 is necessary to induce the opening of a $_{p}$MUC in *Zinnia elegans* (Yu et al., 2002). Both Ca^{2+} and phosphate seem to be the only requirements to induce an increase in mitochondrial permeability produced by $_{p}$MUC opening since CsA acts in species such as *Arabidopsis thaliana* and *Pissum sativum* (Arpagaus et al., 2002; Lin et al., 2006; Scott and Logan, 2008; Tiwari et al., 2002; Vianello et al., 1995) but not on potato or wheat mitochondria, where a $_{p}$MUC has also been detected (Fortes et al., 2001; Virolainen et al., 2002). The effect of other modulators both negative such as spermine (Curtis and Wolpert, 2002), ADP (Fortes et al., 2001), thiol redox agents (Arpagaus et al., 2002), La^{3+} (Scott and Logan, 2008) and ruthenium red (Fortes et al., 2001) and positive such as ROS (Lin et al., 2006; Tiwari et al., 2002) and CAT (Vianello et al., 1995) were tested with positive results in some but not all plant mitochondria which makes it difficult to extrapolate about a general regulatory mechanism in plants. All these observations suggest that the effects of these ions and molecules are tissue and/or species-dependent as seen in mitochondria from other sources (Berman et al., 2000; Friberg et al., 1999).

Studies on diverse plants lead to propose a relationship between MUC opening and cell death. In wheat, oat and potato tuber mitochondria, (Arpagaus et al., 2002; Curtis and Wolpert, 2002; Virolainen et al., 2002) the opening of a Ca^{2+}-induced $_{p}$MUC produces high amplitude swelling with subsequent Cyt *c* release to the cytosol. This observation was soon confirmed in *A. thaliana* mitochondria where the Ca^{2+}-transport inhibitor, La^{3+}, and the $_{m}$MUC inhibitor, CsA, prevented abnormalities in mitochondrial morphology that would have resulted from $_{p}$MUC opening (Scott and Logan, 2008; Tiwari et al., 2002). The phenomenon of massive mitochondrial fragmentation and the early events in apoptosis were related to the release of Cyt *c* once the $_{p}$MUC was induced by Ca^{2+} (Scott and Logan, 2008). This evidence strongly suggests that plant mitochondria may also constitute an attractive model for conducting MUC studies.

7. Concluding remarks

Mitochondrial Unselective Channels appear to be widely distributed in many species. The regulation and possible physiological role of these structures exhibit both, differences and similarities. Still, their importance for cellular bioenergetics cannot be denied. An increasing battery of evidence is building the notion of a basic conserved MUC structure that was subjected to constant change by evolution. Thus, a MUC from wheat or potato tuber may share some features with a similar structure from yeast or rodents. Further comparison between yeast and mammalian channels suggest these structures share the same modulation by a growing set of effectors such as mastoparan. Using non-mammalian mitochondria to study key aspects of PT seems to be an interesting alternative, i.e. fish, plant and yeast mitochondria may constitute effective systems for MUC pharmacological screening and may be considered as reference models for determining the molecular composition of a "standard" MUC, where any putative channel component may be expressed, mutated or deleted. In the case of fish and plant mitochondria, the presence of a MUC with high similarity with the $_{m}$MUC may constitute an advantage. Finally, yeasts such as *S. cerevisiae* may constitute a choice model due to their ability to grow even with dysfunctional mitochondria.

Acknowledgements

This study was partially funded by grants from CONACYT 79989 and DGAPA/UNAM IN217109-3. LALM, SGC, ACO and MGA are CONACYT fellows enrolled in the Biochemistry PhD program at UNAM. The authors wish to thank Ramón Mendez, Armando Zepeda-Bastida, Miriam Vázquez-Acevedo and Yolanda Camacho-Villasana for technical assistance.

References

Alcalá, S., Klee, M., Fernandez, J., Fleischer, A., Pimentel-Muinos, F.X., 2008. A high-throughput screening for mammalian cell death effectors identifies the mitochondrial phosphate carrier as a regulator of cytochrome c release. Oncogene 27, 44–54.

Arpagaus, S., Rawyler, A., Braendle, R., 2002. Occurrence and characteristics of the mitochondrial permeability transition in plants. J. Biol. Chem. 277, 1780–1787.

Averet, N., Aguilaniu, H., Bunoust, O., Gustafsson, L., Rigoulet, M., 2002. NADH is specifically channeled through the mitochondrial porin channel in *Saccharomyces cerevisiae*. J. Bioenerg. Biomembr. 34, 499–506.

Azzolin, L., von Stockum, S., Basso, E., Petronilli, V., Forte, M.A., Bernardi, P., 2010a. The mitochondrial permeability transition from yeast to mammals. FEBS Lett. 584, 2504–2509.

Azzolin, L., Basso, E., Argentón, F., Bernardi, P., 2010b. Mitochondrial Ca^{2+} transport and permeability transition in zebrafish (*Danio rerio*). Biochim. Biophys. Acta 1797, 1775–1779.

Baines, C.P., 2007. The mitochondrial permeability transition pore as a target of cardioprotective signaling. Am. J. Physiol. Heart Circ. Physiol. 293, H903–H904.

Baines, C.P., 2009a. The mitochondrial permeability transition pore and ischemia–reperfusion injury. Basic Res. Cardiol. 104, 181–188.

Baines, C.P., 2009b. The molecular composition of the mitochondrial permeability transition pore. J. Mol. Cell. Cardiol. 46, 850–857.

Baines, C.P., Kaiser, R.A., Purcell, N.H., Blair, N.S., Osinska, H., Hambleton, M.A., Brunskill, E.W., Sayen, M.R., Gottlieb, R.A., Dorn, G.W., Robbins, J., Molkentin, J.D., 2005. Loss of cyclophilin D reveals a critical role for mitochondrial permeability transition in cell death. Nature 434, 658–662.

Ballarin, C., Sorgato, M.C., 1995. An electrophysiological study of yeast mitochondria. Evidence for two inner membrane anion channels sensitive to ATP. J. Biol. Chem. 270, 19262–19268.

Ballarin, C., Sorgato, M.C., 1996. Anion channels of the inner membrane of mammalian and yeast mitochondria. J. Bioenerg. Biomembr. 28, 125–130.

Ballarin, C., Bertoli, A., Wojcik, G., Sorgato, M.C., 1996. Mitochondrial inner membrane channels in yeast and mammals. Soc. Gen. Physiol. Ser. 51, 155–171.

Basso, E., Fante, L., Fowlkes, J., Petronilli, V., Forte, M.A., Bernardi, P., 2005. Properties of the permeability transition pore in mitochondria devoid of cyclophilin D. J. Biol. Chem. 280, 18558–18561.

Basso, E., Petronilli, V., Forte, M.A., Bernardi, P., 2008. Phosphate is essential for inhibition of the mitochondrial permeability transition pore by cyclosporin A and by cyclophilin D ablation. J. Biol. Chem. 283, 26307–26311.

Beauvoit, B., Rigoulet, M., 2001. Regulation of cytochrome c oxidase by adenylic nucleotides. Is oxidative phosphorylation feedback regulated by its end-products? IUBMB Life 52, 143–152.

Berman, S.B., Watkins, S.C., Hastings, T.G., 2000. Quantitative biochemical and ultrastructural comparison of mitochondrial permeability transition in isolated

brain and liver mitochondria: evidence for reduced sensitivity of brain mitochondria. Exp. Neurol. 164, 415–425.
Bernardi, P., 1999. Mitochondrial transport of cations: channels, exchangers, and permeability transition. Physiol. Rev. 79, 1127–1155.
Bernardi, P., Vassanelli, S., Veronese, P., Colonna, R., Szabo, I., Zoratti, M., 1992. Modulation of the mitochondrial permeability transition pore. Effect of protons and divalent cations. J. Biol. Chem. 267, 2934–2939.
Bernardi, P., Veronese, P., Petronilli, V., 1993. Modulation of the mitochondrial cyclosporin A-sensitive permeability transition pore. I. Evidence for two separate Me^{2+} binding sites with opposing effects on the pore open probability. J. Biol. Chem. 268, 1005–1010.
Bernardi, P., Colonna, R., Costantini, P., Eriksson, O., Fontaine, E., Ichas, F., Massari, S., Nicolli, A., Petronilli, V., Scorrano, L., 1998. The mitochondrial permeability transition. Biofactors 8, 273–281.
Bernardi, P., Krauskopf, A., Basso, E., Petronilli, V., Blachly-Dyson, E., Di Lisa, F., Forte, M.A., 2006. The mitochondrial permeability transition from in vitro artifact to disease target. FEBS J. 273, 2077–2099.
Bradshaw, P.C., Pfeiffer, D.R., 2006. Release of Ca^{2+} and Mg^{2+} from yeast mitochondria is stimulated by increased ionic strength. BMC Biochem. 7, 1–4.
Cabrera-Orefice, A., Guerrero-Castillo, S., Luévano-Martínez, L.A., Pena, A., Uribe-Carvajal, S., 2010. Mitochondria from the salt-tolerant yeast *Debaryomyces hansenii* (halophilic organelles?). J. Bioenerg. Biomembr. 42, 11–19.
Carafoli, E., Balcavage, W.X., Lehninger, A.L., Mattoon, J.R., 1970. Ca^{2+} metabolism in yeast cells and mitochondria. Biochim. Biophys. Acta 205, 18–26.
Castrejón, V., Parra, C., Moreno, R., Pena, A., Uribe, S., 1997. Potassium collapses the deltaP in yeast mitochondria while the rate of ATP synthesis is inhibited only partially: modulation by phosphate. Arch. Biochem. Biophys. 346, 37–44.
Chavez, E., Moreno-Sanchez, R., Zazueta, C., Rodriguez, J.S., Bravo, C., Reyes-Vivas, H., 1997. On the protection by inorganic phosphate of calcium-induced membrane permeability transition. J. Bioenerg. Biomembr. 29, 571–577.
Correa, F., Soto, V., Zazueta, C., 2007. Mitochondrial permeability transition relevance for apoptotic triggering in the post-ischemic heart. Int. J. Biochem. Cell Biol. 39, 787–798.
Cortés, P., Castrejón, V., Sampedro, J.G., Uribe, S., 2000. Interactions of arsenate, sulfate and phosphate with yeast mitochondria. Biochim. Biophys. Acta 1456, 67–76.
Cortés-Rojo, C., Calderón-Cortés, E., Clemente-Guerrero, M., Manzo-Avalos, S., Uribe, S., Boldogh, I., Saavedra-Molina, A., 2007. Electron transport chain of *Saccharomyces cerevisiae* mitochondria is inhibited by H_2O_2 at succinate–cytochrome *c* oxidoreductase level without lipid peroxidation involvement. Free Radic. Res. 41, 1212–1223.
Crompton, M., 1999. The mitochondrial permeability transition pore and its role in cell death. Biochem. J. 341 (Pt 2), 233–249.
Crompton, M., McGuinness, O., Nazareth, W., 1992. The involvement of cyclosporin A binding proteins in regulating and uncoupling mitochondrial energy transduction. Biochim. Biophys. Acta 1101, 214–217.
Crompton, M., Virji, S., Ward, J.M., 1998. Cyclophilin-D binds strongly to complexes of the voltage-dependent anion channel and the adenine nucleotide translocase to form the permeability transition pore. Eur. J. Biochem. 258, 729–735.
Curtis, M.J., Wolpert, T.J., 2002. The oat mitochondrial permeability transition and its implication in victorin binding and induced cell death. Plant J. 29, 295–312.
de Chateaubodeau, G., Guerin, M., Guerin, B., 1974. Studies on anionic transport in yeast mitochondria and promitochondria. Swelling in ammonium phosphate, glutamate, succinate and fumarate solutions. FEBS Lett. 46, 184–187.
de Chateaubodeau, G.A., Guerin, M., Guerin, B., 1976. Permeability of yeast mitochondrial internal membrane: structure–activity relationship. Biochimie 58, 601–610.
Dooley, K., Zon, L.I., 2000. Zebrafish: a model system for the study of human disease. Curr. Opin. Genet. Dev. 10, 252–256.
Elrod, J.W., Wong, R., Mishra, S., Vagnozzi, R.J., Sakthievel, B., Goonasekera, S.A., Karch, J., Gabel, S., Farber, J., Force, T., Brown, J.H., Murphy, E., Molkentin, J.D., 2010. Cyclophilin D controls mitochondrial pore-dependent Ca^{2+} exchange, metabolic flexibility, and propensity for heart failure in mice. J. Clin. Invest. 120, 3680–3687.
Fay, J.C., McCullough, H.L., Sniegowski, P.D., Eisen, M.B., 2004. Population genetic variation in gene expression is associated with phenotypic variation in *Saccharomyces cerevisiae*. Genome Biol. 5, R26.
Ferea, T.L., Botstein, D., Brown, P.O., Rosenzweig, R.F., 1999. Systematic changes in gene expression patterns following adaptive evolution in yeast. Proc. Natl. Acad. Sci. USA 96, 9721–9726.
Fontaine, E., Bernardi, P., 1999. Progress on the mitochondrial permeability transition pore: regulation by complex I and ubiquinone analogs. J. Bioenerg. Biomembr. 31, 335–345.
Fortes, F., Castilho, R.F., Catisti, R., Carnieri, E.G., Vercesi, A.E., 2001. Ca^{2+} induces a cyclosporin A-insensitive permeability transition pore in isolated potato tuber mitochondria mediated by reactive oxygen species. J. Bioenerg. Biomembr. 33, 43–51.
Friberg, H., Connern, C., Halestrap, A.P., Wieloch, T., 1999. Differences in the activation of the mitochondrial permeability transition among brain regions in the rat correlate with selective vulnerability. J. Neurochem. 72, 2488–2497.
García, N., Correa, F., Chávez, E., 2005. On the role of the respiratory complex I on membrane permeability transition. J. Bioenerg. Biomembr. 37, 17–23.
García, N., Zazueta, C., Martínez-Abundis, E., Pavón, N., Chávez, E., 2009. Cyclosporin A is unable to inhibit carboxyatractyloside-induced permeability transition in aged mitochondria. Comp. Biochem. Physiol. C Toxicol. Pharmacol. 149, 374–381.
Giorgio, V., Bisetto, E., Soriano, M.E., Dabbeni-Sala, F., Basso, E., Petronilli, V., Forte, M.A., Bernardi, P., Lippe, G., 2009. Cyclophilin D modulates mitochondrial F_oF_1-ATP synthase by interacting with the lateral stalk of the complex. J. Biol. Chem. 284, 33982–33988.
González-Barroso, M.M., Ledesma, A., Lepper, S., Pérez-Magan, E., Zaragoza, P., Rial, E., 2006. Isolation and bioenergetic characterization of mitochondria from *Pichia pastoris*. Yeast 23, 307–313.
Grimm, S., Brdiczka, D., 2007. The permeability transition pore in cell death. Apoptosis 12, 841–855.
Guerin, B., Bunoust, O., Rouqueys, V., Rigoulet, M., 1994. ATP-induced unspecific channel in yeast mitochondria. J. Biol. Chem. 269, 25406–25410.
Gutiérrez-Aguilar, M., Pérez-Vázquez, V., Bunoust, O., Manon, S., Rigoulet, M., Uribe, S., 2007. In yeast, Ca^{2+} and octylguanidine interact with porin (VDAC) preventing the mitochondrial permeability transition. Biochim. Biophys. Acta 1767, 1245–1251.
Gutiérrez-Aguilar, M., Pérez-Marténez, X., Chávez, E., Uribe-Carvajal, S., 2010. In *Saccharomyces cerevisiae*, the phosphate carrier is a component of the mitochondrial unselective channel. Arch. Biochem. Biophys. 494, 184–191.
Halestrap, A.P., 1994. Regulation of mitochondrial metabolism through changes in matrix volume. Biochem. Soc. Trans. 22, 522–529.
Halestrap, A.P., 2009. What is the mitochondrial permeability transition pore? J. Mol. Cell. Cardiol. 46, 821–831.
Halestrap, A.P., Pasdois, P., 2009. The role of the mitochondrial permeability transition pore in heart disease. Biochim. Biophys. Acta 1787, 1402–1415.
Halestrap, A.P., Connern, C.P., Griffiths, E.J., Kerr, P.M., 1997. Cyclosporin A binding to mitochondrial cyclophilin inhibits the permeability transition pore and protects hearts from ischaemia/reperfusion injury. Mol. Cell. Biochem. 174, 167–172.
Hand, S.C., Menze, M.A., 2008. Mitochondria in energy-limited states: mechanisms that blunt the signaling of cell death. J. Exp. Biol. 211, 1829–1840.
Haworth, R.A., Hunter, D.R., 1979. The Ca^{2+}-induced membrane transition in mitochondria. II. Nature of the Ca^{2+} trigger site. Arch. Biochem. Biophys. 195, 460–467.
Holman, J.D., Hand, S.C., 2009. Metabolic depression is delayed and mitochondrial impairment averted during prolonged anoxia in the ghost shrimp, *Lepidophthalmus louisianensis* (Schmitt, 1935). J. Exp. Mar. Bio. Ecol. 376, 85–93.
Hunter, D.R., Haworth, R.A., 1979a. The Ca^{2+}-induced membrane transition in mitochondria. I. The protective mechanisms. Arch. Biochem. Biophys. 195, 453–459.
Hunter, D.R., Haworth, R.A., 1979b. The Ca^{2+}-induced membrane transition in mitochondria. III. Transitional Ca^{2+} release. Arch. Biochem. Biophys. 195, 468–477.
Ichas, F., Mazat, J.P., 1998. From calcium signaling to cell death: two conformations for the mitochondrial permeability transition pore. Switching from low- to high-conductance state. Biochim. Biophys. Acta 1366, 33–50.
Jung, D.W., Bradshaw, P.C., Pfeiffer, D.R., 1997. Properties of a cyclosporin-insensitive permeability transition pore in yeast mitochondria. J. Biol. Chem. 272, 21104–21112.
Kokoszka, J.E., Waymire, K.G., Levy, S.E., Sligh, J.E., Cai, J., Jones, D.P., MacGregor, G.R., Wallace, D.C., 2004. The ADP/ATP translocator is not essential for the mitochondrial permeability transition pore. Nature 427, 461–465.
Korshunov, S.S., Skulachev, V.P., Starkov, A.A., 1997. High protonic potential actuates a mechanism of production of reactive oxygen species in mitochondria. FEBS Lett. 416, 15–18.
Kovaleva, M.V., Sukhanova, E.I., Trendeleva, T.A., Zyl'kova, M.V., Ural'skaya, L.A., Popova, K.M., Saris, N.E., Zvyagilskaya, R.A., 2009. Induction of a non-specific permeability transition in mitochondria from *Yarrowia lipolytica* and *Dipodascus* (*Endomyces*) *magnusii* yeasts. J. Bioenerg. Biomembr. 41, 239–249.
Kowaltowski, A.J., Vercesi, A.E., Rhee, S.G., Netto, L.E., 2000. Catalases and thioredoxin peroxidase protect Saccharomyces cerevisiae against Ca(2+)-induced mitochondrial membrane permeabilization and cell death. FEBS Lett. 473, 177–182.
Krumschnabel, G., Manzl, C., Berger, C., Hofer, B., 2005. Oxidative stress, mitochondrial permeability transition, and cell death in Cu-exposed trout hepatocytes. Toxicol. Appl. Pharmacol. 209, 62–73.
Kushnareva, Y.E., Campo, M.L., Kinnally, K.W., Sokolove, P.M., 1999. Signal presequences increase mitochondrial permeability and open the multiple conductance channel. Arch. Biochem. Biophys. 366, 107–115.
Kushnareva, Y.E., Polster, B.M., Sokolove, P.M., Kinnally, K.W., Fiskum, G., 2001. Mitochondrial precursor signal peptide induces a unique permeability transition and release of cytochrome *c* from liver and brain mitochondria. Arch. Biochem. Biophys. 386, 251–260.
Lee, A.C., Xu, X., Blachly-Dyson, E., Forte, M., Colombini, M., 1998. The role of yeast VDAC genes on the permeability of the mitochondrial outer membrane. J. Membr. Biol. 161, 173–181.
Lemasters, J.J., 2007. Modulation of mitochondrial membrane permeability in pathogenesis, autophagy and control of metabolism. J. Gastroenterol. Hepatol. 22 (Suppl 1), S31–S37.
Lemasters, J.J., Theruvath, T.P., Zhong, Z., Nieminen, A.L., 2009. Mitochondrial calcium and the permeability transition in cell death. Biochim. Biophys. Acta 1787, 1395–1401.
Leung, A.W., Halestrap, A.P., 2008. Recent progress in elucidating the molecular mechanism of the mitochondrial permeability transition pore. Biochim. Biophys. Acta 1777, 946–952.
Leung, A.W., Varanyuwatana, P., Halestrap, A.P., 2008. The mitochondrial phosphate carrier interacts with cyclophilin D and may play a key role in the permeability transition. J. Biol. Chem. 283, 26312–26323.
Lin, J., Wang, Y., Wang, G., 2006. Salt stress-induced programmed cell death in tobacco protoplasts is mediated by reactive oxygen species and mitochondrial permeability transition pore status. J. Plant Physiol. 163, 731–739.
Lohret, T.A., Kinnally, K.W., 1995a. Multiple conductance channel activity of wild-type and voltage-dependent anion-selective channel (VDAC)-less yeast mitochondria. Biophys. J. 68, 2299–2309.
Lohret, T.A., Kinnally, K.W., 1995b. Targeting peptides transiently block a mitochondrial channel. J. Biol. Chem. 270, 15950–15953.

Lohret, T.A., Murphy, R.C., Drgon, T., Kinnally, K.W., 1996. Activity of the mitochondrial multiple conductance channel is independent of the adenine nucleotide translocator. J. Biol. Chem. 271, 4846–4849.

Malhi, H., Gores, G.J., Lemasters, J.J., 2006. Apoptosis and necrosis in the liver: a tale of two deaths? Hepatology 43, S31–S44.

Manon, S., Guerin, M., 1997. The ATP-induced K(+)-transport pathway of yeast mitochondria may function as an uncoupling pathway. Biochim. Biophys. Acta 1318, 317–321.

Manon, S., Roucou, X., Guerin, M., Rigoulet, M., Guerin, B., 1998. Characterization of the yeast mitochondria unselective channel: a counterpart to the mammalian permeability transition pore? J. Bioenerg. Biomembr. 30, 419–429.

Manzl, C., Ebner, H., Kock, G., Dallinger, R., Krumschnabel, G., 2003. Copper, but not cadmium, is acutely toxic for trout hepatocytes: short-term effects on energetics and ion homeostasis. Toxicol. Appl. Pharmacol. 191, 235–244.

Manzl, C., Enrich, J., Ebner, H., Dallinger, R., Krumschnabel, G., 2004. Copper-induced formation of reactive oxygen species causes cell death and disruption of calcium homeostasis in trout hepatocytes. Toxicology 196, 57–64.

Martínez-Caballero, S., Peixoto, P.M., Kinnally, K.W., Campo, M.L., 2007. A fluorescence assay for peptide translocation into mitochondria. Anal. Biochem. 362, 76–82.

Matouschek, A., Rospert, S., Schmid, K., Glick, B.S., Schatz, G., 1995. Cyclophilin catalyzes protein folding in yeast mitochondria. Proc. Natl. Acad. Sci. USA 92, 6319–6323.

McStay, G.P., Clarke, S.J., Halestrap, A.P., 2002. Role of critical thiol groups on the matrix surface of the adenine nucleotide translocase in the mechanism of the mitochondrial permeability transition pore. Biochem. J. 367, 541–548.

Menze, M.A., Hand, S.C., 2009. How do animal mitochondria tolerate water stress? Commun. Integr. Biol. 2, 428–430.

Menze, M.A., Hutchinson, K., Laborde, S.M., Hand, S.C., 2005. Mitochondrial permeability transition in the crustacean *Artemia franciscana*: absence of a calcium-regulated pore in the face of profound calcium storage. Am. J. Physiol. Regul. Integr. Comp. Physiol. 289, R68–R76.

Navarro, R.E., Ramos-Balderas, J.L., Guerrero, I., Pelcastre, V., Maldonado, E., 2008. Pigment dilution mutants from fish models with connection to lysosome-related organelles and vesicular traffic genes. Zebrafish 5, 309–318.

Nicotera, P., Leist, M., Fava, E., Berliocchi, L., Volbracht, C., 2000. Energy requirement for caspase activation and neuronal cell death. Brain Pathol. 10, 276–282.

Palma, E., Tiepolo, T., Angelin, A., Sabatelli, P., Maraldi, N.M., Basso, E., Forte, M.A., Bernardi, P., Bonaldo, P., 2009. Genetic ablation of cyclophilin D rescues mitochondrial defects and prevents muscle apoptosis in collagen VI myopathic mice. Hum. Mol. Genet. 18, 2024–2031.

Pavón, N., Aranda, A., García, N., Hernández-Esquivel, L., Chávez, E., 2009. In hyperthyroid rats octylguanidine protects the heart from reperfusion damage. Endocr. 35, 158–165.

Pereira, C., Silva, R.D., Saraiva, L., Johansson, B., Sousa, M.J., Corte-Real, M., 2008. Mitochondria-dependent apoptosis in yeast. Biochim. Biophys. Acta 1783, 1286–1302.

Pérez-Vázquez, V., Saavedra-Molina, A., Uribe, S., 2003. In *Saccharomyces cerevisiae*, cations control the fate of the energy derived from oxidative metabolism through the opening and closing of the yeast mitochondrial unselective channel. J. Bioenerg. Biomembr. 35, 231–241.

Petronilli, V., Miotto, G., Canton, M., Brini, M., Colonna, R., Bernardi, P., Di Lisa, F., 1999. Transient and long-lasting openings of the mitochondrial permeability transition pore can be monitored directly in intact cells by changes in mitochondrial calcein fluorescence. Biophys. J. 76, 725–734.

Petronilli, V., Penzo, D., Scorrano, L., Bernardi, P., Di Lisa, F., 2001. The mitochondrial permeability transition, release of cytochrome c and cell death. Correlation with the duration of pore openings in situ. J. Biol. Chem. 276, 12030–12034.

Pfeiffer, D.R., Gudz, T.I., Novgorodov, S.A., Erdahl, W.L., 1995. The peptide mastoparan is a potent facilitator of the mitochondrial permeability transition. J. Biol. Chem. 270, 4923–4932.

Prieto, S., Bouillaud, F., Ricquier, D., Rial, E., 1992. Activation by ATP of a proton-conducting pathway in yeast mitochondria. Eur. J. Biochem. 208, 487–491.

Prieto, S., Bouillaud, F., Rial, E., 1996. The nature and regulation of the ATP-induced anion permeability in *Saccharomyces cerevisiae* mitochondria. Arch. Biochem. Biophys. 334, 43–49.

Rasola, A., Bernardi, P., 2007. The mitochondrial permeability transition pore and its involvement in cell death and in disease pathogenesis. Apoptosis 12, 815–833.

Rizzuto, R., Marchi, S., Bonora, M., Aguiari, P., Bononi, A., De Stefani, D., Giorgi, C., Leo, S., Rimessi, A., Siviero, R., Zecchini, E., Pinton, P., 2009. Ca^{2+} transfer from the ER to mitochondria: when, how and why. Biochim. Biophys. Acta 1787, 1342–1351.

Rossi, C.S., Lehninger, A.L., 1964. Stoichiometry of respiratory stimulation, accumulation of Ca^{++} and phosphate, and oxidative phosphorylation in rat liver mitochondria. J. Biol. Chem. 239, 3971–3980.

Roucou, X., Manon, S., Guerin, M., 1995. ATP opens an electrophoretic potassium transport pathway in respiring yeast mitochondria. FEBS Lett. 364, 161–164.

Roucou, X., Manon, S., Guerin, M., 1997. Conditions allowing different states of ATP- and GDP-induced permeability in mitochondria from different strains of *Saccharomyces cerevisiae*. Biochim. Biophys. Acta 1324, 120–132.

Savina, M.V., Emelyanova, L.V., Belyaeva, E.A., 2006. Bioenergetic parameters of lamprey and frog liver mitochondria during metabolic depression and activity. Comp. Biochem. Physiol. B Biochem. Mol. Biol. 145, 296–305.

Scott, I., Logan, D.C., 2008. Mitochondrial morphology transition is an early indicator of subsequent cell death in *Arabidopsis*. New Phytol. 177, 90–101.

Skulachev, V.P., 2006. Bioenergetic aspects of apoptosis, necrosis and mitoptosis. Apoptosis 11, 473–485.

Sokolove, P.M., Kinnally, K.W., 1996. A mitochondrial signal peptide from *Neurospora crassa* increases the permeability of isolated rat liver mitochondria. Arch. Biochem. Biophys. 336, 69–76.

Stuart, R.A., Koehler, C.M., 2007. In vitro analysis of yeast mitochondrial protein import. Curr. Protoc. Cell Biol. 34, 11.19.1–11.19.20.

Szabo, I., Zoratti, M., 1993. The mitochondrial permeability transition pore may comprise VDAC molecules. I. Binary structure and voltage dependence of the pore. FEBS Lett. 330, 201–205.

Szabo, I., De Pinto, V., Zoratti, M., 1993. The mitochondrial permeability transition pore may comprise VDAC molecules. II. The electrophysiological properties of VDAC are compatible with those of the mitochondrial megachannel. FEBS Lett. 330, 206–210.

Telfer, W.R., Busta, A.S., Bonnemann, C.G., Feldman, E.L., Dowling, J.J., 2010. Zebrafish models of collagen VI-related myopathies. Hum. Mol. Genet. 19, 2433–2444.

Theruvath, T.P., Zhong, Z., Currin, R.T., Ramshesh, V.K., Lemasters, J.J., 2006. Endothelial nitric oxide synthase protects transplanted mouse livers against storage/reperfusion injury: role of vasodilatory and innate immunity pathways. Transplant. Proc. 38, 3351–3357.

Tiwari, B.S., Belenghi, B., Levine, A., 2002. Oxidative stress increased respiration and generation of reactive oxygen species, resulting in ATP depletion, opening of mitochondrial permeability transition, and programmed cell death. Plant Physiol. 128, 1271–1281.

Townsend, J.P., Cavalieri, D., Hartl, D.L., 2003. Population genetic variation in genome-wide gene expression. Mol. Biol. Evol. 20, 955–963.

Uribe, S., Rangel, P., Pardo, J.P., 1992. Interactions of calcium with yeast mitochondria. Cell Calcium 13, 211–217.

Varela, C., Cárdenas, J., Melo, F., Agosin, E., 2005. Quantitative analysis of wine yeast gene expression profiles under winemaking conditions. Yeast 22, 369–383.

Velours, J., Rigoulet, M., Guerin, B., 1977. Protection of yeast mitochondrial structure by phosphate and other H^+-donating anions. FEBS Lett. 81, 18–22.

Vianello, A., Macri, F., Braidot, E., Mokhova, E.N., 1995. Effect of cyclosporin A on energy coupling in pea stem mitochondria. FEBS Lett. 371, 258–260.

Virolainen, E., Blokhina, O., Fagerstedt, K., 2002. Ca^{2+}-induced high amplitude swelling and cytochrome c release from wheat (*Triticum aestivum* L.) mitochondria under anoxic stress. Ann. Bot. 90, 509–516.

Volfson, D., Marciniak, J., Blake, W.J., Ostroff, N., Tsimring, L.S., Hasty, J., 2006. Origins of extrinsic variability in eukaryotic gene expression. Nature 439, 861–864.

von Stockum, S., Basso, E., Petronilli, V., Forte, M., Bernardi, P., 2010. A Ca^{2+}-regulated mitochondrial (permeability transition) pore in *Drosophila melanogaster*. Biochim. Biophys. Acta 1797, 131-131.

Walter, L., Miyoshi, H., Leverve, X., Bernard, P., Fontaine, E., 2002. Regulation of the mitochondrial permeability transition pore by ubiquinone analogs. A progress report. Free Radic. Res. 36, 405–412.

Woodfield, K., Ruck, A., Brdiczka, D., Halestrap, A.P., 1998. Direct demonstration of a specific interaction between cyclophilin-D and the adenine nucleotide translocase confirms their role in the mitochondrial permeability transition. Biochem. J. 336 (Pt 2), 287–290.

Yamada, A., Yamamoto, T., Yoshimura, Y., Gouda, S., Kawashima, S., Yamazaki, N., Yamashita, K., Kataoka, M., Nagata, T., Terada, H., Pfeiffer, D.R., Shinohara, Y., 2009. Ca^{2+}-induced permeability transition can be observed even in yeast mitochondria under optimized experimental conditions. Biochim. Biophys. Acta 1787, 1486–1491.

Yu, X.H., Perdue, T.D., Heimer, Y.M., Jones, A.M., 2002. Mitochondrial involvement in tracheary element programmed cell death. Cell Death Differ. 9, 189–198.

Yvert, G., Brem, R.B., Whittle, J., Akey, J.M., Foss, E., Smith, E.N., Mackelprang, R., Kruglyak, L., 2003. Trans-acting regulatory variation in *Saccharomyces cerevisiae* and the role of transcription factors. Nat. Genet. 35, 57–64.

Zazueta, C., Franco, M., Correa, F., García, N., Santamaria, J., Martínez-Abundis, E., Chávez, E., 2007. Hypothyroidism provides resistance to kidney mitochondria against the injury induced by renal ischemia–reperfusion. Life Sci. 80, 1252–1258.

Zheng, Y., Shi, Y., Tian, C., Jiang, C., Jin, H., Chen, J., Almasan, A., Tang, H., Chen, Q., 2004. Essential role of the voltage-dependent anion channel (VDAC) in mitochondrial permeability transition pore opening and cytochrome c release induced by arsenic trioxide. Oncogene 23, 1239–1247.

Zoratti, M., Szabo, I., 1995. The mitochondrial permeability transition. Biochim. Biophys. Acta 1241, 139–176.

Zoratti, M., Szabo, I., De Marchi, U., 2005. Mitochondrial permeability transitions: how many doors to the house? Biochim. Biophys. Acta 1706, 40–52.

Zoratti, M., De Marchi, U., Biasutto, L., Szabo, I., 2010. Electrophysiology clarifies the megariddles of the mitochondrial permeability transition pore. FEBS Lett. 584, 1997–2004.

J Bioenerg Biomembr (2011) 43:323–331
DOI 10.1007/s10863-011-9356-5

Physiological uncoupling of mitochondrial oxidative phosphorylation. Studies in different yeast species

Sergio Guerrero-Castillo · Daniela Araiza-Olivera · Alfredo Cabrera-Orefice · Juan Espinasa-Jaramillo · Manuel Gutiérrez-Aguilar · Luís A. Luévano-Martínez · Armando Zepeda-Bastida · Salvador Uribe-Carvajal

Published online: 10 May 2011

Abstract Under non-phosphorylating conditions a high proton transmembrane gradient inhibits the rate of oxygen consumption mediated by the mitochondrial respiratory chain (state IV). Slow electron transit leads to production of reactive oxygen species (ROS) capable of participating in deleterious side reactions. In order to avoid overproducing ROS, mitochondria maintain a high rate of O_2 consumption by activating different exquisitely controlled uncoupling pathways. Different yeast species possess one or more uncoupling systems that work through one of two possible mechanisms: i) Proton sinks and ii) Non-pumping redox enzymes. Proton sinks are exemplified by mitochondrial unspecific channels (MUC) and by uncoupling proteins (UCP). *Saccharomyces. cerevisiae* and *Debaryomyces hansenii* express highly regulated MUCs. Also, a UCP was described in *Yarrowia lipolytica* which promotes uncoupled O_2 consumption. Non-pumping alternative oxido-reductases may substitute for a pump, as in *S. cerevisiae* or may coexist with a complete set of pumps as in the branched respiratory chains from *Y. lipolytica* or *D. hansenii*. In addition, pumps may suffer intrinsic uncoupling (slipping). Promising models for study are unicellular parasites which can turn off their aerobic metabolism completely. The variety of energy dissipating systems in eukaryote species is probably designed to control ROS production in the different environments where each species lives.

S. Guerrero-Castillo · D. Araiza-Olivera · A. Cabrera-Orefice · J. Espinasa-Jaramillo · M. Gutiérrez-Aguilar · L. A. Luévano-Martínez · A. Zepeda-Bastida · S. Uribe-Carvajal (✉)
Departamento de Genética Molecular, Instituto de Fisiología Celular, Universidad Nacional Autónoma de México, Ciudad Universitaria, Apdo. Postal 70–242, Mexico City, México DF, Mexico
e-mail: suribe@ifc.unam.mx

Keywords Uncoupling · Permeability transition · Uncoupling protein · Branched respiratory chain · *Saccharomyces cerevisiae* · *Yarrowia lipolytica* · *Debaryomyces hansenii*

Introduction

In mitochondria, oxidative phosphorylation results from the coupling between the redox-primary proton pumps in the respiratory chain and the F_1F_0-ATP synthase. The redox H^+ pumps create a pH gradient (ΔpH) used by the F_1F_0-ATP synthase to phosphorylate ADP. The efficiency of this system varies when electrons enter or exit the respiratory chain at different enzymes or when the H^+ gradient is used by secondary pumps for the active transport of proteins, ions and metabolites (Nicholls and Ferguson 2002) (Fig. 1).

Three of the four respiratory complexes in an orthodox respiratory chain are proton pumps. These enzymes oxidize substrates, transferring electron(s) to the next acceptor in the chain and expelling H^+(s) to the intermembrane space. Recycling of the electron within a given pump often results in H^+/e^- stoichiometries higher than 1 (Brandt 2006; Hosler et al. 2006; Trumpower 1990). This high efficiency comes at a price, as redox reactions involve several steps where incomplete reductions transiently convert coenzymes into reactive free radicals (Drose and Brandt 2008; Kushnareva et al. 2002). Therefore, when the mitochondrial ADP concentration drops, the rate of electron flux through the respiratory chain decreases (State IV respiration) and mitochondria become an important source of superoxide and other reactive oxygen species (ROS) (Chen et al. 2003). ROS production has diverse functions, such as signaling and apoptosis (Forman et al. 2010; Perrone et al. 2008).

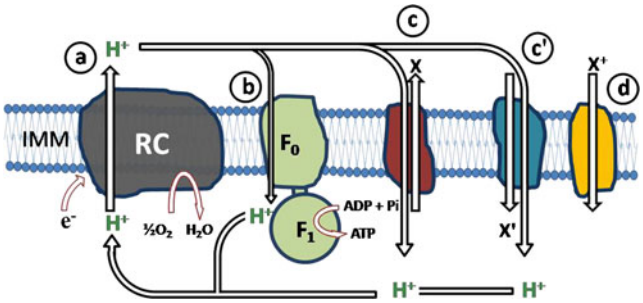

Fig. 1 Oxidative phosphorylation efficiency variations due to different systems that use protons. The proton gradient generated by the respiratory chain may be used by (**a**) the F_1F_0-ATP synthase (F_0F_1) for ADP phosphorylation (**b**) the transport of ions or metabolites across the inner mitochondrial membrane (IMM) either as (**c**) antiporter or (c') symporter. (**d**) ion uniport. RC, respiratory chain

However, overproduction of ROS may lead to ageing and disease (Drakulic et al. 2005; Wilhelm et al. 2006).

The labile nature of the superoxide radical has made difficult the identification of all its mitochondrial sources. Still, it is known that the ubiquinone and flavin oxido-reduction centers produce ROS (Chen et al. 2003; Starkov et al. 2004; Zundorf et al. 2009). During the redox ubiquinone/ubiquinol reaction, oxidized ubiquinone is partially reduced by one electron in the Qo site of the bc_1 complex becoming a potential superoxide source (Drose and Brandt 2008). At a high mitochondrial transmembrane potential, semiquinone accumulates participating in a side reactions that produce ROS (Koshkin et al. 2003; Rottenberg et al. 2009).

In cells and mitochondria there are different enzymes that eliminate ROS, such as Mn^{2+} SOD-dismutases, catalase and glutathione peroxidases. However, ROS overproduction may overwhelm these systems and thus different energy-dissipating uncoupling mechanisms may be activated to prevent such overproduction. These "physiological uncoupling" mechanisms would prevent ROS over-accumulation by inducing increased electron flux (Czarna and Jarmuszkiewicz 2005; Maxwell et al. 1999).

Among plants, yeast and fungi, there are different strategies aimed at preventing ROS overproduction (Kowaltowski et al. 1998; Magnani et al. 2008). In different yeast species it has been observed that oxidative phosphorylation can be uncoupled by different mechanisms (Fig. 2). Oxidative phosphorylation may be uncoupled through dissipation of the H^+ gradient through proton sinks, also termed extrinsic uncouplers (Kadenbach 2003): these may be channels or transporters and are represented by two well studied systems. These are the yeast mitochondrial unspecific channel (MUC) (Manon et al. 1998), which in mammals is known as the permeability transition pore (PTP) (Haworth and Hunter 1979), and the uncoupling proteins (UCP) (Nicholls and Rial 1999) that specifically dissipate H^+ gradients (Fig. 3). The second respiratory chain uncoupling mechanism, also termed intrinsic uncoupling (Kadenbach 2003) is the catalysis of redox reactions without pumping protons. Non-pumping redox enzymes are widely represented in the branched mitochondrial respiratory chains observed in plants and unicellular organisms (Rasmusson et al. 2004; Umbach and Siedow 2000; Wagner and Moore 1997). Among these enzymes, there are type-II NADH dehydrogenases (NDH2) and alternative oxidases (AOX). In addition, the variations in H^+/e^- stoichiometry (slipping) are another source of uncoupling.

Proton dissipating pathways

The mitochondrial unselective channel

Mitochondrial unspecific channels (MUCs) have been detected in yeast such as *Saccharomyces cerevisiae* ($_{Sc}$MUC) (Guerin et al. 1994; Prieto et al. 1992) and *Debaryomyces hansenii* ($_{Dh}$MUC) (Cabrera-Orefice et al. 2010). MUC opening results in a mitochondrial permeability transition (PT) similar to that described in mammals, i.e. a large

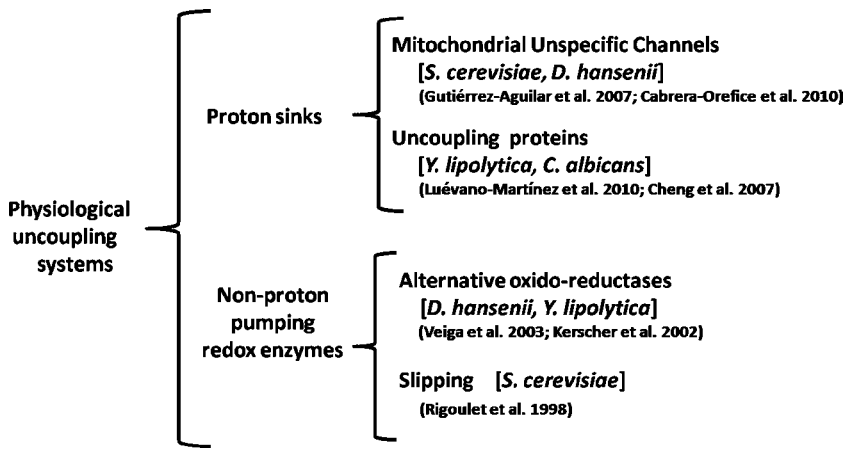

Fig. 2 Physiological uncoupling systems in yeast mitochondria. The rate of oxygen consumption may be accelerated independently of the synthesis of ATP by either depleting the transmembrane pH gradient or by reducing oxygen without contributing to the proton gradient. These mechanisms are present in different yeast species

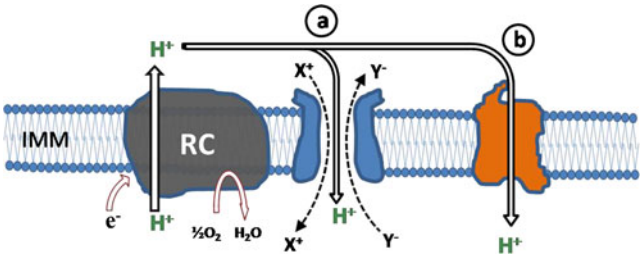

Fig. 3 Proton Sinks. Two proton sink systems are exemplified. Once the (**a**) Respiratory chain establishes a proton gradient, protons may be returned to the matrix through (**b**) unspecific channels or through (**c**) uncoupling proteins that are specific protonophores

increase in conductivity that depletes electrochemical gradients (Azzolin et al. 2010).

The $_{Sc}$MUC has been thoroughly characterized. $_{Sc}$MUC opens in response to ATP, while it is closed by Pi or ADP (Prieto et al. 1995). This suggests that $_{Sc}$MUC is controlled by the phosphorylation potential (Wallace et al. 1994). In addition, both the $_{Sc}$MUC (Perez-Vazquez et al. 2003) and the $_{Dh}$MUC (Cabrera-Orefice et al. 2010) are closed by Mg^{2+} and by Ca^{2+}. Furthermore, the $_{Sc}$MUC seems to be controlled cooperatively by Ca^{2+}, Mg^{2+} and Pi [to be published]. In *S. cerevisiae*, a rise in cytoplasmic [Ca^{2+}] precedes processes such as division, mating (Nakajima-Shimada et al. 2000; Ohya et al. 1991); or even a death program resembling apoptosis (Nakajima-Shimada et al. 2000; Ohya et al. 1991; Pozniakovsky et al. 2005). That is, a rise in $[Ca^{2+}]_{cyt}$ indicates that the cell is about to spend a large amount of energy (Anraku et al. 1991; Manon and Guerin 1998). Both the $_{Sc}$MUC and the $_{Dh}$MUC close in response to low [ATP] or high [Pi] while in contrast, when there is a surplus of ATP and no signals this indicates an oncoming need for energy, yeast MUCs open, dissipating the transmembrane potential and thus allowing the rate of oxygen consumption to increase (Prieto et al. 1992) and the production of ROS to decrease (Korshunov et al. 1997).

In *S. cerevisiae*, Ca^{2+} closes MUC, probably through its interaction with the voltage-dependent anionic channel (VDAC) (Gutierrez-Aguilar et al. 2007). The Ca^{2+}-VDAC interaction has also been proposed for vertebrates (Gincel et al. 2001). In both cases, the possibility that VDAC is a regulatory pore component has been suggested (Baines et al. 2007; Gutierrez-Aguilar et al. 2007). In regard to the possible component of MUC in the IMM, in *S. cerevisiae* it has long been evident that Pi is a strong MUC regulator (Azzolin et al. 2010; Cortes et al. 2000; Jung et al. 1997; Manon and Guerin 1997; Prieto et al. 1992; Velours et al. 1977). From this, it should not be surprising that recent evidence suggests that the mitochondrial phosphate carrier (PiC) is a constituent of the $_{Sc}$MUC: in the absence of PiC, $_{Sc}$MUC changes its solute size exclusion size and Pi sensitivity (Gutierrez-Aguilar et al. 2010). In mammals, PiC has also been proposed to be part of this channel (Leung et al. 2008).

Different modulators of MUCs have been reported depending on the species, strain or even tissue under study (Berman et al. 2000; Fortes et al. 2001; Friberg et al. 1999; Manon et al. 1998), suggesting that MUCs have evolved in response to selective pressure, e.g. in *D. hansenii*, the MUC is closed by monovalent cations (Cabrera-Orefice et al. 2010). This closure probably results in higher production of ATP, as it correlates with increased growth rate and mass yield (Gonzalez-Hernandez et al. 2004) and probably constitutes an adaptation to the high Na^+ contents of sea water (Gustafsson and Norkrans 1976).

Adding to the ongoing debate on the physiological role of MUCs, it is suggested that their role as physiological uncouplers should be considered; i.e. MUCs probably are highly regulated energy dissipative systems that decrease mitochondrial gradients when the demand for energy is low.

PT does not seem to be universal. *Yarrowia lypolytica* and *Endomyces magnusii* undergo PT only upon forced conditions which include incubation with the Ca^{2+} ionophore ETH129 (Kovaleva et al. 2009; Yamada et al. 2009). If MUC- mediated uncoupling is important to inhibit ROS production, and *Y. lipolytica* and *E. magnusii* seem to lack such a structure, then these yeast species should possess alternative uncoupling systems. Indeed, in *Y. lipolytica* mitochondria there are two such systems that might function as uncouplers: an uncoupling protein (Luevano-Martinez et al. 2010) and a branched respiratory chain (Guerrero-Castillo et al. 2009; Kerscher et al. 2002).

Uncoupling proteins

Uncoupling protein (UCP)-like activities have been detected in mitochondria from unicellular organisms, higher eukaryotes and plants (Jarmuszkiewicz et al. 2010). The physiological role of UCPs in unicellular organisms is still debated: the small size of unicellular eukaryotes makes a thermogenic role unlikely, as it is impossible to form a temperature gradient between the cell and the environment although, in *Acanthamoeba castellanii* UCP expression does increase in cells growing at 4 °C (Jarmuszkiewicz et al. 2004). Here, it is proposed that unicellular UCPs are capable of decreasing the mitochondrial $\Delta\Psi$ with the aim of decreasing production of ROS. Also, in unicellular organisms resistance to exogenous ROS is enhanced by UCP activity (Kowaltowski et al. 1998; Ricquier 2005), probably because UCP decreases endogenous ROS production (Krauss et al. 2005) and thus detoxifying enzymes are free to deal with the exogenous species: e.g. strains of *Candida albicans* devoid of UCP are less invasive that the wild type (Cavalheiro et al. 2004; Cheng et al. 2007).

In addition to the available functional evidence, recently a protein exhibiting UCP-like activity was identified in *Y. lipolytica* (Luevano-Martinez et al. 2010). The UCP activity was regulated similarly to the UCP1 from brown adipose tissue. After an extensive phylogenetic search for a UCP ortholog in this yeast, it was demonstrated that the mitochondrial oxaloacetate carrier (OAC) from *Y. lipolytica* is a *bona fide* UCP. The *Y. lipolytica* OAC displayed both, a sulfate/oxaloacetate transport and a UCP behavior. It is noteworthy that in the unicellular organisms where UCP activity has been reported, the green algae *Chlamydomonas reinhardtii*, the amoeba *Dictyostelium discoideum* (DictyBase) and the yeast *Candida albicans* (Cavalheiro et al. 2004; Jarmuszkiewicz et al. 2002) the only UCP-like proteins seem to be the mitochondrial oxaloacetate carriers (results not published). In regard to whether a UCP might prevent ROS overproduction, in *Y. lipolytica,* it has been demonstrated that this protein is over-expressed in the stationary phase, where a degree of uncoupling would be needed to maintain a high rate of oxygen consumption in the absence of ATP synthesis (Luevano-Martinez et al. 2010).

Redox enzymes that do not pump protons

Branched mitochondrial respiratory chains

Redox enzymes lacking pumping activity are constituted by a single protein subunit. These enzymes probably appeared early in the reducing world, before the appearance of oxidative phosphorylation, fulfilling the need to detoxify oxygen from the vicinity of enzymes and membranes. Some prokaryotes still use oxidoreductase-mediated detoxification of oxygen to protect their fragile nitrogen reducing enzymes (Flores-Encarnacion et al. 1999).

Alternative redox enzymes do not contribute to the proton gradient. Branched mitochondrial respiratory chains may contain a number of different enzymes that donate electrons to the quinone pool including complex I (the only proton pump), succinate dehydrogenase, glycerol phosphate dehydrogenase, dihydroorotate dehydrogenase and internal or external type II NADH dehydrogenases. Then the electrons in reduced ubiquinol follow two possible pathways reaching either the cytochrome pathway (complexes III and IV), or the alternative oxidase (AOX). In these respiratory chains, different electron pathways may be envisioned that bypass energy-conserving respiratory complexes I, III and/or IV, i.e. branched chains seem to be able to reduce oxygen while using 0, 1, 2 or 3 proton pumps (Fig. 4).

In mitochondria, the most widely distributed monosubunit redox enzymes are type II NADH dehydrogenases (NDH2) and alternative oxidases (AOX). NDH2s may be located on either surface of the IMM. External NDH2s (NDH2e) oxidize cytosolic NADH, while internal NDH2s (NDH2i) oxidize NADH from the matrix in a rotenone-insensitive reaction. The structure (Fisher et al. 2007; Fisher et al. 2009; Gonzalez-Meler et al. 1999; Kerscher 2000; Melo et al. 2004; Schmid and Gerloff 2004) and kinetics (Fisher et al. 2009; Velazquez and Pardo 2001) of NDH2s from different organisms have been reported. AOX is a single subunit enzyme (Albury et al. 2002; Andersson and Nordlund 1999; Berthold et al. 2000; Moore and Siedow 1991). AOX activity is regulated by nucleotides, by dimerization and/or by α-ketoacids (Hoefnagel et al. 1995; Millar et al. 1993; Millenaar et al. 1998). Some yeast species contain two AOX isoforms, one being constitutively expressed and a second one induced by stress (Siedow and Umbach 2000). It is noteworthy that AOX is present only in fungi that express complex I, possibly because in a respiratory chain without Complex I, any electron reaching AOX would be totally unproductive (Joseph-Horne et al. 2001).

In mitochondria with alternative components, the pathway that electrons follow has to be strictly controlled. A direct reaction between NDH2, ubiquinone and AOX would result in a non-productive, uncoupled pathway, i.e. no protons would be pumped. Furthermore, at the external face of the inner membrane, NDH2 receives the hydride from NADH and takes one H^+, transferring both hydrogen atoms to ubiquinone. Then ubiquinone is regenerated by AOX which in turn transfers its hydrogen atoms to oxygen producing water. This sequence of reactions results in the dissipation of a H^+, i.e. it has a H^+/e^- pumping stoichiometry of −0.5. Therefore, when energy is required, alternative redox enzymes need to be isolated from each other, probably by binding to the proton-pumping complexes. In contrast, when phosphorylation is not active, as in the stationary phase, the non-producing electron transfer between NDH2 and AOX would be useful to maintain a high rate of oxygen consumption at a high transmembrane potential, preventing semiquinone accumulation and decreasing ROS formation (Joseph-Horne et al. 2001).

Proton/electron stoichiometry variations. Slipping

Non-branched respiratory chains seem to use other mechanisms to regulate the efficiency of oxidative phosphorylation (van Dam et al. 1990). Uncoupling may result from increased proton conductance at the lipid bilayer (Luvisetto and Azzone 1989; Luvisetto et al. 1991). A second mechanism would be the decrease in the efficiency of a respiratory pump (slipping) (Pietrobon et al. 1981; Pietrobon et al. 1983). Intrinsic uncoupling or slipping is defined as a decrease in the efficiency of a

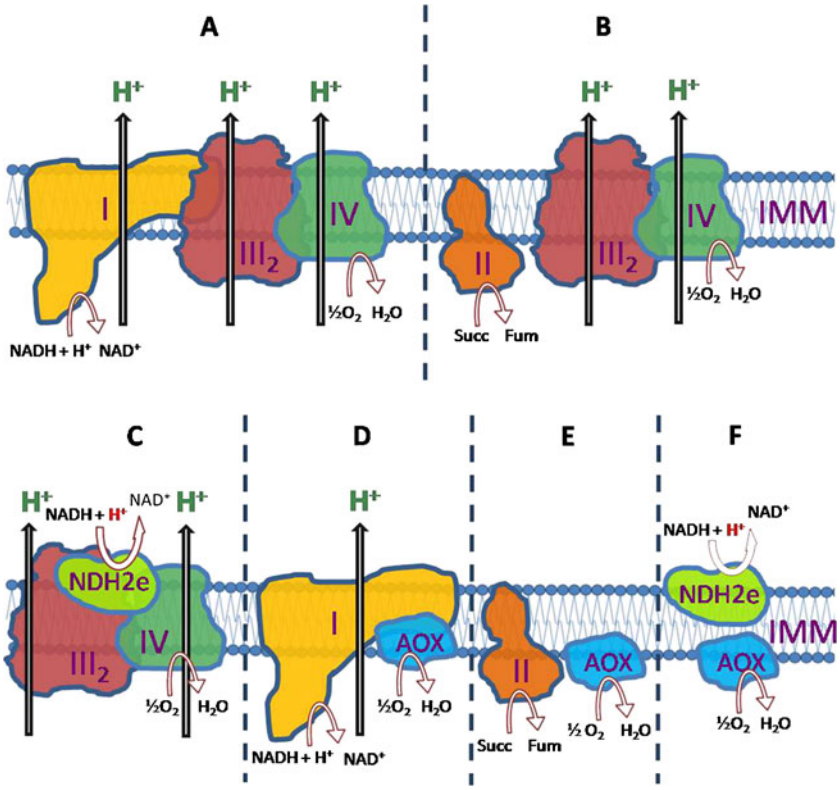

Fig. 4 In a branched respiratory chain the number of proton pumps participating in electron transfer may vary from three to zero. In branched respiratory chains electrons may follow different routes to reach oxygen. Thus the number of proton pumps involved may change: **a** complexes I, III and IV: three proton pumps are involved. **b** from succinate dehydrogenase through the cytochrome pathway, two proton pumps. **c** from NDH2e through complexes III-IV; two proton pumps, although H^+/e^- is 2.5 instead of 3 as in (**b**). **d** from complex I though AOX; one pump. **e** from succinate dehydrogenase through AOX; No proton pumps participate. **f** NDH2e through AOX; zero proton pumps participate and in addition, the combined activity of NDH2e with AOX would consume a H^+ from the intermembrane space, yielding a negative stoichiometry of −0.5 H^+/e^-. Numbers I, II, III_2 and IV represent each of the four respiratory complexes; NDH2e, external NADH dehydrogenase; AOX, alternative oxidase; IMM, inner mitochondrial membrane. Protons in red are used for ubiquinone reduction in the intermembrane side of the IMM, i.e. they do not contribute (**c**) or contribute negatively to the H^+/e^- stoichiometry (**f**)

proton pump (decrease of the H^+/e or H^+/ATP stoichiometry) resulting in a diminished P/O ratio (Kadenbach 2003).

Slipping has been reported in cytochrome c oxidase (Azzone et al. 1985; Frank and Kadenbach 1996). The F_1F_0-synthase can also undergo slipping, hydrolyzing ATP without pumping protons (Feniouk et al. 2005). In addition, protons can reenter the matrix through the pumps without moving electrons backwards or making ATP (Pietrobon et al. 1983).

Slipping accelerates the rate of oxygen consumption as more electrons are needed to maintain a high ΔpH. Normally in the proton pump the chemical reaction and the transport of protons are tightly coupled, while during slipping both processes become independent (Mourier et al. 2010). Upon slipping, the rate of electron flux increases while the proton motive force remains constant and energy is dissipated as heat (Kadenbach 2003).

In *S. cerevisiae* mitochondria, a remarkable change in the stoichiometry of proton pumping has been described. Feeding the respiratory chain with substrates for different quinone reductases leads to an increase in the rate of oxygen consumption without increasing the rate of ATP phosphorylation (Mourier et al. 2010). This phenomenon has been termed active leak and is probably due to slipping of an oxidative phosphorylation pump, although an increase in the proton conductance of the bilayer has not been ruled out.

Interactions between the cytoplasm and mitochondria regulate the efficiency of oxidative phosphorylation

At any given moment the cell´s energy needs determine which metabolic pathways are activated or inhibited (Devin and Rigoulet 2007). The catabolism/anabolism activity ratio is determined by metabolic fluxes (Cascante et al. 1994; Moreno-Sanchez et al. 2010; Ovadi and Saks 2004; Srere 1987). Upon oxygenation, the rate of glycolysis decreases. This may be explained by the allosteric regulation of glycolytic enzymes by ATP and fructose 2,6-bisphosphate and by the competition for ADP and for reducing equivalents observed between glycolysis and

oxidative phosphorylation (Beauvoit et al. 1993; Gosalvez et al. 1974).

In *Saccharomyces cerevisiae*, glycolysis is the main source of ATP; however, in the presence of non-fermentable substrates oxidative phosphorylation becomes the main energy source. During fermentation the genes that encode for oxidative metabolism enzymes stop their expression (Takeda 1981), e.g. glucose addition inhibits the expression of cytochrome c (Thevelein 1994; Zitomer and Nichols 1978), while glycolytic intermediates are accumulated to induce the expression of glycolytic enzymes (Boles et al. 1993).

In *S. cerevisiae* the addition of glucose induces the transition to fermentative metabolism, where glycolysis is increased and oxidative phosphorylation is decreased (den Hollander et al. 1986). This is the Crabtree effect. There are both Crabtree-positive and negative yeast species. Recent sudies indicate that fructose1,6-bisphosphate inhibits oxygen consumption through an interaction with complexes III and IV. In contrast, physiological concentrations of glucose 6-phosphate and fructose 6-phosphate stimulate the respiratory flux, possibly inducing slipping (Diaz-Ruiz et al. 2008).

Unicellular organisms other than yeast

Protists make up the bulk of the eukaryotes, while vertebrates and fungi represent only a small fraction. Protists present a wide variety of physiological properties. There are very few bioenergetics studies on these organisms. *Giardia lamblia* (Hashimoto et al. 1994) and *Entamoeba histolytica* (Tovar et al. 1999) have lost their mitochondria. Other protists, such as some Trichomonadidae and ciliates, have organelles called hydrogenosomes, which are related to mitochondria (de Souza et al. 2009; Mather and Vaidya 2008).

Unicellular parasites have evolved to adapt their metabolism for survival within the host. Depending on the environment and stage in their life cycle, *Plasmodium, Trypanosoma* and *Leishmania* can make a complete switch from a glycolytic to an aerobic metabolism and back, such that in *Plasmodium falciparum* the activities of complex III, IV and dihydroorotate dehydrogenase, are 10 times higher in the sexual than in the asexual stage (Monzote and Gille 2010). Likewise, mitochondria have adapted to the metabolic conditions found within the host, e.g. in the mosquito, *Plasmodium* gametocytes are aerobic and mitochondria are typical. In contrast, in the vertebrate host, sporozoites and merozoites are adapted to microaerophilia and contain few, underdeveloped mitochondria (Segura and Blair 2003).

Throughout the trypanosomatid life cycle, mitochondrial activity varies widely (Schneider 2001). In the bloodstream, these protozoans are anaerobic while in the gut of the insect they perform oxidative phosphorylation. In *Toxoplasma* most energy is obtained from glycolysis, although the mitochondrial DNA sequence of these parasites shows significant differences from the mammalian host, suggesting possible drug targets (Monzote and Gille 2010). Remarkably, the mitochondrial DNAs from trypanosomatids and Apicomplexa lack genes for transfer RNA (Mather and Vaidya 2008).

Concluding remarks

Aerobic metabolism is at the same time highly efficient and very dangerous. The reactive oxygen species produced by the respiratory chain can react with, and damage different components of the cell. Diverse mechanisms have evolved to prevent the deleterious effect of ROS. There are many detoxifying enzymes such as glutathione reductase, superoxide dismutase or catalase. In addition, upriver from these reactions, there are diverse mitochondrial systems designed to prevent ROS overproduction. These systems promote physiological uncoupling to ensure that the redox enzymes in the respiratory chain work at a fast rate, thus preventing reactive intermediates from participating in collateral reactions.

There are two mitochondrial uncoupling mechanisms: a) Those that dissipate the pH gradient and b) Non-productive redox reactions. Both mechanisms are widely spread in nature. Physiological proton sinks are the uncoupling proteins and the mitochondrial unspecific channels, while non productive redox reactions are catalyzed by redox/non-pumping alternative dehydrogenases and by orthodox complexes that undergo slipping.

The relationship between the cytoplasmic and the mitochondrial metabolic pathways needs to be better understood. The ability of some products from glycolysis to regulate oxidative phosphorylation is illustrative. The comparison between Crabtree positive and Crabtree negative yeast species may help understand the mechanisms and consequences of these interactions.

Understanding the mechanisms underlying the control and production of ROS may help to select more resistant organisms for biotechnological applications. Also, various ROS-related diseases have to be understood in order to design better treatments. In this light, it seems useful to know that uncoupling prevents ROS production.

During evolution, each eukaryote species preserved one or more ROS overproduction-prevention mechanism(s). Yeast species are ideal to study each mechanism. Other unicellular organisms may be helpful to understand their ability to shut down aerobic metabolism without being overwhelmed by ROS production.

Acknowledgements Partially funded by grants from CONACYT 79989 and by DGAPA/UNAM, IN217109. SGC, DAO, ACO, MGA and LALM are CONACYT fellows enrolled in the Biochemistry Graduate Program at UNAM. JEJ has a SNI-III aid fellowship. The assistance of Dr Natalia Chiquete-Félix is acknowledged. We thank Dr Soledad Funes-Argüello for critically reading the manuscript.

References

Albury MS, Affourtit C, Crichton PG, Moore AL (2002) Structure of the plant alternative oxidase. Site-directed mutagenesis provides new information on the active site and membrane topology. J Biol Chem 277:1190–1194

Andersson ME, Nordlund P (1999) A revised model of the active site of alternative oxidase. FEBS Lett 449:17–22

Anraku Y, Ohya Y, Iida H (1991) Cell cycle control by calcium and calmodulin in Saccharomyces cerevisiae. Biochim Biophys Acta 1093:169–177

Azzolin L, von Stockum S, Basso E, Petronilli V, Forte MA, Bernardi P (2010) The mitochondrial permeability transition from yeast to mammals. FEBS Lett 584:2504–2509

Azzone GF, Zoratti M, Petronilli V, Pietrobon D (1985) The stoichiometry of H+ pumping in cytochrome oxidase and the mechanism of uncoupling. J Inorg Biochem 23:349–356

Baines CP, Kaiser RA, Sheiko T, Craigen WJ, Molkentin JD (2007) Voltage-dependent anion channels are dispensable for mitochondrial-dependent cell death. Nat Cell Biol 9:550–555

Beauvoit B, Rigoulet M, Bunoust O, Raffard G, Canioni P, Guerin B (1993) Interactions between glucose metabolism and oxidative phosphorylations on respiratory-competent Saccharomyces cerevisiae cells. Eur J Biochem 214:163–172

Berman SB, Watkins SC, Hastings TG (2000) Quantitative biochemical and ultrastructural comparison of mitochondrial permeability transition in isolated brain and liver mitochondria: evidence for reduced sensitivity of brain mitochondria. Exp Neurol 164:415–425

Berthold DA, Andersson ME, Nordlund P (2000) New insight into the structure and function of the alternative oxidase. Biochim Biophys Acta 1460:241–254

Boles E, Heinisch J, Zimmermann FK (1993) Different signals control the activation of glycolysis in the yeast Saccharomyces cerevisiae. Yeast 9:761–770

Brandt U (2006) Energy converting NADH:quinone oxidoreductase (complex I). Annu Rev Biochem 75:69–92

Cabrera-Orefice A, Guerrero-Castillo S, Luevano-Martinez LA, Pena A, Uribe-Carvajal S (2010) Mitochondria from the salt-tolerant yeast Debaryomyces hansenii (halophilic organelles?). J Bioenerg Biomembr 42:11–19

Cascante M, Sorribas A, Canela EI (1994) Enzyme-enzyme interactions and metabolite channelling: alternative mechanisms and their evolutionary significance. Biochem J 298(Pt 2):313–320

Cavalheiro RA, Fortes F, Borecky J, Faustinoni VC, Schreiber AZ, Vercesi AE (2004) Respiration, oxidative phosphorylation, and uncoupling protein in Candida albicans. Braz J Med Biol Res 37:1455–1461

Cortes P, Castrejon V, Sampedro JG, Uribe S (2000) Interactions of arsenate, sulfate and phosphate with yeast mitochondria. Biochim Biophys Acta 1456:67–76

Chen Q, Vazquez EJ, Moghaddas S, Hoppel CL, Lesnefsky EJ (2003) Production of reactive oxygen species by mitochondria: central role of complex III. J Biol Chem 278:36027–36031

Cheng S, Clancy CJ, Zhang Z, Hao B, Wang W, Iczkowski KA, Pfaller MA, Nguyen MH (2007) Uncoupling of oxidative phosphorylation enables Candida albicans to resist killing by phagocytes and persist in tissue. Cell Microbiol 9:492–501

Czarna M, Jarmuszkiewicz W (2005) Activation of alternative oxidase and uncoupling protein lowers hydrogen peroxide formation in amoeba Acanthamoeba castellanii mitochondria. FEBS Lett 579:3136–3140

de Souza W, Attias M, Rodrigues JC (2009) Particularities of mitochondrial structure in parasitic protists (Apicomplexa and Kinetoplastida). Int J Biochem Cell Biol 41:2069–2080

den Hollander JA, Ugurbil K, Brown TR, Bednar M, Redfield C, Shulman RG (1986) Studies of anaerobic and aerobic glycolysis in Saccharomyces cerevisiae. Biochemistry 25:203–211

Devin A, Rigoulet M (2007) Mechanisms of mitochondrial response to variations in energy demand in eukaryotic cells. Am J Physiol Cell Physiol 292:C52–C58

Diaz-Ruiz R, Averet N, Araiza D, Pinson B, Uribe-Carvajal S, Devin A, Rigoulet M (2008) Mitochondrial oxidative phosphorylation is regulated by fructose 1,6-bisphosphate. A possible role in Crabtree effect induction? J Biol Chem 283:26948–26955

Drakulic T, Temple MD, Guido R, Jarolim S, Breitenbach M, Attfield PV, Dawes IW (2005) Involvement of oxidative stress response genes in redox homeostasis, the level of reactive oxygen species, and ageing in Saccharomyces cerevisiae. FEMS Yeast Res 5:1215–1228

Drose S, Brandt U (2008) The mechanism of mitochondrial superoxide production by the cytochrome bc1 complex. J Biol Chem 283:21649–21654

Feniouk BA, Mulkidjanian AY, Junge W (2005) Proton slip in the ATP synthase of Rhodobacter capsulatus: induction, proton conduction, and nucleotide dependence. Biochim Biophys Acta 1706:184–194

Fisher N, Bray PG, Ward SA, Biagini GA (2007) The malaria parasite type II NADH:quinone oxidoreductase: an alternative enzyme for an alternative lifestyle. Trends Parasitol 23:305–310

Fisher N, Warman AJ, Ward SA, Biagini GA (2009) Chapter 17 Type II NADH: quinone oxidoreductases of Plasmodium falciparum and Mycobacterium tuberculosis kinetic and high-throughput assays. Meth Enzymol 456:303–320

Flores-Encarnacion M, Contreras-Zentella M, Soto-Urzua L, Aguilar GR, Baca BE, Escamilla JE (1999) The respiratory system and diazotrophic activity of Acetobacter diazotrophicus PAL5. J Bacteriol 181:6987–6995

Forman HJ, Maiorino M, Ursini F (2010) Signaling functions of reactive oxygen species. Biochemistry 49:835–842

Fortes F, Castilho RF, Catisti R, Carnieri EG, Vercesi AE (2001) Ca2+ induces a cyclosporin A-insensitive permeability transition pore in isolated potato tuber mitochondria mediated by reactive oxygen species. J Bioenerg Biomembr 33:43–51

Frank V, Kadenbach B (1996) Regulation of the H+/e- stoichiometry of cytochrome c oxidase from bovine heart by intramitochondrial ATP/ADP ratios. FEBS Lett 382:121–124

Friberg H, Connern C, Halestrap AP, Wieloch T (1999) Differences in the activation of the mitochondrial permeability transition among brain regions in the rat correlate with selective vulnerability. J Neurochem 72:2488–2497

Gincel D, Zaid H, Shoshan-Barmatz V (2001) Calcium binding and translocation by the voltage-dependent anion channel: a possible regulatory mechanism in mitochondrial function. Biochem J 358:147–155

Gonzalez-Hernandez JC, Cardenas-Monroy CA, Pena A (2004) Sodium and potassium transport in the halophilic yeast Debaryomyces hansenii. Yeast 21:403–412

Gonzalez-Meler MA, Ribas-Carbo M, Giles L, Siedow JN (1999) The effect of growth and measurement temperature on the activity of the alternative respiratory pathway. Plant Physiol 120:765–772

Gosalvez M, Perez-Garcia J, Weinhouse S (1974) Competition for ADP between pyruvate kinase and mitochondrial oxidative phosphorylation as a control mechanism in glycolysis. Eur J Biochem 46:133–140

Guerin B, Bunoust O, Rouqueys V, Rigoulet M (1994) ATP-induced unspecific channel in yeast mitochondria. J Biol Chem 269:25406–25410

Guerrero-Castillo S, Vazquez-Acevedo M, Gonzalez-Halphen D, Uribe-Carvajal S (2009) In Yarrowia lipolytica mitochondria, the alternative NADH dehydrogenase interacts specifically with the cytochrome complexes of the classic respiratory pathway. Biochim Biophys Acta 1787:75–85

Gustafsson L, Norkrans B (1976) On the mechanism of salt tolerance. Production of glycerol and heat during growth of Debaryomyces hansenii. Arch Microbiol 110:177–183

Gutierrez-Aguilar M, Perez-Vazquez V, Bunoust O, Manon S, Rigoulet M, Uribe S (2007) In yeast, Ca2+ and octylguanidine interact with porin (VDAC) preventing the mitochondrial permeability transition. Biochim Biophys Acta 1767:1245–1251

Gutierrez-Aguilar M, Perez-Martinez X, Chavez E, Uribe-Carvajal S (2010) In Saccharomyces cerevisiae, the phosphate carrier is a component of the mitochondrial unselective channel. Arch Biochem Biophys 494:184–191

Hashimoto T, Nakamura Y, Nakamura F, Shirakura T, Adachi J, Goto N, Okamoto K, Hasegawa M (1994) Protein phylogeny gives a robust estimation for early divergences of eukaryotes: phylogenetic place of a mitochondria-lacking protozoan, Giardia lamblia. Mol Biol Evol 11:65–71

Haworth RA, Hunter DR (1979) The Ca2+− induced membrane transition in mitochondria. II. Nature of the Ca2+ trigger site. Arch Biochem Biophys 195:460–467

Hoefnagel MH, Millar AH, Wiskich JT, Day DA (1995) Cytochrome and alternative respiratory pathways compete for electrons in the presence of pyruvate in soybean mitochondria. Arch Biochem Biophys 318:394–400

Hosler JP, Ferguson-Miller S, Mills DA (2006) Energy transduction: proton transfer through the respiratory complexes. Annu Rev Biochem 75:165–187

Jarmuszkiewicz W, Behrendt M, Navet R, Sluse FE (2002) Uncoupling protein and alternative oxidase of Dictyostelium discoideum: occurrence, properties and protein expression during vegetative life and starvation-induced early development. FEBS Lett 532:459–464

Jarmuszkiewicz W, Antos N, Swida A, Czarna M, Sluse FE (2004) The effect of growth at low temperature on the activity and expression of the uncoupling protein in Acanthamoeba castellanii mitochondria. FEBS Lett 569:178–184

Jarmuszkiewicz W, Woyda-Ploszczyca A, Antos-Krzeminska N, Sluse FE (2010) Mitochondrial uncoupling proteins in unicellular eukaryotes. Biochim Biophys Acta 1797:792–799

Joseph-Horne T, Hollomon DW, Wood PM (2001) Fungal respiration: a fusion of standard and alternative components. Biochim Biophys Acta 1504:179–195

Jung DW, Bradshaw PC, Pfeiffer DR (1997) Properties of a cyclosporin-insensitive permeability transition pore in yeast mitochondria. J Biol Chem 272:21104–21112

Kadenbach B (2003) Intrinsic and extrinsic uncoupling of oxidative phosphorylation. Biochim Biophys Acta 1604:77–94

Kerscher SJ (2000) Diversity and origin of alternative NADH: ubiquinone oxidoreductases. Biochim Biophys Acta 1459:274–283

Kerscher S, Drose S, Zwicker K, Zickermann V, Brandt U (2002) Yarrowia lipolytica, a yeast genetic system to study mitochondrial complex I. Biochim Biophys Acta 1555:83–91

Korshunov SS, Skulachev VP, Starkov AA (1997) High protonic potential actuates a mechanism of production of reactive oxygen species in mitochondria. FEBS Lett 416:15–18

Koshkin V, Wang X, Scherer PE, Chan CB, Wheeler MB (2003) Mitochondrial functional state in clonal pancreatic beta-cells exposed to free fatty acids. J Biol Chem 278:19709–19715

Kovaleva MV, Sukhanova EI, Trendeleva TA, Zyl'kova MV, Ural'skaya LA, Popova KM, Saris NE, Zvyagilskaya RA (2009) Induction of a non-specific permeability transition in mitochondria from Yarrowia lipolytica and Dipodascus (Endomyces) magnusii yeasts. J Bioenerg Biomembr 41:239–249

Kowaltowski AJ, Costa AD, Vercesi AE (1998) Activation of the potato plant uncoupling mitochondrial protein inhibits reactive oxygen species generation by the respiratory chain. FEBS Lett 425:213–216

Krauss S, Zhang CY, Lowell BB (2005) The mitochondrial uncoupling-protein homologues. Nat Rev Mol Cell Biol 6:248–261

Kushnareva Y, Murphy AN, Andreyev A (2002) Complex I-mediated reactive oxygen species generation: modulation by cytochrome c and NAD(P)+ oxidation-reduction state. Biochem J 368:545–553

Leung AW, Varanyuwatana P, Halestrap AP (2008) The mitochondrial phosphate carrier interacts with cyclophilin D and may play a key role in the permeability transition. J Biol Chem 283:26312–26323

Luevano-Martinez LA, Moyano E, de Lacoba MG, Rial E, Uribe-Carvajal S (2010) Identification of the mitochondrial carrier that provides Yarrowia lipolytica with a fatty acid-induced and nucleotide-sensitive uncoupling protein-like activity. Biochim Biophys Acta 1797:81–88

Luvisetto S, Azzone GF (1989) Local protons and uncoupling of aerobic and artificial delta muH-driven ATP synthesis. Biochemistry 28:1109–1116

Luvisetto S, Conti E, Buso M, Azzone GF (1991) Flux ratios and pump stoichiometries at sites II and III in liver mitochondria. Effect of slips and leaks. J Biol Chem 266:1034–1042

Magnani T, Soriani FM, Martins Vde P, Policarpo AC, Sorgi CA, Faccioli LH, Curti C, Uyemura SA (2008) Silencing of mitochondrial alternative oxidase gene of Aspergillus fumigatus enhances reactive oxygen species production and killing of the fungus by macrophages. J Bioenerg Biomembr 40:631–636

Manon S, Guerin M (1997) The ATP-induced K(+)-transport pathway of yeast mitochondria may function as an uncoupling pathway. Biochim Biophys Acta 1318:317–321

Manon S, Guerin M (1998) Investigation of the yeast mitochondrial unselective channel in intact and permeabilized spheroplasts. Biochem Mol Biol Int 44:565–575

Manon S, Roucou X, Guerin M, Rigoulet M, Guerin B (1998) Characterization of the yeast mitochondria unselective channel: a counterpart to the mammalian permeability transition pore? J Bioenerg Biomembr 30:419–429

Mather MW, Vaidya AB (2008) Mitochondria in malaria and related parasites: ancient, diverse and streamlined. J Bioenerg Biomembr 40:425–433

Maxwell DP, Wang Y, McIntosh L (1999) The alternative oxidase lowers mitochondrial reactive oxygen production in plant cells. Proc Natl Acad Sci USA 96:8271–8276

Melo AM, Bandeiras TM, Teixeira M (2004) New insights into type II NAD(P)H:quinone oxidoreductases. Microbiol Mol Biol Rev 68:603–616

Millar AH, Wiskich JT, Whelan J, Day DA (1993) Organic acid activation of the alternative oxidase of plant mitochondria. FEBS Lett 329:259–262

Millenaar FF, Benschop JJ, Wagner AM, Lambers H (1998) The role of the alternative oxidase in stabilizing the in vivo reduction state of the ubiquinone pool and the activation state of the alternative oxidase. Plant Physiol 118:599–607

Monzote L, Gille L (2010) Mitochondria as a promising antiparasitic target. Curr Clin Pharmacol 5:55–60

Moore AL, Siedow JN (1991) The regulation and nature of the cyanide-resistant alternative oxidase of plant mitochondria. Biochim Biophys Acta 1059:121–140

Moreno-Sanchez R, Saavedra E, Rodriguez-Enriquez S, Gallardo-Perez JC, Quezada H, Westerhoff HV (2010) Metabolic control analysis indicates a change of strategy in the treatment of cancer. Mitochondrion 10:626–639

Mourier A, Devin A, Rigoulet M (2010) Active proton leak in mitochondria: a new way to regulate substrate oxidation. Biochim Biophys Acta 1797:255–261

Nakajima-Shimada J, Sakaguchi S, Tsuji FI, Anraku Y, Iida H (2000) Ca2+ signal is generated only once in the mating pheromone response pathway in Saccharomyces cerevisiae. Cell Struct Funct 25:125–131

Nicholls DG, Ferguson SJ (2002) Bioenergetics 3. Academic Press, London, ISBN 0125181213

Nicholls DG, Rial E (1999) A history of the first uncoupling protein, UCP1. J Bioenerg Biomembr 31:399–406

Ohya Y, Umemoto N, Tanida I, Ohta A, Iida H, Anraku Y (1991) Calcium-sensitive cls mutants of Saccharomyces cerevisiae showing a Pet- phenotype are ascribable to defects of vacuolar membrane H(+)-ATPase activity. J Biol Chem 266:13971–13977

Ovadi J, Saks V (2004) On the origin of intracellular compartmentation and organized metabolic systems. Mol Cell Biochem 256–257:5–12

Perez-Vazquez V, Saavedra-Molina A, Uribe S (2003) In Saccharomyces cerevisiae, cations control the fate of the energy derived from oxidative metabolism through the opening and closing of the yeast mitochondrial unselective channel. J Bioenerg Biomembr 35:231–241

Perrone GG, Tan SX, Dawes IW (2008) Reactive oxygen species and yeast apoptosis. Biochim Biophys Acta 1783:1354–1368

Pietrobon D, Azzone GF, Walz D (1981) Effect of funiculosin and antimycin A on the redox-driven H+− pumps in mitochondria: on the nature of 'leaks'. Eur J Biochem 117:389–394

Pietrobon D, Zoratti M, Azzone GF (1983) Molecular slipping in redox and ATPase H+ pumps. Biochim Biophys Acta 723:317–321

Pozniakovsky AI, Knorre DA, Markova OV, Hyman AA, Skulachev VP, Severin FF (2005) Role of mitochondria in the pheromone- and amiodarone-induced programmed death of yeast. J Cell Biol 168:257–269

Prieto S, Bouillaud F, Ricquier D, Rial E (1992) Activation by ATP of a proton-conducting pathway in yeast mitochondria. Eur J Biochem 208:487–491

Prieto S, Bouillaud F, Rial E (1995) The mechanism for the ATP-induced uncoupling of respiration in mitochondria of the yeast Saccharomyces cerevisiae. Biochem J 307(Pt 3):657–661

Rasmusson AG, Soole KL, Elthon TE (2004) Alternative NAD(P)H dehydrogenases of plant mitochondria. Annu Rev Plant Biol 55:23–39

Ricquier D (2005) Respiration uncoupling and metabolism in the control of energy expenditure. Proc Nutr Soc 64:47–52

Rottenberg H, Covian R, Trumpower BL (2009) Membrane potential greatly enhances superoxide generation by the cytochrome bc1 complex reconstituted into phospholipid vesicles. J Biol Chem 284:19203–19210

Schmid R, Gerloff DL (2004) Functional properties of the alternative NADH:ubiquinone oxidoreductase from E. coli through comparative 3-D modelling. FEBS Lett 578:163–168

Schneider A (2001) Unique aspects of mitochondrial biogenesis in trypanosomatids. Int J Parasitol 31:1403–1415

Segura C, Blair S (2003) Mitochondria in the Plasmodium genera. Biomedica 23:351–363

Siedow JN, Umbach AL (2000) The mitochondrial cyanide-resistant oxidase: structural conservation amid regulatory diversity. Biochim Biophys Acta 1459:432–439

Srere PA (1987) Complexes of sequential metabolic enzymes. Annu Rev Biochem 56:89–124

Starkov AA, Fiskum G, Chinopoulos C, Lorenzo BJ, Browne SE, Patel MS, Beal MF (2004) Mitochondrial alpha-ketoglutarate dehydrogenase complex generates reactive oxygen species. J Neurosci 24:7779–7788

Takeda M (1981) Glucose-induced inactivation of mitochondrial enzymes in the yeast Saccharomyces cerevisiae. Biochem J 198:281–287

Thevelein JM (1994) Signal transduction in yeast. Yeast 10:1753–1790

Tovar J, Fischer A, Clark CG (1999) The mitosome, a novel organelle related to mitochondria in the amitochondrial parasite Entamoeba histolytica. Mol Microbiol 32:1013–1021

Trumpower BL (1990) Cytochrome bc1 complexes of microorganisms. Microbiol Rev 54:101–129

Umbach AL, Siedow JN (2000) The cyanide-resistant alternative oxidases from the fungi Pichia stipitis and Neurospora crassa are monomeric and lack regulatory features of the plant enzyme. Arch Biochem Biophys 378:234–245

van Dam K, Shinohara Y, Unami A, Yoshida K, Terada H (1990) Slipping pumps or proton leaks in oxidative phosphorylation. The local anesthetic bupivacaine causes slip in cytochrome c oxidase of mitochondria. FEBS Lett 277:131–133

Velazquez I, Pardo JP (2001) Kinetic characterization of the rotenone-insensitive internal NADH: ubiquinone oxidoreductase of mitochondria from Saccharomyces cerevisiae. Arch Biochem Biophys 389:7–14

Velours J, Rigoulet M, Guerin B (1977) Protection of yeast mitochondrial structure by phosphate and other H+− donating anions. FEBS Lett 81:18–22

Wagner AM, Moore AL (1997) Structure and function of the plant alternative oxidase: its putative role in the oxygen defence mechanism. Biosci Rep 17:319–333

Wallace PG, Pedler SM, Wallace JC, Berry MN (1994) A method for the determination of the cellular phosphorylation potential and glycolytic intermediates in yeast. Anal Biochem 222:404–408

Wilhelm J, Fuksova H, Schwippelova Z, Vytasek R, Pichova A (2006) The effects of reactive oxygen and nitrogen species during yeast replicative ageing. Biofactors 27:185–193

Yamada A, Yamamoto T, Yoshimura Y, Gouda S, Kawashima S, Yamazaki N, Yamashita K, Kataoka M, Nagata T, Terada H et al (2009) Ca2+− induced permeability transition can be observed even in yeast mitochondria under optimized experimental conditions. Biochim Biophys Acta 1787:1486–1491

Zitomer RS, Nichols DL (1978) Kinetics of glucose repression of yeast cytochrome c. J Bacteriol 135:39–44

Zundorf G, Kahlert S, Bunik VI, Reiser G (2009) alpha-Ketoglutarate dehydrogenase contributes to production of reactive oxygen species in glutamate-stimulated hippocampal neurons in situ. Neuroscience 158:610–616

Biochimica et Biophysica Acta 1817 (2012) 353–362

Contents lists available at SciVerse ScienceDirect

Biochimica et Biophysica Acta

journal homepage: www.elsevier.com/locate/bbabio

During the stationary growth phase, *Yarrowia lipolytica* prevents the overproduction of reactive oxygen species by activating an uncoupled mitochondrial respiratory pathway

Sergio Guerrero-Castillo, Alfredo Cabrera-Orefice, Miriam Vázquez-Acevedo, Diego González-Halphen, Salvador Uribe-Carvajal *

Dept. of Molecular Genetics, Instituto de Fisiología Celular, Universidad Nacional Autónoma de México, Mexico

ARTICLE INFO

Article history:
Received 19 August 2011
Received in revised form 8 November 2011
Accepted 9 November 2011
Available online 22 November 2011

Keywords:
Yarrowia lipolytica
Mitochondrion
Branched respiratory chain
Alternative NADH dehydrogenase
Physiological uncoupling
Reactive oxygen species, ROS

ABSTRACT

In the branched mitochondrial respiratory chain from *Yarrowia lipolytica* there are two alternative oxido-reductases that do not pump protons, namely an external type II NADH dehydrogenase (NDH2e) and the alternative oxidase (AOX). Direct electron transfer between these proteins is not coupled to ATP synthesis and should be avoided in most physiological conditions. However, under low energy-requiring conditions an uncoupled high rate of oxygen consumption would be beneficial, as it would prevent overproduction of reactive oxygen species (ROS). In mitochondria from high energy-requiring, logarithmic-growth phase cells, most NDH2e was associated to cytochrome *c* oxidase and electrons from NADH were channeled to the cytochromic pathway. In contrast, in the low energy requiring, late stationary-growth phase, complex IV concentration decreased, the cells overexpressed NDH2e and thus a large fraction of this enzyme was found in a non-associated form. Also, the NDH2e–AOX uncoupled pathway was activated and the state IV external NADH-dependent production of ROS decreased. Association/dissociation of NDH2e to/from complex IV is proposed to be the switch that channels electrons from external NADH to the coupled cytochrome pathway or allows them to reach an uncoupled, alternative, ΔΨ-independent pathway.

1. Introduction

Mitochondria from fungi, plants and parasites often contain branched respiratory chains, constituted by orthodox and "alternative" redox enzymes present in different stoichiometries [1–3]. In mitochondria from *Yarrowia lipolytica* the respiratory chain is composed by the four multi-subunit complexes (I to IV) found in animals and plants, plus an external type II NADH dehydrogenase (NDH2e) and an alternative oxidase (AOX) [4]. Both NDH2e and AOX are single-subunit peripheral oxido-reductases that lack proton-pumping activity [5,6].

Branched respiratory chains may include different alternative dehydrogenases that reduce ubiquinone without contributing to the proton gradient. Thus, ubiquinone may be reduced by complex I, succinate-dehydrogenase, glycerol-phosphate dehydrogenase, dihydroorotate-dehydrogenase or by internal or external NDH2s [7,8]. All these enzymes use flavin in the redox reaction [9–11]. From ubiquinol, electrons can reach either complexes III/IV (cytochromic pathway) or an AOX [12]. The many pathways available open the possibility that electrons may reach oxygen with different proton-pumping stoichiometries, even passing only through enzymes that do not translocate protons at all [13], i.e. the ADP:O ratio can vary widely in branched respiratory chains [14].

Structural models of AOX, whether monomeric or dimeric [15–17], suggest it has regulatory sites for nucleotides and/or for α-ketoacids [18,19]. Some yeast species contain only one AOX, which is activated under stress. Other species contain two isoforms of AOX, one constitutive but expressed at low levels and another one inducible under stress [16]. Remarkably, no species is known where the absence of complex-I and the presence of AOX coexist; it has been proposed that such a combination would lead to uncontrolled uncoupling [1,4].

Unless uncoupled respiration is desired, energy-requiring cells must avoid pairing non proton-pumping dehydrogenases with AOX [1]. Therefore, it is of interest to define the usefulness of the non-pumping enzymes. These enzymes might prove useful in medicine and biotechnology; alternative NDH2i (internal NDH2) has been expressed in mammalian cells to partially substitute for a non-functional complex I [20]. In addition, NDH2 has been expressed in

Abbreviations: NDH2e, alternative external NADH dehydrogenase; AOX, alternative oxidase; ΔΨ, transmembrane potential; CCCP, carbonylcyanide-3-chlorophenylhydrazone; ROS, reactive oxygen species

* Corresponding author at: Dept. of Molecular Genetics, Instituto de Fisiología Celular, Universidad Nacional Autónoma de México, Apdo. postal 70-242, 04510 Mexico City, Mexico. Tel.: +52 55 5622 5632.
E-mail address: suribe@ifc.unam.mx (S. Uribe-Carvajal).

0005-2728/$ – see front matter © 2011 Elsevier B.V. All rights reserved.
doi:10.1016/j.bbabio.2011.11.007

aerobic fungi or yeast harboring complex I deficiencies with the aim to analyze mitochondrial function [21,22].

Alternative component activity must be tightly regulated in response to the energy requirements or to the redox state of the cell. In different species of yeast, AOX is over-expressed under stress [23] or in the stationary growth phase [24]. Channeling electrons between a proton-pumping complex and an alternative component would prevent excessive wastage of energy and thus functional associations such as complex I-AOX [25] or NDH2-complexes III/IV [26] have been proposed. In addition, some redox enzymes might alternate between a bound, electron-channeling state and a free, non-channeling state in order to regulate the proton pumping efficiency of the respiratory chain and thus the ADP:O.

Y. lipolytica mitochondria were isolated from cells grown to either the high-energy requiring logarithmic growth phase (log-phase) or the low-energy requiring stationary growth phase (stat-phase) [27–29]. It was observed that in the log-phase, NDH2e-derived electrons were channeled to the cytochromic pathway and NDH2e was bound to complex IV, probably in a complex III/complex IV super-complex. In contrast, in the stat-phase the NDH2e–AOX uncoupled-electron transfer pathway was activated, most likely as a result of the dissociation of NDH2e from complex IV. In these conditions ROS production was largely inhibited, suggesting a physiologic role for uncoupling.

2. Experimental procedures

2.1. Materials

NADH, Glycerol-phosphate, n-propylgallate, n-β-D-dodecylmaltoside, digitonin, mannitol, pyruvate, malate, cytochrome *c*, antimycin-A, rotenone and CCCP were from Sigma Chem. Co. (St. Louis, MO, USA). Coomassie blue G was from Serva (Heidelberg, Germany). The polyclonal antibody against *Y. lipolytica* NDH2e (anti-*Yl*NDH2e) was a kind gift from Dr. Stefan Kerscher, Zentrum der Biologischen Chemie, Frankfurt University, (Germany). Monoclonal antibodies against cytochrome *c* oxidase subunits II and III from *S. cerevisiae* were from Mitoscience (Eugene, OR, USA).

2.2. Strains, culture and isolation of yeast mitochondria

The strains used in this work were the wild type: *Y. lipolytica* E150 (*MatB his1-1 ura3-302 leu2-270 xpr2-322*) and the *Δndh2e* mutant (GB5.2) [30]. All strains were a kind gift from Prof. Ulrich Brandt, ZBC, Frankfurt University (Germany). Cells were grown in YD (Yeast extract 1%, glucose 2%) [31] at 160 rpm, 30 °C for 15 or 96 h to be harvested at the logarithmic or late stationary growth phases, respectively. Cells were washed and re-suspended in 5 mM MES, 0.6 M mannitol, 0.1% BSA (pH 6.8, triethanolamine) and disrupted using a Bead Beater cell homogenizer (Biospec Products, OK, USA) with 0.45 mm glass beads (3×20 s pulses separated by 40 s resting periods). To isolate mitochondria, the homogenate was subjected to differential centrifugation [32] and protein concentration was determined by biuret [33]. Mitochondrial intactness was evaluated by measuring the respiratory controls which were between 2.0 and 3.0 [34]. The integrity of the external mitochondrial membrane was determined by reduction of diaminobenzidine in the presence of 10 μM antimycin A and cytochrome *c* either permeabilized with 0.1 mg/mg protein n-β-D-docecylmaltoside or not. Diaminobenzidine reduction was measured by absorbance changes at 490 nm. In non-permeabilized mitochondria the reaction was 9-fold less than in the presence of detergent. In addition, in the presence of external NADH as a substrate, rotenone inhibited less than 6% of the total oxygen consumption, indicating that external NADH was oxidized mainly by NDH2e.

2.3. Oxygen consumption measurements

The rate of oxygen uptake was measured in an oxygen meter model 782 (Warner/Strathkelvin Instruments) with a Clark type electrode in a 0.1 mL water-jacketed chamber at 30 °C [35] and data were analyzed using the 782 Oxygen System software (Warner/Strathkelvin Instruments). External NADH-dependent respiration was measured in the presence of rotenone in order to inhibit reverse electron transfer from ubiquinol to complex I; rotenone binds to the ubiquinone binding site of complex I [36]. Pyruvate plus malate was used to generate internal NADH which is oxidized by complex I. Cyanide or antimycin A was used to inhibit cytochrome *c* oxidase or the Qi site of complex III, respectively. Since both cyanide and antimycin A inhibit the cytochrome pathway, electrons are diverted towards AOX. The reaction mixture contained 0.6 M mannitol, 5 mM MES (pH 6.8), 20 mM KCl, 4 mM phosphate (the Tris salt was obtained using phosphoric acid and adjusting to pH 6.8 with Tris) and 1 mM $MgCl_2$. Mitochondria were added to a final concentration of 0.5 or 1.0 mg protein/mL. Respiratory controls using either external NADH or succinate were determined in the presence of 2.5 μM rotenone.

2.4. Protein separation by native electrophoresis and in-gel activities

BN- and CN-PAGE were performed as described [37,38]. Mitochondria were solubilized with 2 g n-dodecyl-β-D-maltoside (LM)/g protein, or 4 g digitonin (Dig)/g protein at 4 °C and centrifuged at 100,000 *g* at 4 °C for 25 min. Protein concentration of the supernatants was determined and 0.4 mg protein per well was loaded on 4–12% polyacrylamide gradient gels. For both BN and CN-PAGE digitonin (0.025%) was added to the gel preparation. The cathode buffer for CN-PAGE contained 0.01% LM and 0.05% deoxycholate as described in [39]. In-gel NADH:NBT oxido-reductase activity was determined by incubating the native gels in a mixture containing 10 mM Tris (pH 7.0), 0.5 mg nitro blue tetrazolium bromide (NBT)/mL and 1 mM NADH [40]. In-gel cytochrome *c* oxidase activity was determined using diaminobenzidine and cytochrome *c* as described in [41].

2.5. Ion exchange chromatography and enzymatic activities of the fractions

Mitochondria were solubilized with 0.8 g/g prot n-β-D-dodecylmaltoside (LM) in 1 mM Mg–SO_4, 1 mM PMSF, 50 mM HEPES, pH 8.0 plus 50 μg/mL TLCK (Tosyl-lysyl-chloromethyl ketone). The solubilizate was centrifuged at 100,000×*g* for 30 min and layered on top of a previously equilibrated DEAE-Sepharose column [42]. Once loaded, the column was washed with 3 volumes of 1 mM $MgSO_4$, 50 mM Tris, pH 8.0 and proteins were eluted with a 0–400 mM NaCl gradient. Fractions of 1 mL were collected. The protein concentration in each fraction was estimated spectrophotometrically at 280 nm. For NADH dehydrogenase or cytochrome *c* oxidase activities, 20 μL of each fraction was placed in a well within a micro plate in the presence of the substrate and an electron acceptor and the reaction was followed in a multimodal micro plate reader Synergy Mix, Biotek (VT, USA). Enzyme assays: a) NADH dehydrogenase, following the reduction of nitro blue tetrazolium bromide (NBT) at 570 nm. The reaction mixture was 10 mM Tris, pH 7.0, 1 mM NADH, 0.5 mg/mL NBT; b) Cytochrome *c* oxidase was measured in 50 mM phosphate buffer (sodium) pH 7.4, 2.5 mg/mL horse heart cytochrome *c*, 1 mg/mL diaminobenzidine and cytochrome *c* reduction was followed at 490 nm.

2.6. Immunoassays

Ion exchange chromatography fractions were loaded onto a nitrocellulose membrane for dot blot immunodetection with antibodies

against either NDH2e from *Y. lipolytica* or COXII from *S. cerevisiae*. Blots were quantified using the Image-J software. Also from SDS-Tricine-PAGE, proteins were electro-transferred onto a nitrocellulose membrane (BioRad, Hercules, CA, USA) for immunodetection. Membranes were washed, blocked, and incubated with anti-*Yl*NDH2e [30] (1:1000 for 1 h), using an alkaline phosphatase-conjugated anti-rabbit IgG (1:3000 for 2 h) as secondary antibody. A monoclonal antibody against subunit III of cytochrome *c* oxidase (COX III) from *S. cerevisiae* was used.

2.7. Cytochrome measurements using differential spectrophotometry

Mitochondria (2 mg prot/mL) were added to homogenization buffer without BSA. Absorbance spectra were recorded from 500 to 680 nm in a DW2000 Aminco Spectrophotometer in the presence of ferricyanide to obtain the oxidized spectra, which was assigned as base line. Then, the reduced spectrum was recorded after addition of sodium dithionite to the sample cuvette. Absorption coefficients were: cytochrome *b*, $\varepsilon_{562-575\ nm} = 28.5\ mM^{-1}\ cm^{-1}$ [43]; cytochrome $a + a_3$, $\varepsilon_{603-630\ nm} = 24\ mM^{-1}\ cm^{-1}$ [44].

2.8. Reactive oxygen species measurements

Reactive oxygen species production rates in freshly purified mitochondria were measured using the Amplex Red Hydrogen peroxide/peroxidase method [45] in a Synergy HT multi-mode micro plate reader, Biotek (VT, USA). Hydrogen peroxide formation was determined following resorufin fluorescence as in [46]. Reaction mixture: 0.6 M mannitol, 5 mM MES (pH 6.8), 20 mM KCl, 10 mM phosphate, 1 mM $MgCl_2$, 10 μM Amplex Red (Invitrogen, Molecular Probes, Eugene, OR, USA), 0.1 units/mL horseradish peroxidase and 100 units/mL superoxide dismutase and 0.5 mM NADH or 10 mM pyruvate plus 10 mM malate as substrates. Mitochondria were added to a final concentration of 60 μg protein/well (0.3 mg prot/mL).

3. Results

3.1. In Y. lipolytica mitochondria, direct electron transfer between alternative respiratory chain components is observed only in the stationary phase

In yeast, the need for ATP is high in the logarithmic growth phase (log-phase) and decreases when the cells enter the stationary growth phase (stat-phase) [27]. Consequently, in the log-phase a high rate of oxygen consumption is needed to replenish the electrochemical proton gradient consumed by the synthesis of ATP. In contrast, in the stat-phase less ATP is needed, so a high rate of oxygen consumption would be possible only if a certain degree of uncoupling is promoted [13,14]. The branched mitochondrial respiratory chain from *Y. lipolytica* can probably be uncoupled to different extents, depending on the number of proton pumps participating in the electron pathway followed from different substrates to oxygen [13]. To test for possible electron routes, cells were harvested at two different growth phases and the respiratory activity of isolated mitochondria was evaluated (Fig. 1). The rate of oxygen consumption did not change with the growth phase, although it was always lower using pyruvate plus malate, which are complex I substrates (Fig. 1-A) than when using external NADH, which is oxidized by NDH2e (Fig. 1-B). In contrast, the electron pathway for NDH2e was different depending on the growth phase, as evidenced by the sensitivity to different respiratory inhibitors. In either stage, when using a substrate for complex I, the rate of oxygen consumption was partially inhibited by cyanide (complex IV inhibitor) or by propyl-gallate (AOX inhibitor) and only in the presence of both inhibitors did the rate of oxygen consumption approach complete inhibition. Thus, it seems that the electrons from complex I flow through both the cytochrome pathway and the AOX pathway (Fig. 1-A). In contrast, when NADH was used to feed electrons to NDH2e, the respiratory pathway was different depending on the growth stage of the cell (Fig. 1-B). In mitochondria from log-phase cells, cyanide inhibited most oxygen consumption, while propyl-gallate had negligible effects; the inhibition pattern changed in the stat-phase, where both cyanide and propyl-gallate exhibited partial effects. Again, the simultaneous addition of both inhibitors abolished oxygen consumption completely (Fig. 1-B). Thus, in the log phase the electrons from NDH2e are channeled to the cytochrome pathway and cannot reach AOX, while in the stationary phase the NDH2e to AOX pathway becomes active.

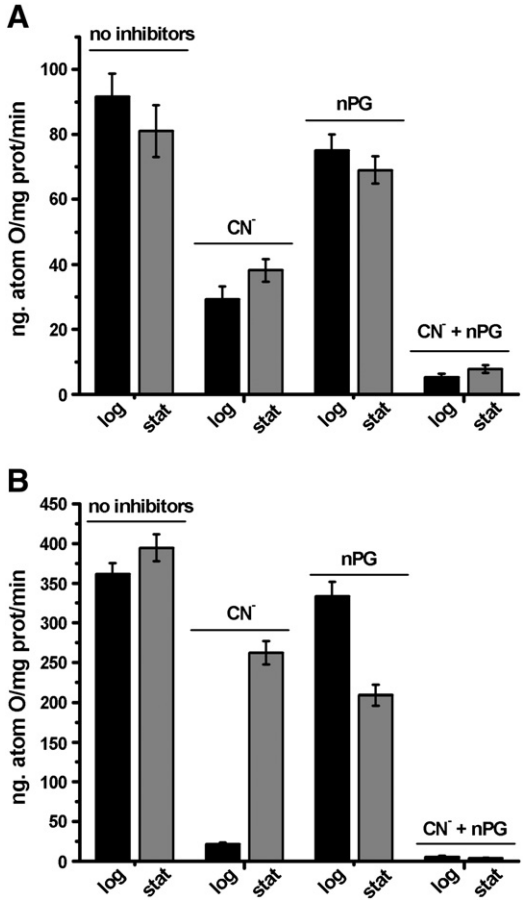

Fig. 1. Effect of oxygen consumption inhibitors on mitochondria isolated from cells grown to the logarithmic or stationary phase. Experimental conditions: 0.6 M mannitol, 5 mM MES, 20 mM KCl, 4 mM phosphate, 1 mM $MgCl_2$, pH 6.8. Oxygen consumption was measured with a Clark electrode in a closed water-jacketed chamber at 30 °C. Rates of respiration were calculated in the presence of 5 mM pyruvate plus malate (A) or 1 mM NADH in the presence of 2.5 μM rotenone (B). Additions as indicated: without inhibitors, in the presence of 100 μM cyanide, 50 μM n-propylgallate or both. Columns indicate mean ± SD (n = 5).

3.2. NDH2e-dependent oxygen consumption is uncoupled in mitochondria from Y. lipolytica in the stationary growth-phase

In mitochondria from *Y. lipolytica* cells grown to either the log- or the stat-phase, the channeling of electrons through NDH2e into the cytochrome pathway was further analyzed by evaluating coupling (Fig. 2). That is, measuring the rate of oxygen consumption in state III and in state IV, as well as the resulting respiratory controls (RC = state III/state IV). In the presence of pyruvate–malate, both the rates of oxygen consumption and the RCs remained high, both in the log-phase and the stat-phase (i.e., $RC_{log} = 2.3 \pm 0.1$ and $RC_{stat} = 2.13 \pm 0.2$) (Fig. 2-A). In contrast, when the NADH-

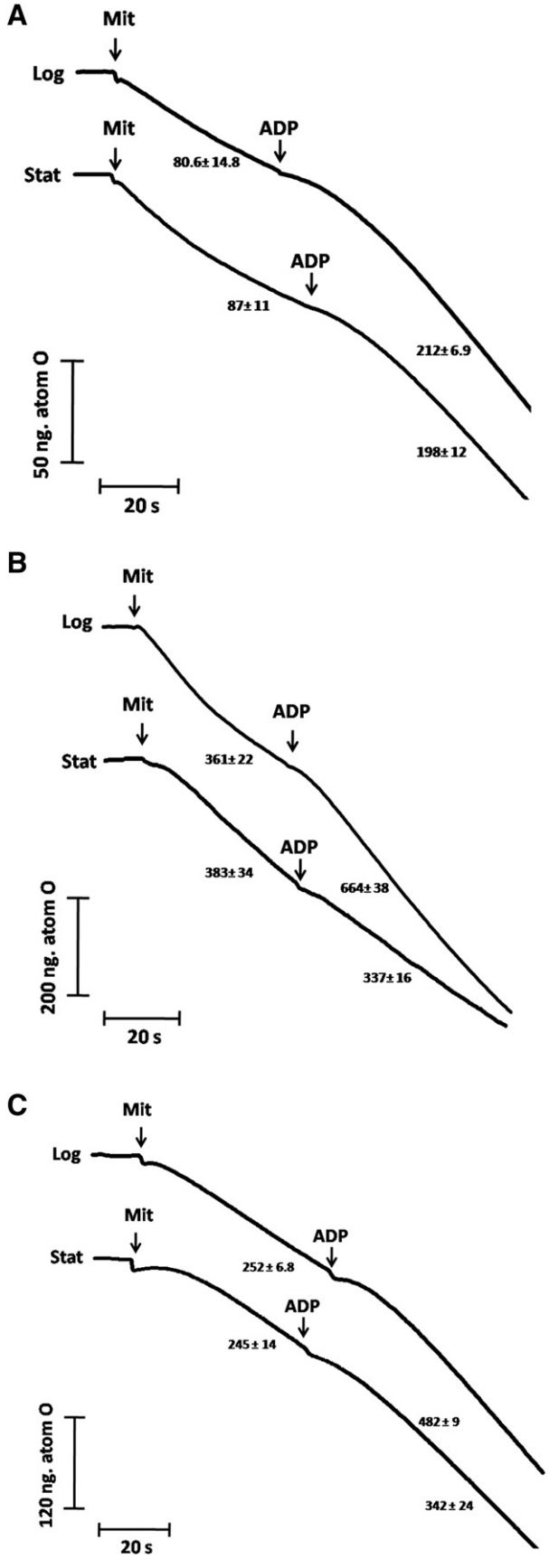

supported respiration was measured, coupling was dependent on the growth phase as follows: in the log-phase, $RC_{log} = 1.82 \pm 0.06$, while in the stat-phase there was no increase in the respiration rate after the addition of ADP (Fig. 2-B). Therefore, it may be concluded that in the stat-phase an uncoupled pathway where electrons enter the respiratory chain at NDH2e, was activated. The NADH-dependent uncoupling was not due to an increase in permeability of the inner mitochondrial membrane, since the response to pyruvate–malate remained intact.

The above results indicate that an NDH2e-dependent uncoupled pathway is activated in the stationary phase, opening the question on whether other non-coupled pathways become active. In this regard, it is known that complex II is not a proton pump, and thus a complex II to AOX pathway would also be fully uncoupled. Thus, we also explored the behavior of electrons coming from succinate (Fig. 2-C). In contrast to the results with NADH, in the presence of succinate the response to ADP was lost only partially in mitochondria from the stationary cells, i.e., $RC_{log} = 1.9 \pm 0.1$, $RC_{stat} = 1.4 \pm 0.1$. That is, even though the RC decreased, it was not abolished, suggesting that even in the stat-phase the electrons from complex II are partially reaching the cytochrome pathway. If there is a physical association between complex II and the III–IV super-complex, this association must be very labile, as it has not been observed in native gel electrophoresis from neither *Y. lipolytica* nor from other mitochondria [26,47]. Altogether the above data indicate that in *Y. lipolytica* a specific NDH2e–ubiquinone–AOX pathway is active in the stat-phase but not in the log-phase.

3.3. In the stationary growth-phase NDH2e is found either free of associated to complex IV

It was previously reported that in spite of the differences in isoelectric points, NDH2e and complex IV co-elute from an ion-exchange chromatography column and also, association of NDH2e with a super-complex III/IV was proposed by native gel experiments [26]. This association was proposed to be the structural basis for the electron channeling between NDH2e and the cytochrome pathway observed in mitochondria isolated from log-phase grown cells [26].

In order to determine the mechanism for the loss of electron channeling detected in the stationary growth phase (Figs. 1 and 2), we tested whether the association between NDH2e and complex IV varied depending on the growth phase of the cells (Fig. 3). Mitochondria from cells in the log (Fig. 3-A) or in the stat-phase (Fig. 3-B) were solubilized and loaded into two independent DEAE-Biogel-A ion-exchange chromatography columns. The concentration of LM used to solubilize was 0.8 mg/mg protein where, contrary to what happens at 2 mg LM/mg protein, supramolecular interactions are partially preserved (Fig. 3). The NADH dehydrogenase activities did vary slightly between the log (Fig. 3-A) and the stationary (Fig. 3-B) growth phase. However, it was difficult to evaluate the change in the specific NDH2e activity due to interference caused by complex I and other enzymes capable of oxidizing NADH. In order to subtract all NADH dehydrogenase activities that were not due to NDH2e it was decided to run a homogenate from a Δndh2e strain through the same column as the WT samples (Fig. 3-C). The Δndh2e sample expressed all NADH activities except NDH2e, and thus it was subtracted from the activities of the WT strain, aiming to obtain a good estimate of the

Fig. 2. Respiratory controls of mitochondria isolated from cells grown to the logarithmic or stationary phase. Reaction mixture: as in Fig. 1 except for the inhibitors. Mitochondria were added to a final concentration of 1 mg prot/mL from cells harvested in the log- (Log) or the stat-phase (Stat). Respiratory substrates were: A) 5 mM pyruvate plus malate; B) 1 mM NADH; C) 10 mM succinate. Where indicated, 1 mM ADP was added. When NADH or succinate was used, 2.5 μM rotenone was added to the reaction mixture. Representative traces are shown (n = 5).

NDH2e activity in the log and the stationary growth phases respectively (Fig. 3-D). Subtraction resulted in 3 peaks of NDH2e which eluted at 150, 190 and 230 mM NaCl. Peaks at 150 and 230 mM closely correspond to two of the peaks observed for cytochrome *c* oxidase activity in Fig. 3-A. In stat-phase, 4 peaks of NDH2e resulted after subtraction of the ΔNDH2e (Fig. 3-D). The first one, eluted at 80 mM NaCl, corresponds to the overexpressed, free-fraction of NDH2e, while the other 3 seem to be the same as in the log-phase. These results were confirmed when the activity profile from the wild type strain in the log-phase (Fig. 3-A) was subtracted from

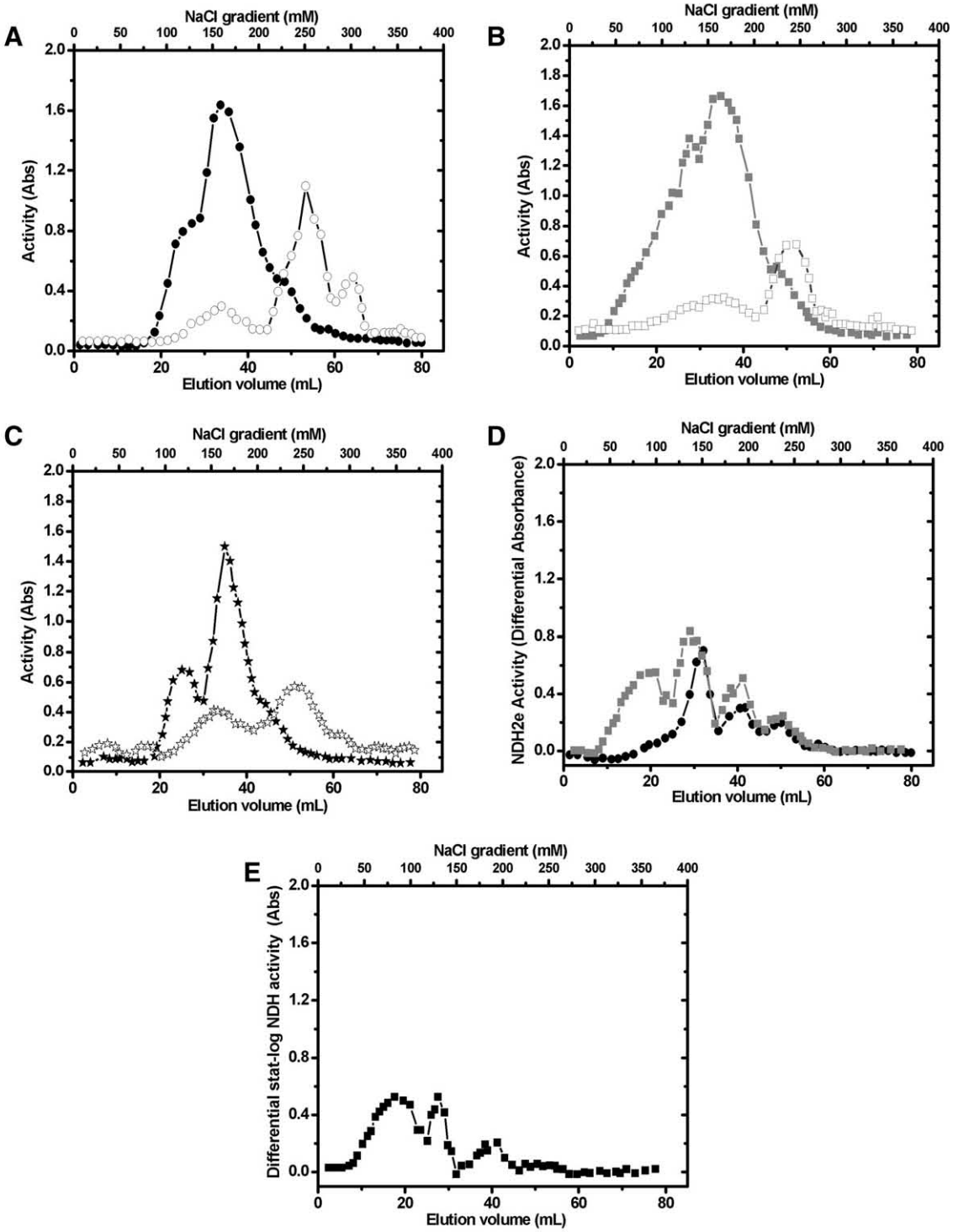

Fig. 3. Ion-exchange chromatographic elution activity and protein profiles of mitochondria from cells harvested at different growth phases. Mitochondrial extracts were loaded on a DEAE-Biogel A gel ion-exchange chromatography column previously equilibrated, washed and eluted using a 0–400 mM NaCl gradient. 1 mL fractions were collected and enzyme activities were measured as described in [26]. NADH dehydrogenase activity (filled symbols); cytochrome *c* oxidase activity (empty symbols). Samples were mitochondria from (A) Log-phase grown cells; (B) Stat-phase grown cells; (C) ΔNDH2e cells. (D) Differential trace for NADH dehydrogenase activity, A minus C (●) and B minus C (■). (E) Differential of stat-phase minus log-phase NADH dehydrogenase activity; both activities were measured from the wild type preparation. (F) Dot blot analysis was conducted on the fractions and results were plotted for NDH2e (G) and for cytochrome *c* oxidase (H). A representative experiment is shown (n = 2).

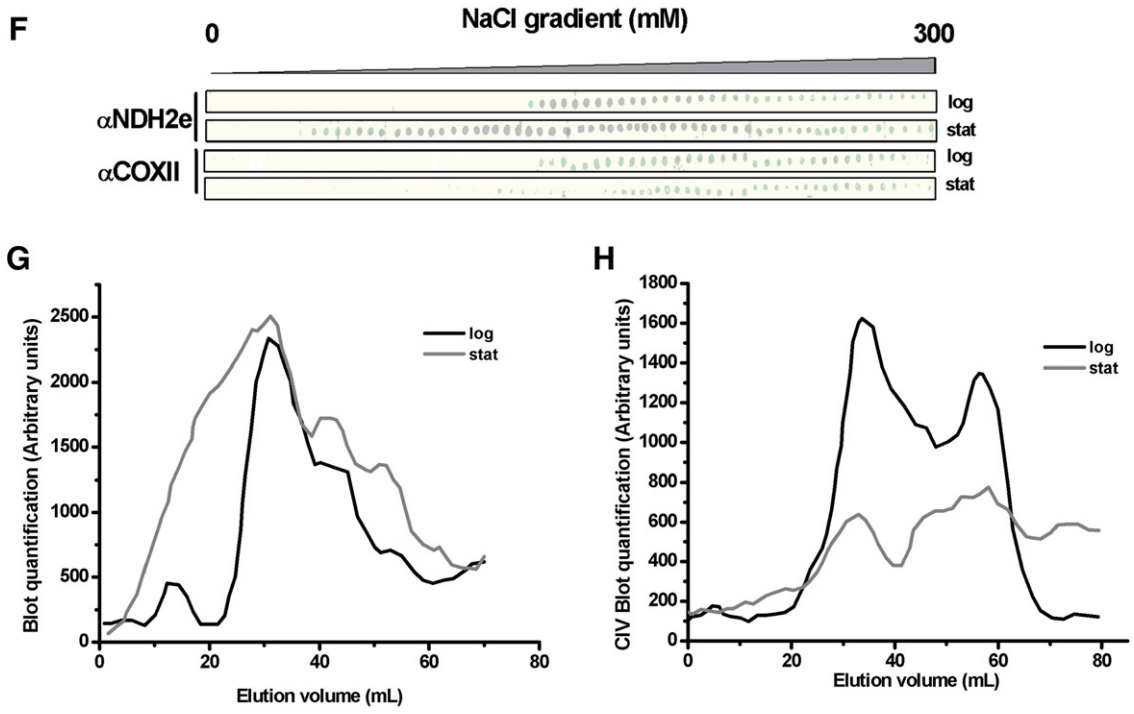

Fig. 3 (*continued*).

the profile from the wild-type strain in stat phase (Fig. 3-B) and in the subtraction (Fig. 3-E) a peak corresponding to a free NDH2e was observed at 80 mM NaCl, i.e. at the same ionic strength as in Fig. 3-D. The results suggest that upon reaching the late stationary phase, a large proportion of NDH2e is detached from complex IV.

In regard to complex IV, it was observed that it eluted in two peaks regardless of the growth phase, suggesting that it eluted as a super-complex in the first peak while the second peak represented the monomeric form of cytochrome *c* oxidase (Fig. 3-A and B). This elution pattern of cytochrome *c* oxidase was not detected in an earlier report using a higher detergent: protein ratio in the chromatography column [26]. Nonetheless, the total activity of cytochrome *c* oxidase seemed to decrease in the stat-phase (Fig. 3-B) as compared to the log-phase (Fig. 3-A). Thus, the release of NDH2e resulting from the increase in this protein combined with a decrease in complex IV might be the mechanism that turns off electron channeling to the cytochromic pathway.

To further characterize the putative growth phase-related redistribution of NDH2e, we performed a dot-blot assay for each of the fractions from the chromatography columns using an anti-*Y. lipolytica* NDH2e antibody and an anti-*S. cerevisiae* COXII subunit antibody to detect the distribution of NDH2e and complex IV in the elution profiles (Fig. 3-F). The immunochemical results confirmed the data obtained from the activity measurements, i.e. in the log-phase most NDH2e co-elutes with complex IV, while in the stat-phase a large proportion of NDH2e dehydrogenase runs free, exiting the column earlier, while only a fraction seems to co-elute with complex IV (Fig. 3-G). In addition, in stat-phase there seems to be an increase in the total amount of NDH2e (Fig. 3-G). When the complex IV immunoblots were quantitated, the presence of two populations of complex IV was observed in both growth phases, suggesting that in addition to the monomeric form of complex IV, a supercomplex containing complex IV was preserved in the column (Fig. 3-H). In addition, in the stat-phase the amount of complex IV seems to decrease (Fig. 3-H).

3.4. In gel activities and spectrophotometric assays confirm that the concentration of NDH2e increases while complex IV decreases

The NDH2e activity seemed to be much higher in the stat-phase than in the log-phase. An increase in the expression of this enzyme would explain the presence of free NDH2e. In addition, an increase in the NDH2e/COX ratio would result from either an increase in NDH2e or a decrease in complex IV. In order to test whether the NDH2/complex IV ratio was increased in the stationary growth phase, in-gel NADH dehydrogenase and cytochrome *c* oxidase activities of digitonin-solubilized mitochondria were measured after hrCN-PAGE (Fig. 4-A). In-gel activity of NADH dehydrogenase stained four bands: the higher molecular mass band was complex I, while the next two bands, marked as NDH2e and NDH2e*, were stained due to the activity of the alternative NADH dehydrogenase, since they were absent in the electrophoretic pattern of the NDH2e deletion mutant. These two bands probably represent bound and free populations of NDH2e. The fourth, lower band, present in all gels, might correspond to the activity of an NADPH dehydrogenase, as it was previously identified by LC-MS/MS analysis [26] and it also appeared in the ΔNDH2e mutant. As expected, cytochrome *c* oxidase in-gel activity revealed several bands probably corresponding to diverse complex IV-containing super-complexes. The lower band corresponds to monomeric complex IV and the upper bands to different complex IV-containing super-complexes.

In the stat-phase an increase in the band marked as NDH2e was observed, which probably corresponds to the free form of the alternative dehydrogenase, while the band marked as NDH2e* did not seem to change as compared with that observed in the log-phase (Fig. 4-A). In parallel, a decrease in cytochrome *c* oxidase activity was detected in the stat-phase, suggesting that complex IV may be down-regulated at the same time as NDH2e expression increases (Fig. 4-A). In addition, western blots of subunit III of cytochrome *c* oxidase indicated that complex IV was found at lower concentrations in the stat- than in the log-phase (Fig. 4-B). To confirm whether complex IV decreased in the stat-phase, the absorption

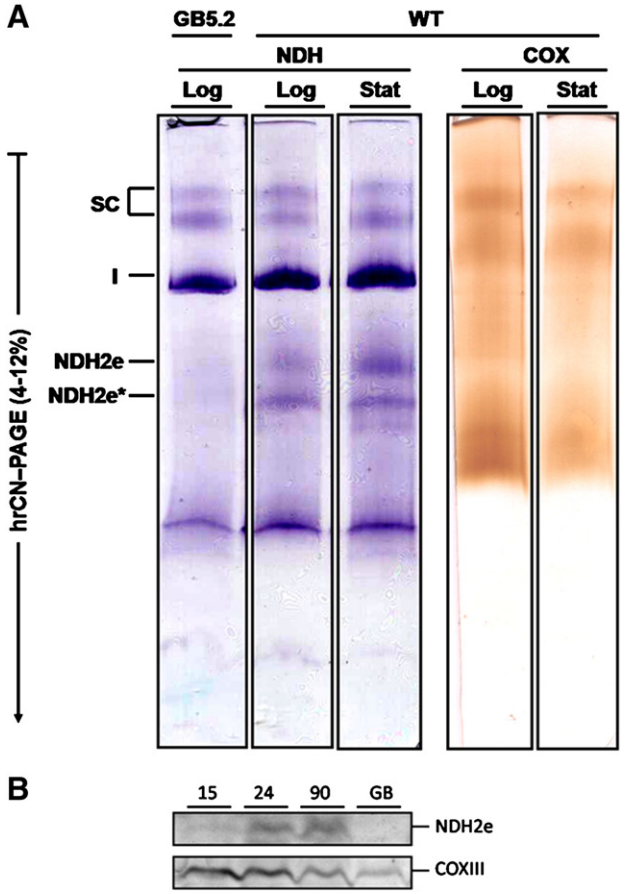

Fig. 4. Activity and protein amounts of NDH2e and complex IV. (A) In-gel NADH dehydrogenase (NDH) or cytochrome *c* oxidase (COX) activities were qualitatively determined after hrCN-PAGE of mitochondria isolated from cells grown to the log-phase (15 h) or to the stat-phase (90 h). In addition to complex-I and NDH2e, other dehydrogenases were detected. The most intensely colored band corresponds to complex I. NDH2e activity could be assigned due to the lack of staining in a *Δndh2e* mutant strain (GB5.2). Two bands corresponding to the alternative enzyme marked as NDH2e and NDH2e* probably correspond to a cytochromic pathway-interacting form and to a free form. I, complex I; IV, complex IV; SC, super-complexes; (B) Western blot of isolated mitochondria for detection of NDH2 and the complex IV subunit COXIII in different growth phases. Numbers indicate time of growth (hours) from the wild type strain; GB, *Δndh2e* mutant strain. A representative gel and blot are shown (n = 3).

spectra of cytochromes *b* and aa_3 and the activity of cytochrome *c* oxidase were measured (Fig. 5). The concentration of cytochrome *b* remained almost constant, while cytochrome $a + a_3$ decreased from 0.07 nmol/mg protein in the log-phase to 0.03 nmol/mg protein in the stat-phase (Fig. 5-A). In these same conditions the rate of oxygen consumption using ascorbate and TMPD also decreased during the stat-phase (Fig. 5-B). Altogether, the differences in the in-gel activities (Fig. 4-A), the decreased complex IV contents detected by western blot (Fig. 4-B) and the absorbance spectra (Fig. 5), are consistent with an increase in the NDH2e:complex IV ratio that in turn would lead to accumulation of non-associated NDH2e that would be free to reduce AOX.

3.5. In mitochondria from cells in the stationary phase, NADH oxidation produces less reactive oxygen species

The uncoupled (NDH2e–AOX) respiratory pathway increased during the stat-phase, although a fraction of NDH2e was still interacting with the cytochrome pathway (Fig. 3). Thus, in the stat-phase the electrons from NDH2e are probably fed to both the cytochromes and the AOX instead of being channeled to the cytochrome bc_1 complex. At high $\Delta\Psi$, complex III has been reported to be an important source of reactive oxygen species (ROS) [48]; therefore, the activation of the alternative pathway would be a most desirable mechanism to decrease the rate of ROS production. To test this hypothesis, the rate of hydrogen peroxide formation was measured in mitochondria isolated from cells either in the log- or the stat-growth phase using NADH or pyruvate–malate as substrates (Fig. 6). In the presence of NADH, mitochondria from log-grown cells exhibited a large rate of ROS production, while those from cells in the stat-phase decreased ROS production, as expected from the activation of the NDH2e–AOX pathway. In contrast it was observed that the pyruvate–malate-supported rate of H_2O_2 production was lower and not modified by the growth phase (Fig. 6). In addition, rotenone blocked electron transfer at the level of complex I, promoting an increase in ROS production from this complex (Fig. 6) as expected from data in the literature [49].

4. Discussion

Depending on the growth phase and metabolic requirements, yeast cells undergo large variations in energy needs [27]. In contrast to multiplying cells, quiescent cells need less ATP, and in this situation a fully coupled, slow respiratory chain would overproduce ROS [50]. In order to increase the rate of oxygen uptake in the stat-phase, the respiratory chain must be partially uncoupled from ATP synthesis. Indeed, uncoupling devices such as the mitochondrial permeability transition and the action of uncoupling proteins have been described [51,52]. Here, the possible existence of a third uncoupling mechanism was explored, namely the activation of an alternate electron transfer pathway in which NADH is oxidized by an alternative dehydrogenase and oxygen is reduced by an alternative oxidase. This alternate route does not pump protons, and therefore does not contribute to $\Delta\Psi$ build-up. In mitochondria from *Arabidopsis thaliana*, the activation of the alternative pathway seems to depend on the pyruvate-mediated stimulation of AOX [19]. Pyruvate or other ketoacids activate AOX at a cysteine residue (C127) located just upstream of the membrane-embedded region [53]. This residue is not present in the *Y. lipolytica* AOX and thus ketoacids do not activate this enzyme. Lack of ketoacid-activation is also observed in the AOX from *Acanthamoeba castellanii* [54].

The energy requirements in a cell should vary widely from the early log-phase, where anabolism is very active and supports rapid rates of cell division and growth, to the stat-phase, a low-energy mode when cells do not grow or reproduce [27]. In quiescent cells fully coupled mitochondria would maintain a high transmembrane potential and low rate of oxygen consumption, overproducing ROS [55]. In these conditions, an increase in the NADH/NAD^+ ratio would down-regulate catabolic pathways both in the cytoplasm and within the mitochondrial matrix. Thus, in the stat-phase the combined activities of the alternative components or the respiratory chain would be most advantageous, as an uncoupled electron flux would be rapid and independent of $\Delta\Psi$, decreasing the rate of ROS production and reestablishing the balance in the NADH/NAD^+ couple needed for an active metabolism.

In the log-phase NADH-derived electrons are channeled to the cytochromic pathway and not to the non-productive AOX. This was demonstrated by the complete inhibition of oxygen consumption mediated by cyanide and by the presence of a high respiratory control. Electron channeling to cytochromes is probably due to the physical interaction of NDH2e with complex IV [26]. By contrast, in the low energy-requiring stationary growth phase, NADH was allowed to reach the alternative electron pathway, as indicated by the partial resistance to cyanide and by the loss of respiratory control. Activation of the alternative pathway was probably due to the combination of the increased expression of NDH2e and the down-regulation of complex IV, which led to the accumulation of high levels

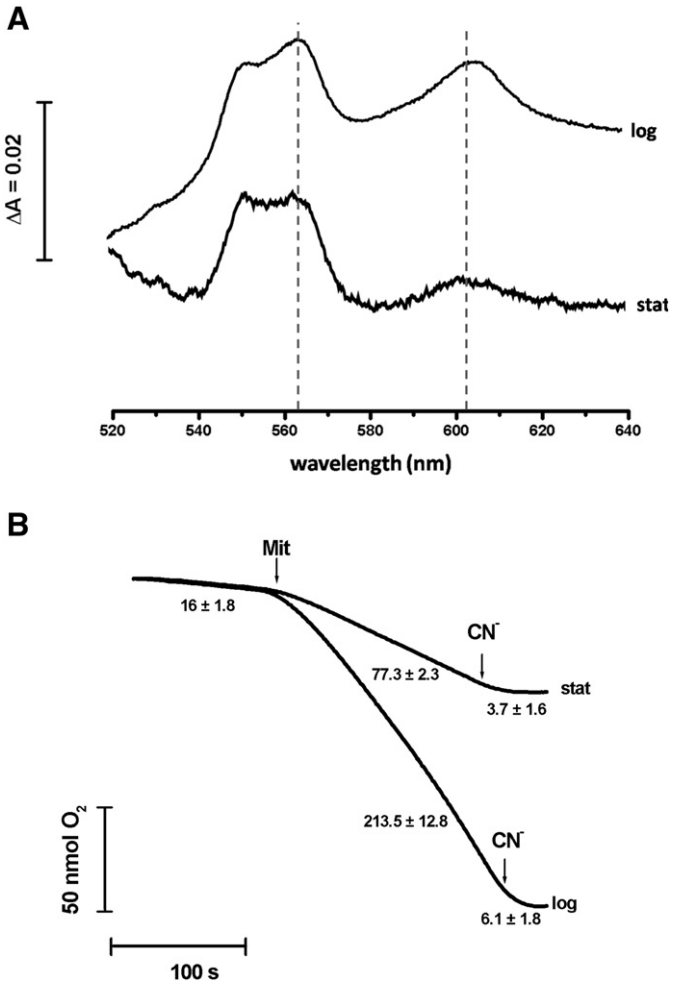

Fig. 5. Differential spectra and cytochrome *c* oxidase activity. (A) Dithionite-reduced minus ferricyanide-oxidized absorbance spectra of mitochondria from cells grown to the logarithmic or to the stationary growth phase. 2 mg/mL mitochondria were added to the reaction mixture described in Fig. 1 and spectra were recorded in an Aminco/Olis DW2000 spectrophotometer. Wavelength limits were 500 and 680 nm. The baseline was recorded after ferrycyanide addition to the reference cuvette. Then, two or three grains of dithionite were added to the sample cuvette and the reduced differential spectrum was recorded. Dashed lines indicate the cytochrome *b* and cytochromes $a+a_3$ peaks. Representative spectra are shown (n = 5). (B) cytochrome c oxidase activity was measured by cyanide-sensitive oxygen consumption in the presence of 5 mM ascorbate, 1 μM, TMPD (Tethrametyl-phenylene-diamine) and 10 μM antimycin A in the same reaction mixture as for Fig. 1.

of free NDH2e. Once released, NDH2e may reduce a non-localized ubiquinone pool which in turn, could be oxidized by AOX.

In bacteria, the contribution of different terminal oxidases to respiration depends heavily on the carbon/energy source [56,57]. By contrast, in mitochondria different respiratory pathways may be switched on and off through dynamic interactions between respiratory enzymes [25]. Through this mechanism, proton pumping would be adjusted to best fit the energy-needs of the cell. In the log-phase, the ability of NDH2e to replenish the cytoplasmic NAD^+ pool would be dependent on the utilization of ATP. However, it may be speculated that in the stat-phase a non-attached NDH2e is needed to oxidize cytoplasmic NADH regardless of a constantly high proton-motive force or the lack of ATP. In other organisms there is ample evidence indicating that AOX is activated in the stat-phase, releasing respiration from ATP production and preventing ROS overproduction [58,59].

Different supercomplexes were detected in mitochondria from *Podospora anserina* at different life stages, allowing to switch on and off selective respiratory pathways that involved either AOX or complexes III/IV [25]. In *Y. lipolytica* grown to the log-phase, NDH2e is bound to super-complex III/IV. In contrast, in the stationary phase overexpressed NDH2e would saturate the binding sites in complex IV, which is present in lower concentrations. The free fraction of NDH2e would not channel electrons to the cytochrome pathway,

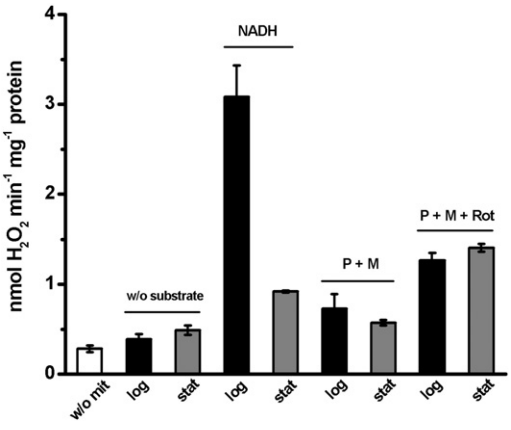

Fig. 6. Reactive oxygen species produced in isolated mitochondria. The production of hydrogen peroxide was measured following resorufin fluorescence in a multiwell microplate reader (Biotek) and the fluorescence increase slope is reported. Reaction mixture: 0.6 M mannitol, 5 mM MES, 20 mM KCl, 0.5 mM $MgCl_2$, 4 mM Pi, 10 μM Amplex Red, 0.1 units/mL horseradish peroxidase, 100 units/mL superoxide dismutase in the presence of 10 mM pyruvate and 10 mM malate or 0.25 mM NADH. Where indicated rotenone was 25 μM. Mean fluorescence ± SD (n = 5).

but instead, reach a non-localized ubiquinone-pool, thus activating the AOX pathway. This alternate electron pathway results in uncoupling of oxidative phosphorylation preventing the overproduction of ROS.

Acknowledgements

Partially funded by grants CONACYT 79989 and DGAPA UNAM IN217109 to SUC and grants CONACYT 128110 and DGAPA UNAM IN203311-3 to DGH. Drs. Gabriel del Río and José Pedraza-Chaverri allowed us to use their spectrometers. The authors thank Ramón Méndez and Natalia Chiquete-Félix for technical assistance. SGC and ACO are CONACYT fellows enrolled in the Biochemistry PhD program at UNAM.

References

[1] T. Joseph-Horne, D.W. Hollomon, P.M. Wood, Fungal respiration: a fusion of standard and alternative components, Biochim. Biophys. Acta 1504 (2001) 179–195.
[2] D. Saisho, E. Nambara, S. Naito, N. Tsutsumi, A. Hirai, M. Nakazono, Characterization of the gene family for alternative oxidase from *Arabidopsis thaliana*, Plant Mol. Biol. 35 (1997) 585–596.
[3] M. Chaudhuri, G.C. Hill, Cloning, sequencing, and functional activity of the *Trypanosoma brucei brucei* alternative oxidase, Mol. Biochem. Parasitol. 83 (1996) 125–129.
[4] S. Kerscher, S. Drose, K. Zwicker, V. Zickermann, U. Brandt, *Yarrowia lipolytica*, a yeast genetic system to study mitochondrial complex I, Biochim. Biophys. Acta 1555 (2002) 83–91.
[5] S.J. Kerscher, Diversity and origin of alternative NADH:ubiquinone oxidoreductases, Biochim. Biophys. Acta 1459 (2000) 274–283.
[6] T. Joseph-Horne, J. Babij, P.M. Wood, D. Hollomon, R.B. Sessions, New sequence data enable modelling of the fungal alternative oxidase and explain an absence of regulation by pyruvate, FEBS Lett. 481 (2000) 141–146.
[7] G. Milani, W. Jarmuszkiewicz, C.M. Sluse-Goffart, A.Z. Schreiber, A.E. Vercesi, F.E. Sluse, Respiratory chain network in mitochondria of *Candida parapsilosis*: ADP/O appraisal of the multiple electron pathways, FEBS Lett. 508 (2001) 231–235.
[8] S. de Vries, C.A. Marres, The mitochondrial respiratory chain of yeast. Structure and biosynthesis and the role in cellular metabolism, Biochim. Biophys. Acta 895 (1987) 205–239.
[9] R. Schmid, D.L. Gerloff, Functional properties of the alternative NADH:ubiquinone oxidoreductase from *E. coli* through comparative 3-D modelling, FEBS Lett. 578 (2004) 163–168.
[10] V. Yankovskaya, R. Horsefield, S. Tornroth, C. Luna-Chavez, H. Miyoshi, C. Leger, B. Byrne, G. Cecchini, S. Iwata, Architecture of succinate dehydrogenase and reactive oxygen species generation, Science 299 (2003) 700–704.
[11] A.M. Melo, T.M. Bandeiras, M. Teixeira, New insights into type II NAD(P)H: quinone oxidoreductases, Microbiol. Mol. Biol. Rev. 68 (2004) 603–616.
[12] A.L. Moore, J.N. Siedow, The regulation and nature of the cyanide-resistant alternative oxidase of plant mitochondria, Biochim. Biophys. Acta 1059 (1991) 121–140.
[13] S. Guerrero-Castillo, D. Araiza-Olivera, A. Cabrera-Orefice, J. Espinasa-Jaramillo, M. Gutierrez-Aguilar, L.A. Luevano-Martinez, A. Zepeda-Bastida, S. Uribe-Carvajal, Physiological uncoupling of mitochondrial oxidative phosphorylation. Studies in different yeast species, J. Bioenerg. Biomembr. 43 (2011) 323–331.
[14] B. Kadenbach, Intrinsic and extrinsic uncoupling of oxidative phosphorylation, Biochim. Biophys. Acta 1604 (2003) 77–94.
[15] D.A. Berthold, M.E. Andersson, P. Nordlund, New insight into the structure and function of the alternative oxidase, Biochim. Biophys. Acta 1460 (2000) 241–254.
[16] J.N. Siedow, A.L. Umbach, The mitochondrial cyanide-resistant oxidase: structural conservation amid regulatory diversity, Biochim. Biophys. Acta 1459 (2000) 432–439.
[17] M.S. Albury, C. Affourtit, P.G. Crichton, A.L. Moore, Structure of the plant alternative oxidase. Site-directed mutagenesis provides new information on the active site and membrane topology, J. Biol. Chem. 277 (2002) 1190–1194.
[18] A.H. Millar, J.T. Wiskich, J. Whelan, D.A. Day, Organic acid activation of the alternative oxidase of plant mitochondria, FEBS Lett. 329 (1993) 259–262.
[19] M.H. Hoefnagel, A.H. Millar, J.T. Wiskich, D.A. Day, Cytochrome and alternative respiratory pathways compete for electrons in the presence of pyruvate in soybean mitochondria, Arch. Biochem. Biophys. 318 (1995) 394–400.
[20] E. Perales-Clemente, M.P. Bayona-Bafaluy, A. Perez-Martos, A. Barrientos, P. Fernandez-Silva, J.A. Enriquez, Restoration of electron transport without proton pumping in mammalian mitochondria, Proc. Natl. Acad. Sci. U. S. A. 105 (2008) 18735–18739.
[21] M.F. Maas, C.H. Sellem, F. Krause, N.A. Dencher, A. Sainsard-Chanet, Molecular gene therapy: overexpression of the alternative NADH dehydrogenase NDI1 restores overall physiology in a fungal model of respiratory complex I deficiency, J. Mol. Biol. 399 (2010) 31–40.
[22] S.J. Kerscher, A. Eschemann, P.M. Okun, U. Brandt, External alternative NADH: ubiquinone oxidoreductase redirected to the internal face of the mitochondrial inner membrane rescues complex I deficiency in *Yarrowia lipolytica*, J. Cell Sci. 114 (2001) 3915–3921.
[23] A.L. Umbach, F. Fiorani, J.N. Siedow, Characterization of transformed *Arabidopsis* with altered alternative oxidase levels and analysis of effects on reactive oxygen species in tissue, Plant Physiol. 139 (2005) 1806–1820.
[24] A.G. Medentsev, V.K. Akimenko, Development and activation of cyanide-resistant respiration in the yeast *Yarrowia lipolytica*, Biochemistry (Mosc.) 64 (1999) 945–951.
[25] F. Krause, C.Q. Scheckhuber, A. Werner, S. Rexroth, N.H. Reifschneider, N.A. Dencher, H.D. Osiewacz, OXPHOS supercomplexes: respiration and life-span control in the aging model *Podospora anserina*, Ann. N. Y. Acad. Sci. 1067 (2006) 106–115.
[26] S. Guerrero-Castillo, M. Vazquez-Acevedo, D. Gonzalez-Halphen, S. Uribe-Carvajal, In *Yarrowia lipolytica* mitochondria, the alternative NADH dehydrogenase interacts specifically with the cytochrome complexes of the classic respiratory pathway, Biochim. Biophys. Acta 1787 (2009) 75–85.
[27] M. Werner-Washburne, E. Braun, G.C. Johnston, R.A. Singer, Stationary phase in the yeast *Saccharomyces cerevisiae*, Microbiol. Rev. 57 (1993) 383–401.
[28] H.I. Boshoff, C.E. Barry III, Tuberculosis — metabolism and respiration in the absence of growth, Nat. Rev. Microbiol. 3 (2005) 70–80.
[29] T. Zakrajsek, P. Raspor, P. Jamnik, *Saccharomyces cerevisiae* in the stationary phase as a model organism — characterization at cellular and proteome level, J. Proteomics 74 (2011) 2837–2845.
[30] A. Garofano, A. Eschemann, U. Brandt, S. Kerscher, Substrate-inducible versions of internal alternative NADH:ubiquinone oxidoreductase from *Yarrowia lipolytica*, Yeast 23 (2006) 1129–1136.
[31] F.M. Perez-Campo, A. Dominguez, Factors affecting the morphogenetic switch in *Yarrowia lipolytica*, Curr. Microbiol. 43 (2001) 429–433.
[32] A. Pena, M.Z. Pina, E. Escamilla, E. Pina, A novel method for the rapid preparation of coupled yeast mitochondria, FEBS Lett. 80 (1977) 209–213.
[33] A.G. Gornall, C.J. Bardawill, M.M. David, Determination of serum proteins by means of the biuret reaction, J. Biol. Chem. 177 (1949) 751–766.
[34] V. Perez-Vazquez, A. Saavedra-Molina, S. Uribe, In *Saccharomyces cerevisiae*, cations control the fate of the energy derived from oxidative metabolism through the opening and closing of the yeast mitochondrial unselective channel, J. Bioenerg. Biomembr. 35 (2003) 231–241.
[35] R.W. Estabrook, Mitochondrial respiratory control and the polarographic measurement of ADP:O ratios, Methods Enzymol. 10 (1967) 41–47.
[36] U. Fendel, M.A. Tocilescu, S. Kerscher, U. Brandt, Exploring the inhibitor binding pocket of respiratory complex I, Biochim. Biophys. Acta 1777 (2008) 660–665.
[37] H. Schagger, Blue-native gels to isolate protein complexes from mitochondria, Methods Cell Biol. 65 (2001) 231–244.
[38] A. Abdrakhmanova, V. Zickermann, M. Bostina, M. Radermacher, H. Schagger, S. Kerscher, U. Brandt, Subunit composition of mitochondrial complex I from the yeast *Yarrowia lipolytica*, Biochim. Biophys. Acta 1658 (2004) 148–156.
[39] I. Wittig, M. Karas, H. Schagger, High resolution clear native electrophoresis for in-gel functional assays and fluorescence studies of membrane protein complexes, Mol. Cell. Proteomics 6 (2007) 1215–1225.
[40] E. Zerbetto, L. Vergani, F. Dabbeni-Sala, Quantification of muscle mitochondrial oxidative phosphorylation enzymes via histochemical staining of blue native polyacrylamide gels, Electrophoresis 18 (1997) 2059–2064.
[41] I. Wittig, H. Schagger, Electrophoretic methods to isolate protein complexes from mitochondria, Methods Cell Biol. 80 (2007) 723–741.
[42] M. Vazquez-Acevedo, P. Cardol, A. Cano-Estrada, M. Lapaille, C. Remacle, D. Gonzalez-Halphen, The mitochondrial ATP synthase of chlorophycean algae contains eight subunits of unknown origin involved in the formation of an atypical stator-stalk and in the dimerization of the complex, J. Bioenerg. Biomembr. 38 (2006) 271–282.
[43] J.A. Berden, E.C. Slater, The reaction of antimycin with a cytochrome b preparation active in reconstitution of the respiratory chain, Biochim. Biophys. Acta 216 (1970) 237–249.
[44] T. Yonetani, Studies on cytochrome oxidase. I. Absolute and difference absorption spectra, J. Biol. Chem. 235 (1960) 845–852.
[45] M. Zhou, Z. Diwu, N. Panchuk-Voloshina, R.P. Haugland, A stable nonfluorescent derivative of resorufin for the fluorometric determination of trace hydrogen peroxide: applications in detecting the activity of phagocyte NADPH oxidase and other oxidases, Anal. Biochem. 253 (1997) 162–168.
[46] S. Drose, U. Brandt, P.J. Hanley, K+-independent actions of diazoxide question the role of inner membrane KATP channels in mitochondrial cytoprotective signaling, J. Biol. Chem. 281 (2006) 23733–23739.
[47] H. Schagger, K. Pfeiffer, The ratio of oxidative phosphorylation complexes I–V in bovine heart mitochondria and the composition of respiratory chain supercomplexes, J. Biol. Chem. 276 (2001) 37861–37867.
[48] H. Rottenberg, R. Covian, B.L. Trumpower, Membrane potential greatly enhances superoxide generation by the cytochrome bc1 complex reconstituted into phospholipid vesicles, J. Biol. Chem. 284 (2009) 19203–19210.
[49] A. Galkin, U. Brandt, Superoxide radical formation by pure complex I (NADH: ubiquinone oxidoreductase) from *Yarrowia lipolytica*, J. Biol. Chem. 280 (2005) 30129–30135.
[50] V. Koshkin, X. Wang, P.E. Scherer, C.B. Chan, M.B. Wheeler, Mitochondrial functional state in clonal pancreatic beta-cells exposed to free fatty acids, J. Biol. Chem. 278 (2003) 19709–19715.
[51] V.G. Tudella, C. Curti, F.M. Soriani, A.C. Santos, S.A. Uyemura, In situ evidence of an alternative oxidase and an uncoupling protein in the respiratory chain of *Aspergillus fumigatus*, Int. J. Biochem. Cell Biol. 36 (2004) 162–172.
[52] Y. Zhu, J. Lu, J. Wang, F. Chen, F. Leng, H. Li, Regulation of thermogenesis in plants: the interaction of alternative oxidase and plant uncoupling mitochondrial protein, J. Integr. Plant Biol. 53 (2010) 7–13.

[53] I. Djajanegara, R. Holtzapffel, P.M. Finnegan, M.H. Hoefnagel, D.A. Berthold, J.T. Wiskich, D.A. Day, A single amino acid change in the plant alternative oxidase alters the specificity of organic acid activation, FEBS Lett. 454 (1999) 220–224.
[54] W. Jarmuszkiewicz, A.M. Wagner, M.J. Wagner, L. Hryniewiecka, Immunological identification of the alternative oxidase of *Acanthamoeba castellanii* mitochondria, FEBS Lett. 411 (1997) 110–114.
[55] M.H. Barros, B. Bandy, E.B. Tahara, A.J. Kowaltowski, Higher respiratory activity decreases mitochondrial reactive oxygen release and increases life span in *Saccharomyces cerevisiae*, J. Biol. Chem. 279 (2004) 49883–49888.
[56] J.A. Megehee, M.D. Lundrigan, Temporal expression of *Mycobacterium smegmatis* respiratory terminal oxidases, Can. J. Microbiol. 53 (2007) 459–463.
[57] G. Morales, A. Ugidos, F. Rojo, Inactivation of the *Pseudomonas putida* cytochrome o ubiquinol oxidase leads to a significant change in the transcriptome and to increased expression of the CIO and cbb3-1 terminal oxidases, Environ. Microbiol. 8 (2006) 1764–1774.
[58] A.L. Umbach, J.N. Siedow, The cyanide-resistant alternative oxidases from the fungi *Pichia stipitis* and *Neurospora crassa* are monomeric and lack regulatory features of the plant enzyme, Arch. Biochem. Biophys. 378 (2000) 234–245.
[59] A.G. Medentsev, A.Y. Arinbasarova, N.P. Golovchenko, V.K. Akimenko, Involvement of the alternative oxidase in respiration of *Yarrowia lipolytica* mitochondria is controlled by the activity of the cytochrome pathway, FEMS Yeast Res. 2 (2002) 519–524.

Biochimica et Biophysica Acta 1837 (2014) 73–84

Contents lists available at ScienceDirect

Biochimica et Biophysica Acta

journal homepage: www.elsevier.com/locate/bbabio

The branched mitochondrial respiratory chain from *Debaryomyces hansenii*: Components and supramolecular organization

Alfredo Cabrera-Orefice, Natalia Chiquete-Félix, Juan Espinasa-Jaramillo, Mónica Rosas-Lemus, Sergio Guerrero-Castillo, Antonio Peña, Salvador Uribe-Carvajal *

Dept. of Molecular Genetics, Instituto de Fisiología Celular, Universidad Nacional Autónoma de México, Mexico City, Mexico

ARTICLE INFO

Article history:
Received 12 June 2013
Received in revised form 23 July 2013
Accepted 25 July 2013
Available online 7 August 2013

Keywords:
Respiratory chain
Debaryomyces hansenii
Alternative oxidase
Alternative NADH dehydrogenase
Glycerol-phosphate dehydrogenase
Supercomplexes

ABSTRACT

The branched respiratory chain in mitochondria from the halotolerant yeast *Debaryomyces hansenii* contains the classical complexes I, II, III and IV plus a cyanide-insensitive, AMP-activated, alternative-oxidase (AOX). Two additional alternative oxidoreductases were found in this organism: an alternative NADH dehydrogenase (NDH2e) and a mitochondrial isoform of glycerol-phosphate dehydrogenase ($_{Mit}$GPDH). These monomeric enzymes lack proton pump activity. They are located on the outer face of the inner mitochondrial membrane. NDH2e oxidizes exogenous NADH in a rotenone-insensitive, flavone-sensitive, process. AOX seems to be constitutive; nonetheless, most electrons are transferred to the cytochromic pathway. Respiratory supercomplexes containing complexes I, III and IV in different stoichiometries were detected. Dimeric complex V was also detected. In-gel activity of NADH dehydrogenase, mass spectrometry, and cytochrome *c* oxidase and ATPase activities led to determine the composition of the putative supercomplexes. Molecular weights were estimated by comparison with those from the yeast *Y. lipolytica* and they were IV_2, I–IV, III_2–IV_4, V_2, I–III_2, I–III_2–IV, I–III_2–IV_2, I–III_2–IV_3 and I–III_2–IV_4. Binding of the alternative enzymes to supercomplexes was not detected. This is the first report on the structure and organization of the mitochondrial respiratory chain from *D. hansenii*.

1. Introduction

The halotolerant, non-pathogenic, oleaginous yeast *Debaryomyces hansenii* is found in the sea and other hyperosmotic habitats [1,2]. *D. hansenii* grows in various environmental conditions including different salt concentrations [3–5], low temperatures [3] and different pHs [3,6]. In addition, *D. hansenii* assimilates many different carbon sources [7–9]. The ability of this yeast to synthesize and store lipids is used in biotechnology to make products of commercial interest, such as cheese [2,10].

D. hansenii has high aerobic metabolism and low fermentative activity which are enhanced by high extracellular NaCl or KCl [11–13]. Isolated *D. hansenii* mitochondria undergo permeability transition due to the opening of a mitochondrial unspecific channel (MUC) [14]. Both, the MUCs from *D. hansenii* ($_{Dh}$MUC) and *S. cerevisiae* ($_{Sc}$MUC) are regulated by effectors such as phosphate, Mg^{2+} or Ca^{2+} [14–19]. The $_{Dh}$MUC is the only MUC reported to date that is closed by Na^{+} or K^{+} [14] probably accounting for the monovalent cation coupling effects observed in whole yeast [12,13].

The mammalian oxidative phosphorylation system contains the four "orthodox" respiratory complexes (I, II, III and IV) plus the F_1F_O-ATP synthase (complex V) [20]. In addition to the above, mitochondria from plants, fungi, protozoa and some animals may contain "alternative" redox enzymes that substitute or coexist with the classical complexes; e.g. alternative NADH dehydrogenases and oxidases [21–25]. In fungi a mammalian-like respiratory complex may be substituted by an alternative enzyme, e.g. in *S. cerevisiae* complex I the oxidoreductase activity was substituted by an internal alternative NADH dehydrogenase [26,27].

The fungal alternative oxidases (AOXs) are single subunit proteins bound to the matrix side of the inner mitochondrial membrane (IMM) [28–31]. The cyanide-resistant AOX transfers electrons from ubiquinol to oxygen. AOX is inhibited by hydroxamic acids and by *n*-alkyl-gallates [29,32]. The presence of AOX constitutes an uncoupled branch of the respiratory chain probably designed to prevent substrate overload and overproduction of reactive oxygen species (ROS) [25,28,33–36].

Alternative type II NADH dehydrogenases (NDH2s) transfer electrons from NADH to ubiquinone without pumping protons [37]. NDH2s are monomeric proteins bound to the inner (NDH2i) or the outer (NDH2e) face of IMM [21,37]. NDH2s are not sensitive to rotenone, but instead are specifically inhibited by flavone [38].

Abbreviations: ADP, adenosine diphosphate; AMP, adenosine monophosphate; AOX, alternative oxidase; BN, blue-native; COX, cytochrome *c* oxidase; CRR, cyanide-resistant respiration; Dig, digitonin; IMM, inner mitochondrial membrane; LC-MS, liquid chromatography mass spectrometry; LM, laurylmaltoside; $_{Mit}$GPDH, glycerol-phosphate dehydrogenase (mitochondrial isoform); MUC, mitochondrial unspecific channel; MW, molecular weight; NDH, NADH dehydrogenase activity; NDH2e, alternative external NADH dehydrogenase; PAGE, polyacrylamide-gel electrophoresis; PG, propyl-gallate; ROS, reactive oxygen species; SDS, sodium dodecyl sulfate; 2D, second dimension

* Corresponding author at: Departamento de Genética Molecular, Instituto de Fisiología Celular, Universidad Nacional Autónoma de México, Ciudad Universitaria, Apdo. Postal 70–242, Mexico City, Mexico. Tel.: +52 55 5622 5632; fax: +52 55 5622 5630.
E-mail address: suribe@ifc.unam.mx (S. Uribe-Carvajal).

0005-2728/$ – see front matter © 2013 Elsevier B.V. All rights reserved.
http://dx.doi.org/10.1016/j.bbabio.2013.07.011

The mitochondrial isoform of glycerol-phosphate dehydrogenase ($_{Mit}$GPDH) is another component of branched respiratory chains [39,40]. $_{Mit}$GPDH oxidizes glycerol-phosphate to dihydroxyacetone-phosphate and reduces ubiquinone. Also, this protein is located on the outer face of the IMM [41]. The peripheral proteins NDH2s, $_{Mit}$GPDH and AOX are not proton pumps [21,29,40].

Two major models describe the structure/function relationship of the respiratory chain. The *fluid* or *random collision* model proposes that respiratory complexes float freely within the IMM and electron transport occurs through the diffusible carriers ubiquinone and cytochrome *c* [42]. On the other hand, the *solid* model proposes that respiratory complexes are organized into stable hetero-oligomers (supercomplexes or "respirasomes") that channel electrons between them [43–46]. There are data that support each model [47]. Kinetic studies show that each respiratory complex can be purified individually, retaining activity [42]. By contrast, blue native gel polyacrylamide electrophoresis (BN-PAGE) reveals the existence of supercomplexes composed of several respiratory complexes [48]. Respiratory supercomplexes can be observed when solubilizing mitochondrial membranes with small amounts of mild detergents such as digitonin [44]. The presence of respiratory supercomplexes has been well documented in mammals [48,49], plants [43,46,50] and different yeast species [51–54]. Additionally, a third model has been proposed: the *plasticity* model, where respiratory complexes undergo a dynamic association-dissociation process and isolated supercomplexes transfer electrons from NADH to oxygen [55]. The plasticity model suggests that complex association/dissociation regulates oxidative phosphorylation [55,56].

Here, the mitochondrial respiratory chain of *D. hansenii*, which has been reported to contain all four mammalian-like respiratory complexes [57] plus a putative stationary-phase-inducible AOX, was characterized [58,59]. This branched respiratory chain contains all the complexes reported [59] plus an external NDH2 and a glycerol-phosphate dehydrogenase. In addition, association of these complexes in different supercomplexes was observed.

2. Materials and methods

2.1. Chemicals

All chemicals were reagent grade. D-sorbitol, D-mannitol, D-glucose, D-galactose, glycerol, Trizma® base (Tris), malic acid, pyruvic acid, citric acid, maleic acid, DL-α-glycerophosphate, NADH, ATP, ADP, rotenone, flavone, antimycin A, propyl-gallate, digitonin, *n*-dodecyl β-D-maltoside (laurylmaltoside), Nitrotetrazolium blue chloride and antifoam A were from Sigma Chem Co. (St Louis, MO). Bovine serum albumin (Probulmin^{TM}) was from Millipore. Yeast extract and bacto-peptone were from BD Bioxon. DL-lactic acid, H_3PO_4, NaCN, KCl, $MgCl_2$ and ethanol were from J.T. Baker. 3,3′-Diaminobenzidine tetrahydrochloride hydrate was from Fluka. Coomassie Blue G was from SERVA (Heidelberg, Germany). Coomassie® brilliant blue G-250 and electrophoresis reagents were from BIO-RAD (Richmond, CA).

2.2. Biologicals

D. hansenii Y7426 strain (US Dept. of Agriculture) was used throughout this work. The strain was maintained in YPGal-NaCl (1% yeast extract, 2% bacto-peptone, 2% D-galactose, 1 M NaCl and 2% bacto-agar) plate cultures. *Yarrowia lipolytica* E150 strain was also used. This strain was maintained in YD (1% yeast extract and 2% D-glucose and 2% bacto-agar) plate cultures.

2.3. Yeast culture and isolation of coupled mitochondria

D. hansenii cells were grown as follows: pre-cultures were prepared inoculating 100 mL of YPLac-NaCl medium (1% yeast extract, 2% bacto-peptone, 2% lactic acid, pH 5.5 adjusted with NaOH and adding NaCl to reach 0.6 M Na^+) containing antifoam A emulsion 50 μL/L. Pre-cultures were grown for 36 h under continuous agitation in an orbital shaker at 250 rpm at 29 °C. Then, each pre-culture was used to inoculate a 750 mL flask with the same medium. Incubation was continued for 24 h (i.e. medium to late logarithmic phase). *D. hansenii* mitochondria were isolated as reported previously [14]. Mitochondria from *Y. lipolytica* were isolated as in [51].

2.4. Protein quantification

Mitochondrial protein was measured by the Biuret method [60]. Absorbance was determined at 540 nm in a Beckman DU-50 spectrophotometer. Bovine serum albumin was used as a standard.

2.5. Oxygen consumption

The rate of oxygen consumption was measured in a YSI-5300 Oxygraph equipped with a Clark-Type electrode (Yellow Springs Instruments Inc., OH) interfaced to a chart recorder. The sample was placed in a water-jacketed chamber at 30 °C. The phosphorylating state (III) was induced with 0.5 mM ADP. The reaction mixture was 1 M sorbitol, 10 mM maleate (pH was adjusted to 6.8 with Tris), 10 mM Tris-phosphate (Pi), 0.5 mM $MgCl_2$ and 75 mM KCl. Mitochondrial protein (Prot) was 0.5 mg/mL; final volume was 1.5 mL. The concentrations of different respiratory substrates and inhibitors are indicated in the legends to the figures.

2.6. Blue native (BN) and 2D SDS-Tricine electrophoresis

BN-PAGE was performed as described in the literature [49]. The mitochondrial pellet was suspended in sample buffer (750 mM aminocaproic acid, 25 mM imidazole (pH 7.0)) and solubilized with 2.0 mg *n*-dodecyl-β-D-maltoside (laurylmaltoside, LM)/mg Prot, or 4.0 mg digitonin (Dig)/mg Prot at 4 °C for 1 h and centrifuged at 33,000 rpm at 4 °C for 25 min. The supernatants were loaded on 4–12% (w/v) polyacrylamide gradient gels. Protein, 0.25 or 0.5 mg per lane was added to 8.5 × 6 cm or 17 × 12 cm gel sizes, respectively. The stacking gel contained 4% (w/v) polyacrylamide. Also, 0.025% digitonin was added to the gel preparation to improve protein band definition [61]. For 2D SDS-Tricine-PAGE, complete lanes from the BN-gels were loaded on 12% polyacrylamide gels to resolve the subunits that constitute each complex. 2D-gels were subjected to Coomassie-staining [61] and silver-staining [62,63]. Apparent molecular weights were estimated using Benchmark Protein (Invitrogen, CA) and Precision Plus Protein^{TM} (BIO-RAD, Richmond, CA) standards.

2.7. In-gel enzymatic activities

In-gel NADH/nitrotetrazolium blue chloride (NTB) oxidoreductase activity was determined incubating native gels in a mixture of 10 mM Tris (pH 7.0), 0.5 mg NTB/mL and 1 mM NADH [64]. Inhibitors such as rotenone and flavone were not able to act on their target enzymes in the gel assays, probably due to dilution into the BN-gel incubation medium, their hydrophobicity or their specific inhibition sites on the protein i.e. the indicator (NTB) seems to receive electrons from flavin prosthetic groups [65], far from the inhibitor blocking sites (near the ubiquinone site) [66,67] (result not shown). In-gel cytochrome *c* oxidase (COX) activity was determined using diaminobenzidine and cytochrome *c* [68]. Cyanide was useful to inhibit COX (Result not shown), but cannot use to unveil the alternative oxidase because there is no method available to measure AOX in-gel activity. In-gel ATPase activity was measured as in [61]. Oligomycin was not able to inhibit this activity (Result not shown) as previously reported in [68].

Table 1
Rates of oxygen consumption in isolated mitochondria from *D. hansenii* in the presence of different respiratory substrates and inhibitors.

Substrate and other additions	Rate of oxygen consumption (natgO · (min · mg Prot)$^{-1}$)	Respiratory control (III/IV)
Pyruvate (10 mM) + malate (10 mM)	123 ± 10*	2.36 ± 0.07
+ADP (500 μM)	290 ± 7**	
+Rotenone (50 μM)	8 ± 1	
+Flavone (500 μM)	114 ± 5	
+Antimycin-A (5 μM)	32 ± 3	
+NaCN (500 μM)	33 ± 2	
+Propyl-gallate (100 μM)	108 ± 6	
Citrate (10 mM) + malate (10 mM)	138 ± 10*	2.17 ± 0.05
+ADP (500 μM)	299 ± 12**	
+Rotenone (50 μM)	11 ± 2	
+Flavone (500 μM)	135 ± 5	
+Antimycin-A (5 μM)	41 ± 3	
+NaCN (500 μM)	39 ± 2	
+Propyl-gallate (100 μM)	128 ± 6	
Succinate (10 mM)	143 ± 11*	1.64 ± 0.08
+ADP (500 μM)	235 ± 14**	
+Rotenone (50 μM)	144 ± 9	
+Flavone (500 μM)	143 ± 11	
+Antimycin-A (5 μM)	38 ± 3	
+NaCN (500 μM)	39 ± 5	
+Propyl-gallate (100 μM)	117 ± 4	
NADH (1 mM)	258 ± 9*	1.23 ± 0.05
+ADP (500 μM)	317 ± 12**	
+Rotenone (50 μM)	243 ± 10	
+Flavone (500 μM)	28 ± 14	
+Antimycin-A (5 μM)	65 ± 3	
+NaCN (500 μM)	65 ± 4	
+Propyl-gallate (100 μM)	204 ± 4	
Glycerol-phosphate (10 mM)	216 ± 10*	1.28 ± 0.03
+ADP (500 μM)	276 ± 11**	
+Rotenone (50 μM)	216 ± 10	
+Flavone (500 μM)	216 ± 10	
+Antimycin-A (5 μM)	39 ± 3	
+NaCN (500 μM)	37 ± 3	
+Propyl-gallate (100 μM)	188 ± 7	

The rates of oxygen consumption were measured in resting state (IV)* and phosphorylating state (III)**. The phosphorylating state was induced with ADP. Rates of oxygen consumption in the presence of inhibitors were measured after a steady state was reached. Reaction mixture: 1 M sorbitol, 75 mM KCl, 10 mM Tris-phosphate, 1 mM $MgCl_2$ and 10 mM maleic acid, pH 6.8 (Tris). Mitochondria 0.5 mg Prot · (mL)$^{-1}$ were added in each assay. Temperature 30 °C. Final volume 1.5 mL. Data from five independent experiments are expressed as the mean ± SD.

2.8. Protein search, alignment and sequence analysis

We used the BLAST website and the NCBI database to search and compare protein sequences from alternative respiratory enzymes. We used the known protein sequences from other yeasts [69–71] to search for possible NDH2s, AOXs and/or $_{Mit}$GPDHs in the *D. hansenii* NCBI database. The identified *D. hansenii* sequences were aligned against those from *S. cerevisiae*, *Y. lipolytica* and/or *C. albicans* using Clustal W 2.0 [72]. The BLAST analysis also indicated the percentages of identity and similarity between amino acid sequences.

2.9. Western blotting

Mitochondrial samples were diluted in 0.5 mL sample buffer (500 mM Tris pH 6.8, 10% glycerol, 10% SDS, 0.05% 2-β-mercaptoethanol and 0.01% bromophenol blue) and boiled for 5 min [73]. SDS-Tricine-PAGE was performed in a 10% polyacrylamide gel. Proteins were electrotransferred to PVDF membranes for immunoblotting using 25 mM potassium phosphate, 25 mM sodium phosphate, 12 mM Tris, 192 mM glycine and 20% methanol, pH 7.0 [74]. Membranes were blocked with 0.5% albumin in TBS/T (50 mM Tris, 100 mM NaCl, pH 7.6, and 0.1% Tween 20) for 1 h and incubated overnight at 4 °C with the primary antibody (monoclonal mouse antibody against the AOX from the higher plant *Sauromatum guttatum* [75]). Then, membranes were washed with TBS/T and incubated at room temperature for 1 h with the horseradish peroxidase (HRP)-conjugated secondary antibody (HRP anti-mouse-igG). Antibodies were diluted in TBS/T. Once the membranes were washed, the bands were developed by chemiluminescence (ECL kit) [76].

2.10. Mass spectrometry

From the BN-gels or 2D SDS-Tricine gels, the indicated bands were excised and sent for protein sequence identification by LC-MS to the University Proteomics Laboratory of the Instituto de Biotecnología, UNAM (Cuernavaca, Morelos, Mexico). Peptides were analyzed in a LC-MS system constituted by an Accela microflux liquid chromatographer (Thermo-Fisher Co., San Jose, CA, USA) with a splitter (1/20), a LTQ Orbitrap Velos mass spectrometer (Thermo-Fisher Co., San Jose, CA, USA) and a nano-electrospray ionization (ESI) system. After tryptic digestion, samples were analyzed in a tandem high-resolution mass spectrometer. Mascot and Protein-Prospector algorithms were used to search all spectrometric results against the NCBInr database. Protein sequence coverage (%) is shown in Tables 3 and 5.

3. Results

3.1. D. hansenii contains a branched mitochondrial respiratory chain

To define the composition of the respiratory chain from *D. hansenii*, we measured the rate of oxygen consumption in isolated mitochondria using different substrates and inhibitors. To prevent the mitochondrial permeability transition (PT), 10 mM phosphate and 75 mM KCl were added (Table 1). As expected [58,59], citrate-malate and pyruvate-malate were efficiently oxidized in a rotenone-sensitive fashion by complex I while succinate was oxidized by complex II. In addition, the complex III inhibitor antimycin-A and the complex IV inhibitor NaCN partially inhibited oxygen consumption. Partial inhibitions indicated the presence of an alternative pathway for oxygen consumption [59]. The presence of an active AOX was confirmed by the partial sensitivity of the rate of oxygen consumption to propyl-gallate (PG). PG was preferred over salicylhydroxamic acid (SHAM) because full inhibition was achieved with 100 μM PG while a higher 500 μM SHAM was needed (Result not shown). Full inhibition of oxygen consumption was achieved by adding NaCN and PG together (Table 1).

The above results confirm the presence of a branched mitochondrial respiratory chain in *D. hansenii* that contains at least all four multisubunit complexes plus an alternative AOX [55,56]. The presence of additional external alternative dehydrogenases was suggested when NADH and glycerol-phosphate were oxidized at high rates (Table 1). Oxidation of these substrates was partially sensitive to both, NaCN or PG, indicating that electrons coming from these substrates could reach either the cytochrome pathway or AOX. The external NADH dehydrogenase (NDH2e) activity was sensitive to flavone, a specific inhibitor of type II NADH dehydrogenases, but it was not sensitive to rotenone. Also, the glycerol-phosphate dehydrogenase ($_{Mit}$GPDH) activity was not sensitive to either rotenone or flavone. Thus, it is suggested that *D. hansenii* contains a branched mitochondrial respiratory chain composed by the four canonical complexes, alternative dehydrogenases (at least NDH2 and $_{Mit}$GPDH) and an AOX.

The substrates predicted to yield a higher number of protons-pumped per electron consumed in the respiratory chain (H^+/e^-) exhibited a higher respiratory control (RC = phosphorylating state (III)/resting state (IV)) than those with a low H^+/e^- (Table 1), i.e., the highest respiratory controls were obtained using pyruvate-malate, RC = 2.35 ± 0.07 or citrate-malate, RC = 2.17 ± 0.05. By contrast,

with succinate a low RC = 1.64 ± 0.08 was observed, while with glycerol-phosphate RC = 1.28 ± 0.03 and with NADH RC = 1.23 ± 0.05.

3.2. The putative mitochondrial NDH2e from D. hansenii is inhibited by flavone and exhibits a high homology with NDH2s from other sources

To confirm the presence of external NDH2(s) in *D. hansenii* the rate of oxygen consumption was titrated with rotenone to inhibit complex I or flavone to inhibit any NDH2 activity present [38]. The rate of oxygen consumption in the absence of inhibitors was taken as 100%. In the presence of pyruvate-malate, respiration was inhibited by rotenone, but it was insensitive to flavone (Fig. 1A). At 5 μM rotenone 50% inhibition was obtained while maximum inhibition of the pyruvate-malate-supported oxygen consumption was reached at 50 μM rotenone (Fig. 1A, full circles). By contrast, with NADH, flavone inhibited oxygen consumption while rotenone exhibited little effect (Fig. 1B). In the presence of NADH, 500 μM flavone led to maximal inhibition (Fig. 1B, empty circles).

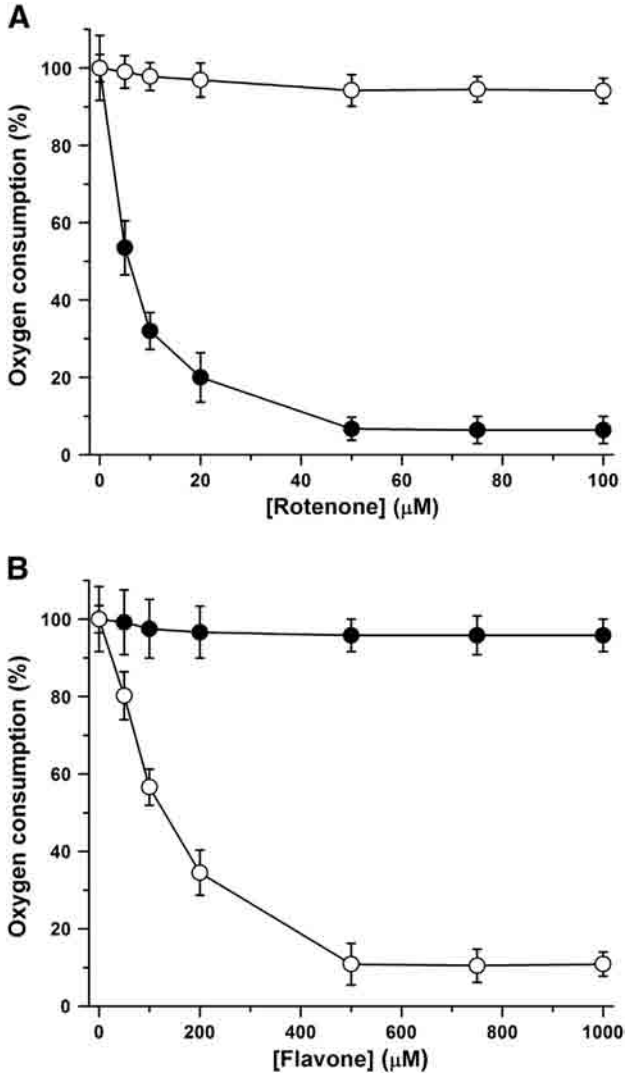

Fig. 1. Inhibition of oxygen consumption in isolated mitochondria from *D. hansenii* with rotenone (A) or flavone (B). The substrate was either 10 mM pyruvate-malate (●) or 1 mM NADH (○). Oxygen measurements were made in the resting state (IV). The reaction mixture was as in Table 1. Data from five independent experiments are expressed as the mean ± SD.

Yeast species may contain different alternative dehydrogenases, e.g. *S. cerevisiae* contains three mitochondrial NDH2 isoforms plus an external $_{Mit}$GPDH [21,40]. To detect possible alternative dehydrogenases in the NCBI database, the genome of *D. hansenii* was analyzed for sequences homologous to those encoding for NDH2s and $_{Mit}$GPDHs in *Y. lipolytica* and *S. cerevisiae*. For NDH2s, the BLAST analysis unveiled a protein sequence with high homology to type II NADH dehydrogenases. This is the hypothetical protein DEHA2D07568p, a 568 amino acid (MW = 63 kDa) precursor. DEHA2D07568p was aligned against the NDH2e sequence from *Y. lipolytica* (YALI0F25135p) and the NDH2s from *S. cerevisiae*, i.e. NDI (YML120c), NDE1 (YMR145c) and NDE2 (YDL085w) (Table 2), exhibiting high sequence similarity. In addition, DEHA2D07568p closely resembles external NDH2s from several fungi and plants (Result not shown). Furthermore, when the conserved motifs described for the NDH2e from *Y. lipolytica* [77] were compared with the DEHA2D07568p, both proteins exhibited highly matching dinucleotide binding sites (for NADH or FAD) and hydrophobic regions (Fig. 2). These results plus the flavone sensitivity strongly suggest that DEHA2D07568p is an NDH2e. In addition, there is a 98.9% probability that this protein is imported into mitochondria as predicted by the MitoProt II-v1.101 program [78]. Analysis of the *D. hansenii* genome did not detect other genes coding for NDH2s.

3.3. D. hansenii has a mitochondrial glycerol-phosphate dehydrogenase ($_{Mit}$GPDH)

Isolated mitochondria from *D. hansenii* oxidized glycerol-phosphate at a high rate (Table 1), suggesting the presence of a mitochondrial GPDH as predicted by Adler and co-workers [79]. Thus, to look for orthologues the *D. hansenii* sequences were aligned against the corresponding genes from *S. cerevisiae* (Gut2p) and *Y. lipolytica* (YALI0B13970p). The analysis unveiled only one candidate sequence, annotated as hypothetical protein DEHA2E08624p; a 652 amino-acid precursor, MW = 72.5 kDa with a 65.9% probability of being imported by mitochondria [78]. DEHA2E08624p sequence is similar to $_{Mit}$GPDHs from other yeast species (Table 2) and with other $_{Mit}$GPDHs stored in the NCBI database. Thus, our data suggest that DEHA2E08624p is a mitochondrial GPDH.

3.4. The AOX in D. hansenii mitochondria is sensitive to AMP

In isolated mitochondria from *D. hansenii* cyanide-resistant respiration (CRR) was ~20–25% of the total. In different organisms this percentage can vary depending on different molecules or environmental

Table 2
D. hansenii putative alternative oxidoreductase sequences. Percentage of identity and similarity with those from other yeast sources.

Sequences	Identity (%)	Similarity (%)
a) NDH2s		
• DEHA2D07568p vs. YALI0F25135p (*Yl*NDH2e)	50	65
• DEHA2D07568p vs. YML120c (*Sc*NDE1)	45	64
• DEHA2D07568p vs. YMR145c (*Sc*NDE2)	52	69
• DEHA2D07568p vs. YDL085w (*Sc*NDI)	50	69
b) $_{Mit}$GPDHs		
• DEHA2E08624p vs. YALI0B13970p (Yl_{Mit}GPDH)	49	64
• DEHA2E08624p vs. Gut2p (Sc_{Mit}GPDH)	58	73
c) AOXs		
• DEHA2C03828p vs. AAQ08895 (*Yl*AOX1)	54	69
• DEHA2C03828p vs. AAQ08896 (*Yl*AOX2)	50	66
• DEHA2C03828p vs. XP_723460 (*Ca*AOX1)	63	73
• DEHA2C03828p vs. XP_723269 (*Ca*AOX2)	65	79

Protein sequences are shown accordingly with their NCBI definition or accession nomenclature.
Abbreviations: *Sc*: *S. cerevisiae*; *Yl*: *Y. lipolytica*; *Ca*: *C. albicans*; NDH2e/NDE: external alternative NADH dehydrogenase; NDI: internal alternative NADH dehydrogenase; AOX1: alternative oxidase isoform 1; AOX2: alternative oxidase isoform 2; Mit: mitochondrial isoform.

Fig. 2. Alignment of the conserved motifs of DEHA2D07568p and *Y. lipolytica* NDH2e amino acid sequences. (:) Conserved substitutions; (.) semi-conserved substitutions. Identical residues in both sequences are shown in gray. Numbers indicate amino acids in the linear sequence of each protein.

conditions, e.g. α-ketoacids, AMP, salts, temperature and mitochondrial-matrix redox state [80–82]. In addition, many plants and microorganisms express AOX in response to ROS or cytochromic pathway inhibitors [83,84]. AOXs from yeast or from *Ustilago maydis* are activated by AMP and possibly by the redox state, but not by α-ketoacids [85]. To test some of the properties of the *D. hansenii* AOX ($_{Dh}$AOX); it was decided to explore the sensitivity to AMP or pyruvate. To measure only CRR, these experiments were conducted in the presence of 500 μM NaCN. Full oxygen consumption inhibition was achieved with 500 μM NaCN plus 100 μM propyl-gallate. It was observed that AMP increased CRR (~15%) while pyruvate had no effects (Fig. 3), i.e. the AOX from *D. hansenii* shares the sensitivity to AMP from other fungi AOXs.

Further analysis of AOX was conducted by comparing the $_{Dh}$AOX hypothetical protein sequence with the constitutive and inducible AOX isoforms (1 and 2, respectively) from *Yarrowia lipolytica* and *Candida albicans*. The BLAST analysis unveiled only one candidate, annotated as hypothetical protein DEHA2C03828p. This sequence corresponds to a 338 amino-acid precursor with a theoretical MW of 39.4 kDa. There is a 97.1% probability that this protein is imported by mitochondria [78]. The DEHA2C03828p sequence has high similarity to the AOXs from both yeast species (Table 2). With the above results, it may be concluded that *D. hansenii* mitochondria contain a branched respiratory chain composed by all four canonical complexes plus three alternative oxido-reductases, namely an NDH2e, a $_{Mit}$GPDH and the $_{Dh}$AOX already reported [59]. Alternative enzymes were analyzed using SDS-Tricine PAGE, western blotting and mass spectrometry (see below).

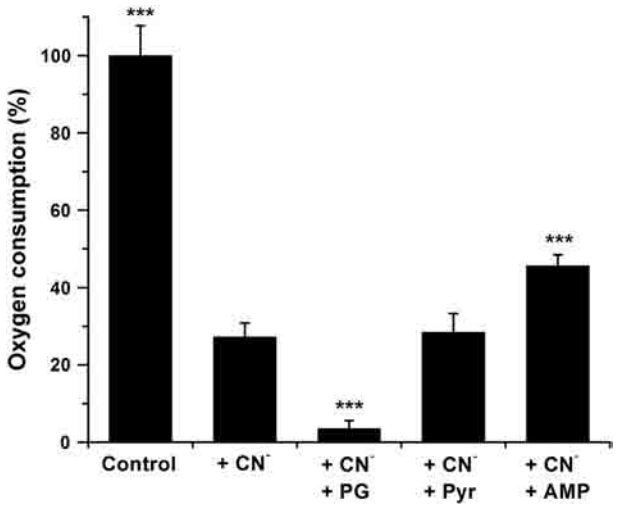

Fig. 3. Activation of the *D. hansenii* AOX by AMP but not by pyruvate (Pyr). Oxygen consumption was measured in state IV with 10 mM succinate as respiratory substrate. 50 μM rotenone was added to inhibit complex I. Cytochrome-dependent oxygen consumption was inhibited with 500 μM NaCN (CN^-). 100 μM propylgallate (PG), 10 mM pyruvate (Pyr) or 1 mM AMP was used as indicated. n = 3 ± SD. One-way ANOVA (Dunnett's multiple comparison test) *P < 0.05 compared to the cyanide-treated sample (second bar).

3.5. In *D. hansenii* mitochondria, respiratory complexes organize into supercomplexes

After detection of the different components of the mitochondrial respiratory chain from *D. hansenii*, it was decided to define whether the respiratory complexes were organized into supercomplexes as described for many other species [48,50,51]. Both *D. hansenii* and *Y. lipolytica* are closely related [69,70], so we decided to use *Y. lipolytica* mitochondrial respiratory complexes and supercomplexes as standards to estimate the MW of those from *D. hansenii*. For BN-PAGE, mitochondrial membranes were solubilized with either laurylmaltoside (LM) or digitonin (Dig). Digitonin was used expecting to preserve associations between respiratory complexes, while laurylmaltoside was expected to allow isolation of the individual complexes. The BN-PAGE results are shown for solubilized mitochondria from *Y. lipolytica* (Fig. 4A) and from *D. hansenii* (Fig. 4B). In LM-solubilized mitochondria, the individual complexes from either *Y. lipolytica* or *D. hansenii* were observed at different migration distances. Migration distances for complexes I, IV and V were reasonably near in both species. By contrast, the complex III band from *D. hansenii* was hardly detectable by BN-PAGE (Fig. 4B lane LM). In fact, the location of complex III was detected only in the 2D Tricine-SDS-PAGE (see below). In digitonin-solubilized mitochondria from both *Y. lipolytica* (Fig. 4A) and *D. hansenii* (Fig. 4B) several high MW bands corresponding to putative respiratory supercomplexes were revealed.

To further characterize the location and composition of each complex and supercomplex, the in-gel enzymatic activities of NADH dehydrogenase (NDH), ATPase and cytochrome *c* oxidase (COX) were assayed in BN-gels (Fig. 4C to E). In the LM solubilized sample, NDH activity

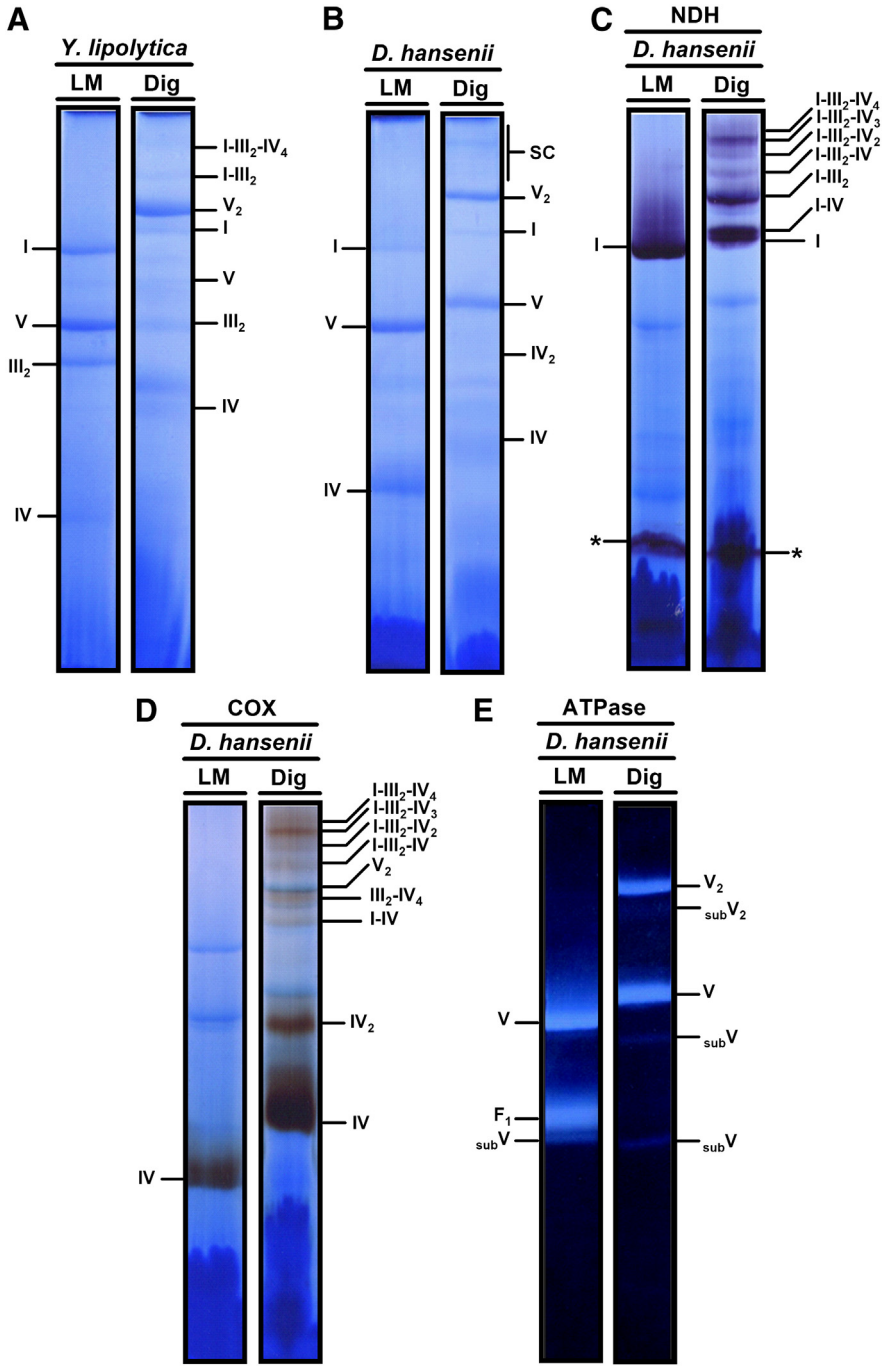

Fig. 4. Respiratory complexes and supercomplexes found in solubilized *D. hansenii* mitochondria. Isolated mitochondria were solubilized with laurylmaltoside (LM) 2.0 mg/mg Prot or digitonin (Dig) 4.0 mg/mg Prot. (A) *Y. lipolytica* solubilizates were resolved by BN-PAGE in a 4–12% polyacrylamide gradient gel and were used as MWs standards. (B) LM- and Dig-solubilizates from *D. hansenii* mitochondria resolved by BN-PAGE. (C) In-gel NADH-dehydrogenase activity (NDH); 1 mM NADH and 0.5 mg/mL nitrotetrazolium blue chloride (NTB). (D) In-gel cytochrome *c* oxidase activity (COX); 0.04% diaminobenzidine and 0.02% cytochrome *c*. (E) In-gel ATPase activity performed in BN-gel; 35 mM Tris, 270 mM glycine, 0.2% $Pb(NO_3)_2$, 14 mM $MgSO_4$ and 8 mM ATP (pH 8.4). I, III_2, IV and V are the mitochondrial mammalian-like complexes. (*) Putative NDH2e. *D. hansenii* supercomplexes (SC) were: I–IV, I–III_2, I–III_2–IV, I–III_2–IV_2, I–III_2–IV_3 and I–III_2–IV_4 where stoichiometries are indicated as sub-indexes. IV_2: complex IV dimer; F_1: soluble domain of complex V; V_2: complex V dimer; subV: complex V sub-complexes.

exhibited two purple bands corresponding to complex I and presumably to the NDH2e (Fig. 4C lane LM). When solubilized with digitonin, higher MW purple bands were detected (Fig. 4C lane Dig). These bands were assigned as supercomplexes containing complex I plus different amounts of either complex III or complex IV (see below). Also, the NDH activity seemed more intense in three bands than in all others, suggesting that complex I-containing supercomplexes were concentrated in these bands. These bands had MWs compatible with their assignment as the complex I band running alone; as a I-IV supercomplex; a I-III_2 supercomplex and a I–III_2–IV_3 supercomplex (Fig. 4C lane Dig; also see Fig. 4D which is described below).

When COX activity was measured, a single brown band was observed in the LM-solubilized lane (Fig. 4D lane LM). It is suggested that this activity is the product of monomeric complex IV. The digitonin lane revealed several brown bands corresponding to monomeric complex IV and to a number of supercomplexes containing complexes I, III_2

and IV (Fig. 4D lane Dig). Supercomplex I-III_2-IV_3 exhibited the highest activity. Also, a faint band, probably corresponding to I–IV supercomplex was detected near complex I.

In regard to in-gel ATPase activity, LM treatment revealed three activity bands that were respectively assigned as the monomeric complex V, the F_1 subunit and a F_1 subcomplex (Fig. 4E lane LM). In the first two bands the ATPase activity was much higher than the activity detected in the subcomplex, indicating that this may be at low concentrations or exhibit less activity. In the digitonin solubilized samples ATPase activity was detected in four bands (Fig. 4E lane Dig). The ATPase activity was more intense in the bands assigned as the complex V dimer and monomer, while the lower intensity bands probably were the F_1 subunit and an F_1F_O-ATP synthase sub-complex. Dimers of complex V have also been detected previously in mitochondria from beef heart, *S. cerevisiae*, *Polytomella* sp. and from other sources by digitonin solubilization or using lower LM/protein ratios [51].

To determine the location of each respiratory complex, including complex III which was not observed in the BN gels, and also whether any given complex was part of a putative supercomplex, complete BN-PAGE lanes from LM- and Dig-solubilized mitochondria were resolved by second dimension denaturing gels (2D Tricine-SDS-PAGE) and subjected to Coomassie-staining (Fig. 5) or silver-staining (Fig. 6), respectively. The second dimension gel from LM-solubilized mitochondria contains the individual subunit signatures [49] from each respiratory complex (Fig. 5). In order to confirm the assignments for complexes I, III, IV and V different bands were excised and sent to protein identification by LC-MS. The 75-kDa subunit from NADH dehydrogenase (I), the core proteins 1 and 2 from the bc_1 complex (III), the COX subunit 2 from cytochrome *c* oxidase (IV) and the gamma (γ) subunit from F_1F_O-ATP synthase (V) were identified with a high sequence coverage (Table 3). In all cases, identified subunits were located at the lane that was previously predicted for a specific respiratory complex. Complex III, which was difficult to see before (Fig 4B, lane LM), could be located next to the complex V monomer (Fig. 5).

In the 2D-gel obtained from digitonin-solubilized mitochondria, the subunit pattern of individual complexes was found also at high MWs indicating the presence of supercomplexes (Fig. 6). The MWs suggested that these supercomplexes contained complexes I, III and IV. In addition, a pattern corresponding to a complex V dimer (V_2) was identified. It is suggested that the supercomplexes detected by BN-gels (Fig. 4) and 2D SDS-Tricine-gels (Figs. 5 and 6) were: IV_2, I–IV, III_2–IV_4, V_2, I-III_2 (S_0), I–III_2–IV (S_1), I–III_2–IV_2 (S_2), I–III_2–IV_3 (S_3) and I–III_2–IV_4 (S_4).

To determine the stoichiometry and the theoretical MWs of these supercomplexes, the MWs of each complex/supercomplex were estimated by measuring the migration distance of the corresponding bands in BN-PAGE of the digitonin solubilizates from *D. hansenii* and interpolating them by linear regression in a log MW vs. migration distance plot from the solubilized mitochondrial respiratory complexes from *Y. lipolytica* that we used as MW standards (Fig. 7). The estimated MWs are shown in Table 4. The composition of each supercomplex was determined by correlating the MW estimates and the presence of NDH, COX and/or ATPase activity in each band. The calculated MWs for complex I, IV and V monomers and complex III dimer were very similar to those from *Y. lipolytica* (Fig. 7). The *D. hansenii* MWs of the supercomplexes were similar to those reported for *Y. lipolytica* [51]. By contrast, the complex V dimers from *D. hansenii* were heavier than expected (Table 4).

In mammalian systems, large supercomplexes containing I_1–III_2–IV_4 and III_2–IV_4 have been detected in BN-gels [49]. Also, mammalian supercomplexes seem to be associated into larger "respiratory strings" [86]. In *D. hansenii*, it seems that complexes I, III_2 and IV organize into supercomplexes suggesting that these mitochondria also possess "respiratory strings" where chain units of the I–III_2–IV_3 supercomplex would attach to each other. In contrast to *Y. lipolytica* [87], NDH2e seems to be detached from the cytochrome-complexes; i.e. in digitonin-treated samples in-gel NADH dehydrogenase activity was absent at the sites where cytochrome complexes migrated (Fig. 4C lane Dig).

At this point, we can conclude that the branched respiratory chain from *D. hansenii* contains a large amount of canonical respiratory complexes (I, III and IV), which may be associated in supercomplexes (Fig. 4). Alternative enzymes probably are independent from the respiratory supercomplexes (at least the NDH2e (Fig. 4C lane Dig). Nevertheless alternative enzyme distribution needs to be explored further.

3.6. Identification of the alternative respiratory enzymes from D. hansenii

NDH2e has already been proposed to correspond to the lower NADH dehydrogenase activity band detected in a BN-gel (Fig. 4C); when this band was subjected to 2D-SDS-Tricine-PAGE different proteins were separated (Fig. 8). Three spots were selected for identification; the

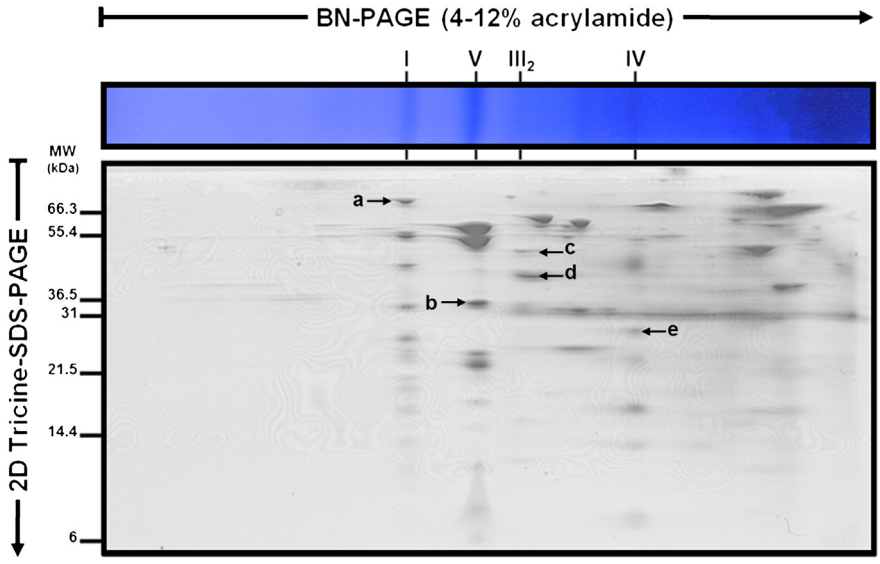

Fig. 5. 2D SDS-Tricine-PAGE of *D. hansenii* mitochondrial respiratory complexes. From the BN-PAGE, the lane containing the laurylmaltoside (LM) solubilized proteins was excised and subjected to 2D SDS-Tricine-PAGE. Bands that appear labeled were cut and sent for protein identification by LC-MS. These results are shown in Table 3. All SDS-Tricine-gels showed were stained with Coomassie® brilliant blue G-250. Respiratory complexes are tagged as in Fig. 4.

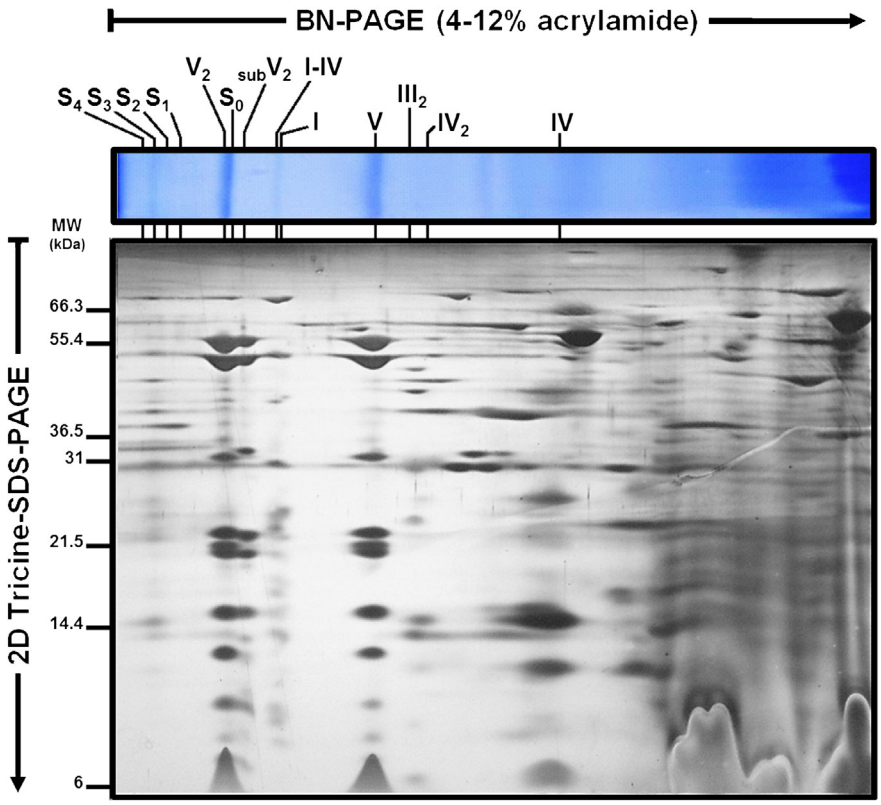

Fig. 6. 2D SDS-Tricine-PAGE of *D. hansenii* mitochondrial supercomplexes. After BN-PAGE, the lane containing the digitonin-solubilized proteins was excised and subjected to 2D-SDS-Tricine-PAGE followed by silver staining. Respiratory complexes are tagged as in Fig. 4. Supercomplex nomenclature: S_0: I–III_2, S_1: I–III_2–IV, S_2: I–III_2–IV_2, S_3: I–III_2–IV_3 and S_4: I–III_2–IV_4.

first corresponded to the hypothetical MW of NDH2e; i.e. 63 kDa (Fig. 8, f) and the other two were chosen due to their high concentration (Fig. 8, bands g and h). The spots were analyzed by LC-MS/MS and the results are shown in Table 5. The first band (f) was reported as the NDH2e hypothetical sequence (DEHA2D07568p) but surprisingly, it also contained the putative $_{Mit}$GPDH (DEHA2E08624p), in spite that the predicted MWs were widely different (63 vs. 72.5 kDa, respectively) (Table 5), i.e. they were in the same spot in the 2D SDS-Tricine-gel (Fig. 8). The presence of both proteins in the asterisked band (excised from the BN-gel, Fig. 4) might reflect a physiological interaction of these alternative dehydrogenases. A similar interaction has been described in *S. cerevisiae* as part of a mitochondrial dehydrogenase membrane complex, which contains different external peripheral alternative dehydrogenases, part of the Krebs cycle enzymes (including complex II), the NDI and other NADH producing enzymes that were not defined [88]. Also, in *D. hansenii* dihydrolipoamide dehydrogenase was identified next to NDH2e and $_{Mit}$GPDH (Fig. 8, g). This protein is part of the pyruvate dehydrogenase and the α-ketoglutarate dehydrogenase complexes [20]. The lower band contained three proteins: the ATP/ADP carrier (ANC); the mitochondrial porin (VDAC) and the phosphate carrier (Fig. 8, h). These proteins are involved in metabolite fluxes and have been proposed to be part of the mitochondrial unspecific channel in other yeast species [89].

In *S. cerevisiae* $_{Mit}$GPDH (Gut2p) has a predicted MW = 72.4 kDa, while the mature form of this protein has a MW = 68.4 kDa [88]. This MW is close to the mature *S. cerevisiae* NDE2 with a MW = 61.7 kDa [88]. In *D. hansenii*, NDH2e exhibited an approximate MW = 60 kDa (Fig. 8) and $_{Mit}$GPDH migrated very near that weight. In silico data and estimated MWs suggested that *D. hansenii* $_{Mit}$GPDH contains a longer signal-sequence than the NDH2e. When both proteins maturate, their MWs become similar and their electrophoretic migration coincides. As a result, both dehydrogenases appeared in the same 2D-gel spot (Fig. 8, f; Table 5).

AOX was identified by mass spectrometry (Fig. 9, upper panel) and by western blotting (WB) (Fig. 9, lower panel). For the western blot, an antibody against AOX from *S. guttatum* was used. Two bands were detected by this procedure (Fig. 9, lower panel). To determine which of these bands contains AOX, they were excised from the gel and sent

Table 3
Proteins identified by LC-MS analysis contained in the indicated bands from the 2D SDS-Tricine-gel (Fig. 5).

Band	Protein name	Accession no.	gI protein	Length[a]	Cov[b] (%)	MW[c] (kDa)
a	NADH-quinone oxidoreductase 75-kDa subunit	DEHA2G06050p	199433960	722	26.7	79
b	F_1F_0-ATP synthase gamma subunit	DEHA2F20658p	202953475	286	36.7	31.3
c	Ubiquinol-cytochrome *c* reductase core protein 1	DEHA2D13640p	199431718	445	31.7	48
d	Ubiquinol-cytochrome *c* reductase core protein 2	DEHA2E09834p	49655402	376	75	39.4
	IDH2 subunit of mitochondrial NAD(+)-dependent isocitrate dehydrogenase	DEHA2G05786p	49657467	365	22.2	39.5
	IDH1 subunit of mitochondrial NAD(+)-dependent isocitrate dehydrogenase	DEHA2C10758p	199430720	359	19.2	38.6
e	Cytochrome *c* oxidase subunit 2	YP_001621413.1	162951843	246	11.7	28.4

[a] Number of amino acids.
[b] Protein sequence coverage.
[c] Predicted molecular weights from the *D. hansenii* NCBI database sequences.

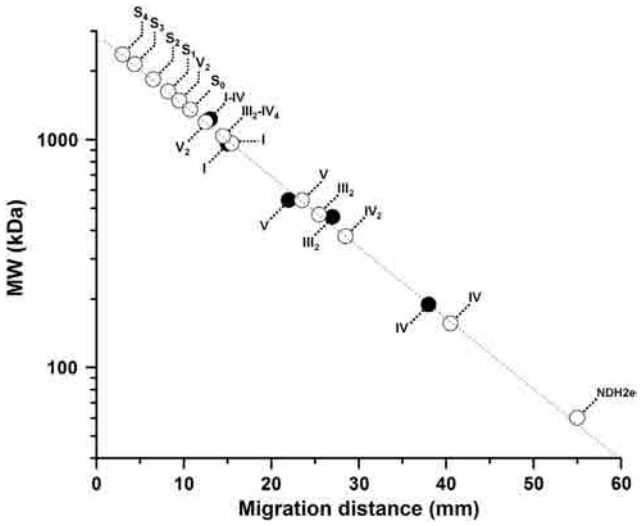

Fig. 7. Molecular weight (MW) estimates of the *D. hansenii* complexes and supercomplexes. The previously characterized molecular masses of *Y. lipolytica* mitochondrial complexes were plotted against their migration distance in BN-PAGE (●). Then, the migration distances of the *D. hansenii* respiratory complexes and supercomplexes (○) were interpolated and their corresponding molecular masses inferred (see values in Table 4). MW values from *Y. lipolytica* complexes I, III_2, IV, V and complex V dimer (V_2) were taken from the previous report by Guerrero-Castillo and co-workers [51]. (*) Putative NDH2e. Note that *y*-axis is in log-scale. Nomenclature for complexes and supercomplexes is as in Figs. 4 and 6.

to LC-MS/MS analysis. AOX was the "i" band (Fig. 9, upper panel) while the "j" band contained the ANC and VDAC (Fig. 9, upper panel). Results are shown in Table 5.

Experimental evidence supports the presence of a branched mitochondrial respiratory chain in *D. hansenii*. This chain contains the multi-subunit complexes I, II, III and IV; there is also a mitochondrial F_1F_O-ATP synthase (complex V), which tends to be a dimer and is detached from the respiratory supercomplexes (Fig. 4E). Three alternative enzymes: NDH2e, $_{Mit}$GPDH and $_{Dh}$AOX were detected as additional components of the branched respiratory chain. Preliminary evidence presented here suggests that multiprotein associations containing the alternative dehydrogenases plus at least two enzymes from the Krebs cycle do exist. Such associations have been described in *S. cerevisiae* [88].

Table 4
Estimated molecular weights (MWs) of the *D. hansenii* complexes and supercomplexes by BN-PAGE.

Complex/supercomplex	Calculated MW[a] (kDa)	Expected MW[b] (kDa)
I	963 ± 49	–
III_2	469 ± 24	–
IV	156 ± 12	–
V	541 ± 28	–
IV_2	377 ± 19	312
I–IV	1035 ± 53	1119
III_2–IV_4	1196 ± 61	1223
I–III_2 (S_0)	1356 ± 35	1432
V_2	1484 ± 76	1082
I–III_2–IV (S_1)	1630 ± 87	1588
I–III_2–IV_2 (S_2)	1842 ± 51	1744
I–III_2–IV_3 (S_3)	2143 ± 59	1900
I–III_2–IV_4 (S_4)	2370 ± 135	2056

Complex and supercomplex nomenclature as in Figs. 4–6.
[a] Calculated MW of the *D. hansenii* complexes and supercomplexes correspond to the mean ± SD from three independent experiments.
[b] Supercomplexes expected MWs correspond to the sum of the individual MW of each respiratory complex according to their stoichiometries (subscript numbers).

4. Discussion

The structure of the branched mitochondrial respiratory chain from *D. hansenii* was analyzed in isolated mitochondria. In addition, we characterized the association pattern of respiratory complexes into respiratory supercomplexes [44,48,49,86]. In agreement with Veiga and co-workers [59], we found that the *D. hansenii* respiratory chain contains all four canonical respiratory complexes I, II, III and IV plus an AOX. In addition, we detected two additional components, namely, an external type II NADH dehydrogenase (NDH2e) and a mitochondrial glycerol-phosphate dehydrogenase ($_{Mit}$GPDH).

AOX activity is resistant to cyanide [58,80]; electrons reach it directly from the ubiquinone pool, as indicated by the resistance of oxygen consumption activity to the complex III inhibitor antimycin-A (Table 1, Fig. 3). Cyanide-resistant, AOX-supported respiration is found in many yeast species, including *D. hansenii* and it has been proposed that AOX regulates energy production in response to different physiological conditions [57–59]. Regulation is the result of a decrease in the electron flux to the cytochromic pathway with the concomitant increase in electron flux to AOX [34–36,87]. Here, it was observed that *D. hansenii* alternative oxidase ($_{Dh}$AOX) is activated by AMP while it is insensitive to α-ketoacids, such as pyruvate. AMP activation is widely reported for AOXs from different yeasts and fungi [21,80,85]. It was suggested that $_{Dh}$AOX activity is induced at the stationary growth phase [59]. In this view, the presence of the AOX could be helpful to diminish the electron flux through the cytochromic pathway and reduce the ATP/O ratio in this physiological condition. In contrast to Veiga and co-workers [59], in our hands $_{Dh}$AOX activity was detected in isolated mitochondria from mid-exponential growth phase cultures. This is probably due to the differences in growth conditions, as we used a non-fermentable carbon source (lactate, see Materials and methods) [14]. This result suggests that $_{Dh}$AOX is active in early growth phases and not only at the stationary phase where it probably acts as an energy sink [35,87]. In cells grown in lactate, $_{Dh}$AOX was detected regardless of the addition of AMP (Table 1, Fig. 3). The role of $_{Dh}$AOX in different growth phases requires further studies.

Two other alternative enzymes, a glycerol-phosphate dehydrogenase and an alternative NADH dehydrogenase were both bound to the external face of the IMM. Electrons were fed to $_{Mit}$GDPH and NDH2e by external glycerol-phosphate or NADH, respectively. These electrons were used to reduce oxygen. From the BLAST analysis of the genomes, we concluded that there is a single gene codifying for each of these

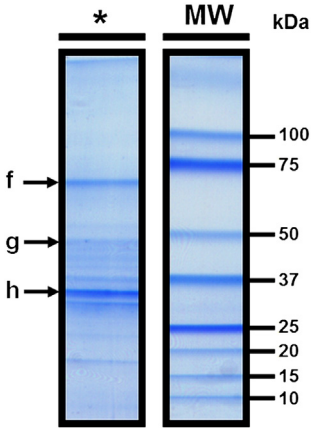

Fig. 8. Identification of the *D. hansenii* alternative NADH dehydrogenase (NDH2e) and the mitochondrial glycerol-posphate dehydrogenase ($_{Mit}$GPDH) by 2D SDS-Tricine-PAGE and LC-MS. (*) NADH dehydrogenase activity band from the BN gel, which was excised and subjected to 2D SDS-Tricine-PAGE in order to separate components. SDS-Tricine-gel was stained with Coomassie® brilliant blue G-250. Both *D. hansenii*. Bands contained f: NDH2e and MitGPDH, g: dihydrolipoamide dehydrogenase (subunit from pyruvate dehydrogenase and α-keto glutarate dehydrogenase) and h: ANC, PiC and VDAC (Table 5).

Table 5
Proteins identified by LC-MS analysis contained in the indicated bands from the SDS-Tricine-gels (Figs. 8 and 9).

Band	Protein name	Accession no.	gI protein	Length[a]	Cov[b] (%)	MW[c] (kDa)
f	Glycerol-3-phosphate dehydrogenase ($_{Mit}$GPDH) precursor	DEHA2E08624p	49655350	652	25.3	72.5
	Mitochondrial external alternative NADH dehydrogenase (NDH2e) precursor	DEHA2D07568p	199431532	568	38.2	63
g	Dihydrolipoamide dehydrogenase	CBS767	49653406	495	58	53.2
h	Major ADP/ATP carrier (ANC) of the mitochondrial inner membrane	DEHA2E12276p	49655508	301	41.5	33
	Voltage-dependent anion channel (VDAC) of the outer mitochondrial membrane	DEHA2D16456p	49654868	282	65.6	29.9
	Mitochondrial phosphate carrier (PiC)	DEHA2B12188p	49653149	307	33.6	32.4
i	Alternative oxidase (AOX) precursor	DEHA2C03828p	199430515	338	36.7	39.4
j	Major ADP/ATP carrier (ANC) of the mitochondrial inner membrane	DEHA2E12276p	49655508	301	38.5	33
	Voltage-dependent anion channel (VDAC) of the outer mitochondrial membrane	DEHA2D16456p	49654868	282	52.1	29.9

[a] Amino acid sequence length.
[b] Protein sequence coverage.
[c] Predicted molecular weights from the *D. hansenii* NCBI database sequences.

proteins and we assigned DEHA2E08624p and DEHA2D07568p as the $_{Mit}$GPDH and the NDH2e, respectively. These sequences were highly homologous to those from *Y. lipolytica* [77] and *S. cerevisiae* [90] (Fig. 2, Table 2).

NDH2e from *D. hansenii* was insensitive to rotenone while it was inhibited specifically by flavone. In isolated mitochondria from *D. hansenii*, 500 μM flavone promoted maximum inhibition of oxygen consumption (Fig. 1B, empty circles), which is similar to the concentrations reported for other organisms, e.g. in isolated mitochondria from *Plasmodium yoelii yoelii* [91] or *Paracoccidioides brasiliensis* [92] exogenous NADH-supported oxygen uptake is inhibited at similar flavone concentrations. In isolated mitochondria from *U. maydis*, complete inhibition is obtained at 250 μM flavone [85]. The flavone-mediated inhibition of the NADH:Q_6 oxidoreductase from *S. cerevisiae* exhibited an IC_{50} = 95 μM, although in the presence of 300 μM flavone, activity was still at 20% [38].

NDH2e has been proposed to compensate for the absence of an aspartate-malate shuttle in ascomycetous fungi [85]. Here, we observed a high rate of exogenous NADH oxidation in isolated mitochondria from *D. hansenii*. Mitochondrial NADH oxidation probably occurs in the intact cell, establishing a NADH/NAD^+ recirculation cycle with the cytosol. Furthermore, probably $_{Mit}$GPDH also constitutes an important mitochondrial sink of redox equivalents [93].

In *D. hansenii* active synthesis and accumulation of glycerol and lipids occur during growth; remarkably, these activities are stimulated by high salt concentrations [79] and $_{Mit}$GPDH seems to participate in both processes. In addition, in *S. cerevisiae*, glycerol-phosphate dehydrogenase is finely regulated by the activity of NDHs, i.e. at saturating NADH, alternative NADH dehydrogenases physically attached to the $_{Mit}$GPDH inhibit the use of glycerol-phosphate and transfer only electrons that come from external NDH [39]. In fact, the presence of both enzymes, whether associated or not, causes competition for the entrance of electrons into the respiratory chain [94].

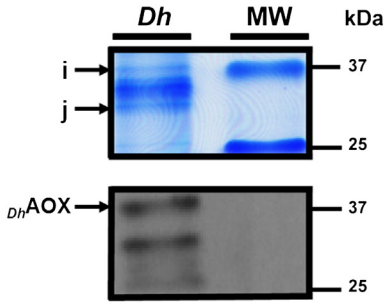

Fig. 9. Identification of the *D. hansenii* alternative oxidase (AOX) by SDS-Tricine-PAGE, western blotting and LC-MS. Total mitochondrial protein extract was subjected to SDS-Tricine-PAGE. SDS-Tricine-gel was stained with Coomassie® brilliant blue G-250 (upper panel). The SDS-Tricine-gel was electrotransferred onto PVDF membrane for western blotting. The membrane was decorated with a monoclonal mouse antibody against the AOX from the higher plant *S. guttatum* (lower panel). The two bands that were resulted immunoreactive in panel A (labeled as "i" and "j") were excised and subjected to identification by LC-MS. These results are shown in Table 5. At the upper panel, *D. hansenii* AOX corresponds to the "i" band. $_{Dh}$AOX: *Debaryomyces hansenii* alternative oxidase.

In *Y. lipolytica* growing in the exponential phase, electrons entering the respiratory chain at NDH2e are channeled to the cytochromic pathway [87]. This reflects the presence of an NDH2e-III_2-IV supercomplex. By contrast, electrons coming from pyruvate-malate (Complex I) or succinate (Complex II) can reach either the cytochromic or the alternative pathways both in *Y. lipolytica* and in *D. hansenii*. The presence of unattached non proton-pumping alternative oxidoreductases (NDH2e, $_{Mit}$GPDH, and $_{Dh}$AOX) probably constitutes a physiological mitochondrial uncoupling mechanism [35]. This is interesting, as *Y. lipolytica* seems to lack the ability to undergo a permeability transition [51,95] while *D. hansenii* does possess a mitochondrial unspecific channel [14]. Electron transfer from the alternative oxidoreductases to AOX constitutes a futile oxygen consumption pathway that needs to be tightly regulated [89]. The presence of this pathway in *D. hansenii* during the exponential growth phase is puzzling, although it may be suggested that it participates in the modulation of ROS production as has been proposed in other branched respiratory chains [35].

In *D. hansenii*, the mammalian-like mitochondrial respiratory complexes I, III and IV are associated in supercomplexes. Supramolecular organization of the respiratory chain has been proposed to promote electron channeling, stabilization of labile multi-subunit complexes and sequestration of free radicals [48]. Consistent association patterns of supercomplexes observed by BN-PAGE, strongly suggest the existence of larger structures such as "respiratory strings" [86] or "respiratory patches" [54]. In *Y. lipolytica* supercomplexes I–III_2, I-III_2-IV_4, I-IV, III_2-IV and III_2-IV_2 and a complex V dimer have been described [51]. In *S. cerevisiae* mitochondria a supercomplex III_2-IV_2 has been detected [96]. In *D. hansenii* respiratory supercomplexes involving complexes I, III and IV were similar to those found in *Y. lipolytica*. Supercomplexes I-III_2, I-III_2-IV_3 and III_2-IV_4 from *D. hansenii* contained the higher NADH dehydrogenase and COX activities as measured in BN-gels (Fig. 4C and D, lanes Dig). These supercomplexes were better observed in the activity staining experiments. In addition, the complex V dimer was easily observed both in the BN-gel and by ATPase activity staining (Fig. 4B and E, lane Dig). The *D. hansenii* F_1F_0-ATP synthase dimer was heavier than the V_2 from *Y. lipolytica*. This is probably due to stronger interactions between the subunits of complex V in these mitochondria than in other yeasts. Another explanation to this observation could be that V_2 may be associated to, and stabilized by the ATP/ADP carrier (ANC) and the phosphate carrier (PiC) in a structure known as the "synthasome" [97]. Molecular weights from the other respiratory complexes were similar to those from *Y. lipolytica*. Moreover, a big difference was observed between the single classical complexes from both *D. hansenii* and *Y. lipolytica* (Fig. 4A and B, lanes LM). In *D. hansenii* respiratory complexes were observed in smaller concentration than complex V. In fact, complex III was not observed in the BN-gels; it was only located by its subunit pattern in the 2D-SDS-Tricine-gels (Fig. 5) and by the identification of the core proteins 1 and 2 by mass

spectrometry (Table 3). Cytochromic complexes III and IV are postulated to be the scaffold of the "respiratory string" [86]. In this case, our observation is unclear, as complex III does not seem to be present in the same amount as complex IV (Fig. 4B, lane LM). These results are not clearly understood and need to be explored further. Still, the electrophoretic migration of respiratory supercomplexes, their putative MWs, their enzymatic activities and the LC-MS identification of some of their subunits indicate that the mitochondrial respiratory chain from *D. hansenii* associates into supercomplexes which are very similar to those detected in organisms studied before such as mammals [44,48,68], plants [43,45,46,50] and other yeasts such as *S. cerevisiae* [44,53] and *Y. lipolytica* [51].

This is the first description of the complete structure of the branched respiratory chain from *D. hansenii*. In addition, we analyzed the supramolecular organization of the classical respiratory complexes in *D. hansenii* mitochondria. Alternative redox enzymes from this yeast do not seem to be attached to supercomplexes at least under our experimental conditions (mid-exponential phase, non-fermentable carbon source), which suggests that the *D. hansenii* alternative oxidoreductases dynamically associate/dissociate with supercomplexes. This would be in agreement with a dynamic *plasticity* model of the oxidative phosphorylation [55], i.e. respiratory components alternate between association in supercomplexes and free forms.

Acknowledgements

Technical assistance was received from Martha Calahorra, Ramón Méndez-Franco and Norma Sánchez. We thank Dr Juan Pablo Pardo for the gift of the AOX antibody. Partially funded by the PAPIIT program and DGAPA/UNAM (grant IN202612). ACO, SGC and MRL are CONACYT fellows enrolled in the Biochemistry Graduate Program at UNAM. This is a partial requirement for the obtention of the PhD degree by ACO.

References

[1] J.C. Gonzalez-Hernandez, C.A. Cardenas-Monroy, A. Pena, Sodium and potassium transport in the halophilic yeast *Debaryomyces hansenii*, Yeast 21 (2004) 403–412.
[2] U. Breuer, H. Harms, *Debaryomyces hansenii*—an extremophilic yeast with biotechnological potential, Yeast 23 (2006) 415–437.
[3] B. Norkrans, Studies on marine occurring yeasts: growth related to pH, NaCl concentration and temperature, Arch. Mikrobiol. 54 (1966) 374–392.
[4] B. Norkrans, A. Kylin, Regulation of the potassium to sodium ratio and of the osmotic potential in relation to salt tolerance in yeasts, J. Bacteriol. 100 (1969) 836–845.
[5] C. Prista, M.C. Loureiro-Dias, V. Montiel, R. Garcia, J. Ramos, Mechanisms underlying the halotolerant way of *Debaryomyces hansenii*, FEMS Yeast Res. 5 (2005) 693–701.
[6] J.A. Hobot, D.H. Jennings, Growth of *Debaryomyces hansenii* and *Saccharomyces cerevisiae* in relation to pH and salinity, Exp. Mycol. 5 (1981) 217–228.
[7] H. Seiler, M. Busse, The yeasts of cheese brines, Int. J. Food Microbiol. 11 (1990) 289–303.
[8] T. Nakase, M. Suzuki, Taxonomic studies on *Debaryomyces hansenii* (Zopf) Lodder et Kreger-Van Rij and related species. II. Practical discrimination and nomenclature, J. Gen. Appl. Microbiol. 31 (1985) 71–86.
[9] T.v.d. Tempel, M. Jakobsen, The technological characteristics of *Debaryomyces hansenii* and *Yarrowia lipolytica* and their potential as starter cultures for production of Danablu, Int. Dairy J. 10 (2000) 263–270.
[10] M.E. Fadda, V. Mossa, M.B. Pisano, M. Deplano, S. Cosentino, Occurrence and characterization of yeasts isolated from artisanal Fiore Sardo cheese, Int. J. Food Microbiol. 95 (2004) 51–59.
[11] N.S. Sanchez, M. Calahorra, J.C. Gonzalez-Hernandez, A. Pena, Glycolytic sequence and respiration of *Debaryomyces hansenii* as compared to *Saccharomyces cerevisiae*, Yeast 23 (2006) 361–374.
[12] N.S. Sanchez, R. Arreguin, M. Calahorra, A. Pena, Effects of salts on aerobic metabolism of *Debaryomyces hansenii*, FEMS Yeast Res. 8 (2008) 1303–1312.
[13] M. Calahorra, N.S. Sanchez, A. Pena, Activation of fermentation by salts in *Debaryomyces hansenii*, FEMS Yeast Res. 9 (2009) 1293–1301.
[14] A. Cabrera-Orefice, S. Guerrero-Castillo, L.A. Luevano-Martinez, A. Pena, S. Uribe-Carvajal, Mitochondria from the salt-tolerant yeast *Debaryomyces hansenii* (halophilic organelles?), J. Bioenerg. Biomembr. 42 (2010) 11–19.
[15] M. Gutierrez-Aguilar, X. Perez-Martinez, E. Chavez, S. Uribe-Carvajal, In *Saccharomyces cerevisiae*, the phosphate carrier is a component of the mitochondrial unselective channel, Arch. Biochem. Biophys. 494 (2010) 184–191.
[16] B. Guerin, O. Bunoust, V. Rouqueys, M. Rigoulet, ATP-induced unspecific channel in yeast mitochondria, J. Biol. Chem. 269 (1994) 25406–25410.
[17] S. Manon, M. Guerin, Investigation of the yeast mitochondrial unselective channel in intact and permeabilized spheroplasts, Biochem. Mol. Biol. Int. 44 (1998) 565–575.
[18] V. Perez-Vazquez, A. Saavedra-Molina, S. Uribe, In *Saccharomyces cerevisiae*, cations control the fate of the energy derived from oxidative metabolism through the opening and closing of the yeast mitochondrial unselective channel, J. Bioenerg. Biomembr. 35 (2003) 231–241.
[19] M. Gutierrez-Aguilar, V. Perez-Vazquez, O. Bunoust, S. Manon, M. Rigoulet, S. Uribe, In yeast, Ca^{2+} and octylguanidine interact with porin (VDAC) preventing the mitochondrial permeability transition, Biochim. Biophys. Acta 1767 (2007) 1245–1251.
[20] D.G. Nicholls, S.J. Ferguson, Bioenergetics 3, Academic Press, London, 2002.
[21] T. Joseph-Horne, D.W. Hollomon, P.M. Wood, Fungal respiration: a fusion of standard and alternative components, Biochim. Biophys. Acta 1504 (2001) 179–195.
[22] I.M. Juszczuk, A.M. Rychter, Alternative oxidase in higher plants, Acta Biochim. Pol. 50 (2003) 1257–1271.
[23] N. Sen, H.K. Majumder, Mitochondrion of protozoan parasite emerges as potent therapeutic target: exciting drugs are on the horizon, Curr. Pharm. Des. 14 (2008) 839–846.
[24] A. McDonald, G. Vanlerberghe, Branched mitochondrial electron transport in the Animalia: presence of alternative oxidase in several animal phyla, IUBMB Life 56 (2004) 333–341.
[25] D. Munro, N. Pichaud, F. Paquin, V. Kemeid, P.U. Blier, Low hydrogen peroxide production in mitochondria of the long-lived *Arctica islandica*: underlying mechanisms for slow aging, Aging cell 12 (2013) 584–592.
[26] R. Buschges, G. Bahrenberg, M. Zimmermann, K. Wolf, NADH: ubiquinone oxidoreductase in obligate aerobic yeasts, Yeast 10 (1994) 475–479.
[27] J. Nosek, H. Fukuhara, NADH dehydrogenase subunit genes in the mitochondrial DNA of yeasts, J. Bacteriol. 176 (1994) 5622–5630.
[28] D.A. Berthold, M.E. Andersson, P. Nordlund, New insight into the structure and function of the alternative oxidase, Biochim. Biophys. Acta 1460 (2000) 241–254.
[29] M.S. Albury, C. Affourtit, P.G. Crichton, A.L. Moore, Structure of the plant alternative oxidase. Site-directed mutagenesis provides new information on the active site and membrane topology, J. Biol. Chem. 277 (2002) 1190–1194.
[30] M.E. Andersson, P. Nordlund, A revised model of the active site of alternative oxidase, FEBS Lett. 449 (1999) 17–22.
[31] A.L. Moore, J.N. Siedow, The regulation and nature of the cyanide-resistant alternative oxidase of plant mitochondria, Biochim. Biophys. Acta 1059 (1991) 121–140.
[32] H. Lambers, The physiological significance of the cyanide-resistant respiration in higher plants, Plant Cell Environ. 3 (1980) 293–302.
[33] D.A. Day, J.T. Wiskich, Regulation of alternative oxidase activity in higher plants, J. Bioenerg. Biomembr. 27 (1995) 379–385.
[34] D.P. Maxwell, Y. Wang, L. McIntosh, The alternative oxidase lowers mitochondrial reactive oxygen production in plant cells, Proc. Natl. Acad. Sci. U. S. A. 96 (1999) 8271–8276.
[35] S. Guerrero-Castillo, D. Araiza-Olivera, A. Cabrera-Orefice, J. Espinasa-Jaramillo, M. Gutierrez-Aguilar, L.A. Luevano-Martinez, A. Zepeda-Bastida, S. Uribe-Carvajal, Physiological uncoupling of mitochondrial oxidative phosphorylation. Studies in different yeast species, J. Bioenerg. Biomembr. 43 (2011) 323–331.
[36] R. El-Khoury, E. Dufour, M. Rak, N. Ramanantsoa, N. Grandchamp, Z. Csaba, B. Duvillie, P. Benit, J. Gallego, P. Gressens, C. Sarkis, H.T. Jacobs, P. Rustin, Alternative oxidase expression in the mouse enables bypassing cytochrome c oxidase blockade and limits mitochondrial ROS overproduction, PLoS Genet. 9 (2013) e1003182.
[37] S. Kerscher, S. Drose, V. Zickermann, U. Brandt, The three families of respiratory NADH dehydrogenases, Results Probl. Cell Differ. 45 (2008) 185–222.
[38] S. de Vries, L.A. Grivell, Purification and characterization of a rotenone-insensitive NADH:Q6 oxidoreductase from mitochondria of *Saccharomyces cerevisiae*, Eur. J. Biochem. 176 (1988) 377–384.
[39] I.L. Pahlman, C. Larsson, N. Averet, O. Bunoust, S. Boubekeur, L. Gustafsson, M. Rigoulet, Kinetic regulation of the mitochondrial glycerol-3-phosphate dehydrogenase by the external NADH dehydrogenase in *Saccharomyces cerevisiae*, J. Biol. Chem. 277 (2002) 27991–27995.
[40] M. Rigoulet, A. Mourier, A. Galinier, L. Casteilla, A. Devin, Electron competition process in respiratory chain: regulatory mechanisms and physiological functions, Biochim. Biophys. Acta 1797 (2010) 671–677.
[41] B. Ronnow, M.C. Kielland-Brandt, GUT2, a gene for mitochondrial glycerol 3-phosphate dehydrogenase of *Saccharomyces cerevisiae*, Yeast 9 (1993) 1121–1130.
[42] C.R. Hackenbrock, B. Chazotte, S.S. Gupte, The random collision model and a critical assessment of diffusion and collision in mitochondrial electron transport, J. Bioenerg. Biomembr. 18 (1986) 331–368.
[43] H. Eubel, J. Heinemeyer, H.P. Braun, Identification and characterization of respirasomes in potato mitochondria, Plant Physiol. 134 (2004) 1450–1459.
[44] H. Schagger, K. Pfeiffer, Supercomplexes in the respiratory chains of yeast and mammalian mitochondria, EMBO J. 19 (2000) 1777–1783.
[45] F. Krause, N.H. Reifschneider, D. Vocke, H. Seelert, S. Rexroth, N.A. Dencher, "Respirasome"-like supercomplexes in green leaf mitochondria of spinach, J. Biol. Chem. 279 (2004) 48369–48375.
[46] H. Eubel, L. Jansch, H.P. Braun, New insights into the respiratory chain of plant mitochondria. Supercomplexes and a unique composition of complex II, Plant Physiol. 133 (2003) 274–286.
[47] G. Lenaz, M.L. Genova, Kinetics of integrated electron transfer in the mitochondrial respiratory chain: random collisions vs. solid state electron channeling, Am. J. Physiol. Cell Physiol. 292 (2007) C1221–C1239.
[48] H. Schagger, Respiratory chain supercomplexes of mitochondria and bacteria, Biochim. Biophys. Acta 1555 (2002) 154–159.
[49] H. Schagger, Respiratory chain supercomplexes, IUBMB Life 52 (2001) 119–128.
[50] N.V. Dudkina, J. Heinemeyer, S. Sunderhaus, E.J. Boekema, H.P. Braun, Respiratory chain supercomplexes in the plant mitochondrial membrane, Trends Plant Sci. 11 (2006) 232–240.

[51] S. Guerrero-Castillo, M. Vazquez-Acevedo, D. Gonzalez-Halphen, S. Uribe-Carvajal, In *Yarrowia lipolytica* mitochondria, the alternative NADH dehydrogenase interacts specifically with the cytochrome complexes of the classic respiratory pathway, Biochim. Biophys. Acta 1787 (2009) 75–85.
[52] H. Boumans, L.A. Grivell, J.A. Berden, The respiratory chain in yeast behaves as a single functional unit, J. Biol. Chem. 273 (1998) 4872–4877.
[53] R.A. Stuart, Supercomplex organization of the oxidative phosphorylation enzymes in yeast mitochondria, J. Bioenerg. Biomembr. 40 (2008) 411–417.
[54] E. Nubel, I. Wittig, S. Kerscher, U. Brandt, H. Schagger, Two-dimensional native electrophoretic analysis of respiratory supercomplexes from *Yarrowia lipolytica*, Proteomics 9 (2009) 2408–2418.
[55] R. Acin-Perez, P. Fernandez-Silva, M.L. Peleato, A. Perez-Martos, J.A. Enriquez, Respiratory active mitochondrial supercomplexes, Mol. Cell 32 (2008) 529–539.
[56] E.J. Boekema, H.P. Braun, Supramolecular structure of the mitochondrial oxidative phosphorylation system, J. Biol. Chem. 282 (2007) 1–4.
[57] A. Veiga, J.D. Arrabaca, M.C. Loureiro-Dias, Cyanide-resistant respiration is frequent, but confined to yeasts incapable of aerobic fermentation, FEMS Microbiol. Lett. 190 (2000) 93–97.
[58] A. Veiga, J.D. Arrabaca, M.C. Loureiro-Dias, Cyanide-resistant respiration, a very frequent metabolic pathway in yeasts, FEMS Yeast Res. 3 (2003) 239–245.
[59] A. Veiga, J.D. Arrabaca, F. Sansonetty, P. Ludovico, M. Corte-Real, M.C. Loureiro-Dias, Energy conversion coupled to cyanide-resistant respiration in the yeasts *Pichia membranifaciens* and *Debaryomyces hansenii*, FEMS Yeast Res. 3 (2003) 141–148.
[60] A.G. Gornall, C.J. Bardawill, M.M. David, Determination of serum proteins by means of the biuret reaction, J. Biol. Chem. 177 (1949) 751–766.
[61] I. Wittig, H. Schagger, Advantages and limitations of clear-native PAGE, Proteomics 5 (2005) 4338–4346.
[62] B.R. Oakley, D.R. Kirsch, N.R. Morris, A simplified ultrasensitive silver stain for detecting proteins in polyacrylamide gels, Anal. Biochem. 105 (1980) 361–363.
[63] W. Wray, T. Boulikas, V.P. Wray, R. Hancock, Silver staining of proteins in polyacrylamide gels, Anal. Biochem. 118 (1981) 197–203.
[64] E. Zerbetto, L. Vergani, F. Dabbeni-Sala, Quantification of muscle mitochondrial oxidative phosphorylation enzymes via histochemical staining of blue native polyacrylamide gels, Electrophoresis 18 (1997) 2059–2064.
[65] M.S. Johnson, S.A. Kuby, Studies on NADH (NADPH)-cytochrome c reductase (FMN-containing) from yeast. Isolation and physicochemical properties of the enzyme from top-fermenting ale yeast, J. Biol. Chem. 260 (1985) 12341–12350.
[66] U. Brandt, A two-state stabilization-change mechanism for proton-pumping complex I, Biochim. Biophys. Acta 1807 (2011) 1364–1369.
[67] M. Iwata, Y. Lee, T. Yamashita, T. Yagi, S. Iwata, A.D. Cameron, M.J. Maher, The structure of the yeast NADH dehydrogenase (Ndi1) reveals overlapping binding sites for water- and lipid-soluble substrates, Proc. Natl. Acad. Sci. U. S. A. 109 (2012) 15247–15252.
[68] I. Wittig, M. Karas, H. Schagger, High resolution clear native electrophoresis for in-gel functional assays and fluorescence studies of membrane protein complexes, Mol. Cell. Proteomics 6 (2007) 1215–1225.
[69] B. Dujon, D. Sherman, G. Fischer, P. Durrens, S. Casaregola, I. Lafontaine, J. De Montigny, C. Marck, C. Neuveglise, E. Talla, N. Goffard, L. Frangeul, M. Aigle, V. Anthouard, A. Babour, V. Barbe, S. Barnay, S. Blanchin, J.M. Beckerich, E. Beyne, C. Bleykasten, A. Boisrame, J. Boyer, L. Cattolico, F. Confanioleri, A. De Daruvar, L. Despons, E. Fabre, C. Fairhead, H. Ferry-Dumazet, A. Groppi, F. Hantraye, C. Hennequin, N. Jauniaux, P. Joyet, R. Kachouri, A. Kerrest, R. Koszul, M. Lemaire, I. Lesur, L. Ma, H. Muller, J.M. Nicaud, M. Nikolski, S. Oztas, O. Ozier-Kalogeropoulos, S. Pellenz, S. Potier, G.F. Richard, M.L. Straub, A. Suleau, D. Swennen, F. Tekaia, M. Wesolowski-Louvel, E. Westhof, B. Wirth, M. Zeniou-Meyer, I. Zivanovic, M. Bolotin-Fukuhara, A. Thierry, C. Bouchier, B. Caudron, C. Scarpelli, C. Gaillardin, J. Weissenbach, P. Wincker, J.L. Souciet, Genome evolution in yeasts, Nature 430 (2004) 35–44.
[70] D.J. Sherman, T. Martin, M. Nikolski, C. Cayla, J.L. Souciet, P. Durrens, Genolevures: protein families and synteny among complete hemiascomycetous yeast proteomes and genomes, Nucleic Acids Res. 37 (2009) D550–D554.
[71] W.K. Huh, S.O. Kang, Characterization of the gene family encoding alternative oxidase from *Candida albicans*, Biochem. J. 356 (2001) 595–604.
[72] M.A. Larkin, G. Blackshields, N.P. Brown, R. Chenna, P.A. McGettigan, H. McWilliam, F. Valentin, I.M. Wallace, A. Wilm, R. Lopez, J.D. Thompson, T.J. Gibson, D.G. Higgins, Clustal W and Clustal X version 2.0, Bioinformatics 23 (2007) 2947–2948.
[73] U.K. Laemmli, Cleavage of structural proteins during the assembly of the head of bacteriophage T4, Nature 227 (1970) 680–685.
[74] H. Towbin, T. Staehelin, J. Gordon, Electrophoretic transfer of proteins from polyacrylamide gels to nitrocellulose sheets: procedure and some applications, Proc. Natl. Acad. Sci. U. S. A. 76 (1979) 4350–4354.
[75] T.E. Elthon, R.L. Nickels, L. McIntosh, Monoclonal antibodies to the alternative oxidase of higher plant mitochondria, Plant Physiol. 89 (1989) 1311–1317.
[76] N. Chiquete-Felix, J.M. Hernandez, J.A. Mendez, A. Zepeda-Bastida, A. Chagolla-Lopez, A. Mujica, In guinea pig sperm, aldolase A forms a complex with actin, WAS, and Arp2/3 that plays a role in actin polymerization, Reproduction 137 (2009) 669–678.
[77] S.J. Kerscher, J.G. Okun, U. Brandt, A single external enzyme confers alternative NADH:ubiquinone oxidoreductase activity in *Yarrowia lipolytica*, J. Cell Sci. 112 (Pt 14) (1999) 2347–2354.
[78] M.G. Claros, P. Vincens, Computational method to predict mitochondrially imported proteins and their targeting sequences, Eur. J. Biochem. 241 (1996) 779–786.
[79] L. Adler, A. Blomberg, A. Nilsson, Glycerol metabolism and osmoregulation in the salt-tolerant yeast *Debaryomyces hansenii*, J. Bacteriol. 162 (1985) 300–306.
[80] A.L. Umbach, J.N. Siedow, The cyanide-resistant alternative oxidases from the fungi *Pichia stipitis* and *Neurospora crassa* are monomeric and lack regulatory features of the plant enzyme, Arch. Biochem. Biophys. 378 (2000) 234–245.
[81] C. Affourtit, K. Krab, A.L. Moore, Control of plant mitochondrial respiration, Biochim. Biophys. Acta 1504 (2001) 58–69.
[82] C.A. Smith, V.J. Melino, C. Sweetman, K.L. Soole, Manipulation of alternative oxidase can influence salt tolerance in *Arabidopsis thaliana*, Physiol. Plant. 137 (2009) 459–472.
[83] S. Sakajo, N. Minagawa, T. Komiyama, A. Yoshimoto, Characterization of cyanide-resistant respiration and appearance of a 36 kDa protein in mitochondria isolated from antimycin A-treated *Hansenula anomala*, J. Biochem. 108 (1990) 166–168.
[84] X. Huang, U. von Rad, J. Durner, Nitric oxide induces transcriptional activation of the nitric oxide-tolerant alternative oxidase in *Arabidopsis* suspension cells, Planta 215 (2002) 914–923.
[85] O. Juarez, G. Guerra, F. Martinez, J.P. Pardo, The mitochondrial respiratory chain of *Ustilago maydis*, Biochim. Biophys. Acta 1658 (2004) 244–251.
[86] I. Wittig, R. Carrozzo, F.M. Santorelli, H. Schagger, Supercomplexes and subcomplexes of mitochondrial oxidative phosphorylation, Biochim. Biophys. Acta 1757 (2006) 1066–1072.
[87] S. Guerrero-Castillo, A. Cabrera-Orefice, M. Vazquez-Acevedo, D. Gonzalez-Halphen, S. Uribe-Carvajal, During the stationary growth phase, *Yarrowia lipolytica* prevents the overproduction of reactive oxygen species by activating an uncoupled mitochondrial respiratory pathway, Biochim. Biophys. Acta 1817 (2012) 353–362.
[88] X. Grandier-Vazeille, K. Bathany, S. Chaignepain, N. Camougrand, S. Manon, J.M. Schmitter, Yeast mitochondrial dehydrogenases are associated in a supramolecular complex, Biochemistry 40 (2001) 9758–9769.
[89] S. Uribe-Carvajal, L.A. Luevano-Martinez, S. Guerrero-Castillo, A. Cabrera-Orefice, N.A. Corona-de-la-Pena, M. Gutierrez-Aguilar, Mitochondrial unselective channels throughout the eukaryotic domain, Mitochondrion 11 (2011) 382–390.
[90] S.J. Kerscher, Diversity and origin of alternative NADH:ubiquinone oxidoreductases, Biochim. Biophys. Acta 1459 (2000) 274–283.
[91] S.A. Uyemura, S. Luo, M. Vieira, S.N. Moreno, R. Docampo, Oxidative phosphorylation and rotenone-insensitive malate- and NADH-quinone oxidoreductases in *Plasmodium yoelii yoelii* mitochondria in situ, J. Biol. Chem. 279 (2004) 385–393.
[92] V.P. Martins, F.M. Soriani, T. Magnani, V.G. Tudella, G.H. Goldman, C. Curti, S.A. Uyemura, Mitochondrial function in the yeast form of the pathogenic fungus *Paracoccidioides brasiliensis*, J. Bioenerg. Biomembr. 40 (2008) 297–305.
[93] M. Klingenberg, Localization of the glycerol-phosphate dehydrogenase in the outer phase of the mitochondrial inner membrane, Eur. J. Biochem. 13 (1970) 247–252.
[94] O. Bunoust, A. Devin, N. Averet, N. Camougrand, M. Rigoulet, Competition of electrons to enter the respiratory chain: a new regulatory mechanism of oxidative metabolism in *Saccharomyces cerevisiae*, J. Biol. Chem. 280 (2005) 3407–3413.
[95] M.V. Kovaleva, E.I. Sukhanova, T.A. Trendeleva, M.V. Zyl'kova, L.A. Ural'skaya, K.M. Popova, N.E. Saris, R.A. Zvyagilskaya, Induction of a non-specific permeability transition in mitochondria from *Yarrowia lipolytica* and *Dipodascus* (*Endomyces*) *magnusii* yeasts, J. Bioenerg. Biomembr. 41 (2009) 239–249.
[96] J. Heinemeyer, H.P. Braun, E.J. Boekema, R. Kouril, A structural model of the cytochrome C reductase/oxidase supercomplex from yeast mitochondria, J. Biol. Chem. 282 (2007) 12240–12248.
[97] C. Chen, Y. Ko, M. Delannoy, S.J. Ludtke, W. Chiu, P.L. Pedersen, Mitochondrial ATP synthasome: three-dimensional structure by electron microscopy of the ATP synthase in complex formation with carriers for Pi and ADP/ATP, J. Biol. Chem. 279 (2004) 31761–31768.

Biochimie xxx (2014) 1–13

Contents lists available at ScienceDirect

Biochimie

journal homepage: www.elsevier.com/locate/biochi

Research paper

Oxidative phosphorylation in *Debaryomyces hansenii*: Physiological uncoupling at different growth phases

Alfredo Cabrera-Orefice [a], Sergio Guerrero-Castillo [a], Rodrigo Díaz-Ruíz [b], Salvador Uribe-Carvajal [a,*]

[a] Dept of Molecular Genetics, Instituto de Fisiología Celular, Universidad Nacional Autónoma de México, Mexico City, Mexico
[b] Facultad de Medicina, Programa de Posgrado en Ciencias Médicas, Odontológicas y de la Salud, Universidad Nacional Autónoma de México, Mexico City, Mexico

ARTICLE INFO

Article history:
Received 10 December 2013
Accepted 3 March 2014
Available online xxx

Keywords:
Debaryomyces hansenii
Physiological uncoupling
NAD^+ loss
AOX
Respiratory complex I
NAD^+ transport

ABSTRACT

Physiological uncoupling of mitochondrial oxidative phosphorylation (OxPhos) was studied in *Debaryomyces hansenii*. In other species, such as *Yarrowia lipolytica* and *Saccharomyces cerevisiae*, OxPhos can be uncoupled through differential expression of branched respiratory chain enzymes or by opening of a mitochondrial unspecific channel ($_{Sc}$MUC), respectively. However *D. hansenii* mitochondria, which contain both a branched respiratory chain and a mitochondrial unspecific channel ($_{Dh}$MUC), selectively uncouple complex I-dependent rate of oxygen consumption in the stationary growth phase. The uncoupled complex I-dependent respiration was only 20% of the original activity. Inhibition was not due to inactivation of complex I, lack of protein expression or to differential expression of alternative oxidoreductases. Furthermore, all other respiratory chain activities were normal. Decrease of complex I-dependent respiration was due to NAD^+ loss from the matrix, probably through an open of $_{Dh}$MUC. When NAD^+ was added back, coupled complex I-activity was recovered. NAD^+ re-uptake was independent of $_{Dh}$MUC opening and seemed to be catalyzed by a NAD^+-specific transporter, which was sensitive to bathophenanthroline, bromocresol purple or pyridoxal-5′-phosphate as described for *S. cerevisiae* mitochondrial NAD^+ transporters. Loss of NAD^+ from the matrix through an open MUC is proposed as an additional mechanism to uncouple OxPhos.

1. Introduction

Some 10^9 years ago, the Great Oxidation Event (GOE) imposed a strong natural selection that led surviving organisms both to profit from the large energy released by water production and to develop protection mechanisms from toxic reactive oxygen species (ROS) [1,2]. Many animals including fish, birds and mammals developed significant barriers to exclude atmospheric oxygen (O_2). These organisms control cellular O_2 concentration tightly [3]. Less developed organisms such as amphibians, crustaceans, plants and unicellulars are permeable to atmospheric O_2 [4,5]. Thus, it is no wonder that bacteria, fungi, plants and lower animals express O_2-detoxifying mechanisms that uncouple oxidative phosphorylation (OxPhos) designed to prevent side reactions that yield ROS [6,7].

In the absence of ATP synthesis (non-phosphorylating state or state IV), mitochondrial respiratory chain activity would be slowed down by the high $\Delta\mu_H^+$ [8] increasing the likelihood that free radicals from complexes I and III react with O_2 to form ROS [6,7]. To avoid this, mitochondria accelerate the rate of oxygen consumption through different physiological mechanisms [8]. These mechanisms may (a) dissipate the proton-gradient (proton sinks) or (b) perform redox reactions without proton pumping [8,9]. Alternative, non-pumping dehydrogenases may compete or even substitute the usual respiratory complexes decreasing the efficiency of the respiratory chain [8]. Proton sinks include mitochondrial unspecific channels (MUCs) [10,11] and uncoupling proteins (UCPs) [12]. On the other hand, non-conservative redox reactions are catalyzed by peripheral alternative oxidoreductases such as mitochondrial glycerol-phosphate dehydrogenases ($_{Mit}$GPDHs), alternative type-II NADH dehydrogenases (NDH2s) and alternative oxidases (AOXs) [13,14]. NDH2s and AOXs do not exist in mammals, which contain four multi-subunit redox complexes, namely I, II, III and IV [15]. By contrast, the “branched” mitochondrial respiratory chains in plants,

* Corresponding author. Departamento de Genética Molecular, Instituto de Fisiología Celular, Universidad Nacional Autónoma de México, Ciudad Universitaria, Apdo. Postal 70-242, Mexico City, Mexico. Tel.: +52 55 5622 5632; fax: +52 55 5622 5630.
E-mail address: suribe@ifc.unam.mx (S. Uribe-Carvajal).

http://dx.doi.org/10.1016/j.biochi.2014.03.003
0300-9084/

fungi, yeast, protozoa and some metazoans do contain this kind of alternative redox enzymes [16–19] and thus electrons may reach O_2 through different routes [20]. In addition, "classical" respiratory complexes may decrease their H^+/e^- stoichiometry (slipping) [21]. To prevent lethal energy depletion, physiological uncoupling has to be strictly regulated [8,22,23].

Mitochondria from different yeast species may possess both, proton sinks and branched respiratory chains. For example, *Saccharomyces cerevisiae* has a mitochondrial unspecific channel ($_{Sc}$MUC) and its respiratory chain possesses multi-subunit complexes II, III and IV, two external type-II NADH dehydrogenases, one internal type-II NADH dehydrogenase and one $_{Mit}$GPDH [24,25]. *Yarrowia lipolytica* does not seem to contain a MUC [26] but instead, it expresses an UCP-like transporter [27] plus a branched respiratory chain containing the four classical complexes, an external alternative NADH dehydrogenase (NDH2e) and an AOX [28]. Interestingly, upon reaching the stationary growth phase *Y. lipolytica*, overexpresses its alternative NDH2e, which then transfers the electrons from NADH directly to quinone and to AOX and to oxygen without pumping a single proton [26] in what should be considered a futile, uncoupled respiration [26,28].

The halotolerant yeast *Debaryomyces hansenii* contains a MUC ($_{Dh}$MUC), which is sensitive to Na^+ and K^+ [29]. This species resists high monovalent cations concentrations [30]. $_{Dh}$MUC was detected in the exponential growth phase [29] but it seems to be active in the stationary phase, where less ATP is required. In addition, *D. hansenii* has a branched mitochondrial respiratory chain containing the four multi-subunit complexes, an AOX, an NDH2e and a $_{Mit}$GPDH [31,32].

While OxPhos in *D. hansenii* is probably optimal during the exponential growth phase, upon entering the stationary phase uncoupling mechanisms should be turned on to maintain a high rate of O_2 consumption and thus inhibit ROS production and regulate the redox state. Here, the expression of the non-proton pumping oxidoreductases and the state of $_{Dh}$MUC was evaluated at different growth phases in an effort to understand the physiological uncoupling mechanisms exhibited by this species. Most of the respiratory chain components in *D. hansenii* remained normal throughout growth. By contrast, the complex I-dependent rate of O_2 consumption was highly decreased and uncoupled. The mechanism for this behavior was explored.

2. Materials and methods

2.1. Chemicals

All chemicals were reagent grade. D-sorbitol, D-glucose, D-galactose, Trizma® base (Tris), malic acid, pyruvic acid, citric acid succinic acid, maleic acid, DL-α-glycerophosphate, NAD^+, NADH, ADP, rotenone, bathophenanthroline, pyridoxal-5′-phosphate, *n*-dodecyl β-D-maltoside (laurylmaltoside), Nitrotetrazolium blue chloride, safranine-O and antifoam A were from Sigma Chem Co. (St Louis, MO). Bovine serum albumin (Probulmin™) was from Millipore. Yeast extract and bacto-peptone were from BD Bioxon. DL-Lactic acid, tannic acid, H_3PO_4, NaCN, KCl and $MgCl_2$ were from J.T. Baker. Zymolyase 20 T was from Seikagaku Corp. (Tokyo, Japan). 3,3′-Diaminobenzidine tetrahydrochloride hydrate was from Fluka. Coomassie Blue G was from SERVA (Heidelberg, Germany). Coomassie® brilliant blue G-250 and electrophoresis reagents were from BIO-RAD (Richmond, CA, USA).

2.2. Biologicals

D. hansenii Y7426 strain (US Dept. of Agriculture) was used. The strain was maintained in YPGal–NaCl (1% yeast extract, 2% bacto-peptone, 2% D-galactose, 1.0 M NaCl and 2% bacto-agar) plate cultures at 4 °C.

2.3. Yeast culture and mitochondrial isolation

D. hansenii cells were grown as follows: pre-cultures were prepared inoculating 100 mL of YPLac–NaCl medium (1% yeast extract, 2% bacto-peptone, 2% lactic acid, pH 5.5 adjusted with NaOH and adding NaCl to reach 0.6 M Na^+) or YPD–NaCl (1% yeast extract, 2% bacto-peptone, 2% D-glucose and 0.6 M NaCl). Antifoam A emulsion 50 μL/L was added to all media. Pre-cultures were grown for 36 h under continuous agitation in an orbital shaker at 250 rpm at 29 °C. Then, each pre-culture was used to inoculate a 750 mL flask with the same medium. Incubation was continued for 15, 18, 24, 48, 72 and 96 h (YPLac–NaCl) or 12, 18, 22, 48, 72 and 96 h (YPD–NaCl). *D. hansenii* mitochondria were isolated as previously reported [29].

2.4. Obtention of permeabilized spheroplasts

D. hansenii spheroplasts were obtained following a method developed for *S. cerevisiae* [33] with some modifications. Briefly, yeast cells were grown in YPLac–NaCl and harvested in either exponential (24 h) or stationary phase (96 h). Cells were washed, centrifuged at 5000 rpm (5 min), resuspended in SH buffer (0.5 M β-mercaptoethanol, 0.1 M Tris, pH 9.3) and incubated at 30 °C for 10 min. Then, cells were centrifuged (5000 rpm, 5 min) and washed twice with 0.5 M KCl, 10 mM Tris, pH 7.0. To obtain spheroplasts, cells were suspended in digesting buffer (1.35 M sorbitol, 1 mM EGTA, 0.2 M phosphate buffer, pH 7.4) containing zymolyase 20 T (5 mg/g biomass dry-weight), which digested the cell wall. Progression of digestion was monitored spectrophotometrically and was stopped when turbidity of a sample suspended in water decreased to 10% of the control. Resulting spheroplasts were centrifuged (2500 rpm, 5 min) and washed three times using protoplast buffer (1.2 M sorbitol, 10 mM Tris–Maleate, pH 6.8). Samples were resuspended in spheroplast buffer (1.0 M sorbitol, 75 mM KCl, 5 mM $MgCl_2$, 0.5 mM EGTA, 20 mM Tris-phosphate, 10 mM Tris-Maleate, 0.2% bovine serum albumin, pH 6.8). Permeabilization was carried out treating spheroplasts at 1 mg protein/mL with nystatin (20 μg/mL) in the presence of constant oxygen, which was bubbled for 10 min. Complete permeabilization was confirmed by monitoring the decrease in the rate of oxygen consumption resulting from the depletion of endogenous respiratory substrates.

2.5. Protein quantification

Mitochondrial or total spheroplast protein was measured by the Biuret method [34]. Absorbance was determined at 540 nm in a Beckman DU-50 spectrophotometer. Bovine serum albumin was used as a standard.

2.6. Oxygen consumption

The rate of oxygen consumption was measured in a Strathkelvin Instruments® 782 Oxygen Meter (North Lanarkshire, Scotland, UK) interfaced to a computer. The sample was placed in a water-jacketed chamber at 30 °C. The phosphorylating state (III) was induced with 0.5 mM ADP. The reaction mixture was 1.0 M sorbitol, 10 mM maleate (pH was adjusted to 6.8 with Tris), 10 mM Tris-phosphate (Pi), 1 mM $MgCl_2$ and 75 mM KCl. Mitochondrial or total spheroplast protein (Prot) were 0.5 or 1.0 mg/mL, respectively; final volume was 1.0 mL. The concentrations of different respiratory substrates and inhibitors are indicated in the legends to the figures.

Please cite this article in press as: A. Cabrera-Orefice, et al., Oxidative phosphorylation in *Debaryomyces hansenii*: Physiological uncoupling at different growth phases, Biochimie (2014), http://dx.doi.org/10.1016/j.biochi.2014.03.003

2.7. Blue native (BN) electrophoresis and in-gel activities

BN-PAGE was performed as described in the literature [35] with slight modifications. Briefly, the mitochondrial pellet was suspended in sample buffer (750 mM aminocaproic acid, 25 mM imidazole (pH 7.0)) and solubilized with 2.0 mg *n*-dodecyl-β-D-maltoside (laurylmaltoside, LM)/mg Prot at 4 °C for 15 min and centrifuged at 33,000 rpm at 4 °C for 25 min. The supernatants were loaded on 4–12% (w/v) polyacrylamide gradient gels. Protein, 0.5 mg per lane was added to a 17 × 12 cm gel. The stacking gel contained 4% (w/v) polyacrylamide. BN-gel was stained with Coomassie® brilliant blue G-250. Semi-quantitative in-gel activities for complex I or IV were performed in BN-gels. In-gel NADH/Nitrotetrazolium blue chloride (NTB) oxidoreductase activity was determined incubating native gels in a mixture of 10 mM Tris (pH 7.0), 0.5 mg NTB/ml and 1 mM NADH [36]. In-gel cytochrome *c* oxidase activity was determined using diaminobenzidine and cytochrome *c* [37].

2.8. Cytochrome measurements using differential spectrophotometry

Mitochondria (2.5 mg Prot/mL) were added to sample buffer (750 mM aminocaproic acid, 25 mM imidazole, pH 7.0) and solubilized with 2.0 mg LM/mg Prot at 4 °C for 15 min and centrifuged at 14,000 rpm at 4 °C for 10 min. Final volume was 2.0 mL. Absorbance spectra from 500 to 650 nm were recorded at room temperature in a DW2000 Aminco spectrophotometer in the presence of ferricyanide to obtain oxidized spectra, which was assigned as base line. Then, the reduced spectrum was recorded after addition of sodium dithionite to the sample cuvette. Absorption coefficients were: cytochrome $a + a_3$, $\Delta\varepsilon_{604-630nm} = 24\ mM^{-1}\ cm^{-1}$ [38]; cytochrome *b*, $\Delta\varepsilon_{563-577nm} = 28.0\ mM^{-1}\ cm^{-1}$ [39]; cytochrome $c + c_1$, $\Delta\varepsilon_{553-539nm} = 19.1\ mM^{-1}\ cm^{-1}$ [40].

2.9. BLAST analysis

BLAST website and the NCBI database were used to search and compare the *D. hansenii* proteome against the two *S. cerevisiae* mitochondrial NAD^+ carrier isoforms (Ndt1p and Ndt2p). BLAST analysis also indicated the percentages of identity and similarity between amino acid sequences.

2.10. Krebs cycle NAD^+-dependent dehydrogenase activities

Pyruvate dehydrogenase (PDH) and malate dehydrogenase (MDH) activities were measured following the reduction of endogenous NAD^+ in a DW2000 AMINCO spectrophotometer (split mode) at room temperature. For both enzymes, the reaction mixture was the same as in respiration measures. Assays were performed based on the protocol reported by Cooney et al. (1981) [41], but no exogenous coenzymes were added. 0.05% (v/v) Triton X-100 was added to solubilize the mitochondrial samples. In order to prevent the oxidation of NADH, 50 μM rotenone was added to fully inhibit complex I [32]. Mitochondria 0.5 mg Prot/mL were added in each assay. Final volume was 2.0 mL. 10 mM pyruvate or 10 mM malate was added to start the reaction. Base line traces were performed in the absence of substrates and subtracted. NADH molar extinction coefficient used was $6.22 \times 10^3\ (M\ cm)^{-1}$.

2.11. Transmembrane potential ($\Delta\Psi$)

The transmembrane potential was determined using 10 μM safranine-O, following the absorbance changes at 511–533 nm [42] in a DW2000 AMINCO spectrophotometer in dual-wavelength mode. Mitochondrial protein was 0.5 mg/mL and final volume 2.0 mL. The concentrations of NAD^+, Pi and other reagents are indicated under each figure. Where indicated, the uncoupler *p*-chloromethoxy-carbonylcyanide phenylhydrazone (CCCP) was added to a final concentration of 5 μM.

3. Results

3.1. Physiological OxPhos uncoupling mechanisms seem to be species-specific

Each yeast species contains specific uncoupling systems. *S. cerevisiae* does not express AOX [43], although it contains a mitochondrial unspecific channel ($_{Sc}$MUC) that opens when ATP increases or phosphate is depleted, while it is closed by ADP or by high phosphate [44]. Thus, it was suggested that the energy charge modulates $_{Sc}$MUC and consequently OxPhos-coupling [45]. *Y. lipolytica* contains a branched respiratory chain, although it does not does not have a MUC [26]. This species undergoes stationary phase-related uncoupling through the overexpression of an alternative NADH dehydrogenase (NDH2e) plus the decrease in complex IV expression, turning on the alternative, non-proton pumping pathway NDH2 to AOX [46]. *D. hansenii* mitochondria express both a MUC and a branched respiratory chain. Monovalent cations close $_{Dh}$MUC, which otherwise is similar to $_{Sc}$MUC [45]. The coexistence of both uncoupling systems in *D. hansenii* led us to search for growth-related physiological uncoupling and for its mechanism(s).

3.2. Respiratory complex I activity decreases at the stationary growth phase

Growth-related uncoupling of OxPhos was measured in *D. hansenii* mitochondria isolated from cells grown for different times in either YPLac–NaCl (Table 1) or YPD–NaCl (Table 2). The rate of O_2 consumption and respiratory controls (RCs) were determined in the presence of substrates for each respiratory chain component. To discard any mitochondrial permeability transition (PT) effect during measurements, experiments were always conducted in the presence of 10 mM phosphate, 1 mM $MgCl_2$ and 75 mM KCl [29]. In the presence of most respiratory substrates, i.e. succinate for complex II, and glycerol-P or NADH for the corresponding alternative dehydrogenases, RCs did not change with incubation time while the rates of O_2 consumption increased slightly in mitochondria from cells grown for 48 h or more (Fig. 1, Tables 1 and 2). By contrast, in the presence of pyruvate–malate, which donates electrons to complex I, wide variations with incubation time were observed: isolated mitochondria from exponential phase lactate-grown cells and glucose-grown cells exhibited a maximum RC = 2.33 (Fig. 1A, Table 1) and RC = 2.2 (Fig. 1B, Table 2), respectively. Then, as cells entered the stationary phase, RCs decreased, i.e. in cells grown in lactate to the stationary phase RC = 1.27 (Fig. 1A, Table 1) while in those grown in glucose RC = 1.25 (Fig. 1B, Table 2). In addition, the rates of oxygen consumption both in the resting state (IV) and in the phosphorylating state (III) were smaller reaching ~15–20% of the activities in exponential phase (Tables 1 and 2). During the transition from the exponential to the stationary growth phase, the rate of oxygen consumption and the RC declined only in the presence of the complex I substrate pyruvate–malate, whereas the other components of the *D. hansenii* mitochondrial respiratory chain remained unaffected.

3.3. Complex I concentration and in-gel activity do not change as *D. hansenii* enters the stationary phase

The complex I-dependent rate of O_2 consumption decreased as growth time increased, which at the stationary phase, might be a

Please cite this article in press as: A. Cabrera-Orefice, et al., Oxidative phosphorylation in *Debaryomyces hansenii*: Physiological uncoupling at different growth phases, Biochimie (2014), http://dx.doi.org/10.1016/j.biochi.2014.03.003

Table 1
Rates of oxygen consumption in isolated mitochondria from *D. hansenii* YPLac−NaCl cultures at different growth times.

Substrate	Culture time (h)	Rate of oxygen consumption (natgO·(min mg Prot)$^{-1}$)		Respiratory control (III/IV)
		State IV*	State III**	
Pyruvate + malate	15	115 ± 14	248 ± 10	2.16 ± 0.09
	20	116 ± 11	262 ± 14	2.25 ± 0.08
	24	120 ± 10	279 ± 12	2.33 ± 0.07
	48	74 ± 8	152 ± 7	2.04 ± 0.05
	72	42 ± 5	59 ± 10	1.41 ± 0.06
	96	22 ± 7	28 ± 8	1.27 ± 0.05
Succinate	15	165 ± 14	280 ± 10	1.69 ± 0.10
	20	176 ± 11	282 ± 5	1.60 ± 0.08
	24	173 ± 15	285 ± 17	1.64 ± 0.10
	48	187 ± 6	284 ± 15	1.52 ± 0.10
	72	219 ± 12	379 ± 10	1.73 ± 0.11
	96	222 ± 8	382 ± 4	1.72 ± 0.05
NADH	15	225 ± 14	279 ± 15	1.24 ± 0.15
	20	235 ± 16	285 ± 13	1.21 ± 0.14
	24	228 ± 5	289 ± 13	1.26 ± 0.04
	48	237 ± 12	293 ± 10	1.24 ± 0.08
	72	283 ± 4	365 ± 9	1.29 ± 0.06
	96	326 ± 7	395 ± 4	1.21 ± 0.03
Glycerol-phosphate	15	211 ± 12	267 ± 11	1.27 ± 0.10
	20	215 ± 8	276 ± 15	1.28 ± 0.09
	24	218 ± 6	279 ± 13	1.28 ± 0.09
	48	232 ± 8	290 ± 12	1.25 ± 0.01
	72	266 ± 14	342 ± 10	1.29 ± 0.12
	96	300 ± 16	351 ± 15	1.17 ± 0.13

The rates of oxygen consumption were measured in resting state (IV)* and phosphorylating state (III)**. State III was induced with 500 μM ADP. Exponential phase samples were 15, 20 and 24 h. Stationary phase samples were 48, 72 and 96 h. 10 mM pyruvate + malate, 10 mM succinate, 1 mM NADH or 10 mM glycerol-phosphate were added in each case. Reaction mixture: 1.0 M sorbitol, 75 mM KCl, 10 mM Tris-phosphate, 1 mM $MgCl_2$ and 10 mM maleic acid, pH 6.8 (Tris). Final volume was 1.0 mL. Temperature = 30 °C. Data from three independent experiments are expressed as the mean ± SD.

physiological mechanism to burn oxygen while producing less ATP; i.e. to block the most efficient ATP-yielding electron entrance of the respiratory chain in the face of a low demand for energy [8]. By contrast, the other respiratory chain components remained fully active (Tables 1 and 2). These results were observed regardless of whether the carbon source was lactate or glucose (Fig. 1). In order to analyze the decrease in pyruvate−malate-dependent respiration observed, it was decided to test whether it was due to a decrease in complex I concentration or to a decrease in the redox activity of this complex.

Mitochondrial samples from cells grown in YPLac−NaCl for 15, 20, 24, 48, 72 and 96 h were solubilized with laurylmaltoside (LM)

Table 2
Rates of oxygen consumption in isolated mitochondria from *D. hansenii* YPD−NaCl cultures at different growth times.

Substrate	Culture time (h)	Rate of oxygen consumption (natgO·(min mg Prot)$^{-1}$)		Respiratory control (III/IV)
		State IV*	State III**	
Pyruvate + malate	12	127 ± 12	250 ± 14	1.97 ± 0.12
	18	123 ± 13	270 ± 15	2.19 ± 0.11
	22	125 ± 15	275 ± 17	2.20 ± 0.13
	48	78 ± 15	149 ± 17	1.91 ± 0.12
	72	45 ± 14	65 ± 16	1.44 ± 0.10
	96	28 ± 17	35 ± 18	1.25 ± 0.11
Succinate	12	166 ± 10	275 ± 18	1.65 ± 0.13
	18	174 ± 14	286 ± 21	1.64 ± 0.14
	22	178 ± 10	295 ± 17	1.65 ± 0.10
	48	180 ± 15	289 ± 9	1.61 ± 0.08
	72	202 ± 18	314 ± 18	1.55 ± 0.12
	96	210 ± 17	345 ± 20	1.64 ± 0.10
NADH	12	222 ± 15	277 ± 14	1.24 ± 0.11
	18	238 ± 15	258 ± 23	1.08 ± 0.13
	22	238 ± 16	282 ± 20	1.18 ± 0.12
	48	244 ± 14	283 ± 14	1.16 ± 0.09
	72	289 ± 18	328 ± 10	1.13 ± 0.11
	96	312 ± 17	351 ± 15	1.13 ± 0.12
Glycerol-phosphate	12	215 ± 12	272 ± 21	1.27 ± 0.14
	18	220 ± 18	269 ± 18	1.22 ± 0.12
	22	222 ± 10	270 ± 11	1.21 ± 0.09
	48	243 ± 13	295 ± 18	1.21 ± 0.10
	72	256 ± 10	330 ± 13	1.29 ± 0.12
	96	290 ± 17	332 ± 18	1.14 ± 0.13

The rates of oxygen consumption were measured in resting state (IV)* and phosphorylating state (III)**. State III was induced with 500 μM ADP. 10 mM pyruvate + malate, 10 mM succinate, 1 mM NADH or 10 mM glycerol-phosphate were added in each case. Reaction mixture was as in Table 1. Exponential phase samples were 12, 18 and 22 h. Stationary phase samples were 48, 72 and 96 h. Data from three independent experiments are expressed as the mean ± SD.

Please cite this article in press as: A. Cabrera-Orefice, et al., Oxidative phosphorylation in *Debaryomyces hansenii*: Physiological uncoupling at different growth phases, Biochimie (2014), http://dx.doi.org/10.1016/j.biochi.2014.03.003

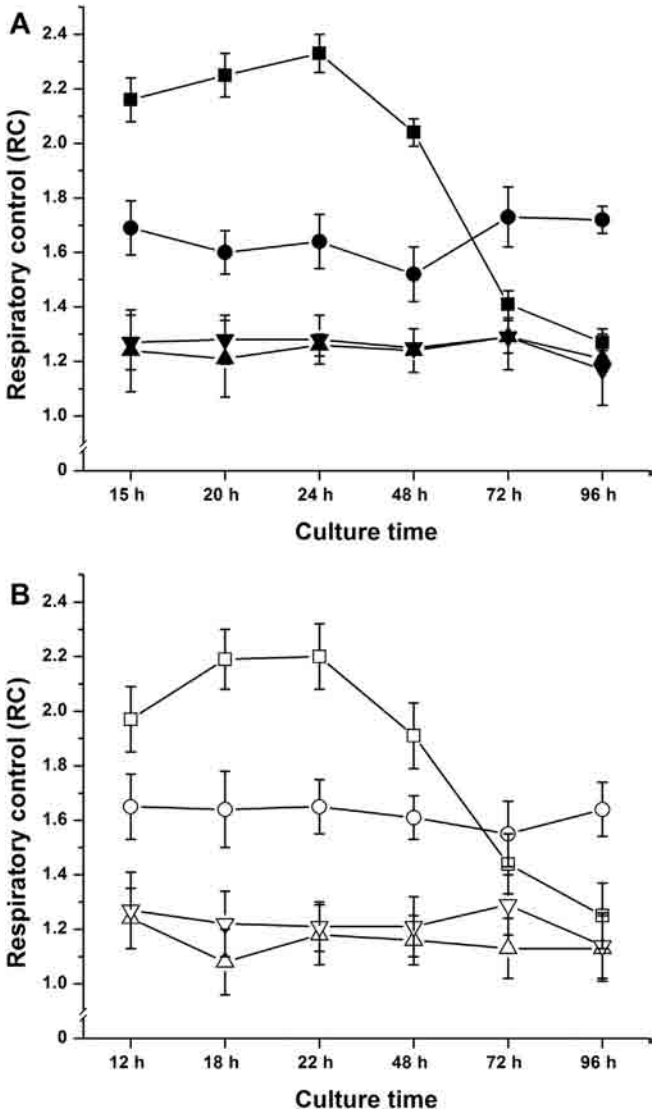

Fig. 1. Respiratory controls (RCs) of isolated mitochondria from *D. hansenii* grown in different carbon sources for different times. Respiratory chain substrates were: 10 mM pyruvate plus 10 mM malate (squares); 10 mM succinate (circles); 1 mM NADH (triangles) or glycerol-phosphate (inverted triangles). (A) RCs of exponential phase (15, 20 and 24 h) and stationary phase (48, 72 and 96 h) samples from YPLac–NaCl cultures (full symbols). (B) RCs of exponential phase (12, 18 and 22 h) and stationary phase (48, 72 and 96 h) samples from YPD–NaCl cultures (empty symbols). Reaction mixture was as in Table 1. Data from three independent experiments are expressed as the mean ± SD. RC values are shown in Tables 1 and 2.

and subjected to BN-PAGE [47]. It was observed that the protein bands that correspond to complexes I, IV and V were similar at all incubation times (Fig. 2A). The complex V (F_1F_0-ATP synthase) band was used as the loading control. In-gel enzymatic activities were also evaluated. NADH dehydrogenase in-gel activity (NDH) seemed to remain constant at the different culture times tested (Fig. 2B); i.e. complex I in-gel activity suggested that the activity of this complex was constant throughout growth.

3.4. Complex III and complex IV were not modified during growth

Electron transport using NADH, glycerol-phosphate or succinate as substrates, was not altered during growth, suggesting that the respiratory complex III–cyt *c*–complex IV segment was not modified. This was suggested by measuring in-gel cytochrome *c* oxidase activity (COX), which remained constant throughout growth (Fig. 2C). It is difficult to detect the *D. hansenii* ubiquinol:cytochrome *c* oxidoreductase (complex III) in BN-gels [32] and thus the in-gel complex III activity was not measured. Nonetheless, cytochrome contents were estimated in differential spectra at two different growth times in LM-solubilized mitochondrial samples from cells grown for 24 or 96 h. The concentration of cytochromes $a + a_3$ at 24 h was 0.217 ± 0.07 nmol/mg Prot and it varied very little at 96 h where it was 0.202 ± 0.13 nmol/mg Prot. At 24 h cytochrome $b = 0.318 \pm 0.06$ and $c + c_1 = 0.375 \pm 0.03$ nmol/mg Prot, respectively. At 96 h, cyt $b = 0.2 \pm 0.07$ and cyt $c + c_1 = 0.227 \pm 0.05$ nmol/mg Prot; i.e. complex III concentration decreased approximately 40% in the stationary phase, even when the rate of oxygen consumption through the III to IV cytochromic pathway remained the same (Table 1).

3.5. AOX expression in D. hansenii

In mitochondria from stationary phase grown cells, inhibition and uncoupling of the respiratory activity were evident only when the respiratory substrate was pyruvate–malate. This behavior was not due to changes in the expression or activity of complex I or any other complex (Fig. 2). To understand the decrease in complex I activity, it was decided to test whether known uncoupling mechanism(s) was (were) triggered. Two such possibilities were the activation of AOX leading to a non-productive pathway similar to the one described in *Y. lipolytica* [46] or a possible uncoupling role of the $_{Dh}$MUC.

In order to determine the pattern of AOX expression in *D. hansenii*, cells were cultured in either YPLac–NaCl or YPD–NaCl media and harvested at different times throughout the exponential and stationary phases. Then mitochondria were isolated and the rate of O_2 consumption before and after the addition of 500 μM NaCN was measured. The remaining activity was termed Cyanide Resistant Respiration (CRR) (Fig. 3). In lactate (Fig. 3A), CRR appeared early in the exponential growth phase and was ~20–25% of the total respiratory activity throughout growth. When the AOX activator AMP [32] was added, CRR increased by ~13–15% in all samples (Fig. 3A). By contrast, in YPD–NaCl grown cells (Fig. 3B) *D. hansenii* AOX ($_{Dh}$AOX) activity was absent at 12 h of growth, it was low at 18 h, where CRR ~13% and became fully active in the mid-exponential phase at 18 h where CRR ~20–25% and did not change further (Fig. 3B). In isolated mitochondria from YPD–NaCl grown cells AMP had no effects at 12 h, suggesting that $_{Dh}$AOX was not present; at 18 h CRR increased about 5% and a maximal activation of ~15% was observed at 22 h and thereafter (Fig. 3B). Thus, in our hands expression of $_{Dh}$AOX was dependent on the carbon source. Using glucose, a fermentable carbon source, CRR appeared in the late exponential phase while, when provided with a non-fermentable carbon source (lactate), CRR was already fully present at 12 h and remained constant throughout growth. Moreover, $_{Dh}$AOX expression did not seem to affect coupling. Thus, at variance with *Y. lipolytica*, AOX does not seem to participate in the uncoupling of *D. hansenii* mitochondria.

3.6. Krebs cycle dehydrogenases remain active, but mitochondria lose NAD^+ throughout growth

Krebs cycle NAD^+-dependent dehydrogenases provide the electrons for complex I, and thus an inhibition of these enzymes might account for the low rate of O_2 consumption observed with pyruvate–malate. To test whether these enzymes become inhibited during growth, pyruvate dehydrogenase (PDH) and malate dehydrogenase (MDH) activities were measured in permeabilized mitochondria. Both activities were lower at the later growth stages (results not shown). However, addition of 1 mM NAD^+ increased enzymatic activities to values similar to those observed in the

Please cite this article in press as: A. Cabrera-Orefice, et al., Oxidative phosphorylation in *Debaryomyces hansenii*: Physiological uncoupling at different growth phases, Biochimie (2014), http://dx.doi.org/10.1016/j.biochi.2014.03.003

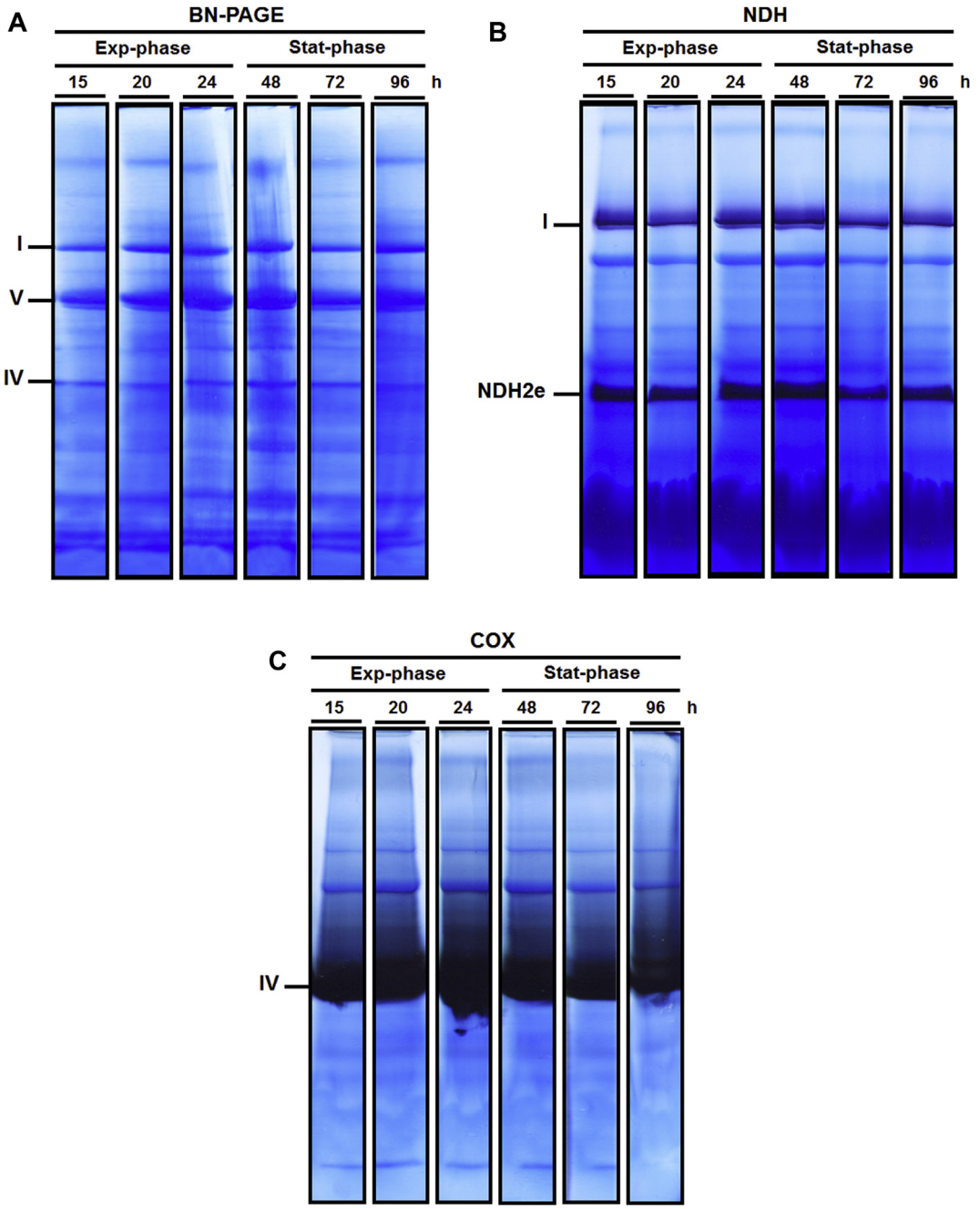

Fig. 2. In-gel NADH dehydrogenase (NDH) and cytochrome *c* oxidase (COX) activities of solubilized mitochondria from *D. hansenii* grown for different times. Isolated mitochondria (obtained from YPLac–NaCl cultures) were solubilized with lauryl-maltoside (LM) 2.0 mg/mg Prot. Growth phases and culture times are shown over each lane. (A) Different mitochondrial solubilizates were resolved by BN-PAGE in a 4–12% polyacrylamide gradient gel. The BN-gel was stained with Coomassie® brilliant blue G-250. Complex V was used as loading control. (B) In-gel NADH-dehydrogenase activity (NDH); 1 mM NADH and 0.5 mg/mL Nitrotetrazolium blue chloride (NTB). (C) In-gel cytochrome *c* oxidase activity (COX); 0.04% diaminobenzidine and 0.02% cytochrome *c*. I, IV and V are the classical respiratory complexes. NDH2e corresponds to the alternative external NADH dehydrogenase. Representative gels from triplicates.

samples from exponential phase (results not shown); i.e. Mitochondrial NAD^+ was lost as the stationary phase was approached. Both PDH and MDH were fully functional as observed when the NAD^+ pool was replenished.

3.7. *In stationary phase mitochondria, NAD^+ partially restores the rate of oxygen consumption and OxPhos coupling*

We observed that during growth, both PDH and MDH became inhibited by the lack of endogenous NAD^+ and that the addition of this coenzyme fully restored their activities. A previous report indicates that isolated mitochondria from *Polytomella* sp. do not establish a $\Delta\Psi$ unless NAD^+ is added [48]. Indeed, a NAD^+ specific mitochondrial transporter has been reported in *S. cerevisiae*, mammalians and plants [49–51]. Thus, NAD^+ was added to isolated mitochondria from *D. hansenii* grown to the stationary phase. In mitochondria from 96 h-grown cells, up to 1 mM NAD^+ increased the pyruvate–malate-promoted rate of O_2 consumption in the resting state (IV) (Table 3). In contrast, no significant effect of NAD^+ was observed in mitochondria from exponential phase (24 h) cells

Please cite this article in press as: A. Cabrera-Orefice, et al., Oxidative phosphorylation in *Debaryomyces hansenii*: Physiological uncoupling at different growth phases, Biochimie (2014), http://dx.doi.org/10.1016/j.biochi.2014.03.003

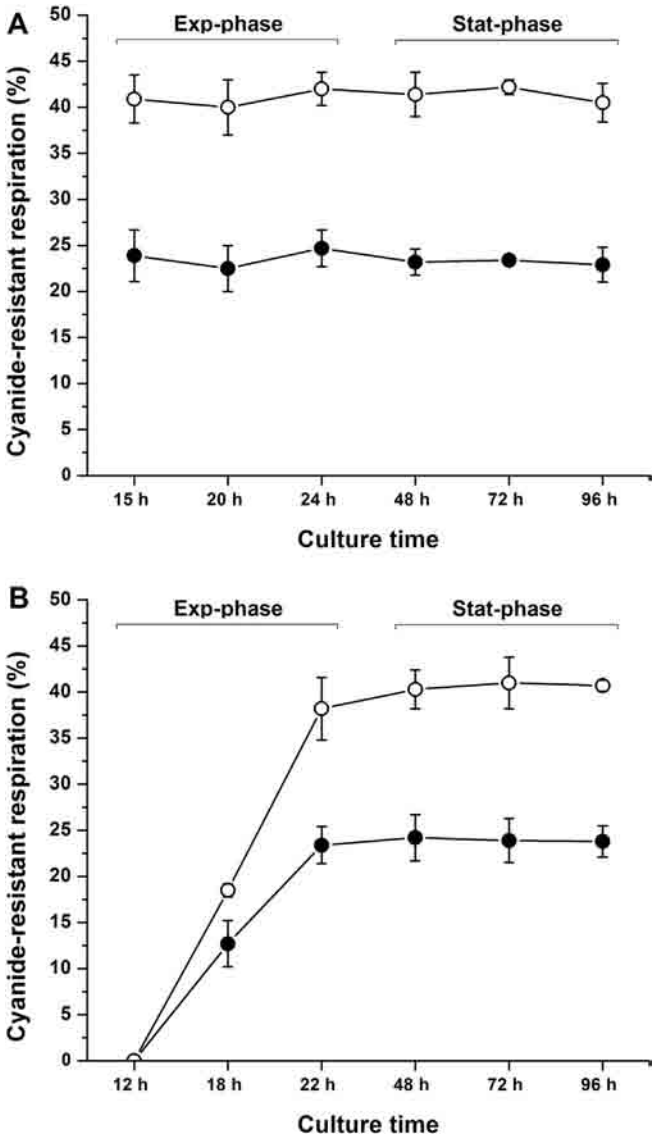

Fig. 3. Cyanide-resistant respiration (CRR) in *D. hansenii* isolated mitochondria grown to different phases using glucose or lactate as carbon sources. Oxygen consumption was measured in state IV with 10 mM succinate as respiratory substrate. 50 μM rotenone was added to inhibit complex I. CRR was assessed by the addition of 500 μM NaCN. Isolated mitochondria 0.5 mg Prot·(mL)$^{-1}$ were added in each assay. (A) CRR percentage of exponential phase (15, 20 and 24 h) and stationary (48, 72 and 96 h) phase samples that were obtained from YPLac–NaCl cultures (black dots). (B) CRR percentage of exponential phase (12, 18 and 22 h) and stationary (48, 72 and 96 h) phase samples that were obtained from YPD–NaCl cultures (black dots). In both panels, CRR was activated with 1 mM AMP (empty symbols). Reaction mixture was as in Table 1. Data from three independent experiments are expressed as the mean ± SD.

(Table 3). NAD^+ addition resulted in a partial recovery of respiratory activity (Table 3) and coupling (Fig. 4). The RC of isolated mitochondria from *D. hansenii* grown for different times was measured. In the presence of pyruvate–malate and during the exponential growth phase, from 15 to 24 h a consistently high RC ~2.3 was detected. Then, as the culture aged, RCs decreased such that at 48 h, RC ~2, at 72 h, RC ~1.4 and at 96 h, RC ~1.3 (Fig. 4, full squares). The decrease in RC observed in the presence of pyruvate–malate at the later growth times was prevented by adding NAD^+, such that at both 72 and 96 h, RC ~1.8 (Fig. 4, empty squares). The decrease in RC was specific for the complex I substrate pyruvate–malate, as demonstrated by a constant RC ~1.7 observed throughout growth when the substrate was succinate regardless of whether NAD^+ was added (Fig. 4, empty circles) or not (Fig. 4, full circles). The results suggest that when approaching the stationary phase, mitochondria from *D. hansenii* undergo complex-I specific uncoupling, which is reversed by the addition of NAD^+.

3.8. In stationary phase D. hansenii mitochondria, NAD^+ escapes the matrix, probably through the $_{Dh}$MUC

To use pyruvate–malate efficiently, isolated mitochondria from *D. hansenii* stationary phase grown-cells required replenishment of the NAD^+ pool, which was lost during growth, probably exiting through an open MUC [52]. In order to explore the behavior of $_{Dh}$MUC in the exponential and in the stationary growth phases, mitochondrial transmembrane potentials ($\Delta\Psi$) were measured at phosphate (Pi) 0.4 mM, where the $_{Dh}$MUC is open or at Pi 10 mM where the $_{Dh}$MUC is closed [29]. In mitochondria from cells grown to the exponential phase (Fig. 5A and B), and in the presence of pyruvate–malate and high Pi, $\Delta\Psi$ were high and stable with (Fig. 5A, trace c) or without added NAD^+ (Fig. 5A, trace a). In the presence of NAD^+ (Fig. 5A, trace c), maximal $\Delta\Psi$ seemed to be reached faster. In low Pi a $\Delta\Psi$ was not established and no NAD^+ effect was observed (Fig. 5A, traces b, d). In the presence of succinate (Fig. 5B) at high Pi, $\Delta\Psi$ was high and stable; a slight delay in $\Delta\Psi$ rise was observed when NAD^+ was added, i.e. a faster $\Delta\Psi$ was established in the absence (Fig. 5B, trace a) than in the presence of NAD^+ (Fig. 5B, trace c). Once more, at low Pi, $\Delta\Psi$ was not established regardless of NAD^+ (Fig. 5B, traces b, d).

In mitochondria from cells grown to the stationary phase (Fig. 5C and D) and in the presence of pyruvate–malate and high Pi, a partial $\Delta\Psi$ was established (Fig. 5C, trace a). Then, in the presence of NAD^+, $\Delta\Psi$ was significantly higher (Fig. 5C, trace c). Again, at low Pi a $\Delta\Psi$ failed to be established with (Fig. 5C, trace d) or without NAD^+ (Fig. 5C, trace b). When succinate was used as a substrate no effect of NAD^+ on $\Delta\Psi$ was observed and at high Pi, $\Delta\Psi$ was high (Fig. 5D, traces a, c) while at low Pi, $\Delta\Psi$ was minimal (Fig. 5D, traces b, d).

In the presence of high Pi, when $_{Dh}$MUC is closed, NAD^+ addition to mitochondria from cells grown to the stationary phase resulted in $\Delta\Psi$ increase. This suggests that the uptake of NAD^+ follows another transport route. To explore this, NAD^+ was added during $\Delta\Psi$ measurements at both phosphate concentrations and using pyruvate–malate as respiratory substrate (Fig. 6A). At high Pi, $\Delta\Psi$ was increased upon NAD^+ addition (Fig. 6A, trace a), i.e. NAD^+ entered mitochondria even when $_{Dh}$MUC was closed. By contrast, at low Pi, NAD^+ did not raise the $\Delta\Psi$ (Fig. 6A, trace b). Additional $\Delta\Psi$ measurements were performed in stationary phase mitochondria to discard a direct effect of NAD^+ on $_{Dh}$MUC. To do this, mitochondria were incubated 30 s at low Pi in the absence (Fig. 6B trace a) or presence of NAD^+ (Fig. 6B trace b) and no $\Delta\Psi$ was established. Then, when 10 mM Pi was added a $\Delta\Psi$ was established which was higher in the NAD^+-preincubated organelles (Fig. 6B, trace b) than in the controls (Fig. 6B, trace a).

3.9. The aging-related mitochondrial loss of NAD^+ does not result from the isolation procedure, as it is already observed in spheroplasts

In regard to the possible mechanism of mitochondrial NAD^+ depletion observed in the stationary phase, two possibilities were considered. Either NAD^+ loss occurred during mitochondrial isolation and was due to enhanced organelle fragility or this exit occurred *in situ*. To test these possibilities, we decided to measure the NAD^+-dependent respiratory activity in permeabilized spheroplasts, i.e. in wall-less, substrate-permeable cells. Thus, respiratory activity and coupling were measured in *D. hansenii* permeabilized spheroplasts from both exponential (24 h) and

Table 3
Effect of the NAD^+ on the respiratory activity and coupling of *D. hansenii* isolated mitochondria from 24 or 96 h of growth.

Substrates	Exponential phase (24 h)			Stationary phase (96 h)		
	Rate of oxygen consumption (natgO·(min mg Prot)$^{-1}$)		Respiratory control (III/IV)	Rate of oxygen consumption (natgO·(min mg Prot)$^{-1}$)		Respiratory control (III/IV)
	State IV*	State III**		State IV*	State III**	
Pyruvate + malate						
$-NAD^+$	120 ± 10	279 ± 12	2.33 ± 0.07	22 ± 7	28 ± 8	1.27 ± 0.05
$+NAD^+$	130 ± 12	307 ± 15	2.36 ± 0.13	72 ± 10	126 ± 17	1.75 ± 0.15
Succinate						
$-NAD^+$	173 ± 15	285 ± 17	1.64 ± 0.10	222 ± 8	382 ± 4	1.72 ± 0.05
$+NAD^+$	170 ± 3	270 ± 18	1.59 ± 0.10	215 ± 14	348 ± 16	1.62 ± 0.13

Reaction mixture was as in Table 1. *Resting state (IV); **phosphorylating state (III). State III was induced with 500 μM ADP. NAD^+ was added to a final concentration of 1 mM. 10 mM pyruvate + malate or 10 mM succinate were added in each case. Data from three independent experiments are expressed as the mean ± SD.

stationary phase (96 h) grown cells (Table 4). Respiratory substrates, ADP, Tris-phosphate, NAD^+ and $MgCl_2$ concentrations (see Table 4 legend) were raised to obtain maximal respiratory rates and coupling [33]. In the presence of pyruvate–malate or succinate, respiration was slower than in isolated mitochondria and RC was slightly lower (Table 3), e.g. in 24 h-grown samples spheroplasts exhibited RC = 1.83 while in isolated mitochondria RC = 2.33 (Tables 3 and 4). The rates of O_2 consumption for exponential vs. stationary phase spheroplasts were compared. Using succinate as the electron donor, the rates of O_2 consumption and coupling were similar in both growth phases, with or without added NAD^+ (Table 4). When the NAD^+-dependent substrate pyruvate–malate was added, exponential phase spheroplasts exhibited the same rate of oxygen consumption and RC regardless of whether NAD^+ was added. By contrast, stationary phase spheroplasts exhibited a smaller rate of O_2 consumption and a low RC. Then, the addition of NAD^+ to stationary phase spheroplasts fully restored both the rate of oxygen consumption and the RC (Table 4). These results in spheroplasts, where mitochondrial integrity is highly conserved strongly support the notion that the depletion of mitochondrial NAD^+ does occur in the intact cell during aging.

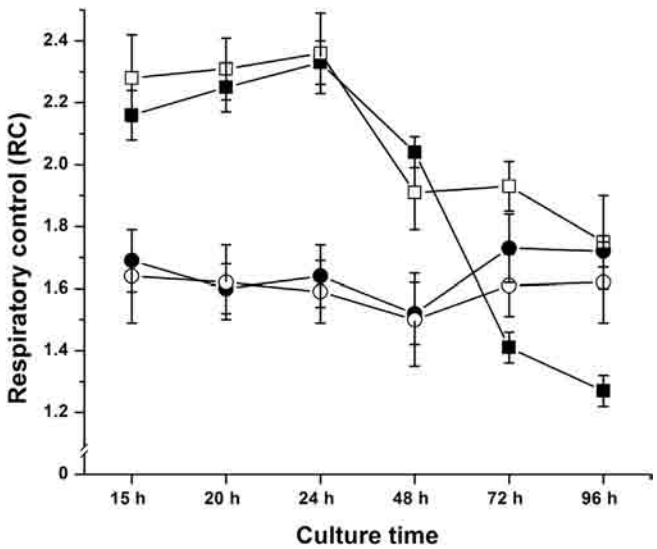

Fig. 4. Effect of the NAD^+ on the respiratory coupling of mitochondria isolated from *D. hansenii* grown for different times. Respiratory control values were obtained from oxygen consumption data that are shown in Table 3 and from other of different culture times (data not shown). 10 mM pyruvate plus 10 mM malate (squares) or 10 mM succinate (circles) were used as electron donors. Respiratory coupling was tested in the absence (full symbols) or the presence (empty symbols) of 1 mM NAD^+. Isolated mitochondria were obtained from YPLac–NaCl cultures. Reaction mixture was as in Table 1. Data from three independent experiments are expressed as the mean ± SD.

3.10. NAD^+-uptake mechanism

It was decided to determine whether *D. hansenii* contains a specific NAD^+ transporter. *S. cerevisiae* does contain two mitochondrial specific NAD^+ carriers: (a) Ndt1p and (b) Ndt2p with a protein sequence of 373 and 335 residues, respectively [50]. BLAST analysis against the sequences from *S. cerevisiae* was performed and a *D. hansenii* ortholog protein of 390 residues, annotated as DEHA2B09284p was found. DEHA2B09284p appears in the NCBI bank as a hypothetical pyruvate transporter and similar to ADP/ATP translocase. Nonetheless, our analysis exhibited identity and similarity percentages of 49% and 63% with the Ndt1p and 45% and 60% with the Ndt2p. The *E*-values for each isoform alignment were 8×10^{-102} and 2×10^{-88}, respectively. These values were very small indicating an excellent alignment and sequence coverage (83–86%). Thus, it is suggested that DEHA2B09284p is the NAD^+ carrier and belongs to the mitochondrial carrier family (MCF).

To further characterize the NAD^+ uptake mechanism, it was decided to test some of the different inhibitors of the reconstituted *S. cerevisiae* NAD^+ transporter that have been reported [50]. We chose pyridoxal 5′-phosphate, bathophenanthroline, bromocresol purple and tannic acid. These molecules were reported to be potent NAD^+-transporter inhibitors and at the same time are not known to inhibit other mitochondrial transporters such as the ATP/ADP translocase (carboxyatractyloside [53] and bongkrekic acid [54]) or the phosphate carrier (mersalyl) [55,56]. The rate of O_2 consumption was measured in mitochondria from stationary phase-grown cells using pyruvate–malate as the substrate. As expected from the results above (Table 3), in the absence of NAD^+ (Fig. 7) a low rate of O_2 consumption was observed. Also as expected, this rate was higher in the presence of NAD^+ (Fig. 7). However, in the presence of each of the transport inhibitors, addition of NAD^+ was failed to accelerate the rate of O_2 consumption, suggesting that a specific NAD^+ transporter had been blocked (Fig. 7). In mitochondria from exponential growth cells the rate of O_2 consumption was always high, regardless of whether the NAD^+ transport inhibitors were added or not (results not shown). A fourth inhibitor, tannic acid, was tested; however, this compound inhibited respiratory activity in all cases suggesting that it must have other targets (result not shown). Thus, even though NAD^+ seems to exit mitochondria under open $_{Dh}$MUC conditions, its uptake probably occurs through a NAD^+-specific transporter. Besides $_{Dh}$MUC opening, the loss and uptake of NAD^+ probably constitutes an additional mechanism to control OxPhos during growth in *D. hansenii*.

4. Discussion

During different stages of growth, yeast cells undergo remarkable metabolic changes in response to energy requirements [57]. In

Please cite this article in press as: A. Cabrera-Orefice, et al., Oxidative phosphorylation in *Debaryomyces hansenii*: Physiological uncoupling at different growth phases, Biochimie (2014), http://dx.doi.org/10.1016/j.biochi.2014.03.003

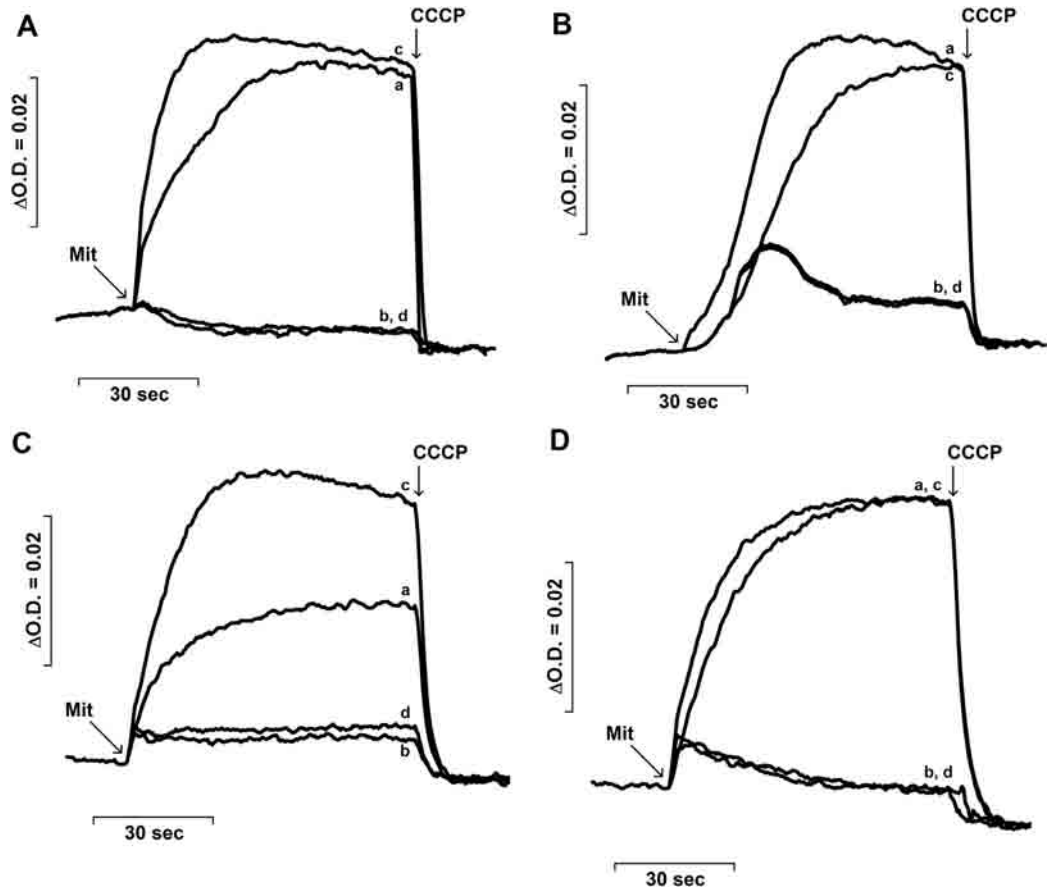

Fig. 5. Effect of NAD^+ on the transmembrane potential ($\Delta\Psi$) of mitochondria isolated from *D. hansenii* grown to exponential or stationary phases. Reaction mixture: 1 M sorbitol, 10 μM safranine-O and 10 mM maleic acid, pH 6.8 (Tris). Final volume 2.0 mL; room temperature. Phosphate concentrations were: 0.4 mM (traces b, d) or 10 mM (traces a, c). 10 mM pyruvate plus 10 mM malate was tested in isolated mitochondria from exp-phase (24 h) (A) and stat-phase (96 h) (C). 10 mM succinate was tested in isolated mitochondria from exp-phase (24 h) (B) and stat-phase (96 h) (D). 1 mM NAD^+ was added to the reaction mixture in traces c and d. Where indicated, mitochondria (Mit) 0.5 mg Prot·$(mL)^{-1}$ and CCCP 5 μM were added. Representative traces from three independent experiments.

the exponential growth phase, highly replicative cells must produce a large amount of ATP to contend with active anabolic pathways [58]. However, entering the stationary growth phase, cell division stops and ATP needs decrease considerably [8,59]. In this situation, the mitochondrial respiratory chain would work at a low rate, promoting ROS formation and losing the control of the cellular redox state [8,46]. Non-fermentative or Crabtree-negative yeast species (e.g. *Y. lipolytica*, *D. hansenii*, *Candida albicans*, etc.), where mitochondrial OxPhos is the main ATP source would be at a larger disadvantage [43]. Crabtree-positive yeast species, such as *S. cerevisiae*, probably need to face this problem only in the presence of non-fermentative carbon sources. To avoid ROS overproduction, there must be some mechanisms that increase the rate of O_2 consumption through physiological uncoupling [8]. Uncoupling systems must be finely regulated and become activated only under low energy-demand conditions; e.g. the stationary phase [8,46].

D. hansenii contains two physiological uncoupling systems. The first system involves the alternative redox enzymes: NDH2e, $_{Mit}$GPDH and AOX [32,60]. The electron transfer through these oxidoreductases is non-conservative and independent of the synthesis of ATP [8,32]. Therefore, even if alternative oxidoreductases are not protonophores, i.e. classic uncouplers, the final result is the increase in the rate of O_2 consumption, which is uncoupled from the synthesis of ATP [8,9]. The second is the permeability transition (PT) triggered by the opening of mitochondrial unspecific channel (MUC) [29]. PT is defined as the increase in the unselective transport of ions and metabolites across the mitochondrial inner membrane with a molecular mass cutoff of 1.1–1.5 kDa [61,62]. PT dissipates all electrochemical gradients and promotes mitochondrial swelling [44]. Both systems were previously described in *D. hansenii* mitochondria isolated from exponential phase grown cells [29,32] and they were further studied here, aiming to understand physiological uncoupling in *D. hansenii*.

In the stationary growth phase, *D. hansenii* mitochondria exhibited a fall in the complex I-dependent rate of O_2 consumption and coupling, which did not occur in the presence of other electron donors such as NADH, succinate or glycerol-phosphate. This behavior was apparently caused by a loss of NAD^+ from the mitochondrial matrix. It is likely that upon aging NAD^+ exited mitochondria through $_{Dh}$MUC that appears to be open during the stationary growth phase, causing the dissipation of $\Delta\Psi$ and electrochemical gradients [8,52,63]. This uncoupling would increase the rate of O_2 consumption by the respiratory chain, preventing ROS overproduction and reestablishing the balance in the NADH/NAD^+ needed for both cytosolic and mitochondrial metabolic pathways.

Open MUC-related NAD^+ loss was previously described in *S. cerevisiae* and in intact immortalized human microvascular endothelial cells (HMEC-1) by Bradshaw and Pfeiffer [52] and by Dumas and co-workers [63], respectively. In the first case, endogenous NAD^+ was lost only from swollen mitochondria, decreasing the complex I-dependent respiratory activity. NAD^+ addition restored the decreased rate of oxygen consumption in these mitochondria [52]. On the other hand, HMEC-1 cells opened the permeability transition pore (PTP) [63]; i.e. the mammalian

Please cite this article in press as: A. Cabrera-Orefice, et al., Oxidative phosphorylation in *Debaryomyces hansenii*: Physiological uncoupling at different growth phases, Biochimie (2014), http://dx.doi.org/10.1016/j.biochi.2014.03.003

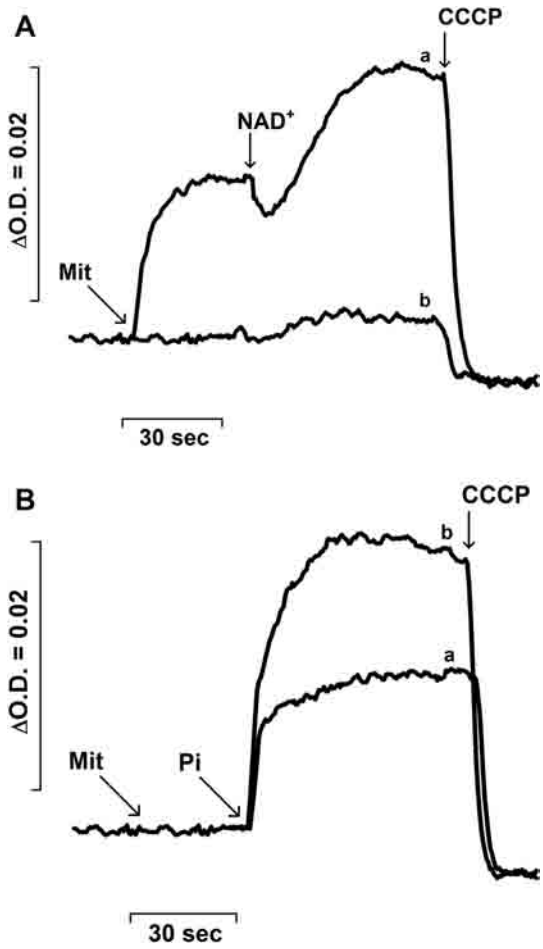

Fig. 6. NAD^+-mediated increase in $\Delta\Psi$ of isolated mitochondria from *D. hansenii* grown to the stationary phase. Reaction mixture: 1 M sorbitol, 10 μM safranine-O and 10 mM maleic acid, pH 6.8 (Tris) and 10 mM pyruvate plus 10 mM malate as respiratory substrate. Final volume 2.0 mL; room temperature. Where indicated, mitochondria (Mit) 0.5 mg Prot·$(mL)^{-1}$, 1 mM NAD^+, 10 mM Pi and CCCP 5 μM were added. (A) Phosphate concentrations were: 0.4 mM (trace b) or 10 mM (trace a). (B) NAD^+ concentrations were: 0 mM (trace a) or 1 mM (trace b); no phosphate was added before the 10 mM marked addition. Representative traces from three independent experiments.

counterpart of MUC [44], in the presence of the Ca^{2+} ionophore A23187. In this situation, matrix NAD(P)H loss and swelling were described; cyclosporine A was prevented both events [63].

In *S. cerevisiae*, NAD^+ is synthesized outside the mitochondria and imported by two isoforms of a NAD^+ carrier named Ndt1p and Ndt2p, respectively [50]. Both carriers import NAD^+ by unidirectional transport or by exchange with nucleotide monophosphates, such as AMP, GMP and their deoxyderivatives [64]. Also, these transporters belong to the mitochondrial carrier family (MCF); i.e. a family of nuclear-codified mitochondrial proteins that exhibits a conserved six-transmembrane-helix structure [65]. In stat-growth phase *D. hansenii* isolated mitochondria, the complex I-dependent rate of O_2 consumption and coupling was partially restored by NAD^+ addition to the reaction mixture. Furthermore, NAD^+ addition fully restored both parameters in permeabilized spheroplasts. A high phosphate concentration (10 or 20 mM) was added to close the $_{Dh}$MUC. In this condition, NAD^+ was imported into mitochondria probably through a specific carrier and not by $_{Dh}$MUC. Searching for this protein, a possible candidate annotated as DEHA2B09284p was found in the NCBI database, which shows a great similarity to Ndt1p and Ndt2p. In addition, the putative *D. hansenii* NAD^+ transporter also shares with the *S. cerevisiae* Ndt1p and Ndt2p the sensitivity to at least three NAD^+ transporter inhibitors; i.e. bathophenanthroline, pyridoxal-5′-phosphate and bromocresol purple [50,66].

Results strongly suggest that a physiological stationary-phase-related loss of matrix NAD^+ occurred before the isolation of mitochondria. Matrix NAD^+ loss has been described in mitochondria from *Polytomella* sp. [48] and from *S. cerevisiae* [52]. In *D. hansenii*, it seems that mitochondria from stationary phase-grown cells did retain some NAD^+ as they were able to support remnants of complex I-linked respiratory activity. The traces of matrix NAD^+ could be useful to maintain basal metabolite fluxes through the Krebs cycle and other NAD^+-dependent mitochondrial pathways. We propose that the decrease in complex I-linked respiratory activity promoted by NAD^+ loss constitutes a novel ATP-overproduction prevention/physiological uncoupling mechanism.

Since NAD^+ addition did not fully restore the respiratory activity promoted by pyruvate–malate in stationary growth phase mitochondria it was thought that further modifications were present and thus, all other, classical or alternative respiratory components were measured. Complexes I and IV and the NDH2e activities remained constant throughout growth. Complex III did decrease in stat-growth phase samples. As complexes I, III and IV from this yeast are organized into supercomplexes [32] and these associations have been related to electron channeling [67], the decrease in complex III might affect supercomplex assembly, detaching some of the complexes I and IV. If so, a lower electron transfer through the cytochromic pathway would be expected when using complex I-electron donors. Supercomplex assembly dynamics in this species needs to be studied. In addition, respiratory activities and coupling in the presence of succinate, NADH or glycerol-phosphate were not affected by the decrease of complex III. This behavior could be due

Table 4
Effect of the NAD^+ on the respiratory activity and coupling of *D. hansenii* permeabilized spheroplasts from 24 or 96 h of growth.

Substrates	Exponential phase (24 h)			Stationary phase (96 h)		
	Rate of oxygen consumption (natgO·(min mg Prot)$^{-1}$)		Respiratory control (III/IV)	Rate of oxygen consumption (natgO·(min mg Prot)$^{-1}$)		Respiratory control (III/IV)
	State IV*	State III**		State IV*	State III**	
Pyruvate + malate						
$-NAD^+$	11.5 ± 0.2	21.1 ± 2.0	1.83 ± 0.18	4.9 ± 1.3	5.3 ± 1.3	1.08 ± 0.02
$+NAD^+$	11.8 ± 1.2	22.5 ± 3.2	1.91 ± 0.12	11.1 ± 1.2	20.7 ± 3.3	1.86 ± 0.10
Succinate						
$-NAD^+$	12.6 ± 0.7	18.7 ± 0.4	1.49 ± 0.08	12.2 ± 2.8	18.5 ± 2.8	1.54 ± 0.15
$+NAD^+$	11.9 ± 1.4	17.9 ± 0.4	1.51 ± 0.21	13.3 ± 2.4	18.8 ± 2.4	1.42 ± 0.08

Spheroplasts were permeabilized with 20 μg/mL nystatin in the presence of constant oxygen bubbling. Rates of oxygen consumption were measured in resting state (IV)* and phosphorylating state (III)**. State III was induced with 5 mM ADP. NAD^+ was added to a final concentration of 5 mM. 20 mM pyruvate + malate or 20 mM succinate were added in each case. Reaction mixture: 1.0 M sorbitol, 75 mM KCl, 20 mM Tris-phosphate, 5 mM $MgCl_2$, 0.5 mM EGTA and 10 mM maleic acid, pH 6.8 (Tris). Final volume was 1.0 mL. Temperature = 30 °C. Data from three independent experiments are expressed as the mean ± SD.

Please cite this article in press as: A. Cabrera-Orefice, et al., Oxidative phosphorylation in *Debaryomyces hansenii*: Physiological uncoupling at different growth phases, Biochimie (2014), http://dx.doi.org/10.1016/j.biochi.2014.03.003

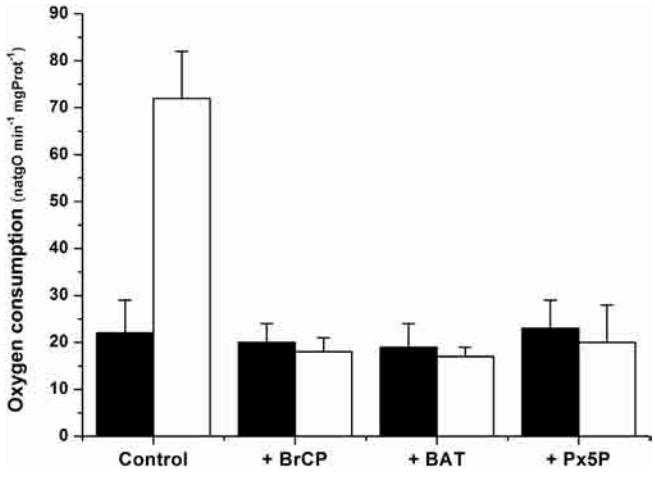

Fig. 7. Effect of NAD^+-mitochondrial transporter inhibitors on the rate of oxygen consumption in state IV of mitochondria isolated from *D. hansenii* grown to the stationary phase. Mitochondria isolated from 96 h grown cells. Oxygen consumption was measured in resting state (IV) with (white bars) or without (black bars) 1 mM NAD^+. 10 mM pyruvate–malate was used as electron donor. Inhibitors concentrations were: 0.3 mM bromocresol purple (BrCP); 5 mM bathophenanthroline (BAT) and 5 mM pyridoxal 5′-phosphate (Px5P). Inhibitors were added to the reaction mixture before addition of mitochondria. Reaction mixture was as in Table 1. Data from three independent experiments, expressed as the mean ± SD.

to the lack of supercomplex attachments reported for complex II, NDH2e or $_{Mit}$GPDH [32].

In *Y. lipolytica*, a supercomplex formed by the alternative external NADH dehydrogenase ($_{Yl}$NDH2e) and complexes III and IV has been described [26]. This association exists only in the exponential growth phase and blocks the electron flux from exogenous NADH to the alternative pathway. However, during the stationary phase, the $_{Yl}$NDH2e-III–IV supercomplex dissociates and allows the flow of electrons through both the cytochromic pathway and the alternative pathway [46]. In *D. hansenii* it is not clear whether alternative components attach to large I–III–IV supercomplexes, as no associations between NDH2e with the cytochrome complexes III and IV have been observed in the exponential growth phase [32]. Both *Y. lipolytica* and *D. hansenii* possess identical composition of their respiratory chains and yet, component associations between classical and alternative enzymes seem to be different, at least in the exponential phase [26,32]. In *D. hansenii* regardless of the substrate, electrons are transferred by both pathways [32].

In lactate-containing media, $_{Dh}$AOX is fully expressed and active in all growth phases. By contrast, in glucose-containing media, $_{Dh}$AOX was not present in the early exponential growth phase and only in the late-exponential and stationary growth phases was $_{Dh}$AOX activity detected. These results are interesting because $_{Dh}$AOX expression seems to be controlled by the carbon source and not only by the growth phase, as suggested others (2003) [60]. In *S. cerevisiae*, lactate can be directly oxidized by two mitochondrial lactate dehydrogenase (LDH) isoforms located in the outer side of the inner mitochondrial membrane or by another matrix LDH isoform [25,68,69]. LDH membrane isoforms oxidize D-lactate or L-lactate to pyruvate and are able to donate electrons directly to cytochrome *c* [69]. Matrix LDH isoform uses D-lactate to produce pyruvate in a NAD^+-dependent fashion [70]. *D. hansenii* must contain at least one of these proteins in order to assimilate lactate during growth. A higher rate of ATP synthesis in the presence of lactate would be expected, saturating and slowing the rate of electron transport, rather than using glucose. It is proposed that to prevent this, *D. hansenii* expresses AOX in all growth phases, establishing an escape route to move electrons and avoid ROS overproduction. This putative function of AOX is amply proposed in the literature [8,14,60,71].

5. Conclusions

In the stationary growth phase, *D. hansenii* mitochondria decreased their complex I-dependent rate of oxygen consumption and coupling. This was caused by a loss of NAD^+ from the mitochondrial matrix. In isolated mitochondria from stationary phase grown cells, addition of NAD^+ partially restored both O_2 consumption and RC. Furthermore, NAD^+ addition to permeabilized spheroplasts from cells grown to the stationary growth phase fully restored complex I-dependent respiration and coupling. NAD^+ seems to be transported by a putative specific carrier annotated as DEHA2B09284p, which is similar to those from *S. cerevisiae* (Ndt1p and Ndt2p). The NAD^+ effect was inhibited by bathophenanthroline, pyridoxal-5′-phosphate and bromocresol purple which are known to inhibit the reconstituted mitochondrial NAD^+-transporters. OxPhos parameters did not change in the presence of succinate, NADH or glycerol-phosphate under in any growth condition. In addition, $_{Dh}$AOX expression seems to be controlled by both the carbon source and the growth phase. It is suggested that upon reaching the stationary growth phase *D. hansenii* activates $_{Dh}$MUC (consequently losing mitochondrial matrix NAD^+) as a physiological uncoupling mechanism.

Conflict of interest

There are no conflicts of interest associated with this publication. The manuscript has been read and approved by all named authors for submitting to Biochimie.

Acknowledgments

Authors thank Natalia Chiquete-Félix, Martha Calahorra, Ramón Méndez-Franco and Norma Sánchez for technical assistance. We thank Dr. Antonio Peña for the gift of *D. hansenii* Y7426 strain, reagents and use of equipment. Also thank Dr. Diego González-Halphen and Miriam Vázquez-Acevedo for BN-PAGE assistance. Partially funded by the PAPIIT Program and DGAPA/UNAM grant IN202612. ACO is a CONACYT fellow enrolled in the Biochemistry Graduate Program at UNAM.

References

[1] N. Lane, Oxygen: the Molecule that made the World, Oxford University Press, USA, 2004.
[2] A.L. Sessions, D.M. Doughty, P.V. Welander, R.E. Summons, D.K. Newman, The continuing puzzle of the great oxidation event, Curr. Biol. 19 (2009) R567–R574.
[3] T.L. Clanton, M.C. Hogan, L.B. Gladden, Regulation of cellular gas exchange, oxygen sensing, and metabolic control, Compr. Physiol. 3 (2013) 1135–1190.
[4] T. Fenchel, B. Finlay, Oxygen and the spatial structure of microbial communities, Biol. Rev. Camb. Philos. Soc. 83 (2008) 553–569.
[5] C.C. Hsia, A. Schmitz, M. Lambertz, S.F. Perry, J.N. Maina, Evolution of air breathing: oxygen homeostasis and the transitions from water to land and sky, Compr. Physiol. 3 (2013) 849–915.
[6] S. Drose, U. Brandt, The mechanism of mitochondrial superoxide production by the cytochrome bc_1 complex, J. Biol. Chem. 283 (2008) 21649–21654.
[7] Y. Kushnareva, A.N. Murphy, A. Andreyev, Complex I-mediated reactive oxygen species generation: modulation by cytochrome c and NAD(P)$^+$ oxidation–reduction state, Biochem. J. 368 (2002) 545–553.
[8] S. Guerrero-Castillo, D. Araiza-Olivera, A. Cabrera-Orefice, J. Espinasa-Jaramillo, M. Gutierrez-Aguilar, L.A. Luevano-Martinez, A. Zepeda-Bastida, S. Uribe-Carvajal, Physiological uncoupling of mitochondrial oxidative phosphorylation. Studies in different yeast species, J. Bioenerg. Biomembr. 43 (2011) 323–331.
[9] B. Kadenbach, Intrinsic and extrinsic uncoupling of oxidative phosphorylation, Biochim. Biophys. Acta 1604 (2003) 77–94.

[10] S. Manon, M. Guerin, Investigation of the yeast mitochondrial unselective channel in intact and permeabilized spheroplasts, Biochem. Mol. Biol. Int. 44 (1998) 565–575.
[11] R.A. Haworth, D.R. Hunter, The Ca^{2+}-induced membrane transition in mitochondria. II. Nature of the Ca^{2+} trigger site, Arch. Biochem. Biophys. 195 (1979) 460–467.
[12] D.G. Nicholls, E. Rial, A history of the first uncoupling protein, UCP1, J. Bioenerg. Biomembr. 31 (1999) 399–406.
[13] A.G. Rasmusson, K.L. Soole, T.E. Elthon, Alternative NAD(P)H dehydrogenases of plant mitochondria, Annu. Rev. Plant Biol. 55 (2004) 23–39.
[14] A.L. Umbach, J.N. Siedow, The cyanide-resistant alternative oxidases from the fungi *Pichia stipitis* and *Neurospora crassa* are monomeric and lack regulatory features of the plant enzyme, Arch. Biochem. Biophys. 378 (2000) 234–245.
[15] D.G. Nicholls, S.J. Ferguson, Bioenergetics 3, Academic Press, London, 2002.
[16] T. Joseph-Horne, D.W. Hollomon, P.M. Wood, Fungal respiration: a fusion of standard and alternative components, Biochim. Biophys. Acta 1504 (2001) 179–195.
[17] A. McDonald, G. Vanlerberghe, Branched mitochondrial electron transport in the animalia: presence of alternative oxidase in several animal phyla, IUBMB Life 56 (2004) 333–341.
[18] N. Sen, H.K. Majumder, Mitochondrion of protozoan parasite emerges as potent therapeutic target: exciting drugs are on the horizon, Curr. Pharm. Des. 14 (2008) 839–846.
[19] D. Munro, N. Pichaud, F. Paquin, V. Kemeid, P.U. Blier, Low hydrogen peroxide production in mitochondria of the long-lived *Arctica islandica*: underlying mechanisms for slow aging, Aging Cell 12 (2013) 584–592.
[20] S. Kerscher, S. Drose, V. Zickermann, U. Brandt, The three families of respiratory NADH dehydrogenases, Results Probl. Cell Differ. 45 (2008) 185–222.
[21] M. Rigoulet, X. Leverve, E. Fontaine, R. Ouhabi, B. Guerin, Quantitative analysis of some mechanisms affecting the yield of oxidative phosphorylation: dependence upon both fluxes and forces, Mol. Cell. Biochem. 184 (1998) 35–52.
[22] M. Crompton, The mitochondrial permeability transition pore and its role in cell death, Biochem. J. 341 (Pt. 2) (1999) 233–249.
[23] A.P. Halestrap, C. Brenner, The adenine nucleotide translocase: a central component of the mitochondrial permeability transition pore and key player in cell death, Curr. Med. Chem. 10 (2003) 1507–1525.
[24] S. de Vries, L.A. Grivell, Purification and characterization of a rotenone-insensitive NADH: Q6 oxidoreductase from mitochondria of *Saccharomyces cerevisiae*, Eur. J. Biochem. 176 (1988) 377–384.
[25] M. Rigoulet, A. Mourier, A. Galinier, L. Casteilla, A. Devin, Electron competition process in respiratory chain: regulatory mechanisms and physiological functions, Biochim. Biophys. Acta 1797 (2010) 671–677.
[26] S. Guerrero-Castillo, M. Vazquez-Acevedo, D. Gonzalez-Halphen, S. Uribe-Carvajal, In *Yarrowia lipolytica* mitochondria, the alternative NADH dehydrogenase interacts specifically with the cytochrome complexes of the classic respiratory pathway, Biochim. Biophys. Acta 1787 (2009) 75–85.
[27] L.A. Luevano-Martinez, E. Moyano, M.G. de Lacoba, E. Rial, S. Uribe-Carvajal, Identification of the mitochondrial carrier that provides *Yarrowia lipolytica* with a fatty acid-induced and nucleotide-sensitive uncoupling protein-like activity, Biochim. Biophys. Acta 1797 (2010) 81–88.
[28] S. Kerscher, S. Drose, K. Zwicker, V. Zickermann, U. Brandt, *Yarrowia lipolytica*, a yeast genetic system to study mitochondrial complex I, Biochim. Biophys. Acta 1555 (2002) 83–91.
[29] A. Cabrera-Orefice, S. Guerrero-Castillo, L.A. Luevano-Martinez, A. Pena, S. Uribe-Carvajal, Mitochondria from the salt-tolerant yeast *Debaryomyces hansenii* (halophilic organelles?), J. Bioenerg. Biomembr. 42 (2010) 11–19.
[30] U. Breuer, H. Harms, *Debaryomyces hansenii* — an extremophilic yeast with biotechnological potential, Yeast 23 (2006) 415–437.
[31] A. Veiga, J.D. Arrabaca, M.C. Loureiro-Dias, Cyanide-resistant respiration, a very frequent metabolic pathway in yeasts, FEMS Yeast Res. 3 (2003) 239–245.
[32] A. Cabrera-Orefice, N. Chiquete-Felix, J. Espinasa-Jaramillo, M. Rosas-Lemus, S. Guerrero-Castillo, A. Pena, S. Uribe-Carvajal, The branched mitochondrial respiratory chain from *Debaryomyces hansenii*: components and supramolecular organization, Biochim. Biophys. Acta 1837 (2014) 73–84.
[33] N. Averet, V. Fitton, O. Bunoust, M. Rigoulet, B. Guerin, Yeast mitochondrial metabolism: from in vitro to in situ quantitative study, Mol. Cell. Biochem. 184 (1998) 67–79.
[34] A.G. Gornall, C.J. Bardawill, M.M. David, Determination of serum proteins by means of the biuret reaction, J. Biol. Chem. 177 (1949) 751–766.
[35] H. Schagger, Respiratory chain supercomplexes, IUBMB Life 52 (2001) 119–128.
[36] E. Zerbetto, L. Vergani, F. Dabbeni-Sala, Quantification of muscle mitochondrial oxidative phosphorylation enzymes via histochemical staining of blue native polyacrylamide gels, Electrophoresis 18 (1997) 2059–2064.
[37] I. Wittig, M. Karas, H. Schagger, High resolution clear native electrophoresis for in-gel functional assays and fluorescence studies of membrane protein complexes, Mol. Cell. Proteomics 6 (2007) 1215–1225.
[38] G.C. Steffens, R. Biewald, G. Buse, Cytochrome *c* oxidase is a three-copper, two-heme-A protein, Eur. J. Biochem. 164 (1987) 295–300.
[39] J.A. Berden, E.C. Slater, The reaction of antimycin with a cytochrome *b* preparation active in reconstitution of the respiratory chain, Biochim. Biophys. Acta 216 (1970) 237–249.
[40] D.E. Green, J. Jarnefelt, H.D. Tisdale, Studies on the elecron transport system. XIV. The isolation and properties of soluble cytochrome c_1, Biochim. Biophys. Acta 31 (1959) 34–46.
[41] G.J. Cooney, H. Taegtmeyer, E.A. Newsholme, Tricarboxylic acid cycle flux and enzyme activities in the isolated working rat heart, Biochem. J. 200 (1981) 701–703.
[42] K.E. Akerman, M.K. Wikstrom, Safranine as a probe of the mitochondrial membrane potential, FEBS Lett. 68 (1976) 191–197.
[43] A. Veiga, J.D. Arrabaca, M.C. Loureiro-Dias, Cyanide-resistant respiration is frequent, but confined to yeasts incapable of aerobic fermentation, FEMS Microbiol. Lett. 190 (2000) 93–97.
[44] S. Manon, X. Roucou, M. Guerin, M. Rigoulet, B. Guerin, Characterization of the yeast mitochondria unselective channel: a counterpart to the mammalian permeability transition pore? J. Bioenerg. Biomembr. 30 (1998) 419–429.
[45] S. Uribe-Carvajal, L.A. Luevano-Martinez, S. Guerrero-Castillo, A. Cabrera-Orefice, N.A. Corona-de-la-Pena, M. Gutierrez-Aguilar, Mitochondrial unselective channels throughout the eukaryotic domain, Mitochondrion 11 (2011) 382–390.
[46] S. Guerrero-Castillo, A. Cabrera-Orefice, M. Vazquez-Acevedo, D. Gonzalez-Halphen, S. Uribe-Carvajal, During the stationary growth phase, *Yarrowia lipolytica* prevents the overproduction of reactive oxygen species by activating an uncoupled mitochondrial respiratory pathway, Biochim. Biophys. Acta 1817 (2012) 353–362.
[47] H. Schagger, K. Pfeiffer, The ratio of oxidative phosphorylation complexes I–V in bovine heart mitochondria and the composition of respiratory chain supercomplexes, J. Biol. Chem. 276 (2001) 37861–37867.
[48] A. Jimenez-Suarez, M. Vazquez-Acevedo, A. Rojas-Hernandez, S. Funes, S. Uribe-Carvajal, D. Gonzalez-Halphen, In *Polytomella* sp. mitochondria, biogenesis of the heterodimeric COX2 subunit of cytochrome *c* oxidase requires two different import pathways, Biochim. Biophys. Acta 1817 (2012) 819–827.
[49] P. Rustin, B. Parfait, D. Chretien, T. Bourgeron, F. Djouadi, J. Bastin, A. Rotig, A. Munnich, Fluxes of nicotinamide adenine dinucleotides through mitochondrial membranes in human cultured cells, J. Biol. Chem. 271 (1996) 14785–14790.
[50] S. Todisco, G. Agrimi, A. Castegna, F. Palmieri, Identification of the mitochondrial NAD^+ transporter in *Saccharomyces cerevisiae*, J. Biol. Chem. 281 (2006) 1524–1531.
[51] M. Neuburger, R. Douce, Slow passive diffusion of NAD^+ between intact isolated plant mitochondria and suspending medium, Biochem. J. 216 (1983) 443–450.
[52] P.C. Bradshaw, D.R. Pfeiffer, Loss of NAD(H) from swollen yeast mitochondria, BMC Biochem. 7 (2006) 3.
[53] X. Roucou, S. Manon, M. Guerin, Conditions allowing different states of ATP- and GDP-induced permeability in mitochondria from different strains of *Saccharomyces cerevisiae*, Biochim. Biophys. Acta 1324 (1997) 120–132.
[54] M. Crompton, S. Virji, J.M. Ward, Cyclophilin-D binds strongly to complexes of the voltage-dependent anion channel and the adenine nucleotide translocase to form the permeability transition pore, Eur. J. Biochem. 258 (1998) 729–735.
[55] P. Cortes, V. Castrejon, J.G. Sampedro, S. Uribe, Interactions of arsenate, sulfate and phosphate with yeast mitochondria, Biochim. Biophys. Acta 1456 (2000) 67–76.
[56] M. Gutierrez-Aguilar, X. Perez-Martinez, E. Chavez, S. Uribe-Carvajal, In *Saccharomyces cerevisiae*, the phosphate carrier is a component of the mitochondrial unselective channel, Arch. Biochem. Biophys. 494 (2010) 184–191.
[57] M. Werner-Washburne, E. Braun, G.C. Johnston, R.A. Singer, Stationary phase in the yeast *Saccharomyces cerevisiae*, Microbiol. Rev. 57 (1993) 383–401.
[58] S.M. Jazwinski, The retrograde response: when mitochondrial quality control is not enough, Biochim. Biophys. Acta 1833 (2013) 400–409.
[59] J.V. Gray, G.A. Petsko, G.C. Johnston, D. Ringe, R.A. Singer, M. Werner-Washburne, "Sleeping beauty": quiescence in *Saccharomyces cerevisiae*, Microbiol. Mol. Biol. Rev. 68 (2004) 187–206.
[60] A. Veiga, J.D. Arrabaca, F. Sansonetty, P. Ludovico, M. Corte-Real, M.C. Loureiro-Dias, Energy conversion coupled to cyanide-resistant respiration in the yeasts *Pichia membranifaciens* and *Debaryomyces hansenii*, FEMS Yeast Res. 3 (2003) 141–148.
[61] D.W. Jung, P.C. Bradshaw, D.R. Pfeiffer, Properties of a cyclosporin-insensitive permeability transition pore in yeast mitochondria, J. Biol. Chem. 272 (1997) 21104–21112.
[62] A.P. Halestrap, What is the mitochondrial permeability transition pore? J. Mol. Cell. Cardiol. 46 (2009) 821–831.
[63] J.F. Dumas, L. Argaud, C. Cottet-Rousselle, G. Vial, C. Gonzalez, D. Detaille, X. Leverve, E. Fontaine, Effect of transient and permanent permeability transition pore opening on NAD(P)H localization in intact cells, J. Biol. Chem. 284 (2009) 15117–15125.
[64] F. Palmieri, G. Agrimi, E. Blanco, A. Castegna, M.A. Di Noia, V. Iacobazzi, F.M. Lasorsa, C.M. Marobbio, L. Palmieri, P. Scarcia, S. Todisco, A. Vozza, J. Walker, Identification of mitochondrial carriers in *Saccharomyces cerevisiae* by transport assay of reconstituted recombinant proteins, Biochim. Biophys. Acta 1757 (2006) 1249–1262.
[65] F. Palmieri, C.L. Pierri, A. De Grassi, A. Nunes-Nesi, A.R. Fernie, Evolution, structure and function of mitochondrial carriers: a review with new insights, Plant J. 66 (2011) 161–181.
[66] F. Palmieri, B. Rieder, A. Ventrella, E. Blanco, P.T. Do, A. Nunes-Nesi, A.U. Trauth, G. Fiermonte, J. Tjaden, G. Agrimi, S. Kirchberger, E. Paradies,

Please cite this article in press as: A. Cabrera-Orefice, et al., Oxidative phosphorylation in *Debaryomyces hansenii*: Physiological uncoupling at different growth phases, Biochimie (2014), http://dx.doi.org/10.1016/j.biochi.2014.03.003

A.R. Fernie, H.E. Neuhaus, Molecular identification and functional characterization of *Arabidopsis thaliana* mitochondrial and chloroplastic NAD^+ carrier proteins, J. Biol. Chem. 284 (2009) 31249–31259.
[67] H. Schagger, K. Pfeiffer, Supercomplexes in the respiratory chains of yeast and mammalian mitochondria, EMBO J. 19 (2000) 1777–1783.
[68] X. Grandier-Vazeille, K. Bathany, S. Chaignepain, N. Camougrand, S. Manon, J.M. Schmitter, Yeast mitochondrial dehydrogenases are associated in a supramolecular complex, Biochemistry 40 (2001) 9758–9769.
[69] A. Mourier, J. Vallortigara, E.D. Yoboue, M. Rigoulet, A. Devin, Kinetic activation of yeast mitochondrial D-lactate dehydrogenase by carboxylic acids, Biochim. Biophys. Acta 1777 (2008) 1283–1288.
[70] A. Chelstowska, Z. Liu, Y. Jia, D. Amberg, R.A. Butow, Signalling between mitochondria and the nucleus regulates the expression of a new D-lactate dehydrogenase activity in yeast, Yeast 15 (1999) 1377–1391.
[71] D.P. Maxwell, Y. Wang, L. McIntosh, The alternative oxidase lowers mitochondrial reactive oxygen production in plant cells, Proc. Natl. Acad. Sci. U. S. A. 96 (1999) 8271–8276.

Please cite this article in press as: A. Cabrera-Orefice, et al., Oxidative phosphorylation in *Debaryomyces hansenii*: Physiological uncoupling at different growth phases, Biochimie (2014), http://dx.doi.org/10.1016/j.biochi.2014.03.003

Oxígeno, para bien y para mal

Emilio Espinoza Simón[a], Mónica Rosas Lemus[a], Alfredo Cabrera Orefice[a], Cristina Uribe Álvarez[a], Natalia Chiquete Félix[a], Salvador Uribe Carvajal[a]

El oxígeno ayuda a aprovechar la energía de los nutrientes, sin embargo, también produce especies reactivas de oxígeno (ERO), que en exceso, reaccionan con las moléculas del organismo y las destruyen. Esto provoca envejecimiento y, eventualmente, la muerte. Las diferentes especies biológicas han evolucionado para regular la formación de las ERO. La alimentación y el estilo de vida ejercen una fuerte influencia sobre la capacidad del organismo para lidiar con las ERO.

Desde su aparición hace 3,500 millones de años, los seres vivos proliferaron y se diversificaron hasta que hace 2,000 millones de años la concentración de oxígeno atmosférico aumentó 100,000 veces, lo que indujo la extinción de alrededor del 80% de las especies biológicas. Este aumento se debió a la actividad de las cianobacterias fotosintéticas cuya actividad metabólica libera oxígeno como subproducto y a la toxicidad de los derivados parcialmente reducidos del oxígeno que se conocen como ERO.

A partir de las especies que sobrevivieron a la oxigenación masiva de la atmósfera se desarrollaron los organismos aerobios. Es decir, células que utilizan al oxígeno como aceptor de electrones, lo que libera grandes cantidades de energía en un proceso conocido como respiración aerobia. La cadena respiratoria aerobia se localiza en la membrana plasmática de las bacterias o en la membrana interna mitocondrial de los eucariontes.

La fosforilación oxidativa mitocondrial resulta del acoplamiento entre 2 procesos **(figura 1)**. Primero, la cadena respiratoria bombea protones al espacio extramembranal usando la energía del flujo de electrones desde diversos donadores hasta el oxígeno, este proceso genera un "gradiente" de protones, es decir una diferencia de sus concentraciones a cada lado de la membrana. Luego el complejo V o adenosintrifosfato (ATP) sintetasa libera la energía almacenada en el gradiente de protones para la fosforilación, es decir la síntesis de ATP, a partir de una molécula de adenosindifosfato (ADP) y un fosfato. La cadena respiratoria acepta equivalentes reductores de diversos sustratos como el nicotinamida adenindinucleótido reducido (NADH) y el flavín adenin dinucleótido reducido ($FADH_2$). El nicotinamida adenindinucleótido (NAD^+) es reducido a NADH por diversas enzimas entre las que se encuentran algunas del ciclo de Krebs, como

[a]Laboratorio 305 Oriente. Departamento de Genética Molecular. Instituto de Fisiología Celular. UNAM. México, DF.

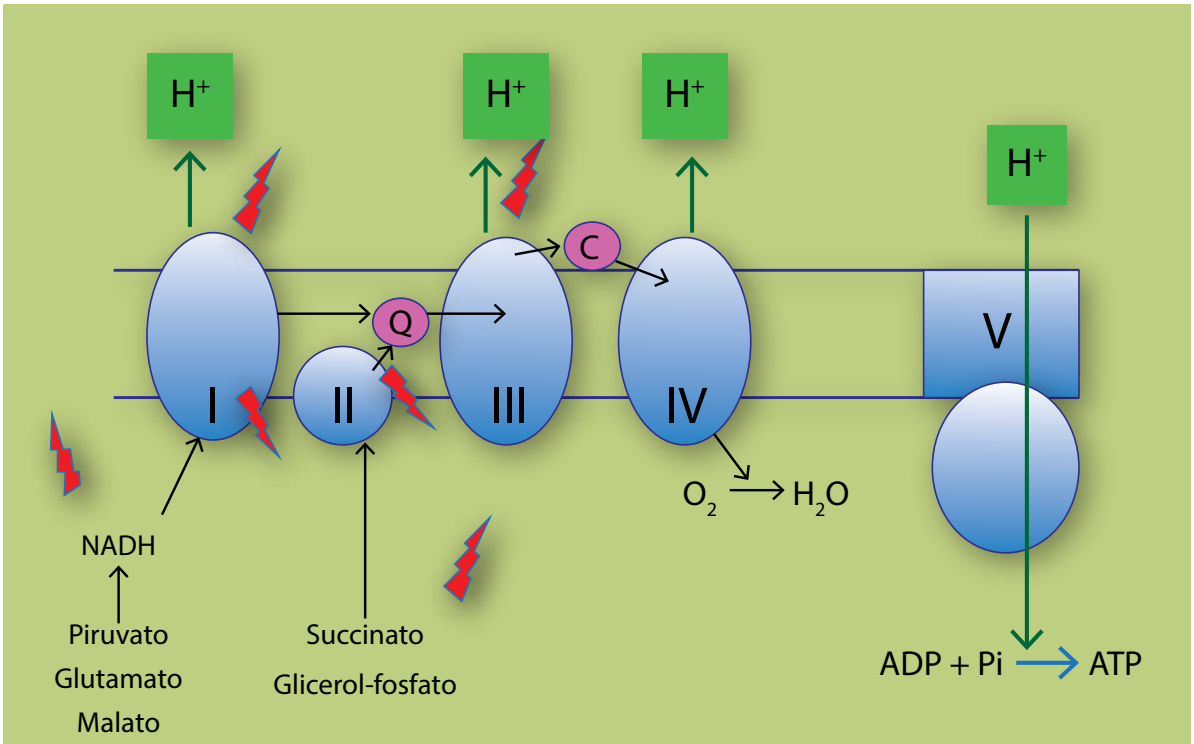

Figura 1. Estructura de la cadena respiratoria mitocondrial de mamíferos donde se muestra el flujo de electrones entre los intermediarios del ciclo de Krebs y la cadena respiratoria (flechas negras) hasta reducir al oxígeno obteniendo agua; el bombeo de protones hacia el espacio intermembranal (arriba) por los complejos I, III y IV y el regreso a la matriz mitocondrial a través del complejo V (complejos en azul) para energizar la síntesis de ATP (flechas verdes). La fuga de radicales libres proviene de diversas fuentes (flechas rojas) como las deshidrogenasas dependientes de NADH, los complejos I, II y III y la glicerol fosfato dehidrogenasa. La coenzima Q y el citocromo c (círculos rosa) transportan electrones entre los complejos de la cadena.

la piruvato deshidrogenasa, la alfa-ceto glutarato deshidrogenasa y la malato deshidrogenasa; luego el NADH es oxidado en el complejo I (NADH: coenzima Q óxido-reductasa). El $FADH_2$ proviene de la succinato dehidrogenasa o de la glicerol fosfato deshidrogenasa y alimenta al complejo II (FADH2: coenzima Q óxido-reductasa). Los electrones captados en los complejos I y II son cedidos a través de la coenzima Q al complejo III (coenzima Q: citocromo c óxido-reductasa) y luego, a través del citocromo C al complejo IV (citocromo-oxidasa). El complejo IV reduce al oxígeno para producir agua.

El flujo de electrones es ilustrado con flechas negras **(figura 1)**. Los electrones arrastran protones y 3 de los complejos respiratorios (I, III y IV) aprovechan la liberación de energía de las óxido-reducciones catalizadas para bombear los protones al espacio intermembranal y así almacenar la energía en forma de un gradiente de protones (**figura 1**, flechas y cuadros verdes). Los protones fluyen de regreso al interior mitocondrial a través de la ATP sintetasa o complejo V liberando energía que se usa para sintetizar ATP **(figura 1)**.

La eficiencia del metabolismo aerobio es unas 15 veces mayor que la del metabolismo anaerobio y por ello, los organismos que generaron un metabolismo aerobio pudieron crecer y llegaron a dominar la Tierra. Sin embargo, esa eficiencia tiene un elevado precio. Durante la respiración se generan radicales libres (especies químicas con electrones desaparea-

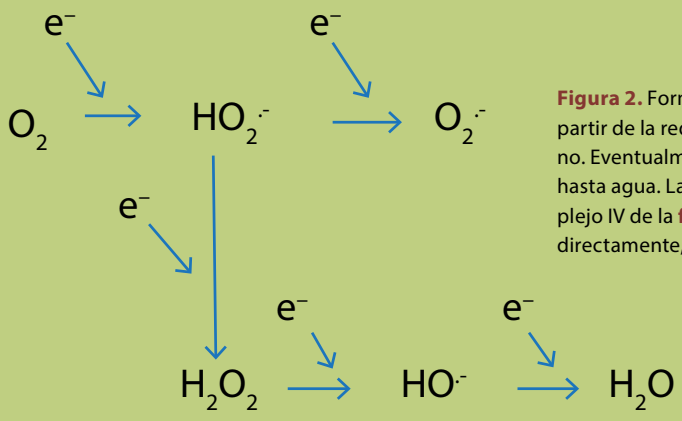

Figura 2. Formación de radicales libres de oxígeno a partir de la reducción parcial de la molécula de oxígeno. Eventualmente, las ERO se detoxifican al reducirse hasta agua. La citocromo oxidasa mitocondrial (complejo IV de la **figura 1**) reduce el oxígeno hasta agua directamente, sin pasar por estos intermediarios.

dos) que pueden reaccionar inespecíficamente con el oxígeno del medio y generar ERO (**figura 1**, flechas rojas).

Las ERO, que también son radicales libres, reaccionan rápidamente con los lípidos formando malondialdehido y 4-hidroxinonenal, oxidan las bases del DNA formando 8- hidroxiguanosina, además de carbonilar, nitrar y glutationilar a las proteínas. Estas modificaciones eventualmente conducen a la muerte celular.

Las principales ERO son el ion superóxido ($O_2^{\cdot-}$), el ion hidroperóxido ($HOO^{\cdot}$) y el ion hidroxilo ($HO^{\cdot}$), además del peróxido de hidrógeno (H_2O_2) que no es un radical libre pero es muy reactivo. Su génesis por introducción de electrones individuales provenientes de radicales libres se muestra en la **figura 2**.

Los organismos, lo mismo una bacteria que un humano, necesitan defenderse de las ERO. Las defensas son de 2 tipos: el primero es la desactivación de las ERO catalizada por enzimas como la superóxido-dismutasa (SOD), la catalasa y el sistema de la glutatión-peroxidasa/reductasa. La SOD convierte al radical superóxido en peróxido de hidrógeno, mientras que la catalasa transforma al peróxido de hidrógeno en agua. Estas 2 reacciones deben estar estrechamente coordinadas. Por ejemplo, en humanos la SOD se codifica en el cromosoma 21; si hay 3 cromosomas 21, en lugar de 2, se expresa un exceso de SOD que produce tanto peróxido de hidrógeno que la catalasa no logra eliminarlo y daña a las células. El sistema de la glutatión peroxidasa/reductasa usa al glutatión, un tripéptido antioxidante que contiene cisteína.

La glucólisis anaerobia genera 2 moléculas de ATP por glucosa consumida, mientras que la combinación de glucólisis con fosforilación oxidativa genera entre 36 y 38 moléculas de ATP por glucosa.

El segundo mecanismo de protección consiste en abatir la formación intracelular de las ERO. La aceleración de la velocidad del paso de electrones por la cadena respiratoria abate la producción de las ERO mediante 2 mecanismos: disminuye la concentración de oxígeno en la célula y elimina rápidamente a los radicales libres, antes de que puedan participar en reacciones inespecíficas.

Las mitocondrias, paradójicamente parecen ser la clave del manejo de las ERO. Si bien la cadena respiratoria mitocondrial produce una gran cantidad de radicales libres, es también gracias a la actividad de la cadena respiratoria mitocondrial que se evita que esos radicales libres se combinen con oxígeno y se produzcan ERO.

En humanos, las ERO tienen un papel relevante en procesos tan variados como el síndrome de Down (trisomía 21), la gangrena, el daño postis-

Foto: Tsutomu Takasu

El ejercicio regular, físico y muy probablemente intelectual y la ingesta de antioxidantes polifenólicos incrementan la biogénesis y la respiración mitocondrial en tejido nervioso, adiposo y muscular. En modelos animales se observó que la biogénesis y la función mitocondrial neuronal de la descendencia son beneficiadas por la práctica constante de ejercicio.

químico, cerebral o miocárdico, el envejecimiento fisiológico de los organismos y las enfermedades neurodegenerativas.

En pacientes con la enfermedad de Parkinson se observó una actividad deficiente del complejo I mitocondrial en la sustancia nigra, mientras que en la enfermedad de Huntington existe una baja actividad del complejo II en el cerebro de pacientes en etapas avanzadas y en la corteza temporal de pacientes con síndrome de Alzheimer se observa deficiencia del complejo III.

Diversos estudios demostraron que el ejercicio regular, físico y muy probablemente intelectual y la ingesta de antioxidantes polifenólicos incrementan la biogénesis y la respiración mitocondrial en tejido nervioso, adiposo y muscular en sujetos obesos, diabéticos y sanos. En modelos animales se observó que la biogénesis y la función mitocondrial neuronal de la descendencia son beneficiadas por la práctica constante de ejercicio. Asimismo, la restricción calórica preserva la función mitocondrial promoviendo la biogénesis mitocondrial y mejorando la eficiencia bioenergética.

El elixir de la juventud es el propio sudor. Conforme acumulamos años, es necesario luchar (en el gimnasio y en la pista de atletismo) por formar biomasa muscular y mantener el metabolismo aerobio funcionando. Así se producirán más mitocondrias y se evitará el daño inducido por las ERO. En este sentido, se ha demostrado que aún cuando un sujeto físicamente activo no necesariamente viva más tiempo, su calidad de vida será muy superior al que es sedentario. Evitar el exceso en la ingesta en alimentos también ayuda a aumentar la población mitocondrial. ●

BIBLIOGRAFÍA

Gregory MA, Gill DP, Petrella RJ. Brain health and exercise in older adults. Curr Sport Med Rep. 2013;12(4):256-71.

Lane N. Oxygen: the molecule that made the world. Oxford: Oxford University Press; 2003.

Sena LA, Chandel NS. Physiological roles of mitochondrial reactive oxygen species. Mol Cell. 2012;48(2):158-67.

Toledo FG, Goodpaster BH. The role of weight loss and exercise in correcting skeletal muscle mitochondrial abnormalities in obesity, diabetes and aging. Moll Cell Endocrinol. 2013;379(1-2):30-4.